

**Identification and Characterization of Protein-based Arsenic
Resistance Mechanisms in *Pseudomonas mendocina*
SMSKVR-3 Isolated from Khetri Copper Mines**

THESIS

Submitted in partial fulfillment
of the requirements for the degree of

DOCTOR OF PHILOSOPHY

by

SHRADDHA MISHRA

Under the Supervision of

Prof. SANJAY KUMAR VERMA

&

Co-Supervision of

Prof. SURESH GUPTA



**BIRLA INSTITUTE OF TECHNOLOGY AND SCIENCE, PILANI,
RAJASTHAN-333031, INDIA**

2022

**BIRLA INSTITUTE OF TECHNOLOGY AND SCIENCE,
PILANI, RAJASTHAN, INDIA**

CERTIFICATE

This is to certify that the thesis entitled “**Identification and Characterization of Protein-based Arsenic Resistance Mechanisms in *Pseudomonas mendocina* SMSKVR-3 Isolated from Khetri Copper Mines**” and submitted by **Shraddha Mishra**, ID No. **2014PHXF0001P** for the award of Ph.D. of the Institute embodies original work done by him/her under my supervision.

Signature (Supervisor) :

Name (Supervisor) : **Sanjay Kumar Verma**

Designation : **Professor**

Department of Biological Sciences,

BITS Pilani, Pilani Campus.

Signature (Co-Supervisor) :

Name (Co-Supervisor) : **Suresh Gupta**

Designation : **Professor**

Department of Chemical Engineering,

BITS Pilani, Pilani Campus.

Date:

*Dedicated to My Beloved
Grandparents*

ACKNOWLEDGEMENTS

First and foremost, I would like to thank God for always showering blessings on me, keeping me healthy, and guiding me towards the right path.

My sincere gratitude to my supervisor Prof. Sanjay Kumar Verma, Department of Biological Sciences, BITS Pilani for giving me the opportunity of pursuing Ph.D. under his guidance and benefiting me with his wealth of knowledge and experience. The encouragement and motivation given by him have immensely helped me during the difficult stages of my research. I will be obliged and thankful to him forever for making me so confident and helping me to improve my analytical skills.

I sincerely thank Prof. Souvik Bhattacharyya, Vice-Chancellor, Prof. Sudhirkumar Barai, Director, and Prof. Ashoke Kumar Sarkar (Former Director) BITS Pilani, Pilani campus for providing laboratory facilities which helped me to complete the research work successfully.

I am grateful to my Co-supervisor, Prof. Suresh Gupta, Department of Chemical Engineering, BITS Pilani for his support, availability, and guidance during the project work as well as throughout the research.

I want to especially thank Prof. Jitendra Panwar and Prof. Prabhat Nath Jha, Department of Biological Sciences, BITS Pilani, members of my Doctoral Advisory Committee for their support and encouragement. My sincere gratitude to them for giving their valuable time whenever I required any suggestion. They also helped a lot in learning microbiology during my 5 years of microbiology lab teaching experience which allowed me to improve my teaching skills. My heartfelt gratitude to the head of the Department of Biological Sciences Prof. P. R. Deepa for providing all the departmental facilities, guidance, and support. I also acknowledge all the faculties of the Department of Biological Sciences, BITS Pilani for their help, directions, suggestions, and friendliness. My biggest thanks to all the non-teaching staff of the Department of Biological Sciences for helping me with the issues related to my research as well as departmental work.

I am so much grateful to Waste Water and Energy management (WWE-BITS, Pilani), BITS Pilani, and the Council of Scientific and Industrial Research (CSIR) for providing me financial assistance during my research work.

I deeply thank *P. mendocina* SMSKVR-3 for so much tolerance towards arsenic and other heavy metals without that I would have never completed my Ph.D. You provided me a direction to work for the Ph. D. and future too.

It was a great opportunity to have Mr. Shivam Agarwal, Ms. Saumya Singh, Ms. Niharika Singh, and Ms. R. Sreenidhi as project students who worked in the same area as a part of their M.E. project work. I especially want to thank Ms. R. Sreenidhi for helping me to learn several bioinformatics tools that were required for my research work. I am thankful

ACKNOWLEDGEMENTS

to my group members Mr. Sandeep and Mrs. Poonam for always cooperating in the lab work. I am so much thankful to the former lab members of our group, Prof. S. Ramachandran, Dr. Pankaj Jain, Dr. Sachi Singh, Dr. Prakash, Dr. Jola Sunil Dubey, and Dr. A. Senthil Nagappan, and for their guidance, support, and motivation. My heartfelt thanks to the entire EMB Lab. family for being so cooperative and friendly. I always feel so fortunate to get this opportunity to work with the hardworking, dedicated, and extremely talented lab. members who always maintained constructive and peaceful lab. environment.

My heartfelt thanks to my seniors Dr. Vidushi Asati, Dr. Monika M Jangir, Dr. Gagandeep Singh Saggu, Dr. Panchsheela, Dr. Arpit Bhargava, Dr. Gurpreet, Dr. Zarna Pala, Dr. Rajnish Singh, Dr. Isha Pandey, and Dr. Kuldeep Gupta for always helping and encouraging me. I would especially like to thank Venkataraghavan Ragunathan, Anna University, Chennai for teaching me Autodock which helped me to complete the bioinformatic part of my work.

I would like to thank my friends Dr. Amritanjali, Dr. Sonam Shrama, Ms. Nidhi Gaur, Mr. Dheeraj Singh, Mr. Shashank, Ms. Rinki Gupta, Dr. Archana Singh, Dr. Anupama Rani, Mrs. Poonam Shah, Ms. Nirupama Dixit, Ms. Paramita Chawley, Mr. Dilip, Mr. Azeem for always encouraging, motivating, and supporting me during difficult times. My heartfelt thanks to Mrs. Monica Sandhu Paul for her immense support, love, and guidance during my research. I would also like to thank Dr. Anil Rai for making me the part of several musical events in the institute and always encouraging me for the singing.

Word can never be enough to thank my parents who always believed in me and supported in the decision of pursuing a Ph.D. I am so much indebted to them for their blessings, prayers, love, encouragement, care, and support at every moment of my life and most importantly the patience they carried during my Ph.D. journey. I am also grateful to my elder brother, Dr. Abhishek Mishra, and younger brother, Mr. Abhinandan Mishra for always dreaming so big for me and inspiring me to do that. Thanks for holding my hands from childhood till now and always loving and supporting me at every stage of my life. I am so much thankful to my sister-in-law, Dr. Arti Nirmal for always inspiring, loving, supporting, and giving valuable suggestions whenever I needed them. I would also like to thank my little angel, Ms. Mishika Mishra, for loving me so much, giving me so many precious happy moments, and being my little inspiration. I would also like to thank my entire family (uncles, aunts, and cousins) for always supporting and believing me.

Shraddha Mishra

Abstract

Considering the potential application of arsenic-resistant bacteria as well as proteins expressed by them for arsenic bioremediation and biosensor development, 7 bacterial strains (SMSKVR-1, SMSKVR-2, SMSKVR-3, SMSKVW-1, SMSKVW-2, SMSKVW-3, and SMSKVW-4) were isolated from the khetri copper mines, Rajasthan, India. The strain SMSKVR-3 was selected for further studies because of its faster growth in 300 mM As(V) containing media. The biochemical and complete molecular characterization of SMSKVR-3 has led to its identification as *Pseudomonas mendocina* with 99.04% identity to *P. mendocina* strain ATCC 25411. Although it showed growth under a wide range of temperature, pH, and salt (NaCl) concentrations, the optimum growth was observed at temperature 30 °C, pH 7, and 0.25% (w/v) NaCl concentration. The toxic effect of As(V) and As(III) on *P. mendocina* SMSKVR-3 was studied using growth curve analysis and scanning electron microscopy in the absence (control) and presence of 300 mM As(V) and 1.34 mM As(III). In the presence of As(V) and As(III), no significant change in the growth pattern and cellular morphology was observed, indicating the efficient arsenic detoxification mechanisms in *P. mendocina* SMSKVR-3. The studies conducted to identify the arsenic resistance mechanisms in *P. mendocina* SMSKVR-3 suggested the role of siderophores, metal/metalloid-antibiotic cross-tolerance, arsenate reduction, and polyphosphate bodies. This was confirmed by the PCR amplification of arsenate reductase (*arsC*), polyphosphate kinase (*ppk1*), efflux RND transporter component & gene for arsenic resistance protein *arsH* along with the whole-genome sequencing of *P. mendocina* SMSKVR-3. The whole-genome sequencing revealed the presence of several other genes related to arsenic resistance such as genes for arsenical-resistance protein (ACR3), MFS-type efflux pump (ArsJ) specific for 1-arseno-3-phosphoglycerate, arsenical resistance operon repressor (ArsR), and NAD-dependent glyceraldehyde-3-phosphate dehydrogenase. To investigate the proteins involved in As(V) tolerance in *P. mendocina* SMSKVR-3, proteomic studies including 2-DGE followed by MALDI-TOF/TOF MS and whole proteome analysis using LC-MS/MS were performed. The 8 h incubation time and 300 mM As(V), concentration were optimized by protein expression analysis using SDS-PAGE to conduct further proteomic studies. Based on the % volume and fold expression in the 2-DGE, three exclusively expressed protein spots and one overexpressed spot were selected. The MALDI TOF/TOF MS analysis has proved that these protein spots correspond to ribosome-recycling

factor, polyphosphate: ADP/GDP phosphotransferase, ribonuclease P protein component, and cobalt-precorrin-5B C(1)-methyltransferase. A MASCOT score of 54, 81, 94, and 100% confirms this finding. These proteins may be playing an indirect role in As(V) resistance. The whole proteome comparative study of *P. mendocina* SMSKVR-3 in the absence and presence of As(V) seems to be in agreement with the whole-genome analysis showing the over-expression of proteins such as ArsC family reductase, glyceraldehyde-3-phosphate dehydrogenase, NAD-dependent aldehyde dehydrogenase, and arsenical resistance protein ArsH under As(V) stress. Several other stress-related proteins such as superoxide dismutase, universal stress protein, and UspA domain-containing protein having an indirect role in As(V) resistance were also over-expressed under As(V) stress. The proteins specifically expressed under As(V) stress included stress-related proteins such as OsmC family peroxiredoxin, NAD(P)H-quinone oxidoreductase, response regulator receiver protein, BolA family protein, glutathione synthase, and phosphate-specific transport system protein (PhoU). All of these proteins allow *P. mendocina* SMSKVR-3 to tolerate higher As(V) concentrations. The *in silico* study of As(V) binding with the arsenic resistance proteins ArsC and ArsH was conducted to show their applicability in the As(V) bioremediation and biosensor development. Both ArsC and ArsH exhibited significant binding with As(V) ion with the binding energies of -4.31 and -4.60 kcal/mol, respectively. The docking study revealed the binding of As(V) ion with the Glu 73, Leu 76, Ala 79, Arg 78, and Lys 111 residues of the ArsC protein and Ser 39, Lys 43, Ser 44, Phe 45, and Ser 46 residues of the B-chain of ArsH protein. Overall, the present study shows various arsenic-specific proteins to be responsible for higher As(V) resistance in *P. mendocina* SMSKVR-3 that can significantly bind with the As(V) and can be employed in bioremediation and arsenic biosensor development.

Contents

	Page No.
<i>Acknowledgements</i>	i-ii
<i>Abstract</i>	iii-iv
<i>Contents</i>	v-vi
<i>List of figures</i>	vii-xi
<i>List of tables</i>	xii-xiii
<i>List of abbreviations</i>	xiv-xv
Chapter I Introduction	1-23
1.1 General introduction	2-3
1.2 Detection of arsenic in environmental samples	3-7
1.3 Bioremediation of arsenic-containing pollutants	7-9
1.4 Evolution of arsenic resistance in bacteria	9-10
1.5 Arsenic resistant bacteria	10-13
1.4 Bacterial arsenic resistance mechanisms	13-15
1.7 Binding of arsenic with prokaryotic proteins	16-18
1.8 Proteomic approaches to study the arsenic-induced protein expression in the bacteria	19-20
1.9 Bioinformatics approaches for studying the interaction of proteins with arsenic	20-21
1.10 Gaps in the existing research	21-22
1.11 Objectives of the present research	22-23
Chapter II Materials and Methods	24-54
2.1 Isolation of arsenic resistant bacterial strains from khetri copper mines	25-26
2.2 Identification and characterization of the isolated strains of bacteria	26-33
2.3 Study of physiological parameters required for the bacterial growth	33-34
2.4 Analysis of the growth curve	34

2.5 Study of the cellular morphology by scanning electron microscopy (SEM)	35
2.6 Investigation of the possible arsenate resistance mechanisms in <i>P. mendocina</i> SMSKVR-3	35-41
2.7 Whole-genome sequencing analysis of <i>P. mendocina</i> SMSKVR-3 to explore the presence of arsenate resistance genes	41-43
2.8 Analysis of the proteins involved in arsenate resistance by proteomic approaches	43-51
2.9 <i>In silico</i> study of the binding of arsenate with the selected arsenic binding proteins	51-54
Chapter III Results and Discussion	55-147
3.1 Isolation and characterization of arsenic resistant bacterial strains from khetri copper mines	56-65
3.2 Study of physiological parameters required for the bacterial growth	65-66
3.3 Analysis of the growth curve	67-68
3.4 Study of cellular morphology under arsenic stress using SEM analysis	68-70
3.5 Investigation of the arsenate resistance mechanisms in <i>P. mendocina</i> SMSKVR-3	70-81
3.6 Whole-genome sequencing analysis of <i>P. mendocina</i> SMSKVR-3 to explore the presence of arsenate resistance genes	82-92
3.7 Analysis of the differential protein expression in <i>P. mendocina</i> SMSKVR-3 using 2-DGE	93-107
3.8 Analysis of the whole-cell proteins under arsenate stress	107-131
3.9 <i>In silico</i> study of the binding of arsenate with the selected arsenic binding proteins	132-147
Chapter IV Summary and Conclusions	148-152
<i>Future scope of the work</i>	153
<i>References</i>	154-176
Appendix	177-187
<i>List of Publications (Appendix I)</i>	177-181
<i>Biography (Appendix II)</i>	182-184
<i>Appendix III-V</i>	185-187

List of Figures

Fig. No.	Caption	Page No.
Fig. 1.1	Basic functional mechanism of a whole-cell biosensor involving different reporter proteins for detection which include color change, luminescence, or fluorescence	5
Fig. 1.2	Overall representation of arsenic resistance mechanisms found in different microbes	14
Fig. 2.1	Map of the study area	26
Fig. 3.1	Different sites of sample collection in the khetri copper mines	57
Fig. 3.2	Gram staining of the isolated bacterial strains	59
Fig. 3.3	Molecular characterization of the isolates, (a) genomic DNA of the isolates, (b) amplified 16S rRNA genes from the isolates, (c) BOX-PCR profile of all the isolates	60
Fig. 3.4	Morphology of SMSKVR-3 in M9-minimal media-agar plate	62
Fig. 3.5	Neighbour-joining phylogenetic tree based on 16S rRNA gene sequences, showing the position of SMSKVR-3 and other related genera. The 16S rRNA gene sequence of the <i>E. coli</i> K-12 was used as an outgroup. Bootstrap values (%) are based on 1000 replicates	64
Fig. 3.6	Study of different physiological parameters (a) temperature, (b) pH, and (c) salt (NaCl) concentrations required for the growth of <i>P. mendocina</i> SMSKVR-3.	66
Fig. 3.7	Growth curve of <i>P. mendocina</i> SMSKVR-3 in the presence of (a) only M9 minimal media, (b) M9 media having 300 mM arsenate, and (c) M9 media supplemented with 1.34 mM arsenite	67
Fig. 3.8	Scanning electron microscopy image of <i>P. mendocina</i> SMSKVR-3; a(i), (ii) & (iii) without any treatment (control); a(iv), (v) & (vi) treated with 300 mM arsenate; a(vii), (viii) & (ix) treated with 1.34 mM arsenite at 20000 x magnification; b(i), (ii) & (iii) enlarged image (50000 x) of <i>P. mendocina</i> SMSKVR-3 under control, As(V) treated, and As(III) treated conditions	69
Fig. 3.9	Siderophores production by <i>P. mendocina</i> SMSKVR-3 in King's B-agar plate with chrome azurol S dye supplemented with (a) Fe(III), (d) As(V), and (g) As(III) inoculated with negative control (<i>E. coli</i> DH5 α); King's B media plate with chrome azurol S dye supplemented with (b) Fe(III), (e) As(V), and (h) As(III) inoculated with the positive control (<i>P. aeruginosa</i>); King's B-agar plate with chrome azurol S dye supplemented with (c) Fe(III), (f) As(V), and (i) As(III) inoculated with <i>P. mendocina</i> SMSKVR-3 and incubated for 48 h	71

Fig. 3.10	Silver nitrate microtiter plate assay for the analysis of arsenate reduction by <i>P. mendocina</i> SMSKVR-3. In each well of microtitre plate 80 µl of 0.2 M Tris-HCl buffer (pH 7.5), 1.33 mM As(V), 20 µl of bacterial cells (OD ₆₀₀ range 0.6-0.7) or 20 µl of 0.2 M Tris-HCl buffer (pH 7.5) in control was added. After the incubation for (A) 24 h, (B) 48 h, and (C) 72 h picture was taken after the addition of 100 µl of 0.1 M AgNO ₃	75
Fig. 3.11	Role of polyphosphate bodies in response to 300 mM As(V) in <i>P. mendocina</i> SMSKVR-3; (a) concentration of polyphosphate, (b) concentration of deposited As(V) on the cell surface, (c) concentration of intracellular As(V)	79
Fig. 3.12	Schematic representation of probable mechanisms of arsenic resistance in <i>P. mendocina</i> SMSKVR-3	80
Fig. 3.13	PCR amplification of the genes involved in arsenate resistance in <i>P. mendocina</i> SMSKVR-3. Lane 1 & 5: 100-10000 bp ladder (SM0331), Lane 2-4: genes involved in arsenate resistance including arsenate reductase, polyphosphate kinase & efflux RND transporter component, Lane 8: arsenic resistance protein (ArsH)	81
Fig. 3.14	Organism annotation based on the top BLASTX hits	83
Fig. 3.15	Phylogenetic tree constructed based on the whole-genome sequence of <i>P. mendocina</i> SMSKVR-3 and other closest reference and representative genomes belonging to the same genus	84
Fig. 3.16	Annotation of the genes based on their biological process	85
Fig. 3.17	Annotation of the genes based on their molecular function	86
Fig. 3.18	Annotation of the genes based on their cellular component	86
Fig. 3.19	Circular graphical representation of the complete genome annotation of the <i>P. mendocina</i> SMSKVR-3. The outer to inner rings include (1) the contigs, (2) forward strand CDS, (3) reverse strand CDS, (4) RNA genes, (5) CDS with homology to known antimicrobial resistance genes, (6) CDS with homology to known virulence factors, (7) GC content, and (8) GC skew. The circular graphical map was constructed using PATRIC (version 3.6.9)	87
Fig. 3.20	Pie chart representing an overview of the subsystem for the <i>P. mendocina</i> SMSKVR-3 genome based on the analysis using PATRIC. The count of the subsystem and genes have been listed right side in parentheses	88
Fig. 3.21	Study of protein expression in <i>P. mendocina</i> SMSKVR-3 at (a) 0 h, (b) 4 h, (c) 8 h, (d) 16 h, and (e) 24 h under arsenate untreated (control; C1, C2 and C3) and 300 mM As(V) treated (Treated; T1, T2 and T3) condition	94

Fig. 3.22	Graphical representation of the SDS-PAGE analysis of the proteins over-expressed and under-expressed at different time intervals under As(V) treated condition in <i>P. mendocina</i> SMSKVR-3	95
Fig. 3.23	SDS- PAGE analysis of the protein expression in <i>P. mendocina</i> SMSKVR-3 under the increasing concentration of As(V)	96
Fig. 3.24	Analysis of protein expression in <i>P. mendocina</i> SMSKVR-3 using 2-DGE without As(V) treatment (control) (a), and with 300 mM As(V) treatment (b)	97
Fig. 3.25	2-DGE gel images showing uniquely expressed proteins in the sample treated with 300 mM arsenate after analysis using Image Master 2D Platinum 7.0 software	98
Fig. 3.26	2-DGE gels showing differentially expressed protein in (a) control (without arsenate), and (b) treated (300 mM arsenate) samples after analysis using Image Master 2D Platinum 7.0 software	98
Fig. 3.27	Expression-based categorization of proteins under the (a) control, and (b) treated (300 mM arsenate) conditions in the form of the pie charts; (c) graphical representation of the differentially expressed proteins under 300 mM arsenate treatment	99-100
Fig. 3.28	Protein spots expressed exclusively in (a) untreated (control), and (b) 300 mM arsenate treated condition represented in terms of % volume (only % volume ≥ 0.1 has been considered)	101
Fig. 3.29	Graphical representation of the under-expressed or over-expressed protein spot in arsenate treated sample in comparison to control sample in terms of fold change (a); over-expression and under-expression of proteins in As(V) treated sample in comparison to control represented as a heat map (b)	102-103
Fig. 3.30	MALDI-TOF/TOF MS spectra and MASCOT histogram plot of the selected spot (a) 4472, (b) match spot 15, (c) 4483, and (d) 4422. In the MASCOT histogram plot, a protein score of >50 is considered as a significant score ($p < 0.05$)	104-105
Fig. 3.31	Venn diagram of the total identified proteins in <i>P. mendocina</i> SMSKVR-3 under 300 mM As(V) treated and control (untreated) conditions	108
Fig. 3.32	Pie chart representing the distribution of proteins expressed specifically in the control sample based on their (a) biological process, (b) molecular function, and (c) cellular component	110
Fig. 3.33	Pie chart representing the distribution of proteins expressed specifically in the 300 mM As(V) treated sample based on their (a) biological process, (b) molecular function, and (c) cellular component	112
Fig. 3.34	Pie chart representing the distribution of proteins showed downregulation in the 300 mM As(V) treated sample (in comparison to control) based on	117

	their (a) biological process, (b) molecular function, and (c) cellular component	
Fig. 3.35	Pie chart representing the distribution of proteins showed upregulation in the 300 mM As(V) treated sample (in comparison to control) based on their (a) biological process, (b) molecular function, and (c) cellular component	119
Fig. 3.36	The Heat map of differentially expressed proteins in As(V) treated sample (in comparison to control). The result of samples in duplicates has been represented. Over-expressed and under-expressed proteins have been shown in green and red colors respectively. The level of expression has been represented in the form of relative abundance on the bar shown right side	120
Fig. 3.37	Differential expression of proteins belonging to cell adhesion, signal transduction, chemotaxis, motility, and receptor family represented in terms of \log_2 value of the abundance ratio (treated/control)	127
Fig. 3.38	Differential expression of the proteins related to stress response represented in terms of \log_2 value of the abundance ratio (treated/control)	130
Fig. 3.39	Overview of the whole-cell proteomic analysis of <i>P. mendocina</i> SMSKVR-3 under the As(V) stress representing some important proteins upregulated, downregulated, and specifically expressed	131
Fig. 3.40	Presence of secondary structures in <i>P. mendocina</i> SMSKVR-3 (a) ArsC, and (B) ArsH proteins analyzed by PSIPRED	135
Fig. 3.41	PDBSum-PROCHECK analysis of the protein structures: (a) Ramachandran plot of the SWISS-MODEL structure of the ArsC (b) Ramachandran plot of the SWISS-MODEL structure of the ArsH showing amino acid residues in allowed and disallowed regions	137
Fig. 3.42	Analysis of the ERRAT score for (a) Structure of ArsC protein obtained from SWISS-MODEL, (b) SWISS-MODEL structure of the homotetrameric structure of ArsH- chain A, (c) ArsH chain B, (d) ArsH chain C, and (e) ArsH chain D	138-139
Fig. 3.43	Best protein models obtained by SWISS-MODELER for (a) ArsC protein containing one chain only, and (b) homotetrameric ArsH proteins where green color represents chain A, yellow- chain B, blue- chain C, and red-chain D	140
Fig. 3.44	Docking of arsenate ion ligand with the <i>P. mendocina</i> SMSKVR-3 ArsC protein (a) complete protein structure, and (b) putative binding site in the protein involving Glu 73, Leu 76, Ala 79, Arg 78, and Lys 111	142
Fig. 3.45	Docking of arsenate ion ligand with the <i>P. mendocina</i> SMSKVR-3 ArsH protein (a) complete protein structure, and (b) putative binding site in the protein involving Ser 39, Lys 43, Ser 44, Phe 45, and Ser 46 of the chain B	143

-
- Fig. 3.46 Molecular dynamic simulation studies of ArsC and ArsH proteins using iMODS. Different simulation plots represent (a) and (b) index of deformability, (c) and (d) eigenvalues, and (e) and (f) NMA variance for the *P. mendocina* SMSKVR-3 ArsC and ArsH proteins, respectively 145

List of Tables

Table No.	Caption	Page No.
Table 1.1	Arsenic-resistant bacterial species isolated from different geographical locations and their tolerance to different arsenic species	11-12
Table 1.2	Arsenic binding proteins and their binding sites identified in different bacterial species	17-18
Table 2.1	Primers used in the PCR amplification of arsenic resistance genes	40
Table 3.1	Partial characterization of isolated bacteria based on 16S rRNA gene sequencing	61
Table 3.2	Biochemical characterization of selected isolate (SMSKVR-3)	63
Table 3.3	Cross-tolerance of selected isolate for other heavy metals and metalloid(s)	73
Table 3.4	Sensitivity of <i>P. mendocina</i> SMSKVR-3 towards different antibiotics	74
Table 3.5	Overall properties of the <i>P. mendocina</i> SMSKVR-3 genome	82
Table 3.6	Annotated subclasses, subsystems, and gene products related to transport	90-91
Table 3.7	Genes related to arsenic resistance in <i>P. mendocina</i> SMSKVR-3 genome	92
Table 3.8	Identification of selected protein spots using MALDI-TOF/TOF MS analysis followed by MASCOT database search	105
Table 3.9	Proteins exclusively expressed in <i>P. mendocina</i> SMSKVR-3 under As(V) treated condition	114-115
Table 3.10	The membrane and transport-related proteins downregulated under As(V) treated condition in <i>P. mendocina</i> SMSKVR-3	123-124
Table 3.11	The membrane and transport-related proteins upregulated under As(V) treated condition in <i>P. mendocina</i> SMSKVR-3	125
Table 3.12	Physiochemical characteristics and numbers of cysteine residues in ArsC and ArsH proteins	133

Table 3.13	Motifs present in proteins determined by the MotifFinder	134
Table 3.14	Content of different secondary structures in ArsH and ArsC proteins	134
Table 3.15	Ramachandran plot analysis and ERRAT scores of the proteins 3D structures obtained by different modeling tools	136
Table 3.16	Free energies of the binding and inhibition constants obtained by the docking of <i>P. mendocina</i> SMSKVR-3 proteins ArsC and ArsH with the As(V) ion	144

List of Abbreviations

AAS	Atomic absorption spectrophotometer
ACN	Acetonitrile
AFS	Atomic fluorescence spectrometry
ATP	Adenosine triphosphate
BCA	Bicinchoninic Acid
BLAST	Basic local alignment search tool
BP	Biological process
BSA	Bovine serum albumin
CAS	Chrome-azurol-S
CBB	Coomassie brilliant blue
CC	Cellular component
CDART	Conserved Domain Architecture Retrieval Tool
CDD	Conserved Domain Database
CDS	Coding sequences
CFU	Colony-forming unit
CTAB	Cetyltrimethylammonium bromide
2-DGE	2-Dimensional gel electrophoresis
ETAAS	Electrothermal atomic absorption spectroscopy
ETICPMS	Electrothermal vaporization inductively coupled plasma mass
DMA	Dimethylarsine
DMSO	Dimethyl sulfoxide
DNA	Deoxyribonucleic acid
dNTPs	Deoxynucleotide triphosphate
ETC	electron transport chain
FDR	false discovery rate
FMN	Flavin mononucleotide
GMO	Genetically modified organism
GO	Gene ontology
GOE	Great Oxidation Event
GRAVY	Grand average of hydropathicity
GSH	Glutathione
<i>HCCA</i>	α -Cyano-4-hydroxycinnamic acid
HGAAS	Hydride generation atomic absorption spectroscopy
HGAFS	Hydride generation atomic fluorescence spectrometry
HMMs	hidden markov models
ICPMS	Inductively coupled mass spectrometry
ICP-OES	Inductively coupled plasma - optical emission spectrometry
IDA	Iodoacetamide
IEF	Iso-electric focusing
IMViC	Indole, methyl red test, Voges-Proskauer test
kHz	kilohertz
LB	Luria Bertani
LOD	Limit of detection
LOV	Light-oxygen-voltage
MALDI-TOF	Matrix-Assisted Laser Desorption Ionization-Time of Flight

MF	Molecular function
MIC	Minimal inhibitory concentration
mM	milimolar
MMA	Monomethylarsine
MSA	Multiple Sequence Alignment
MTs	Metallothioneins
NADPH	Nicotinamide adenine dinucleotide phosphate
NCBI	National center for biotechnology information
nm	nanometer
NMR	Nuclear magnetic resonance
OD	Optical density
PANNZER2	Protein ANNotation with Z-scoRE
PATRIC	PATHosystems Resource Integration Centre
PBS	Phosphate-buffered saline
PCR	Polymerase chain reaction
Prodigal	Prokaryotic Dynamic Programming Gene-finding Algorithm
PSIPRED	PSI-blast-based secondary structure PREDiction
PSM	Peptide spectrum match
QDs	Quantum dots
RAST	Rapid Annotations using Subsystems Technology
RNA	Ribonucleic acid
rRNA	Ribosomal RNA
RT	Room temperature
ROS	Reactive oxygen species
SDS-PAGE	Sodium dodecyl sulfate-polyacrylamide gel electrophoresis
SEM	Scanning electron microscopy
SOPMA	Self-Optimized Prediction Method with Alignment
SPCEs	Screen-printed carbon electrodes
TBS	Tris-buffered saline
TCA	Tricarboxylic acid cycle
TCEP	Tris (2-carboxyethyl) phosphine
TFA	Trifluoroacetic acid
WHO	World Health Organization
ZOI	Zone of inhibition

Chapter I

Introduction

1.1 General introduction

Arsenic (As) is a metalloid that is the 20th most widely distributed element in nature exists in the combined form covering 0.00005% of the earth's crust (Jha et al., 2017). Arsenic is typically present in organic and inorganic forms in the soil in which inorganic forms are more predominant. The inorganic forms of arsenic include more than 300 minerals such as arsenates (e.g. arseniosiderite, parasymplectite, pharmacosiderite, scorodite), arsenites, arsenides, sulfides (e.g., arsenopyrite, pyrite, loellingite, realgar), sulfosalts, native elements, and metal alloys. The organic forms of arsenic are mostly found in living organisms and are less toxic. Organic forms include the compounds such as monomethylarsine (MMA), dimethylarsine (DMA), trimethylarsine (TMA), lewisite, adamsite, and arsenocholine (Shrivastava et al., 2015).

Arsenic is most commonly found in two oxidation states in nature; trivalent arsenite [(As(III))] and pentavalent arsenate [As(V)]. However, the other oxidation states of arsenic including -3 (arsenides) and 0 (elemental arsenic) are also present in nature. Though naturally present in the environment, it has become a contaminant from past few decades due to anthropogenic activities such as the use of arsenic-containing pesticide/herbicides, excessive mining, industrial and medical waste discharge, usage of wood preservatives, and burning of fossil fuels (Dey et al., 2016; Kale et al., 2015). The permissible limit of arsenic in the drinking water has been reduced to 10 $\mu\text{g L}^{-1}$ by the WHO above which, it is considered toxic for human beings (Gudlavalleti et al., 2017). Both the As(V) and As(III) are known to be toxic causing cellular damage but As(III) is more toxic than As(V) because of its higher water solubility. The As(V) shows an analogy to the phosphate and enters through the phosphate channels inside the biological system. It inhibits various metabolic activities requiring phosphorylation and ATP synthesis (Dey et al., 2016; Shrivastava et al., 2015). However, As(III) imposes toxicity by binding with the thiol groups present in the cysteine residues of the proteins or enzymes and thus inactivating them (Finnegan & Chen, 2012). The common disease symptoms instigated by arsenic toxicity include nausea, abdominal pain, and diarrhea. However, chronic arsenic exposure causes severe effects such as cutaneous lesions, leukomelanosis, melanosis, ischemic heart disease, keratosis, superficial cuticular diseases, and impaired cognitive abilities and motor functions. It also causes skin, liver, kidney, bladder, and lung cancers (Shrivastava et al., 2015). Thus, to prevent the toxic exposure of arsenic, it

is essential to have an efficient arsenic detection and removal strategy to detect and remove it from the contaminated environmental sites.

Microorganisms routinely exposed to arsenic have developed resistance to mitigate its toxic effect by several mechanisms such as methylation, oxidation, and reduction converting it to the less toxic form. Various proteins and enzymes present in the microorganisms help in this process. The application of these arsenic-resistant microorganisms provides a cost-effective and eco-friendly approach for its removal from the contaminated area (Bahar et al., 2013). Various enzymes have also been employed for the bioremediation of different organic and inorganic pollutants (Mousavi et al., 2021) which shows the higher potential of enzymes involved in arsenic resistance, in the arsenic bioremediation process. The arsenic binding ability of the enzymes or proteins involved in the arsenic-resistance mechanism has also been applied for the development of arsenic-specific biosensors providing high specificity (Male et al., 2007). These studies show the extensive requirement of studying the bacterial proteomic profile in the presence of arsenic to get a deep insight into various arsenic-induced proteins as well as proteins having affinity toward arsenic. Proteomics provides the systematic study of the change in cellular protein expression under altered environmental conditions such as stress caused by the exposure of metals (Ge et al., 2016). The proteomic response of different bacteria under arsenic stress needs to be explored as there are very few reports in this area. The study of the interaction between protein/enzyme and arsenic could provide an in-depth view of its mechanism of action and the binding sites involved in it, thus showing its potential for application in bioremediation and biosensor development.

The present study focuses on the isolation and characterization of the arsenic-resistant bacteria from the metal-contaminated site and the analysis of the arsenic resistance mechanisms using the proteomic approaches. The study also includes the screening of candidate proteins that can be exploited for the development of arsenic bioremediation strategy and biosensor, using *in silico* arsenic binding study.

1.2 Detection of arsenic in environmental samples

To avoid the toxic exposure of arsenic through contaminated water or consumption of plants growing on arsenic-contaminated soil, it is of utmost importance to detect it precisely. To detect the contamination level of arsenic in the environment, various detection methods are

used which include common laboratory methods and biosensor-based methods which have been described below.

1.2.1 Methods used in laboratory

The common laboratory techniques applied for the arsenic detection include colorimetric, electrochemical, spectrometry-based [e.g., absorption spectrophotometer (AAS), atomic fluorescence spectrometry (AFS), inductively coupled mass spectrometry (ICPMS), electrothermal vaporization inductively coupled plasma mass spectrometry (ETICPMS), electrothermal atomic absorption spectroscopy (ETAAS), hydride generation atomic fluorescence spectrometry (HGAFS), hydride generation atomic absorption spectroscopy (HGAAS), etc.], chromatography, neutron activated analysis and electrophoresis. Most of the accepted laboratory methods for arsenic detection provide a limit of detection (LOD) of $1 \mu\text{g L}^{-1}$. All of these methods provide good reproducibility and high throughput analysis but have high maintenance costs as well as the requirement of trained technicians (Yogarajah & Tsai, 2015).

1.2.2 Biosensors for arsenic detection

The biosensor is an analytical device that contains a sensitive biological recognition element associated with a physicochemical detector (Chambers et al., 2008; Turner, 2000). The biological recognition element can be an enzyme, whole-cell, antibody, or DNA, and a detector can be optical, electrochemical, or thermal. Along with these elements, an amplification unit is also associated with biosensors that provide quantitative or semi-quantitative data based on the concentration of the analyte (Kaur et al., 2015; Park et al., 2013; Singh et al., 2008). Various biosensors have been developed for the detection of arsenic employing strong and specific interaction between the analyte and biological recognition element to provide high selectivity and sensitivity. The biorecognition element generates an enhanced or reduced biochemical signal that is converted into a coherent signal by the detector. Depending on the biorecognition element biosensors can be whole cell-based or cell-free/biomolecules-based.

1.2.2.1 Whole cell-based biosensors

The bacterial whole cell-based biosensors are constructed taking advantage of the cellular metabolic processes such as the metal resistance mechanism of the bacterial cell. The whole cell-based biosensors for arsenic detection are mostly based on the bacterial repressor protein ArsR of the *ars* operon which binds specifically with As(III). In the presence of As(III), ArsR binds with it causing its release from the promoter site and subsequent reporter gene synthesis. The living microorganisms are used for biosensing in whole cell-based biosensors. The change occurring in the cellular metabolism, pH, or gene expression upon binding of arsenic with ArsR is quantified using techniques such as electrochemical and optical sensing. The common reporter proteins used in the construction of whole cell-based biosensors are green fluorescent protein (*gfp* gene), luciferase (*lux* gene), and β -galactosidase (*lacZ* gene) (Diesel et al., 2009; Gudlavalleti et al., 2017; Merulla et al., 2013). These whole cell-based arsenic biosensors allow a limit of detection (LOD) in the order of $1 \mu\text{gL}^{-1}$ (Yogarajah & Tsai, 2015). The functional mechanism of a basic whole cell-based biosensor has been shown in Fig. 1.1. There are some limitations of whole cell-based biosensors including their non-feasibility.

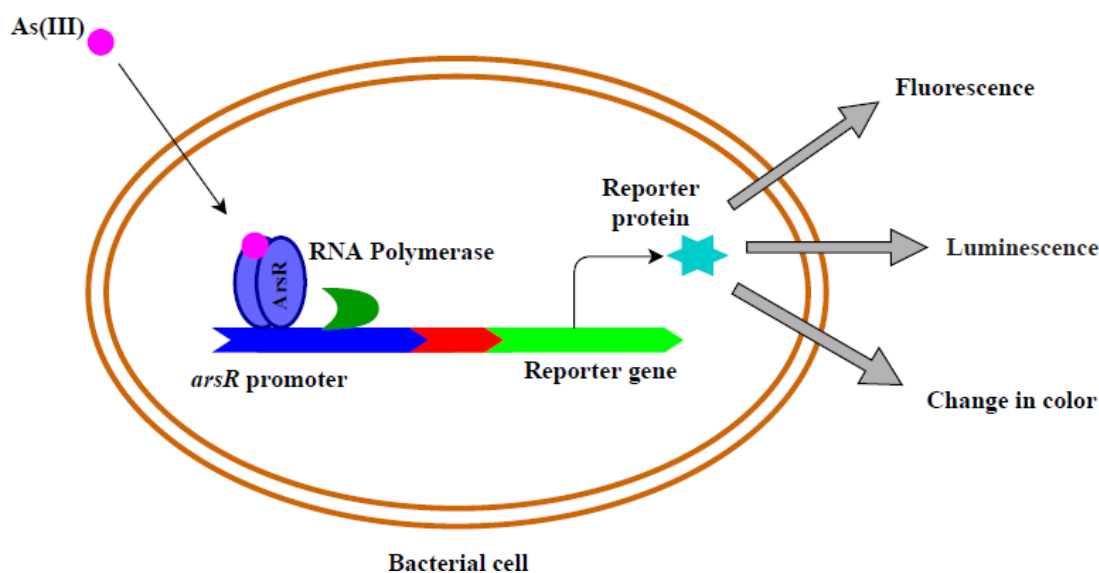


Fig. 1.1 Basic functional mechanism of a whole-cell biosensor involving different reporter proteins for detection which include color change, luminescence, or fluorescence.

1.2.2.2 Cell free/ biomolecule-based biosensors

Several cell-free biosensors have been constructed for the detection of arsenic, based on its affinity with different types of biomolecules such as DNA, RNA, and proteins (Merulla et al., 2013). These biosensors have certain advantages over whole cell-based biosensors such as long time storage using the freeze-drying technique, quick response upon the reaction with the target analyte, better sensitivity with the detection limit in the nanomolar range, better chemical tolerance, high selectivity, robustness, resistance against the disturbance caused by environmental factors and not releasing genetically modified organism (GMO) in the environment (Zhang et al., 2020). In a DNA-based biosensor, DNA is used as a biorecognition element to measure its interaction with the target analyte employing electrochemical transduction (Tencaliec et al., 2006). The interaction of DNA with the target analyte (heavy metals such as arsenic) is electrostatic which can involve negatively charged phosphate groups, binding with minor and major grooves of DNA double helix, or intercalation between the stacked base pairs (Arora et al., 2007; Kaur et al., 2015). The interaction between the DNA and the heavy metals is studied either by native state DNA (such as *Calf Thymus* or double-stranded DNA) or denatured DNA (single-stranded DNA) applying electrochemical techniques having high sensitivity, improved signal to noise ratio, fast analytical process, and low cost. Generally, voltammetry or chronopotentiometry techniques have been used for the detection of the analyte (Babkina et al., 2004; Oliveira et al., 2008; Tencaliec et al., 2006; Turdean, 2011; Wong et al., 2007).

Several biosensors have been constructed employing aptamers (that are artificial single-stranded DNA or RNA) as biorecognition units (Kaur et al., 2015). These biosensors provide selective molecular recognition of target analytes and are referred as aptamer-based biosensors or aptasensors. Aptamers have been used for the construction of the biosensor for arsenic detection because of their unique recognition ability, easy construction, fast response, and high sensitivity (Zhang et al., 2018). Aptamer-based biosensors are divided into the broad category of fluorescence-based, colorimetric, and electrochemical aptasensor based on the detection system.

The protein-based biosensor comprises enzymes, peptides, or metallothionines as biorecognition elements. The protein-based As(III) biosensor employs different arsenic binding proteins, peptides, or metallothionines based on their thiophilic nature. Four different mechanisms of interaction of As(III) with sulfhydryl group of the proteins are reported including inhibition, coordination, oxidation, and oxidative coupling (Kaur et al., 2015). The function of biosensors having enzymes as a sensory element is based on the inhibition mechanism. Various enzymes and small peptides used in the development of biosensors include acetylcholinesterase (Stoytcheva et al., 1998), acid phosphatases (Cosnier et al., 2006; Sanllorrente-Méndez et al., 2012), polyphenol oxidases (Cosnier et al., 2006), arsenite oxidase (Male et al., 2007), cytochrome C (Fuku et al., 2012) and L-cysteine (Sarkar et al., 2010). Some fluorescently labeled phytochelatin-like peptides have also been used for biosensor development which can differentiate between As(III) and As(V) species in the wastewater sample (Parker et al., 2005). Low molecular weight proteins (approximately 6500 dalton) metallothioneins (MTs) which contain 30% cysteine residues have been widely applied for the arsenic biosensor development because of their strong affinity with the target metal, low cost, and simplicity (Smith & Nordberg, 2015). Some examples of metallothionein based arsenic biosensors include MTs physically adsorbed onto paper discs placed on screen-printed carbon electrodes (SPCEs) (Irvine et al., 2017), CdSe/ZnS core-shell quantum dots (QDs) capped with cysteine-rich ligand glutathione (GSH) (De Villiers et al., 2015), engineered flavin mononucleotide (FMN) chromophore-based light-oxygen-voltage (LOV) domain sensing fluorescent proteins (iLOV protein) (Ravikumar et al., 2017) and phage display library having peptide (sequence: T-Q-S-Y-K-H-G) (Yang et al., 2018).

1.3 Bioremediation of arsenic-containing pollutants

The contamination of arsenic has become a global problem that requires the development of As-remediation techniques to remove it from the contaminated sites. Various physicochemical techniques for example ion exchange, adsorption, electroplating, filtration, reverse osmosis, chemical precipitation, and co-precipitation have been widely used for the removal of arsenic (Hassan et al., 2009). However, these methods suffer from the limitations of producing toxic by-products, inefficiency, high cost of maintenance, and difficulties in operation (Srivastava & Dwivedi, 2015; Ungureanu et al., 2015). Bioremediation is a better alternative for arsenic

removal as it doesn't have these limitations. Bioremediation employs the application of biological species or their components to remove the contaminants from the environment (Shukla & Srivastava, 2017). Bioremediation has been categorized into microbial remediation, phytoremediation, phytobial remediation, simultaneous biosorption and bioaccumulation, phytosuction separation technique, and microbial fuel cells techniques. Waste generated from agriculture, biomass, and by-products of living organisms are also being utilized in the bioremediation process nowadays (Shukla & Srivastava, 2017). The selection of microorganisms in the microbial remediation process is dependent on the bacterial capacity to transform, sequester, and/or degrade the pollutant present in the sample. The microbial uptake of the metal ion can be of two types biosorption or bioaccumulation. The microbe accumulates or entraps uptaken metal ions in the cellular structure which requires initial binding of the positively charged metal ions with the negatively charged hydroxyl, thiol, phosphate, sulfate, and amino groups present on the bacterial cell wall. This passive process is called biosorption and is not dependent on the metabolic cycle of the microorganism. However, in the biological system, the active transport of the metals across the cell can also occur. The metal uptake process involving both active and passive metal uptake mechanisms (biphasic uptake) is termed as bioaccumulation which is exploited in microbial metal remediation studies using live microbial cells (Verma & Singh, 1991).

1.3.1 Enzymes (proteins) utilized in bioremediation

The enzymes play a very important role in the bioremediation of various pollutants including organic (e.g., azo dyes, PAHs, organocyanides, polymers, etc.) and inorganic (e.g., chromium, mercury, and lead) pollutants because of their highly specific nature. For the bioremediation of the pollutants, several enzymes isolated from different microbial species have been used as they provide a practical, efficient, and cost-effective approach for bioremediation. The enzymes used for the bioremediation of organic pollutants include hydrolases (EC 3), esterases (3.1), nitrilases (EC 3.5.5.1), organophosphorus, hydrolase (EC 3.1.8.2), and cytochrome p450 monooxygenase (EC 1.14.14.1) which are derived from the microorganisms such as bacteria and fungi. The inorganic pollutants include heavy metals and metalloids such as Cr, Pb, Hg, As, etc. Metallothioneins and phytochelatin are the low molecular weight metal-binding peptides produced by the microorganisms to detoxify the metals through

sequestration. For example, phytochelatins are synthesized by the phytochelatin synthase enzyme which along with GSH chelates the heavy metals (Cobbett & Goldsbrough, 2002; Kang et al., 2007). However, these metal-binding peptides are non-specific and can chelate any heavy metal. Microorganisms have developed specific resistance pathways for several heavy metals involving enzymes as the crucial element (Singh et al., 2008). The toxic organic form of mercury is converted to a less toxic form (metallic Hg) by the mercuric reductase enzyme produced in the cells of mercury-resistant bacteria (Bafana et al., 2017). The chromium resistant bacteria produce enzymes such as chromate reductase, cytochrome c3, and Ni-Fe hydrogenase which can reduce hexavalent chromium [Cr(VI)] to a less toxic form (Bai et al., 2018; Chen & Tian, 2021). In microorganisms, the pathways involved in arsenic resistance include enzymes such as arsenate reductase and arsenite oxidase (Mousavi et al., 2021). All of these enzymes are very specific to their respective heavy metal or metalloid and can be employed for the development of the enzyme-based bioremediation process. However, further studies are needed to understand their mechanism of action and activity. New enzymes can also be isolated to improve the efficiency of the bioremediation process.

The cell-free biosensor-based arsenic detection and bioremediation techniques involving arsenic-binding proteins show their potential role in arsenic detection and removal. Thus, the study of arsenic resistance mechanisms present in the bacteria including several arsenic-binding as well as arsenic-induced proteins could provide a great opportunity to develop an efficient, cost-effective, selective, and sensitive strategy for arsenic bioremediation and biosensor development using these proteins.

1.4 Evolution of arsenic resistance in bacteria

One of the major challenges faced by the microorganisms growing in the metal-contaminated area is to endure the toxicity caused by the presence of toxic metals or metalloids. To understand the commencement of this protective mechanism among the microorganisms the study of the earlier evolution of the Earth and its lifeforms is essential. However, there are very limited pieces of information are available on the adaptive response of the microorganisms to this environmental challenge because of the scarcity of fossil records. To understand this process, the example of hydrothermal vents or hot springs present in the

oceans can be considered which contains a relatively higher concentration (>0.020 mM) of arsenic in the dissolved state and shows an analogy to the niches present on the primordial Earth. The presence of arsenic in the primordial earth led to the emergence of the arsenic resistance mechanisms involving its transport and biotransformation in the microorganisms (Kulp et al., 2008; Lebrun et al., 2003; Oremland et al., 2009). However, the chemistry of the arsenic present on the Earth's surface and the ocean got altered due to the rise of atmospheric oxygen that occurred ~ 2.4 billion years ago and termed as the Great Oxidation Event (GOE) (Oremland & Stolz, 2003; Zhu et al., 2014). The primordial Earth consisted of reduced arsenic species [As(III)] predominantly in comparison to the oxidized one [As(V)] due to the reducing or anoxic atmosphere and ocean environment which got altered after the GOE (Duval et al., 2008; Lebrun et al., 2003; Oremland et al., 2009). Due to the increased oxygen level in the environment which was $\sim 1\%$ of the today's oxygen level, the arsenic-containing minerals started releasing As(V) predominantly as continental arsenic to the oceans. This occurred due to the oxidative weathering of the minerals containing As, causing the emergence of oxidized arsenic species in the environment (Fru et al., 2015; Fru et al., 2019). This shift in the bioavailability and oxidation state of the arsenic enforced a strong selection pressure on the microorganism present on the ancient earth to acquire novel mechanisms of arsenic resistance such as arsenate reductases (ArsC) and efflux permease (ArsB). However, before the GOE the traces of As(V) in the Archean would have formed due to the selection pressure on them. This formation of As(V) led to the arsenic oxidation processes like nitrate-dependent respiration and anoxygenic photosynthesis (Chen et al., 2020).

1.5 Arsenic resistant bacteria

As mentioned in the previous section, the microorganisms such as bacteria may gradually develop resistance to toxic metal or metalloids if it is present in their surrounding environment. However, tolerance to the low concentrations of arsenic is seen in the majority of the bacterial species. The bacteria growing in the environment with arsenic contamination show higher tolerance to it. Various arsenic resistance bacteria have been reported from the arsenic-contaminated water and soils which are listed in Table 1.1. The bacteria belonging to the genera *Agrobacterium/Rhizobium*, *Ochrobactrum*, and *Achromobacter* were predominant

Table 1.1 Arsenic-resistant bacterial species isolated from different geographical locations and their tolerance to different arsenic species.

Isolated bacteria	Site of the isolation	Tolerance for As ⁺⁵ (mM)	Tolerance for As ⁺³ (mM)	Reference
<i>Pseudomonas putida</i> RS-4 and RS-5	Gold-silver mines, Republic of Korea	66.7	26	(Chang et al., 2008)
<i>Agrobacterium/Rhizobium</i>	Groundwater sample, West Bengal	≥100	≥10	(Sarkar et al., 2013)
<i>Ochrobactrum</i>	Groundwater sample, West Bengal	≥100	≥10	(Sarkar et al., 2013)
<i>Achromobacter</i> (SW4)	Groundwater sample, West Bengal	≥100	≥10	(Sarkar et al., 2013)
<i>Flavobacterium arsenatis</i> sp. nov.	High-arsenic sediment, Jiangnan Plain, China.	40	20	(Ao et al., 2014)
<i>Enterobacter</i> sp. (MNZ1)	Wastewater sample, Kala Shah Kakoo, Pakistan	-	4.01	(Abbas et al., 2014)
<i>Klebsiella pneumoniae</i> (MNZ4 and MNZ6)	Wastewater sample, Kala Shah Kakoo, Pakistan	-	4.94	(Abbas et al., 2014)
<i>Pseudomonas</i> sp. (ARS1)	Agricultural soil, Chianan Plain in southwestern Taiwan	320	30	(Das et al., 2014)
<i>Geobacillus</i> sp. ASR4	Agricultural soil, Chianan Plain in southwestern Taiwan	300	10	(Das et al., 2014)
<i>Exiguobacterium</i> sp. (As-9)	Arsenic rich soil, Chhattisgarh, India	700	10	(Pandey & Bhatt, 2015)
<i>Bacillus</i> sp. (As-14)	Arsenic rich soil, Chhattisgarh, India	700	10	(Pandey & Bhatt, 2015)
<i>Bacillus</i> sp. (SW2)	Groundwater, Burdwan, West Bengal, India	60.1	7.34	(Dey et al., 2016)
<i>Aneurinibacillus aneurinilyticus</i>	Groundwater, Burdwan, West Bengal, India	60.1	7.34	(Dey et al., 2016)
<i>Brevibacterium linens</i> strain AE038-8	Groundwater Tucumán, Argentina	1000	75	(Maizel et al., 2016)
<i>Pseudomonas</i> strain As-11	Arsenic contaminated water, Babagorgor Spring, west of Iran	270.7	43.4	(Jebelli et al., 2017)
<i>Klebsiella oxytoca</i> N53	As-containing wastewater irrigated cropland	550	200	(Qamar et al., 2017)
<i>Staphylococcus</i> sp. strain TA6	Groundwater, Jorhat, Assam	250	30	(Das & Barooah, 2018)

<i>Bacillus aryabhatai</i> MCC3374	Agricultural field, West Bengal, India	100	20	(Ghosh et al., 2018)
<i>Pseudaminobacter arsenicus</i> sp. nov.	Arsenic-rich aquifers, Jiangnan Plain in Hubei, China.	47.5	10	(Mu et al., 2019)
<i>Bacillus cereus</i> (P2Ic, P1C1Ib)	Brazilian gold mining area	-	40.1	(Aguilar et al., 2020)
<i>Lysinibacillus boronitolerans</i> (P2IIIb)	Brazilian gold mining area	-	40.1	(Aguilar et al., 2020)

among the arsenic-resistant bacteria isolated from the groundwater contaminated with arsenic in West Bengal, India. These bacterial genera were able to use arsenic as electron-donor for their chemolithotrophic growth and were able to tolerate 100 mM of As(V) and 10 mM of As(III) (Sarkar et al., 2013). The bacterial species *A. aneurinilyticus* and *Bacillus* sp. isolated from the groundwater from West Bengal exhibited tolerance to 60.1 mM of As(V) and 7.34 mM As(III). Tolerance to 4.01 and 4.94 mM of As(III) was detected for three bacterial strains *Enterobacter* sp. (MNZ1), *K. pneumoniae* MNZ4, and MNZ6 isolated from the wastewater of Kala Shah Kakoo, Pakistan (Abbas et al., 2014). Three bacterial species, *Pseudomonas* sp., *Geobacillus* sp., and *B. aryabhatai* MCC3374, isolated from the agricultural soils are reported to exhibit tolerance to 320, 300, 100 mM of As(V) and 30, 10, 20 mM of As(III) (Das et al., 2014; Ghosh et al., 2018). *K. oxytoca* N53, isolated from the cropland irrigated with arsenic-contaminated wastewater, was found to be hyper tolerant to As(V) and As(III) with the tolerance of 550 mM and 200 mM respectively (Qamar et al., 2017). Tolerance to 700 mM As(V) was obtained for *Exiguobacterium* sp. and *Bacillus* sp. isolated from the arsenic-rich soil of Chhattisgarh. A very high tolerance to As(V) (1000 mM) was represented by *B. linens* strain AE038-8 which was isolated from the groundwater of Tucumán, Argentina with 75 mM As(III) tolerance (Maizel et al., 2016). The bacterial species, *B. cereus* (P2Ic, P1C1Ib), and *L. boronitolerans* (P2IIIb), isolated from the gold mining area in Brazil exhibited tolerance to 40.1 mM of As(III) (Aguilar et al., 2020). However, *P. putida* strain RS-4 and RS-5 isolated from the gold-silver mines in the Republic of Korea showed tolerance to 66.7 mM As(V) and 26 mM As(III) (Chang et al., 2008) The other arsenic-resistant bacteria included a novel *F. arsenatis* sp. nov., *Staphylococcus* sp. strain TA6, and *Pseudomonas* strain As-11 having resistance to 40, 250, and 270.7 mM of As(V) and 20, 30, and 43.4 mM As(III) (Ao et al., 2014; Das & Barooah, 2018; Jebelli et al., 2017). All these studies show the diversity of

arsenic-resistant bacteria in different environmental sites such as groundwater and agricultural soils. However, very few studies are there on the arsenic-resistant bacteria from mining areas. Some studies have shown the presence of arsenic-resistant bacteria in the gold and silver mining area which gives us an opportunity to explore several other mining areas for their presence and to study their arsenic resistance mechanisms. The ability of the bacteria to tolerate higher concentrations of toxic arsenic species is conferred by the expression of different arsenic resistance genes present in the bacterial genome.

1.6 Bacterial arsenic resistance mechanisms

The microorganisms growing in the arsenic-rich environment have the ability to develop several resistance mechanisms to mitigate its toxic effects. In the majority of the prokaryotes, the arsenic [both As(V) and As(III)] resistance is contributed by *ars* operon which can be present either in genomic or plasmid DNA (Cervantes et al., 1994). The structure of As(III) is similar to glycerol and thus it enters the cells through the aquaglyceroporin channel GlpF (glycerol channel). However, the entry of As(V) in the bacterial cell occurs through the phosphate transporters such as Pst and Pit due to their structural similarity with phosphate ions (Rosen, 2002). The *ars* operon was first reported in *E. coli* plasmid R773 containing the three most important genes *arsR*, *arsB*, and *arsC*, while two extra genes *arsD* and *arsA* have also been reported in some operons (Rosen, 2002; Shi et al., 1996; Xu et al., 1998). ArsR and ArsD are regulatory proteins encoded by *arsR* and *arsD* gene whereas *arsA* encodes a transport ATPases. The arsenic pump ArsB is encoded by *arsB* gene and arsenate reductase is encoded by *arsC* gene (Fig. 1.2). The regulatory proteins ArsR and ArsD are repressor proteins and are homodimers containing two monomers of 117 and 120 amino acid residues, respectively. Repressor ArsR binds to the operator side of DNA and represses the expression of operon to a basal level in the absence of As(III), while it dissociates from the DNA due to conformational changes when bound to the As(III) under the As(III) rich condition leading to the transcription of genes present in *ars* operon. The ArsD protein is a weak repressor that binds at the same operator site but the binding affinity of ArsD is two times lower than the ArsR. Due to the low affinity, it binds with the *ars* operon when produced in high concentration binding with a high level of As(III) (Ben Fekih et al., 2018). This binding characteristic of ArsD allows it to regulate the concentration of ArsB inside the cell which can

otherwise be toxic for the bacteria. Besides working as a repressor, it also acts as arsenic metallochaperone by delivering As(III) to ATPase (Shen et al., 2013; Yang et al., 2010). The ArsR and ArsD together form a regulatory circuit to control the arsenic level inside the cell by controlling the expression of *arsRDABC* operon at both high and low levels of As(III).

The evolution of cytoplasmic arsenate reductase (ArsC) in bacteria has enhanced the arsenic detoxification ability of bacteria by broadening the range of arsenic resistance from As(III) to As(V). In the bacteria, the detoxification of As(V) is performed by arsenate reductase protein (ArsC) which transforms As(V) to As(III). There are two families of ArsC proteins based on different types of electron donors that are required for the reduction process:

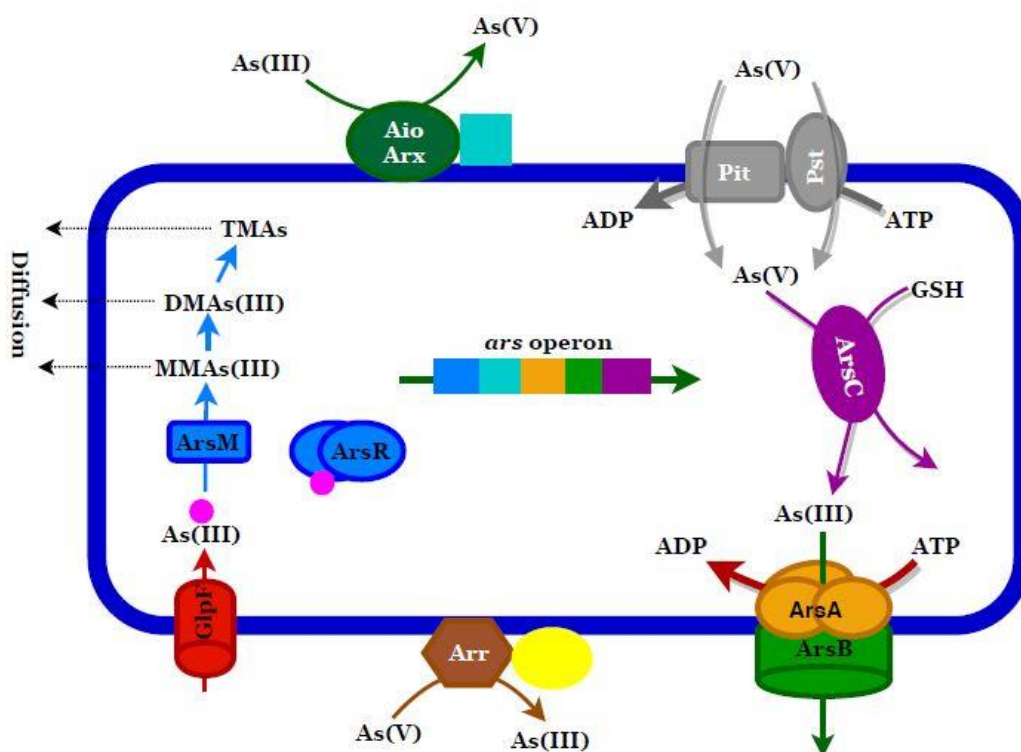


Fig. 1.2 Overall representation of arsenic resistance mechanisms found in different microbes.

ArsC coupled with glutaredoxin (eg. *E. coli* plasmid R773) and ArsC coupled with thioredoxin (eg. *S. aureus* plasmid pI258). An aquaglyceroporin channel, AqpS discovered in the *ars* operon of *Sinorhizobium meliloti* also provides As(V) resistance. It replaces the function of ArsB by coupling with ArsC throwing As(III) out of the cell (Yan et al., 2019;

Yang et al., 2005; Yang et al., 2011). Various bacterial phyla use As(V) as the terminal electron acceptor for growing anaerobically which involves reduction of As(V) by periplasmic respiratory arsenate reductase (ArrAB) encoded by the *arr* operon. The As(V) reducing gene was first identified in Strain MIT-13 later known as *Geospirillum arsenophilus* (Ahmann et al., 1994). The purified and characterized structure of Arr from *Chrysiogenes arsenatis* has shown that it is a heterodimer containing a large catalytic subunit, ArrA (87 kDa), and a small subunit, ArrB (29 kDa) (Yan et al., 2019).

Another mechanism of arsenic detoxification is its oxidative methylation by the enzyme As(III) S-adenosylmethionine methyltransferase (ArsM) which transfers methyl group S-adenosylmethionine to As(III) and reduces it with glutathione and other thiol-containing compounds in three successive steps. This pathway was proposed in the fungus *Scopulariopsis brevicaulis* and functions as the same manner in the prokaryotes (Challenger, 1945). The final product of this process is trimethyl arsine (TMA) which is volatile and is considered nontoxic (Kruger et al., 2013; Qin et al., 2006).

The ability of bacteria to detoxify arsenic by oxidizing it is known for a long time. In most of the As(III) oxidizing organisms, it is catalyzed by an arsenite oxidase designated as AioAB which is a homodimer molybdoenzyme belonging to the dimethyl sulfoxide (DMSO) reductase family. Another arsenite oxidase ArxAB belongs to the DMSO reductase family and was discovered in *Alkalilimnicola ehrlichii* strain MLHE-1, which in the presence of nitrate, catalyzes the anaerobic oxidation of As(III). It has been speculated that ArxAB would have catalyzed the light-driven As(III) oxidation during anoxygenic photosynthesis (Kruger et al., 2013; Oremland et al., 2009).

The proteins involved in the arsenic-resistance mechanisms represent a specific affinity towards the arsenic for detoxifying it. Some amino acid residues present in the proteins, such as cysteine are involved in the binding of arsenic with that protein. Different binding sites present in the proteins can be examined to check their interaction with the arsenic to develop the arsenic bioremediation strategies as well as biosensors for its detection using that protein.

1.7 Binding of arsenic with prokaryotic proteins

Arsenic is reported to bind different proteins in order to impose toxicity. As(III) imparts toxicity by binding with the sulfhydryl groups of cysteine residues present in the proteins (Bhattacharjee et al., 1995; Shi et al., 1996; Yang et al., 2010). However, the As(V) ion (HAsO_4^{2-}) which is a structural analog of the phosphate (HPO_4^{2-}), replaces the phosphate thereby inhibiting various biochemical reactions such as the production of adenosine triphosphate (ATP) in oxidative phosphorylation (Shen et al., 2013). The regulatory protein (ArsR) of the *ars* operon of *E. coli* plasmid R773 binds with As(III) at cysteine residues, Cys32, Cys34, and Cys37 (Shi et al., 1994). The binding of As(III) with ArsD protein also involves three conserved cysteine residues Cys12, Cys13, and Cys18, all of which forms As(III) binding site (Ajees & Rosen, 2015; Ye et al., 2010). ArsA is an ATPase that has two nucleotide-binding domains A1 and A2 connected with a short linker and a metalloid binding domain formed by cysteine residues Cys113, Cys172, and Cys422 having high affinity for the As(III) transferred by ArsD (Ajees & Rosen, 2015). Various arsenic binding proteins present in the bacterial cell have been listed in Table 1.2.

The enzyme arsenate reductase (ArsC) isolated and purified from *E. coli* plasmid R773 is well-characterized arsenic transforming enzyme. It has Cys12 residue in the active site which is involved in As(V) binding surrounded by an arginine triad consisting of Arg60, Arg 94, and Arg 107 residues. The mutagenesis study has shown the role of Arg60 in product formation along with a stable covalently bound Cys12-thiol-dihydroxyarsenite intermediate having no charge in the arsenic atom (DeMel et al., 2004). The characterization of ArsC protein (belonging to the Grx-linked prokaryotic arsenate reductase family) using the bioinformatic approach has revealed the presence of four residues Glu9, Asp53, Arg86, and Glu100 in the active site of the protein involved in As(V) binding. This protein was obtained from arsenic-resistant bacteria *Deinococcus indicus* DR1. The above study has reported a different mechanism of As(V) degradation due to the convergent evolution of ArsC gene, which uses a mix of positively- and negatively charged residues in the active site unlike the active site of *E. coli* where Cys 12 is a crucial residue (Chauhan et al., 2019).

Table 1.2 Arsenic binding proteins and their binding sites identified in different bacterial species.

Arsenical compound	Protein	Organism	Binding site	Kd or Ki/Km (μM)	Reference
As(V)	Ornithine carbamoyltransferase	<i>E. coli</i> W	-	5100	(Legrain & Stalon, 1976)
As(V)	Ornithine carbamoyltransferase	<i>E. coli</i> W	-	1800	(Legrain & Stalon, 1976)
4-(4-aminophenylarsonic acid)	Alkaline phosphatase	<i>E. coli</i>	-	0.13	(Szajn et al., 1977)
As(V)	Ornithine carbamoyltransferase	<i>E. coli</i>	-	5000	(Wargnies et al., 1979)
As(V)	Catabolic ornithine carbamoyltransferase	<i>P. putida</i>	-	85000	(Wargnies et al., 1979)
As(V)	Yeast triosephosphate isomerase	<i>E. coli</i>	-	9600	(Nickbarg & Knowles, 1988)
As(V)	binding-protein-dependent galactose transport in proteoliposomes	<i>S. typhimurium</i>	-	10000	(Richarme, 1988)
(CH ₃) ₂ AsSCH ₂ CONH ₂	EcoRI methyl transferase(methylase)	<i>E. coli</i>	(Cys) residue located close to a tryptophan (Trp) site	0.053	(Tsao & Maki, 1991)
As(III)	Arsenite pump Ars ATPase	<i>E. coli</i>	-	100	(Dey et al., 1994)
As(V)	Arsenate reductase	<i>S. aureus</i>	-	1	(Ji et al., 1994)
As(V)	PTPase	<i>Yersinia</i>	Cys(X)sArg active site motif	882	(Zhang et al., 1994)
As(V)	α -glucan phosphorylase	<i>T. thermophilus</i>	-	4100	(Boeck & Schinzel, 1996)
As(V)	Arsenate reductase (ArsC)	SES-3	-	200	(Newman et al., 1998)
As(V)	Arsenate reductase (Arr)	<i>C. arsenatis</i>	-	300	(Krafft & Macy, 1998)
As(V)	Protein tyrosine phosphatase	<i>Yersinia</i>	active site Cys403 sulfhydryl	1030	(Keng et al., 1999)
As(V)	Protein tyrosine phosphatase	<i>Yersinia</i>	active site Arg409	4660	(Keng et al., 1999)
As(V)	Trehalose phosphorylase	<i>S. commune</i>	-	3800	(Eis & Nidetzky, 2002)
As(III)	Arsenate reductase	<i>S. aureus</i>	Cys-X5-R motif	377	(Messens et al., 2002)
As(V)	Arsenate reductase	<i>S. aureus</i>	Cys10-X5-Arg16 segment	0.066	(Messens et al., 2002)
As(V)	Arsenate reductase	<i>S. aureus</i>	Cys10-X5-Arg16 segment	68	(Messens et al., 2002)
As(V)	Respiratory arsenate reductase	<i>B. seleitireducens</i>	-	34	(Afkar et al., 2003)
As(V)	Arsenate reductase	<i>S. aureus</i> plasmid pI258	P-loop(Cys10, Thr11, Gly12, Asn13, Ser14, Cys15, Arg16) structural motif	9-81	(Roos et al., 2006)
As(V)	Arsenate reductase	<i>B. subtilis</i>	P-loop(Cys10, Thr11, Gly12, Asn13, Ser14, Cys15, Arg16) structural motif	47-64	(Roos et al., 2006)
PAO	thioredoxin	<i>E. coli</i>	two vicinal cysteines in the -CysGlyProCys-region of the Trx	0.1	(Wang et al., 2007)
MMAIII	thioredoxin	<i>E. coli</i>	two vicinal cysteines in the -CysGlyProCys-region of the Trx	0.23	(Wang et al., 2007)
DMAIII	thioredoxin	<i>E. coli</i>	two vicinal cysteines in the -CysGlyProCys-region of the Trx	3	(Wang et al., 2007)

As(V)	arsenate reductase	<i>Pseudomonas</i> sp.	-	400	(Joshi et al., 2008)
As(V)	Respiratory arsenate reductase (Arr)	<i>Shewanella</i>	-	5	(Malasarn et al., 2008)
As(III)-BAL	Betaine aldehyde dehydrogenase	<i>P. aeruginosa</i>	thiol of Cys286	128	(González-Segura et al., 2009)
As(V)	Oxyanion-binding subunit AioX	<i>Rhizobium</i> sp. str. NT-26	sulphur atom of Cys106 of Tyr88, Cys106, Tyr131, Ser161, Ser163, His192, and Asp210 binding pocket	0.17	(Badilla et al., 2018)
As(V)	Oxyanion-binding subunit ArxX	<i>A. ehrlichii</i> str. MLHE-1	sulfur atom of Cys106 of Tyr88, Cys106, Tyr131, Ser161, Ser163, His192, and Asp210 binding pocket	0.28	(Badilla et al., 2018)
As(V)	Oxyanion-binding subunit ArrX	<i>C. arsenatis</i>	sulphur atom of Cys106 of Tyr88, Cys106, Tyr131, Ser161, Ser163, His192, and Asp210 binding pocket	1	(Badilla et al., 2018)

Biomethylation of arsenic is known to be catalyzed by S-adenosylmethionine methyltransferases (ArsM). The analysis of various ArsM orthologs having As(III) methylation activities has revealed that it requires four conserved cysteine residues (Cys A, B, C, and D) for its activity. A novel ArsM characterized from *Bacillus* sp. CX-1 [having low sequence similarities ($\leq 39\%$) to other ArsMs] has represented only three conserved cysteine residues with the missing CysB residue. However, the mutation study has shown that only conserved cysteines (CysC and D) at positions 145th and 195th are required for the methylation of As(III) and methylarsenite [MAs(III)] (Huang et al., 2018).

A new subfamily of arsenic oxyanion-binding proteins including AioX from *Rhizobium* sp. str. NT-26 and its orthologs ArxX and ArrX from *A. ehrlichii* str. MLHE-1 and *C. arsenatis* respectively have been isolated and characterized (Badilla et al., 2018). The binding of arsenic with these arsenic binding proteins has shown that ArrX binds with As(V) while AioX and ArxX bind with As(III) in the binding region that is conserved in all the three proteins. The structure of apo and As(III)-bound AioX was also determined by the crystal structure of phosphate-bound AioX which showed the formation of a link between the sulfur atom of Cys106 of AioX binding pocket (containing Tyr88, Cys106, Tyr131, Ser161, Ser163, His192, and Asp210) and As(III).

1.8 Proteomic approaches to study the arsenic-induced protein expression in the bacteria

As described earlier, the exposure of bacteria to arsenic induces arsenic resistance machinery which includes various arsenic-induced and arsenic binding proteins. To study the expression of these proteins, several methods have been used. One such method is indirect DNA microarray which provides a global analysis of the bacterial gene expression in response to arsenic exposure. However, the gene expression data provided by DNA microarray does not correlate with the abundance of protein in the cell and it also does not consider the modifications caused due to the post-translational changes in the proteins (Krizek et al., 2003). Proteomics provides a better alternative to understand the differential protein expression as it produces information on microbial activity in the form of protein abundance, indicating the microbial reaction upon the metal exposure. Different proteomic tools such as Two-dimensional electrophoresis (2-DGE), micro-fluidics, and protein microarray have been used to understand the differential expression of the proteins under arsenic stress. However, there are some drawbacks of these techniques such as 2-DGE does not provide the data of entire microbial proteome as it cannot resolve hydrophobic proteins; protein microarray has limited affinity reagents and cannot be applied on the samples of variable sources; protein microarray requires suitable immobilization techniques for quantitative protein analysis. These drawbacks can be overcome by liquid chromatography in conjunction with mass spectrometry (LC-MS/MS), which is extensively used for quantitative analysis of the protein expression (Sun et al., 2011). In the LC-MS/MS, the separation of proteins is performed by LC followed by their split into fragment ions based on their mass/charge ratio (m/z). The generated fragment ions are then detected and identified by MS. The LC-MS/MS has made it very easy to interpret the role of proteins expressed in microorganisms under metal stress.

The expression of proteins under arsenic stress in the *Pseudomonas*, *Chromobacterium*, *Staphylococcus sp*, and *Thiomonas* has been studied using the proteomics approach (Bryan et al., 2009; Ciprandi et al., 2012; Patel et al., 2007; Srivastava et al., 2012). However, all these studies have been performed using modern soft ionization techniques. Recently, the whole proteomic response of *Brevibacterium casei* #NIOB88, and *Staphylo-*

coccus sp. NIOSBK35 has been studied under arsenic stress using the LC-MS QtoF technique (Shah & Damare, 2020; Shah & Damare, 2018). However, there are very few studies on the whole proteome analysis of bacterial species under arsenic stress which can be explored to get more information about the different types of proteins expressed under arsenic stress and their potential role in arsenic detoxification.

1.9 Bioinformatics approaches for studying the interaction of proteins with arsenic

As mentioned earlier, various approaches such as arsenic-specific DNA aptamer as a biorecognition element have been utilized for the detection and removal of arsenic and its derivatives from the arsenic-containing waste (Kim et al., 2009). However, a new approach that requires more exploration is the recognition of arsenic by the arsenic-specific protein or peptides. The ability of the proteins or peptides to recognize arsenic ions can be studied using *in silico* or bioinformatics approaches such as molecular docking and molecular dynamics (MD) simulation studies which could be further validated using biophysical techniques such as nuclear magnetic resonance (NMR) and circular dichroism (CD) spectroscopy (Sahu et al., 2019). The study of the interaction of protein/peptide with arsenic ion requires a good quality 3D structure of that protein or peptide which can be generated using various molecular modeling tools based on homology modeling. This allows the understanding of the mode of the action of these proteins without the presence of detailed 3D structure information. The docking of the ligand in the active site of the receptor protein allows to locate the ligand-binding site along with the ligand's active site geometry, which can be determined by evaluating the free energy of the binding. The primary requirement for the correct protein-ligand binding is to obtain a single and lowest free energy docked configuration. It is based on the assumption that the binding of the protein with the ligand leads to a significant loss in the entropy of the configuration requiring it to balance the enthalpy (Sorin et al., 2017). The docking study requires a good quality 3D structure of both the ligand as well as the protein. Various software packages such as AutoDock, GRID, GLIDE, etc. are available to study the docking between ligand and protein.

Thus based on the proteomic and bioinformatic approach the suitable protein candidates for the development of arsenic bioremediation strategy and biosensor can be identified.

The earlier study conducted on the copper tailing waste of the khetri copper mines in our laboratory has exhibited the presence of 1.08 mM of arsenic in it (Kumar, 2017). Several copper ores such as enargite (Cu_3AsS_3) & tennantite ($\text{Cu}_{12}\text{As}_4\text{S}_{13}$) also contain arsenic in small amounts (Tongamp et al., 2009; Yin et al., 2014). This indicates the possibility of obtaining arsenic-resistant bacteria from the mining environment. Based on this observation the present study focuses on obtaining the arsenic-resistant bacteria from different locations of the khetri copper mines located in the Jhunjhunu district of Rajasthan, India. This will help us to explore the arsenic resistance mechanism and proteomic response of these bacteria under arsenic stress. The specificity of the identified proteins for arsenic can also be analyzed to investigate their potential role in bioremediation and arsenic-specific biosensor development.

1.10 Gaps in the existing research

Arsenic-resistant bacteria have been reported from diverse sampling sites such as arsenic-contaminated groundwater, soil, rhizospheric region, etc. However, there are very few reports on the arsenic resistance mechanisms of the bacteria found in the mining area. The mining areas exhibit higher possibilities of obtaining the arsenic-resistant bacteria as the ores of several metals contain arsenic in small amounts. The copper mining area is least explored in the aspect of the identification of arsenic-resistant bacteria and thus has been selected in the present study. Based on the survey of previous studies conducted on arsenic resistant bacteria following gaps were identified-

- A lot of studies have been conducted on the isolation and characterization of the arsenic-resistant bacteria from the arsenic-contaminated water and soils but there are very few reports exploring the arsenic-resistant bacteria from the mining area. Amongst different mining areas studied for the isolation of arsenic-resistant bacteria, the copper mining areas are the least explored ones. Therefore, the present study focuses on the copper mining site for exploring arsenic-resistant bacteria.

- The genomic study provides an opportunity to explore the genes responsible for the particular characteristics of the bacteria. The earlier studies provide information about the genome sequence of several arsenic-resistant bacteria isolated from the arsenic-contaminated ground-water and soil samples. However, there are still opportunities to explore the genome sequences of arsenic-resistant bacterial strains from different other sites such as mining areas to analyze the presence of genes responsible for arsenic resistance as well as other novel arsenic resistance genes. In the present study, genomic analysis has been performed to understand the arsenic resistance mechanism in the bacteria by analyzing the suitable genes.
- Investigation of the proteomic response of the bacteria under the arsenic stress and unstressed conditions could provide information about the arsenic resistance mechanisms confirming the expression of arsenic resistance genes present in the genome. It can also provide information about the altered expression of several proteins under arsenic stress and their direct or indirect role in arsenic resistance. There are primitive studies on the whole proteome response of bacteria under arsenic stress. The present study makes an attempt to understand the whole-cell proteome response of bacteria under arsenate stress.
- The proteins having arsenic binding property can be exploited for the development of bioremediation strategies to remove the arsenic from the contaminated samples as well as biosensor development. However, very few arsenic-induced proteins have been used for this purpose to date. Thus, the other arsenic-induced proteins are needed to be explored which can be applied for the arsenic bioremediation and biosensor development.

1.11 Objectives of the present research

Based on the research gaps, the present research work focuses on the isolation and characterization of arsenate-resistant bacteria from the khetri copper mines and exploring the possible arsenate resistance mechanisms using different approaches including biochemical tests and assays, genomics, and proteomic studies. The study also includes the analysis of different arsenic-induced/binding proteins in the selected bacteria using the whole-cell

proteomic approach which can be employed in arsenic bioremediation from the arsenic-contaminated samples and the development of protein-based arsenic biosensors. The objective of the present research includes:

1. Isolation and identification of arsenic-resistant microbial strains from the metal-contaminated site.
2. Identification of arsenic resistance mechanisms in selected strain.
3. Molecular characterization of the arsenic-binding protein(s).
4. *In silico* study of selected arsenic-binding protein(s) for its application in bioremediation and biosensor development.

Chapter II

Materials and Methods

2.1 Isolation of arsenic resistant bacterial strains from khetri copper mines

Isolation of arsenic-resistant bacteria from khetri copper mines involved sample collection from different sites of khetri copper mines followed by enrichment of culture, serial dilution, plating, subculturing, and characterization.

2.1.1 Collection of samples from khetri copper mines

The arsenic-resistant bacteria were isolated from the soil, water, and slag samples collected from the metal-contaminated site of the khetri copper mines which is situated in the Jhunjhunu district of Rajasthan, India, and geographically located at the point coordinates of 75°46'32.33" E, 28°0'53.66" N (Fig. 2.1). The rhizospheric region of the healthy plants growing in the metal-contamination zone was selected for the collection of the rhizospheric soil samples, the wastewater discharge area was selected for the collection of the water sample, and the slag dumping area was selected for the collection of slag samples. The samples were collected in quadruplets from each site which were further mixed. The samples were transported in sterile containers and were stored at 4°C until further use. After the collection of the samples, the pH of the samples was measured using EUTECH CyberScan pH 1100 pH meter.

2.1.2 Culture Media

A chemically defined M9 minimal medium was used for the isolation and further cultivation of isolated bacteria. M9 Minimal media was prepared from 5X M9 minimal salt that was purchased from HiMedia, India. It contains (per liter); disodium hydrogen phosphate (Na_2HPO_4) 33.90 g, potassium dihydrogen phosphate (KH_2PO_4) 15.00 g, sodium chloride (NaCl) 2.50 g, ammonium chloride (NH_4Cl) 5.00 g. The 5X M9 minimal salt was prepared separately by dissolving in water and autoclaved at 121 °C temperature and 15 psi pressure for 20 min. The 1X concentration of this 5X M9 minimal salt was used for the media preparation. Filter-sterilized glucose (11.1 mM) solution and 1 mM of autoclaved $\text{MgSO}_4 \cdot 7\text{H}_2\text{O}$ solution were added afterward and the rest of the volume was made up by autoclaved double-distilled H_2O . The pH of the media was 7.0 ± 0.2 (Atlas, 2010).



Fig. 2.1 Map of the study area.

2.1.3 Isolation of arsenic resistant bacteria using enrichment culture technique

To isolate the bacteria from the collected samples, the standard enrichment culture technique was used. For this purpose, As(V) concentrations ranging from 2-300 mM were selected based on the available literature. After the enrichment of bacteria in As(V)-containing M9 minimal media for 7-8 days at 30 ± 2 °C in an orbital shaker, the bacterial strains were isolated by serially diluting the samples up to 10^{-6} dilution followed by spread plating of 0.1 ml of diluted sample on M9 minimal media-agar plate further incubating it at 30 ± 2 °C for 24-72 h. For the long-term storage of the isolated bacterial strains, glycerol stocks were prepared that contain 800 μ l of freshly grown bacterial culture and 200 μ l of 100% (v/v) glycerol.

2.2 Identification and characterization of the isolated strains of bacteria

Identification and characterization of isolated bacterial strains included different biochemical tests and molecular characterization by 16S rRNA gene sequencing.

2.2.1 Gram's staining

Gram staining and typing were performed by following the standard method using Himedia's Gram staining- Kit. Staining was performed by flooding the bacterial smear with crystal violet solution for 30 sec and then washing with water. It was then treated with Gram's iodine (moderant) solution for 1 min, followed by washing with water. Then the decolorization was performed for a maximum of 30 sec followed by counterstaining using safranin for 30 sec. After both the steps, the slide was washed with water (Coico, 2006). The clean air-dried slide was then visualized under oil immersion (100X) using Olympus CX31 bright and phase-contrast microscope.

2.2.2 Genomic DNA isolation

Bacterial genomic DNA was isolated using QIAamp® DNA Mini Kit (QIAGEN- mini 51304). To isolate the bacterial genomic DNA, 1 ml of freshly grown bacterial culture was taken in a 1.5 ml microcentrifuge tube and centrifuged at 7500 rpm for 5 min. According to the volume of the pellet, 180 µl of ATL buffer was added along with the 20 µl of proteinase K provided. The solution was mixed by vortexing and then incubated at 56 °C until the cells lysed completely (around 1.5 h). The bacterial sample was vortexed occasionally during the incubation so that solution gets mixed homogenously and then briefly centrifuged to remove the water droplets present inside the lid. Then the 4 µl of 100 mg/ml of RNase A was added to it, mixed for 15 s by pulse vortexing followed by incubation at RT (15-25 °C) for 2 min. Brief centrifugation was performed to remove the water droplets from the lid. After that, 200 µl of buffer AL was added, mixed well by pulse vortexing for 15 s, and incubated at 70 °C for 10 min followed by brief centrifugation to remove the water inside the lid. Then 200 µl of 96-100% ethanol was added to the sample, mixed by pulse vortexing for 15 s, and briefly centrifuged to remove the water droplets present inside the lid. The obtained mixture was applied carefully to the QIAamp Mini spin column that was present inside a 2.0 ml collection tube without letting the rim get wet and centrifuged at 8000 rpm for 1 min. The QIAamp Mini spin column was then placed in a clean 2.0 ml collection tube, 500 µl of buffer AW1 was added into it without wetting the rim and centrifuged at 8000 rpm for 1 min. The column was placed in a clean 2.0 ml collection tube, 500 µl of buffer AW2 was added into it followed by

centrifugation at full speed (14000 rpm) for 3 min. The column was again placed in a clean 2.0 ml collection tube and centrifuged at full speed for 1 min to eliminate the residual buffer. To elute the genomic DNA, the column was placed in a clean 1.5 ml microcentrifuge tube to which 200 µl of AE buffer was added, the mixture was incubated at RT for 1 min and then centrifuged at 8000 rpm for 1 min (the elution was performed in two steps by sequentially adding 100 µl of AE buffer two times).

2.2.3 Fingerprinting of isolated strains using BOX-PCR

The BOX-PCR analysis is based on the amplification of dispersed-repeat motifs called BOX elements which are scattered throughout the bacterial genome. It is used to differentiate isolated bacteria at the strain level (Brusetti et al., 2008). The PCR reaction was performed in the total reaction volume of 25 µl that contained 2.5 µl of 1X PCR buffer A (containing 15 mM MgCl₂), 2.5 µl of 10 mM dNTP (2.5 mM each), 10 pmol of BOXA1R primer (5' - CTACGGCAAGGCGACGCTGACG- 3'), 50 ng of genomic DNA, 0.5 µl of Taq DNA polymerase (3U/µl). All the reagents used for PCR amplification were obtained from Genei, India except the primers which were synthesized by Sigma-Aldrich, India. The nuclease-free water used for setting up the PCR reaction was obtained from HiMedia, India. To set up the PCR reaction a thermal cycler (Bio-Rad T100, USA) was used involving initial denaturation at 94 °C for 5 min followed by 34 cycles of denaturation at 94 °C for 1 min, annealing at 42 °C for 1 min, elongation at 72 °C for 8 min and a final extension at 72 °C for 10 min (Mishra et al., 2015). The fingerprints obtained by PCR were analyzed in 2.5 % agarose gel stained with 0.5 µg ml⁻¹ of ethidium bromide and visualized under the Biorad gel documentation (Chemi-Doc) system.

2.2.4 Polymerase chain reaction (PCR) amplification of 16S rRNA gene

The isolated bacterial strains were partially characterized by the amplification and sequencing of the partial 16S rRNA gene. The extraction of the total genomic DNA of the isolate was done as described above (section 2.2.2). The 16S rRNA gene was amplified from the extracted genomic DNA by PCR in a 50 µl reaction mixture using universal 27F forward primer (5'-AGAGTTTGATCMTGGCTCAG- 3') and universal 1492R reverse primer (5'-GGTTACCTTGTTACGACTT- 3') (Hussein & Joo, 2017; Song & Leff, 2005) which were

obtained from Sigma-Aldrich. The volumes of the components of the reaction mixture and the condition of the PCR reaction were standardized. The reaction mixture contained 5 μ l of 10 X Taq buffer A (containing 15 mM MgCl₂), 10 pmol of each forward and reverse primer, 10 mM of dNTP (2.5 mM each), 1.98 U of Taq DNA polymerase, and 10 ng of template DNA. The PCR reaction was set up in a thermal cycler (Bio-Rad T100, USA) involving the following steps: initial denaturation at 94 °C for 5 min followed by 35 cycles of each step consisting of denaturation at 94 °C for 1 min, annealing at 50 °C for 30 s, elongation at 72 °C for 1 min 30 s and a final extension at 72 °C for 5 min. The analysis of the PCR amplified product was done by agarose gel electrophoresis using 0.8% agarose gel. The DNA bands were visualized by staining the gel with 0.5 μ g ml⁻¹ of ethidium bromide. The Thermo Scientific GeneRuler DNA Ladder Mix (SM0331) was used to analyze the size of obtained DNA bands.

2.2.5 Partial sequencing of 16S rRNA of the isolates and phylogenetic analysis

The partial sequencing of 16S rRNA of the isolates involved partial length (<1000 bp) sequencing of a single strand of the 16S ribosomal DNA. The sequencing was performed by 27F forward and 1492R reverse primers using the ABI 3730 XL DNA sequencer from the University of Delhi South Campus (UDSC) Department of Biochemistry, New Delhi, India. The obtained sequences were compared against the GeneBank database using the NCBI Basic Local Alignment Tool (BLAST) (<https://blast.ncbi.nlm.nih.gov/Blast.cgi>) program. The sequences were further submitted to the NCBI database.

All the isolated strains were able to grow in the M9 minimal media containing 300 mM As(V) were partially characterized. However, strain SMSKVR-3 showed the fastest growth in the arsenate-containing media and was thus selected for further studies.

2.2.6 Morphological and biochemical characterization of SMSKVR-3

The morphological characterization included the study of colony morphology and gram staining characteristics of the isolate. The study of the colony morphology was performed by streaking the fresh culture of bacteria on the M9-agar plate followed by incubating the plates at 30 \pm 2 °C for 24 h. Under the study of colony morphology, various characteristics of the colony such as margin, form, texture, appearance, elevation, optical property, and

pigmentation were observed. The biochemical characterization of the isolate was performed using Himedia's Biochemical test kit including several biochemical tests such as the utilization of lysine, ornithine, citrate, and malonate, phenylalanine deamination, nitrate reduction, H₂S production, Voges Proskauer's, methyl red, indole, esculin hydrolysis, urease, arabinose, xylose, adonitol, rhamnose, cellobiose, melibiose, saccharose, raffinose, trehalose, glucose, lactose and oxidase tests (Satyapal et al., 2018). All the biochemical tests were performed in triplicates using the freshly grown culture of selected bacteria having an optical density of 0.6 at 600 nm.

2.2.7 Molecular characterization of SMSKVR-3

Molecular characterization of isolated bacteria included amplification, sequencing, and phylogenetic analysis of 16S rRNA gene present in bacterial genomic DNA. It involved isolation of genomic DNA (section 2.2.2) from the bacterial cell followed by PCR amplification of 16S rRNA gene using universal primers, sequencing, and phylogenetic analysis. The PCR amplification of the 16S rRNA gene has been already described in section 2.2.4.

2.2.7.1 Cloning and sequencing of 16S rRNA gene

The amplified 16S rRNA gene was sequenced from the DNA sequencing facility at the Department of Biochemistry, University of Delhi South Campus (UDSC), New Delhi, India. The double-stranded full-length sequencing of the 16S rRNA gene was performed using the primer walking technique for which the amplified 16S rRNA gene product was cloned in pCR™2.1-TOPO® vector followed by transformation into the *E. coli* DH5α cells. For cloning, TOPO® TA Cloning® Kit (Invitrogen, India) was used.

2.2.7.1.1 Competent cells preparation

E. coli DH5α host cells were grown overnight at 37 °C on an LB agar plate. After that, a single colony from the streaked plate was inoculated in 10 ml of LB broth and incubated overnight at 37 °C in a shaking incubator at 120 rpm. After obtaining the full growth, 300 ml of LB broth was inoculated with 1% (v/v) of this overnight grown culture and incubated at 37 °C under shaking at 120 rpm until the OD_{600nm} value reached 0.25-0.30. The culture was

incubated on ice for 10-15 min and then centrifuged at 6000 rpm for 8 min at 4 °C. The supernatant was discarded without disturbing the pellet, which was further gently resuspended in 100 ml of ice-cold 0.1 M calcium chloride (CaCl₂), incubated on ice for 20 min, and again centrifuged at 6000 rpm for 8 min at 4 °C. The pellet obtained after centrifugation was gently re-suspended in 12 ml of ice-chilled CaCl₂, and after that, 1.8 ml of 100% (v/v) glycerol was added to the resuspended cells to make a final concentration of 15% (v/v) and mixed well by gentle stirring. After incubating the cells on ice for 10 min, they were distributed in ice-chilled microcentrifuge tubes as 300 µl aliquots and then stored at -80 °C until the use.

2.2.7.1.2 TOPO® TA Cloning and transformation reaction

The TOPO® TA cloning reaction was set up by adding the components as provided in the table below. All the ingredients were added, mixed gently, and incubated at RT (22-23 °C) for 5 min.

Contents	Volume (µl)
Fresh PCR product	4
Salt solution	1
Water	Add to a total vol. of 5 µl
TOPO vector	1
Total	6

After the cloning reaction, the obtained cloned product was transformed into the competent cells of *E. coli* DH5α. To perform the transformation, the competent cells stored at -80 °C were thawed on ice, and 10 µl of the cloned product was added to 100 µl of competent cells. The suspension was mixed well by gentle tapping and left on ice for 25 min after that the heat shock was given to the mixture by incubating it in the water bath at 42 °C for 90 seconds followed by immediately placing it on ice. Then 800 µl of LB broth was added to the sample, mixed well, and incubated at 37 °C for 45 min followed by centrifugation at 3000 rpm for 5 min. After pelleting down the cells, 750 µl of supernatant was removed, and the pellet was re-suspended in the remaining supernatant. It was then plated on LB agar plates containing 100 µg/ml ampicillin and spread with 40 µl of 40 mg/ml X-gal followed by incubating plates at 37 °C for 14-15 h. The screening of transformants was performed by blue-white colony screening.

2.2.7.1.3 Screening of recombinant clone using colony PCR

Based on the blue-white colony screening, 7 white colonies were selected to analyze the presence of the gene of interest. All the selected colonies were picked from the plate under sterile conditions and streaked on the fresh LA plates containing antibiotic and X-gal followed by incubating overnight at 37 °C. The colonies were suspended in 10 µl of nuclease-free water in a 0.5 µl Eppendorf tube and heated to 95 °C for 10 min to lyse the cells. The lysed cells were then centrifuged at 6000 rpm for 5 min and 5 µl of the supernatant was used to set up the PCR reaction to amplify the cloned 16S rRNA gene as described in section 2.2.4. The amplified PCR products were analyzed in 0.8% agarose gel.

2.2.7.1.4 Plasmid isolation and amplification of the 16S RNA gene

The final confirmation of successful cloning was done by amplifying the cloned 16S rRNA gene from the cloned-TOPO vector. For that, the plasmid DNA was isolated from the recombinant clone containing transformed cells using QIAprep® Spin Miniprep Kit (QIAGEN, India). For plasmid isolation, the recombinant clone containing bacterial colony was inoculated in 10 ml of 100 µg/ml ampicillin containing LB broth and incubated at 37 °C overnight. After incubation, the plasmid DNA was isolated by the standard method as described in the kit. After the isolation, the plasmid concentration was determined using the nanodrop at the wavelengths of 260 and 280 nm. The PCR amplification of the cloned 16S rRNA gene was performed as described in section 2.2.4.

2.2.7.2 Sequencing and phylogenetic analysis

The cloned PCR product was sequenced by primer walking technique using ABI 3730 XL DNA sequencer employing M13 F(-21) forward (5' GTAAAACGACGGCCAGT 3') and M13 R reverse (5' AACAGCTATGACCATG 3') primers. The sequences obtained from both the forward and reverse primers were matched and compared against GeneBank databases employing NCBI Basic Local Alignment Tool (BLAST) (<https://blast.ncbi.nlm.nih.gov/Blast.cgi>) following alignment by MEGA6 tool using ClustalW. To calculate the evolutionary distance between sequences Jukes and Cantor method

was used, followed by the construction of the phylogenetic tree using the “neighbor-joining” method. The obtained 16S rRNA gene sequence was deposited in the NCBI database.

2.3 Study of physiological parameters required for the bacterial growth

Physiological parameter study involved examining the optimum temperature, pH, and salt concentration required for the optimum growth of selected bacteria.

2.3.1 The optimum temperature

The effect of different temperatures on the growth of selected bacterial isolate was determined by inoculating 1% (v/v) freshly grown culture ($OD_{600nm} = 0.6$) of bacterial isolate in 10 ml of M9 media in 25 ml flasks having pH 7.0 ± 0.2 and incubating them at 25, 28, 30, 33, 37 and 40 ± 2 °C temperatures under continuous shaking at 120 rpm for 24 h. For each temperature, flasks were inoculated in triplicates. The optical density (OD) was measured at 600 nm along with the estimation of total intracellular protein concentration as described further in section 2.8.1.2 reflecting the bacterial growth.

2.3.2 The optimum pH

The optimum pH necessary for the growth of the selected isolate was determined by inoculating the 1% (v/v) of freshly grown bacterial culture having $OD_{600nm} = 0.6$ in 10 ml of M9 minimal media containing 11.1 mM glucose and 1 mM $MgSO_4 \cdot 7H_2O$ in the 25 ml flask. The pH of the media was adjusted to 3, 5, 7, 9, and 11 in triplicates along with the control having the respective pH without bacterial culture. The pH of the media was adjusted using 1N HCl and 1N NaOH. All the flasks were incubated at 30 ± 2 °C in an orbital shaker at 120 rpm for 24 h followed by the measurement of OD at 600 nm and determination of protein concentration.

2.3.3 The salt concentration

To study the effect of different salt concentrations on the growth of bacterial isolate, 0.50, 0.75, 1.25, 2.25, 3.25, 4.25, and 5.25% (w/v) of NaCl was incorporated in M9 minimal media having pH 7.0 ± 0.2 . The salt-containing media was then inoculated with the 1% (v/v) freshly

grown culture of bacteria having $OD_{600nm} = 0.6$ and incubated at 30 ± 2 °C and 120 rpm in an orbital shaker for 24 h. For each NaCl concentration, the OD was measured at 600 nm and total intracellular protein concentration was calculated.

2.4 Analysis of the growth curve

To analyze the growth curve of selected bacteria 1% (v/v) inoculum of the bacteria having 7.65×10^{13} CFU ml⁻¹ cells was inoculated in 100 ml of M9 media supplemented with 300 mM of As(V). The As(V) or As(III) free minimal media served as control. All experiments were conducted in triplicates. For comparison sake, the bacterial growth was also studied in the presence of 1.34 mM of As(III), a concentration that is reported to be toxic to other wild-type gram-negative prokaryotes (Tariq et al., 2018; Edmundson & Horsfall, 2015). All the flasks were incubated in continuous shaking at 30 ± 2 °C and 120 rpm in an orbital shaker. To measure the growth of the bacteria, the optical density of the media was measured every 2 h at 600 nm using Thermo Scientific™ Multiskan™ GO microplate spectrophotometer (Ndeddy Aka & Babalola, 2017). The doubling time of bacteria was calculated in each condition by plotting a graph of log (OD) vs time (h) using the following equation-

$$\text{Doubling time (T}_d\text{)} = \ln(2)/\text{growth rate (r)}$$

Where,

$$N(t) = N(0)e^{rt} \text{ or } r = \ln [N(t)/N(0)]/t$$

$$N(t) = \text{No. of cells at time } t$$

$$N(0) = \text{No. of cells at time } 0$$

$$r = \text{growth rate}$$

$$t = \text{time (in hours)}$$

2.5 Study of the cellular morphology by scanning electron microscopy (SEM)

The SEM analysis of the selected isolate was performed in the absence and presence of the arsenate and arsenite. To perform this a freshly grown (till mid-log phase) liquid culture of bacteria was taken that was grown in the absence (control) and presence of 300 mM arsenate and 1.34 mM arsenite in M9 minimal media. A thin layer of bacterial smear was prepared on the glass slides and heat-fixed by passing into the flame 4-5 times for 1-2 s. The bacterial smear was further fixed by 2.5% (v/v) aqueous glutaraldehyde solution for 1 h that was followed by dehydration of smear by passing through the 35-100% (v/v) of ethanol solution gradually and drying at room temperature overnight. For each condition, the slides were prepared in triplicates. Then the gold-coating of the bacterial smear on the slides was performed followed by observation of slides under 20 kV scanning electron microscope (FEI™ Thermo Fisher Scientific, Apreo SEM) to study the bacterial cell morphology under the arsenic unstressed and stressed condition (Dey et al., 2016).

2.6 Investigation of the possible arsenate resistance mechanisms in *P. mendocina* SMSKVR-3

To investigate the arsenate resistance mechanism in *P. mendocina* SMSKVR-3 several tests including siderophore production, cross heavy metal/metalloid tolerance, antibiotic susceptibility, arsenic biotransformation, the role of polyphosphate bodies in cellular arsenic removal were performed. All of which are either directly or indirectly assisting in bacterial arsenic resistance.

2.6.1 Siderophore production test

The siderophore production by selected isolate was detected by the universal chemical assay which involves the use of chrome azurol S (CAS) in King's medium B consisting of (per 1000 ml media) 20 g protease peptone, 1.5 g K₂HPO₄, 1.5 g MgSO₄, 10 ml glycerol, and pH of 6.8±0.2. The CAS assay solution was prepared by following the standard method described by Schwyn & Neilands, 1987. To test the siderophore production, the CAS-agar plates were inoculated with 1 µl of freshly grown bacterial culture in triplicates along with one negative and positive control and incubated at 30±2 °C for 48-96 h. *P. aeruginosa* was used as a

positive control which is known to produce siderophores (Arora & Verma, 2017), and *E. coli* DH5 α was used as a negative control (Tabatabai et al., 2008). The formation of a yellow-orange halo zone around the bacterial growth area was considered a positive result for the siderophore production assay.

2.6.2 Cross heavy metal/metalloid-tolerance study

The study of cross heavy metal/metalloid-tolerance in the selected isolated strain included different concentrations of heavy metal and metalloid ions such as As(V), As(III), Mn(II), Mo(VI), Fe(III) Cd(II), Cu(II), Zn(II), Ni(II), Co(II), Cr(VI) and Hg(I). To perform the cross-tolerance test 1% (v/v) inoculum of the freshly grown culture of bacteria having 2.7×10^{12} CFU ml⁻¹ (log phase culture) was inoculated in 2 ml of M9 minimal media supplemented with above mentioned heavy metal/metalloid ions in a concentration range of 0.02-26.88 mM. After the inoculation, the media containing bacteria and metal ions was incubated at 30 \pm 2 °C for 48 h. To determine the minimal inhibitory concentration (MIC) the OD was taken at 600 nm followed by the viability test by plating the bacterial culture on M9-agar plates. For all the concentrations of heavy metal/metalloid, the experiment was performed in triplicates along with the control without bacterial inoculation (Rahman et al., 2014). As the source of metal ions, salts of respective heavy metal/metalloid ions were used including NaAsO₂, MnCl₂.4H₂O, Na₂MoO₄, FeCl₃, CdCl₂.H₂O, CuSO₄.5H₂O, ZnSO₄.7H₂O, NiCl₂.6H₂O, CoCl₂.6H₂O, K₂Cr₂O₇, and HgCl₂. A stock solution of 10000 mg/L in Milli-Q water was prepared for As(V), As(III) however for other heavy metals 1000 mg/L stock solution was prepared.

2.6.3 Antibiotic susceptibility determination

To determine the antibiotic sensitivity of isolated bacteria, a pure colony of culture was inoculated in M9 minimal media broth at 30 \pm 2 °C for 15-16 h (until the log phase is achieved). The freshly grown bacterial suspension was then spread evenly over the surface of the M9 minimal media agar plate. The inoculated plates were allowed to dry for 15 min, followed by placing the antibiotic-containing diffusion discs over the plates ensuring proper contact between disc and agar surface. Susceptibility test of 6 types of antibiotics was performed by disc diffusion method as described by Bauer et al. (1966) using commercially available

antibiotic discs including ampicillin (10 µg), chloramphenicol (30 µg), kanamycin (30 µg), tetracycline (30 µg), vancomycin (30 µg), and streptomycin (10 µg) (purchased from HiMedia, India). Plates containing antibiotic discs were incubated at 30 °C for 24 h, and after that, the zone of inhibition (ZOI) was measured including the diameter of the discs. To express the result sensitive (S), intermediate (I), and resistant (R) terms were used (Bauer et al., 1966).

2.6.4 Determination of arsenic biotransformation using a qualitative assay

The study of arsenic biotransformation involved the qualitative detection of arsenate reduction and/or arsenite oxidation using the microtiter plate assay. Microplate assay was performed by growing the bacteria in 20 ml of M9 minimal medium without arsenic at 30±2 °C on an incubator shaker (120 rpm) until the optical density at 600 nm reached 0.4-0.6. After that, the cell suspension was centrifuged at 5000 rpm for 15 min, washed, and finally suspended in 1 ml sterilized deionized water. The bacterial cell suspension (20 µl) was inoculated in a 96-well plate containing 80 µl of 0.2 M Tris-HCl buffer (pH 7.5) along with either (a) 1.33 mM As(V) or (b) 1.33 mM As(V) and incubated for 24, 48 and 72 h. The bacteria-free suspension having either As(V) or As(III) was used as the control. To confirm the biotransformation of arsenic, 100 µl of 0.1 or 0.2 M of silver nitrate (AgNO₃) solution was added to the wells. For each condition, the experiment was performed in triplicates (Simeonova et al., 2004).

2.6.5 Determination of polyphosphate (polyP) bodies concentration

Determination of polyP bodies inside the cells of selected bacteria was performed at 0, 0.5, 4, 8, 24, and 48 h of intervals in M9 minimal media under the arsenate stress (300 mM) to explore the role of these polyPs in intracellular arsenic removal. The isolation of polyP bodies from the bacterial cells was performed from 10 ml of bacterial culture which was grown until the OD_{600nm} reached 0.6. The bacterial culture was then treated with 300 mM of As(V) followed by incubation at 30±2 °C in an incubator shaker (120 rpm) for the above-mentioned time intervals. For each time interval, the experiment was conducted in triplicates. To obtain the cell pellet, the bacterial culture was centrifuged at 10000 g for 10 min at 4 °C which was followed by the extraction of polyP bodies from the cells using the alkaline hypochlorite method which takes advantage of the insolubility of polyP bodies in alkaline hypochlorite (Rao et al., 1985; Singh et al., 1992). The obtained cell pellet was then suspended in 500 µl

of a solution containing 1 mM NaF and 0.145 M NaCl and re-centrifuged. The supernatant was discarded and the pellet was re-suspended in 0.1 ml of alkaline hypochlorite (NaOCl) solution (pH 9.8) followed by incubation at 30 ± 2 °C for 60 min. After the incubation, the insoluble fraction was collected from the solution by centrifugation at 21000 g for 15 min and then re-suspended in 133 μ l of wash solution containing 0.1 M NaCl, 5 mM EDTA, and 1 mM NaF (pH 4.6). After that, the solution was centrifuged at 21000 g for 15 min and the obtained residue was solubilized in 0.1 ml of 0.154 M NaCl solution (pH 7.0) followed by again centrifugation at 10000 g for 10 min to obtain the supernatant fluid containing the polyP bodies. The collected supernatant was mixed with an equal volume of 1 M HCl and given heat treatment at 100 °C for 15 min that led to the hydrolysis of polyP bodies and formation of inorganic phosphate which was then quantified by the method of Murphy and Riley (1962).

To quantify the inorganic phosphate in the sample 100 μ l of the sample was diluted with Milli-Q water to make up the final volume of 8 ml and then 1.6 ml of freshly prepared mixed reagent was added into it along with the blank solution containing 8 ml of Milli-Q water. The mixed reagent contained 5 N sulfuric acid (125 ml), ammonium molybdate (37.5 ml), ascorbic acid solution (75 ml), and potassium antimonyl tartrate (12.5 ml). After adding the mixed reagent, the solution was mixed by shaking and left for 5-10 min at RT until the development of blue color. After that, the OD of the solution was measured at 882 nm using the Thermo Scientific™ Multiskan™ GO microplate spectrophotometer. The concentration of inorganic phosphate in the solution was calculated from the standard graph prepared from potassium dihydrogen phosphate (Murphy & Riley, 1962).

2.6.6 Quantification of intracellular and surface-bound arsenic concentration

The quantification of intracellular and surface-bound arsenic was performed to understand the role of polyP bodies in arsenic resistance. To quantify the arsenic concentration in the time interval of 0, 0.5, 4, 8, 24, and 48 h, 400 ml of M9 minimal media was inoculated with 1% (v/v) of completely grown primary culture of bacteria and allowed to grow until the OD at 600 nm reaches to 0.6-0.7. Then the 10 ml of this bacterial culture was distributed in 25 ml flasks and treated with 300 mM of As(V) followed by incubation at 30 ± 2 °C in an incubator shaker for the above-mentioned time intervals. For each time interval, the experiment was

conducted in triplicates. The cell pellets at the different time intervals were obtained by centrifuging bacterial culture at 10000 g for 10 min at 4 °C and the obtained cell pellet was stored at 4 °C until further use. The surface-bound arsenic was analyzed by washing the cell pellet with 1 mM EDTA (pH 7.8) followed by centrifugation at 10000 g for 5 min and collection of the supernatant which contained surface-bound arsenic. The bacterial cell pellet was dried for 24 h at room temperature and then digested with 1 ml of 30% HNO₃ (v/v) involving incubation for 48 h at room temperature. After acid digestion, the bacterial culture containing solution was sonicated 5 times involving the 10 s pulse of 10 kHz and then centrifuged at 13000 g for 20 min. The obtained supernatant was diluted in a ratio of 1:5 to measure the intracellular arsenic concentration (Tu et al., 2013). The fractions containing surface-bound arsenic were also diluted according to the detection range of the instrument and arsenic concentration was measured using Inductively Coupled Plasma-Optical Emission Spectrometer (ICP-OES) - Optima 7000 DV (with Autosampler, S10 Series), Perkin Elmer. To correlate the arsenic concentration with the bacterial cell number at each time point, cell counting at each time point was performed.

2.6.7 PCR amplification of genes involved in arsenate resistance in *P. mendocina* SMSKVR-3

Based on the results of the above-mentioned studies, different genes playing a role in arsenate resistance were selected and amplified using PCR to check their presence in the *P. mendocina* SMSKVR-3 genome. The selected genes included arsenate reductase (glutaredoxin) (ArsC), polyphosphate kinase 1 (PPK1), efflux RND transporter component and, arsenical resistance protein ArsH. The primers used for PCR amplification of the respective genes were designed manually based on the gene sequence of *P. mendocina* available in the NCBI-GeneBank database. The primers were synthesized from Integrated DNA Technologies (IDT), India. The PCR conditions were optimized for each gene. The list of primer sequences used in PCR amplification of different genes has been listed in Table 2.1.

Table 2.1 Primers used in the PCR amplification of arsenic resistance genes.

Target gene	Primer Name	Primer Sequence (5'-3')	Amplicon size (bp)
Arsenate reductase (<i>arsC</i>)	ArsCF	ATGACCGACCTGACCCTCTACCA	354
	ArsCR	TCATGCCAGCAGCTCCAGGAC	
Polyphosphate kinase (<i>ppk1</i>)	PPK1F	ATGAACAGCGAAGGACTCAACAGC	2168
	PPK1R	ACCGGGGCCGTGAGCTTTTCCA	
Efflux RND transporter component	RNDF	TGAAACGCAGCATGATTCT	1652
	RNDR	ATGGGAATTGCTGTGGCT	
Arsenic resistance protein (<i>arsH</i>)	ArsHF	ATCCTGCTGCTGTACGGCTCCACC	607
	ArsHR	GCTGATTGACGCGCTTGGACAGTTC	

2.6.7.1 Amplification of *arsC* gene

To amplify *ArsC* gene having amplicon length of 354 nt, a 25 µl PCR reaction was set up including 2.5 µl of 10X PCR reaction buffer B, 1.5 µl of 25 mM MgCl₂, 0.5 µl of 10 mM dNTP (2.5 mM each), 5 pmol of each forward (*ArsCF*) and reverse (*ArsCR*) primers, 60 ng DNA template and 0.2 µl of taq DNA polymerase (3U/µl). The PCR reaction involved initial denaturation at 94 °C for 3 min which was followed by 35 cycles of steps consisting of denaturation at 94 °C for 30 s, annealing at 59 °C for 30 s, elongation at 72 °C for 30 s, and a final extension at 72 °C for 5 min.

2.6.7.2 Amplification of *ppk1* gene

The *PPK1* gene having expected amplicon length of 2168 nt was amplified using PCR by setting up a 25 µl reaction containing 2.5 µl of 10X PCR reaction buffer A, 0.5 µl of 10 mM dNTP (2.5 mM each), 5 pmol of each forward (*PPK1F*) and reverse (*PPK1R*) primers, 60 ng DNA template and 0.2 µl of taq DNA polymerase (3U/µl). The PCR reaction involved initial denaturation at 94 °C for 3 min which was followed by 35 cycles of steps consisting of denaturation at 94 °C for 30 s, annealing at 60.2 °C for 45 s, elongation at 72 °C for 1 min, and a final extension at 72 °C for 5 min.

2.6.7.3 Amplification of efflux RND transporter component gene

The amplification of efflux RND transporter component gene (1652 nt amplicon length) was performed by setting up a 25 µl reaction having 2.5 µl of 10X PCR reaction buffer B, 1.5 µl of 25 mM MgCl₂, 0.5 µl of 10 mM dNTP (2.5 mM each), 5 pmol of each forward (RNDF) and reverse (RNDR) primers, 60 ng DNA template and 0.2 µl of taq DNA polymerase (3U/µl). The PCR reaction involved initial denaturation at 94 °C for 3 min which was followed by 35 cycles of steps consisting of denaturation at 94 °C for 30 s, annealing at 55 °C for 45 s, elongation at 72 °C for 1 min and a final extension at 72 °C for 5 min.

2.6.7.4 Amplification of *arsH* gene

To amplify *ArsH* gene (amplicon length=607 nt) a 50 µl PCR reaction was set up containing 5 µl of 10X PCR reaction buffer A, 1 µl of 10 mM dNTP (2.5 mM each), 10 pmol of each forward (*ArsHF*), and reverse (*ArsHR*) primers, 120 ng DNA template and 0.4 µl of Taq DNA polymerase (3U/µl). The PCR reaction involved initial denaturation at 95°C for 2 min which was followed by 35 cycles of steps consisting of denaturation at 95 °C for 15 s, annealing at 62 °C for 15 s, elongation at 68 °C for 45 s and a final extension at 68 °C for 5 min.

The agarose gel electrophoresis was performed on 1.2% agarose gel for the analysis of PCR amplified products which were then visualized after staining with the ethidium bromide.

2.7 Whole-genome sequencing analysis of *P. mendocina* SMSKVR-3 to explore the presence of arsenate resistance genes

The whole-genome sequencing analysis was performed to analyze the genome structure of *P. mendocina* SMSKVR-3 along with the validation of the presence of genes related to arsenate resistance. The whole-genome sequencing analysis included isolation of genomic DNA from the bacteria followed by genome sequencing, assembly, gene prediction, and annotation.

2.7.1 Extraction of genomic DNA, genome sequencing, and assembly

The extraction of genomic DNA from *P. mendocina* SMSKVR-3 was performed as described in section 2.2.2. After the extraction, its presence was confirmed in 0.8% agarose gel followed by quantification using nanodrop (Simplinano). The Illumina HiSeqX10 paired-end sequencing platform was used for the *de novo* whole-genome assembly. The raw reads obtained from Illumina paired-end sequencing were quality checked using FastQC that included analysis of base quality score distributions, the average base content per read, and GC distribution in the reads. Before performing the genome assembly, the pre-processing of fastq files was performed using AdapterRemoval-V2 (version 2.3.1) software (<https://github.com/mikkelschubert/adapterremoval>) (Schubert et al., 2016). The adapter sequences were trimmed and the reads were filtered out which has a quality score <30 in any of the paired-end reads. Unicycler (version 0.4.8) assembler (<https://github.com/rwick/Unicycler>) was used for the *de novo* assembly of the data generated from the Illumina paired-end sequencing (Wick et al., 2017). Unicycler is an open-source GPLv3 that is used to assemble the genome of the bacteria from the data of the combination of short and long reads. The initial assembly graph was generated from the shorts reads using the SPAdes assembler which is a *de novo* assembler then from the information of short and long reads the graph was simplified. The statistical analysis of the assembled data was performed using QUAST (version 4.6) (Gurevich et al., 2013). The BUSCO (version 4.1.4) (Simão et al., 2015) was used for the generation of conserved gene levels.

2.7.2 Gene prediction and genome annotation

The prediction of coding sequences (CDS) from the Unicycler assembled contigs of *P. mendocina* SMSKVR-3 genome was performed using the Prokaryotic Dynamic Programming Gene-finding Algorithm (Prodigal) (version 2.6.3) gene prediction software (<https://github.com/hyattpd/Prodigal>) (Hyatt et al., 2010). The annotation process of predicted genes included matching the gene sequences with the UniProt database using BLASTX (version 2.6.0 program), organism annotation, and gene ontology (GO) annotation. The comparison of predicted genes with the UniProt database was done using the BLASTX program considering the E-value cutoff to be 10^{-3} . It was followed by filtering out the best BLASTX hit based on the query coverage, similarity score, identity, and description of each

gene. For the organism annotation, the organism's name was extracted from the top BLASTX hits. After the organism annotation, the gene ontology (GO) terms of the genes were mapped under three broad categories including biological process (BP), molecular function (MF), and cellular component (CC). The other annotation tools PATRIC (version 3.6.9) (PATHosystems Resource Integration Centre) (Davis et al., 2020) that uses RAST (Rapid Annotations using Subsystems Technology) (Brettin et al., 2015) server was also used for the annotation, circular map generation, and phylogenetic analysis.

2.7.3 Alignment of the genome and phylogenetic analysis

The phylogenetic analysis of the *P. mendocina* SMSKVR-3 genome with the other reference and representative genome was performed using the PATRIC (version 3.6.9). PATRIC includes reference and representative genomes in the phylogenetic analysis which are selected and categorized manually by the NCBI staff. The identification of the closest reference and representative genome was performed by Mash/MinHash (Ondov et al., 2016). The phylogenetic placement of the genome was done by the selection of PATRIC global protein families (PGFams) (Davis et al., 2016) which was followed by the alignment of protein sequence from these families using MUSCLE (Edgar, 2004) and nucleotide mapping of each sequence to the protein alignment. The amino acid and nucleotide alignments were joined into a data matrix that was analyzed using RaxML (Stamatakis, 2014) with fast bootstrapping (Stamatakis et al., 2008) that has been represented as the support value in the tree.

2.8 Analysis of the proteins involved in arsenate resistance by proteomic approaches

The study of the proteome of *P. mendocina* SMSKVR-3 under arsenate stressed and unstressed conditions were performed to understand the mechanism of As(V) resistance in the bacteria. This study included one-dimensional SDS-PAGE analysis, 2-DGE followed by MALDI-TOF/TOF MS analysis, and the study of the entire cellular proteome by LC-MS/MS analysis.

2.8.1 Analysis of protein expression in *P. mendocina* SMSKVR-3 by SDS-PAGE

The SDS-PAGE analysis was performed to optimize the arsenate exposure time for the differential expression of proteins and also to optimize the concentration of arsenate required to induce the differential proteomic response.

2.8.1.1 Study of differential protein expression under arsenate stress

The protein expression profile of bacterial isolate *P. mendocina* SMSKVR-3 was studied under arsenate stress. The well-grown culture of bacteria was inoculated in M9 minimal media containing M9 minimal salt (5X) diluted to 1X (HiMedia, India), 1 mM MgSO₄·7H₂O (Sigma-Aldrich), and 11.1 mM glucose (CDH fine chemicals, India). The first two media components were sterilized separately by autoclaving at 120 °C and 15 psi for 20 min, whereas glucose solution was sterilized by filtration. The media containing inoculum was kept at 30±2 °C and 120 rpm until OD_{600nm} reached 0.4-0.5. After that, 10 ml of bacterial culture was distributed in 25 ml flasks in triplicates and treated with 300 mM of arsenate [sodium arsenate dibasic heptahydrate (NaHAsO₄·7H₂O) (Sigma-Aldrich) salt was used] and kept at 30±2 °C in shaking (120 rpm) for 0, 4, 8, 16, and 24 h along with the control without arsenate treatment. After each time interval, samples were collected and centrifuged at 8000 rpm, 4 °C for 10 min. The pellet was washed using 1X phosphate buffer saline (PBS), pH 7.2±0.2 followed by centrifugation at 13000 rpm, 4 °C for 1 min. After that 40 µl of protease inhibitor (cOmplete Mini, Roche Diagnostics, Germany) was added to the pellet and incubated at 37 °C for 1 h under continuous shaking at 150 rpm. The samples were spun for a short duration and then sonicated using Microson XL-2000 Ultrasonic cell disruptor, Misonix, New York at 10 kHz, 10-second pulse for 10 times under ice-chilled condition. The cell debris were removed by centrifuging the samples at 8000 rpm, 4 °C for 20 min and the supernatant containing whole-cell protein was stored at -20 °C until further use.

2.8.1.2 Estimation of total cell proteins

The quantification of total protein content in crude cell extract was performed using QuantiPro™ BCA Assay Kit from Sigma-Aldrich employing bovine serum albumin (BSA) to plot the standard curve for the protein estimation. A stock solution of BSA having 1 mg/ml concentration was diluted to different concentrations (0.5, 5.0, 10, 20, and 30 µg/ml) using

MilliQ water in triplicates. The reagents provided in the kit were used to make the final BCA reagent (as mentioned in the kit manual) and then this reagent was added to the protein solution in a 1:1 ratio along with a blank that contained MilliQ water. The solution was mixed and incubated at 60 °C in a water bath for 1h and then absorbance was taken at 562 nm. The values of protein concentrations versus absorbance were used to plot the standard curve. The following equation obtained from the graph ($R^2= 0.99$) was used to determine the concentration of protein in the samples-

$$Y= 0.0209X-0.0004$$

where, Y=absorbance at 562 nm, and X=concentration of protein ($\mu\text{g/ml}$)

2.8.1.3 Analysis of protein expression by SDS-PAGE

To study the expression of proteins at different time intervals under arsenate stressed and unstressed (control) conditions, the SDS-PAGE analysis was performed. For which the 15 μg of total protein from each sample was loaded to 12% SDS-PAGE gel followed by gel running at 40 mV until the staining of the proteins and then at 80 mV, in a Biorad Protean cell. To detect the protein bands, the gels were stained overnight with coomassie brilliant blue (CBB) G-250 followed by destaining and analysis of gels using Biorad gel documentation (Chemidoc) system. To determine the approximate molecular weight of the protein bands ThermoFisher Scientific PageRuler™ unstained protein ladder was used which has a molecular weight range from 10-200 kDa.

2.8.1.4 Effect of arsenate concentration on protein induction

The effect of As(V) concentration on protein induction or the concentration of As(V) required to induce the significant change in the protein expression in *P. mendocina* SMSKVR-3 was determined. For which the fresh bacterial culture (10 ml) having $\text{OD}_{600\text{nm}}$ 0.4-0.5 was treated with As(V) concentrations 0.067, 0.67, 2, 10, 50, 200, and 300 mM respectively in triplicates in separate flasks along with the control which was kept untreated. The incubation of all the flasks was done at 30 ± 2 °C and 120 rpm for 8 h followed by extraction and quantification of total protein from each sample as mentioned before. To analyze the protein expression 12% SDS-PAGE gel was used and 15 μg of protein sample was loaded.

2.8.2 Protein expression analysis by two-dimensional gel electrophoresis (2-DGE) followed by MALDI-TOF/TOF MS analysis of the selected protein spots

The differential protein expression study of the sample treated with As(V) for 8 h was performed by 2-DGE to understand the change in protein expression under As(V) stress in comparison to control which was untreated. It was followed by the selection of protein spots and MALDI-TOF/TOF MS analysis of those selected spots.

2.8.2.1 2-DGE

To perform the iso-electric focusing (IEF) of the control (without arsenate treatment) and arsenate treated protein samples, 300 µg of each protein sample were loaded onto the pre-casted (immobilized pH gradient) IPG strips which have 18 cm length and pH gradient of 4-7. The sample was run using Ettan™ IPGphor3 system from GE Healthcare. The IPG strips were then equilibrated in equilibration buffer followed by further separation of protein in the second dimension on 10% SDS-PAGE gel employing Ettan™ DALTsix Gel Electrophoresis Unit from GE Healthcare.

2.8.2.2 Image processing and analysis of 2-DGE gels

The 2-DGE gels were scanned utilizing Epson Expression 11000XL Scanner and the scanned gel images were analyzed using Image Master 2D Platinum 7.0 Software. The gels were processed as a project into a match set to detect the spots selecting the smooth min. area and saliency parameters to be 2, 5, and 5 respectively. It was followed by manual editing and defining landmarks for the spots that were common in gels. After matching the gels, spot IDs were assigned to all the spots with the help of the software. The differential expression of the protein was analyzed by comparing the matched spots of the treated and control samples and spots with the fold change >2 and <0.5 were considered as over-expressed and under-expressed respectively. The spots that were present either in the control or treated sample's gel were considered unique spots.

2.8.2.3 Spot selection and in-gel digestion

The selected protein spots from the 2-DGE gel were excised and de-stained for 15 min by 15 mM potassium hexacyanoferrate (III) [$K_3[Fe(CN)_6]$] and 50 mM Hypo in a ratio of 1:1. After de-staining the spot containing gels were washed and dehydrated with 25 mM ammonium bicarbonate and acetonitrile (ACN) solutions. The samples were then treated with 100 mM DTT for 1 h at 56 °C followed by 250 mM iodoacetamide (IDA) for 45 min in the dark. Later the samples were trypsin digested and incubated at 37 °C overnight leading to the formation of tryptic peptides which were then extracted by 0.1% (v/v) trifluoroacetic acid (TFA) in water. It was followed by the vacuum drying and dissolution of obtained peptides in 5 μ l of TA buffer which contains a 1:1 ratio of 0.1% (v/v) TFA and 100% (v/v) ACN. Finally, the extracted tryptic peptides (1.5 μ l) were mixed with 1.5 μ l of 5 mg ml⁻¹ α -Cyano-4-hydroxycinnamic acid (HCCA) matrix containing 1:2 ratio of 0.1% (v/v) TFA and 100% (v/v) ACN followed by spotting 2 μ l of this mixture onto the MALDI (Matrix-Assisted Laser Desorption/Ionization) plate.

2.8.2.4 MALDI-TOF/TOF MS analysis

For MALDI-TOF/TOF MS analysis, the mixture containing HCCA matrix and peptides was spotted on the MALDI plate (MTP 384 ground steel from Bruker Daltonics, Germany). After spotting it was dried and analyzed by the MALDI TOF/TOF ULTRAFLEX III instrument (Bruker Daltonics, Germany) using standard peptides (PEPMIX mixture) having a mass range of 1046-3147 Da (obtained from Bruker) for external calibration. The MS-MS analysis was performed in reflectron ion mode employing 500 laser shots at a mass detection range of 500-5000 m/z using FLEX ANALYSIS SOFTWARE (Version 3.3). To identify the proteins, the obtained masses were further analyzed by the MASCOT search in the “Capra hircus” database. The protein showing a MASCOT score of ≥ 50 is considered as the significant match for the protein to be identified.

2.8.3 Analysis of the whole-cell proteins under arsenate stress

To get a detailed view of the proteins involved in arsenate resistance in *P. mendocina* SMSKVR-3, the analysis of the entire proteome of the bacteria was performed. The whole-

cell proteome analysis included extraction of the proteins from the cell followed by LC-MS/MS analysis, data processing, and gene ontology analysis.

2.8.3.1 Extraction of whole-cell proteins

Based on the result of SDS-PAGE analysis of samples exposed to arsenate for different time intervals, 8 h exposure time was selected for the analysis of whole-cell proteome under arsenate unstressed (control) and stressed (treated) conditions. This study was conducted to analyze the differential protein expression as well as the proteins that are specifically expressed under arsenate stress.

The freshly grown primary culture of bacteria (1% v/v) was inoculated in 50 ml of sterilized M9 minimal media in 250 ml Erlenmeyer flask and incubated at 30 ± 2 °C and 120 rpm until the OD at 600 nm reaches between 0.4-0.5 (2.62×10^{11} CFU/ml). After growing the bacteria up to a desired optical density, 10 ml of bacterial culture were distributed in separate 25 ml flasks adding 300 mM of arsenate (treated) in duplicate flasks while keeping the other two untreated (control). The flasks containing bacterial cultures were then incubated at 30 ± 2 °C and 120 rpm for 8 h followed by the extraction of intracellular proteins.

The extraction of intracellular proteins was performed by the guanidine hydrochloride (GnHCl) method (Subedi et al., 2019). The bacterial suspension was centrifuged at 8000 rpm for 4 min at 4 °C to pellet down the cells which were then washed twice with 1 ml of freshly prepared 1X Tris-buffered saline (TBS). The cell pellet was collected by centrifuging the suspension at 13000 rpm for 1 min. The freshly prepared protease inhibitor was added to the cell pellet and mixed by vortexing followed by incubation on ice for 20 min. After this, the cell lysis was performed by adding the 100 µl of hot 6M GnHCl (prepared in 0.1M Tris having pH 8.5), vortexing, and incubating at 90 °C in a water bath for 10 min. The suspension was then sonicated with the 10-second pulse of 10 kHz until the solution appears clear and then incubated at 90 °C for 5 min. To obtain the intracellular protein, the sonicated solution was centrifuged at 15000 rpm for 20 min. The supernatant was collected and stored at -20 °C until further use. The quantification of protein was performed using the BCA method using lysis buffer as the blank.

2.8.3.2 Sample preparation for liquid chromatography-mass spectrometry/mass spectrometry (LC-MS/MS) analysis

Before the introduction of protein samples for LC-MS/MS analysis, they were processed. The 25 μ l of protein extracts were reduced with 5 mM of Tris (2-carboxyethyl) phosphine (TCEP) which cleaves the disulfide bonds present in the proteins and denatures it followed by the alkylation of proteins using 50 mM iodoacetamide. It binds with the cysteine residues of the protein and inhibits the disulfide bond formation also inhibiting the cysteine peptidases. After reduction and alkylation, the proteins were digested with trypsin (1:50 ratio of enzyme/lysate containing protein) for 16 h at 37 °C. To remove the salts from the obtained digests, a C18 silica cartridge was used followed by vacuum drying using a speed vac. The obtained dried pellet was further resuspended in buffer A containing 5% (v/v) acetonitrile and 0.1% (v/v) formic acid.

2.8.3.3 LC-MS/MS analysis of peptide mixtures

The LC-MS/MS analysis of digested protein samples was performed using Thermo Fisher Scientific EASY-nLC 1000 system which is coupled with Thermo Fisher-QExactive equipped with a nanoelectrospray ion source. For this, the peptide mixture (1.0 μ g) was injected in PicoFrit column having 15 cm length, 360 μ m outer diameter, 75 μ m inner diameter, 10 μ m tip and filled with 2.0 μ m of C18-resin (Dr. Maesch, Germany). The peptide samples were loaded with buffer A followed by elution with 0-40% gradient of buffer B that contains 95% (v/v) acetonitrile and 0.1% (v/v) formic acid at 300 nl/min flow rate for 100 min. The MS1 and MS2 spectra were collected at 70000 and 17500 resolutions, respectively. The acquisition of MS data was done using a data-dependent top10 method that dynamically chooses the most abundant precursor ions from the survey scan.

2.8.3.4 LC-MS/MS data processing

All the acquired raw data was processed, and the generated raw files were analyzed by Proteome Discoverer (v2.2) software against the uniprot reference proteome database of *P. mendocina*. The Sequest search was performed setting the precursor mass tolerance of ± 10 ppm and fragment mass tolerance of 0.5 Da. The enzyme specificity was set for the enzyme trypsin/P (cleavage at the C terminus of “K/R: unless followed by “P”) that was used to

generate peptides along with the missed cleavage value to be two. The carbamidomethyl on cysteine was considered as fixed modification and oxidation of methionine and N-terminal acetylation was considered as variable modifications for the database search. The peptide spectrum match (PSM) and false discovery rate (FDR) were set to 0.01 FDR. The student's t-test was used to obtain the significance of match and the $-\log$ value of the student's t-test's P-value was calculated. Where P-value represents the probability of an observed match to be a random event. Thus, protein or MS/MS spectra showing a small P-value is not a random event.

A comparison was done between the protein expressed in the presence and absence of arsenate to determine the upregulation or downregulation of different proteins. The ion abundance data of peptides was used to calculate the ratio of peptides in control and treated samples to compare the expression of proteins in these samples. The fold change calculation was performed by executing \log_2 normalization of the dataset followed by the analysis of their expression pattern. Protein/peptides showing a \log_2 abundance ratio greater than 1 were considered as upregulated however a \log_2 abundance ratio less than -1 was considered as downregulation as described by Shah and Damare (2018).

2.8.3.5 Analysis of the Gene Ontology and enrichment

Functional annotation and enrichment of differentially expressed proteins, proteins unique in untreated control, and proteins unique in arsenate treated sample was performed using the PANNZER2 (Protein ANNotation with Z-scoRE) webserver. This server is available at <http://ekhidna2.biocenter.helsinki.fi/sanspanz/> and provides a completely automated service for the functional annotation of protein of unknown function present in a prokaryotic or eukaryotic cell (Törönen et al., 2018). This web server provides fast Gene Ontology (GO) annotations and free text description (DE) predictions. PANNZER2 utilizes the ARGOT scoring function for the analysis of the protein sequences. The input data for the analysis is given either by pasting the protein sequence in FASTA format into the given text box or by uploading the FASTA file. In the next step, the scientific name (*P. mendocina*) needs to be entered. The analysis was performed in batch queue mode as input data contained >10 protein sequences. After the completion of the analysis, PANNZER2 provides the links to download different tables and to view the prediction summary. The summary table contains different columns having information about query header, gene name, description GO- ID, and function

prediction under biological process (BP), molecular function (MF), and cellular component (CC) categories. The GO annotations having ARGOT rank 1 (highest confidence prediction or highest ARGOT score) were filtered out from the mixture of GO annotations. In each BP, MF, and CC category, the proteins were further subdivided into different groups that were represented in the form of a pie chart showing the percentage of protein annotations present in each group.

2.9 *In silico* study of the binding of arsenate with the selected arsenic binding proteins

Based on the result of whole-cell proteomics of *P. mendocina* SMSKVR-3, two proteins involved in the arsenic resistance mechanism, ArsC and ArsH were selected for the *in silico* study. This study included the analysis of physicochemical and functional characteristics of the proteins, protein secondary structure prediction, modeling of protein 3D structure using different modeling tools, selection of the best model based on its quality, studying the affinity of the As(V) ion with the protein by docking, and deformability and stability study of As(V)-docked protein structure.

2.9.1 Analysis of the physicochemical and functional characteristics of the proteins

The proteomic analysis of the *P. mendocina* SMSKVR-3 under As(V) stress exhibited the expression of several arsenic binding proteins among which the ArsC and ArsH were selected for the As(V) binding study. Both of these proteins are known for As(V) resistance in different microorganisms. The amino acid sequences of the proteins were obtained from the LC-MS/MS analysis. The analysis of physicochemical properties of the proteins was performed by the Expasy-ProtParam (Gasteiger et al., 2005) tool which allows the estimation of various physical and chemical properties of the proteins including the composition of amino acid, molecular weight, isoelectric point (pI), half-life, theoretical aliphatic index, instability index, and grand average of hydropathicity (GRAVY). The isoelectric point of a protein is the pH at which the net charge on the protein is zero. At the pH corresponding to the pI value, the protein has minimum solubility in the water or salt solution and thus gets precipitated. The determination of the pI value of the protein is applied in the designing of the protein purification process. The half-life of a protein is the time at which half of the protein quantity is degraded inside the biological system. It also determines the time up to which a protein will

remain stable. The aliphatic index and instability index are the measure of thermostability and stability of the proteins, respectively. The GRAVY is the ratio of the sum of the hydropathy values of the individual amino acid residues and the length of the amino acid sequence. The identification of the disulfide bonds present in the proteins was performed by CYS_REC (Bhattacharya et al., 2018) that analyzes the total number of cysteines, their positions, and the pattern of the most probable S-S bond pairs in the proteins using primary sequence data. To predict the families of the protein sequences, the Pfam database was used containing a large collection of protein families represented by MSA and hidden Markov models (HMMs) (Mistry et al., 2021). For the prediction of the domains, the Conserved Domain Database (CDD) (Lu et al., 2020) and the Conserved Domain Architecture Retrieval Tool (CDART) (Geer et al., 2002) were used. The CDD contains the collection of MSA data of various known protein domains and full-length proteins for the identification of conserved domains. The CDART uses a protein domain profile to search for similar protein and group proteins having similarities with the query sequence. It assigns a similarity score based on their architecture. The analysis of the motif region of the protein was performed using the MotifFinder using the PROSITE tool (Sigrist et al., 2002) (<https://www.genome.jp/tools/motif/>).

2.9.2 Protein secondary structure prediction

The secondary structure of the protein which mainly consists of α -helix, β -sheets, coils, and turns was determined using the Self-Optimized Prediction Method with Alignment (SOPMA) (Geourjon & Deléage, 1995). The SOPMA is an improved version of the SOPM method which takes the information from the alignment of the sequences belonging to the same family. The protein structure pattern such as transmembrane regions and coiled coils were predicted using PSIPRED 4.0 (PSI-blast-based secondary structure PREDiction) (Buchan & Jones, 2019) web service which uses artificial neural network machine learning in its algorithm to predict the secondary structure of the protein from the primary structure.

2.9.3 Prediction of the active sites

The physicochemical properties of the protein are determined by either the positioning of specific amino acids or the presence of cavities on the surface of the protein. To understand the structural basis of the protein functioning, the mapping of the residues having functional

importance is performed. The mapping of the active site residues present in *P. mendocina* SMSKVR-3 ArsC and ArsH proteins was performed using the CASTp which is an online tool to locate cavities and ligand binding pockets (Tian et al., 2018). The CASTp uses the annotation obtained from PDB, Online Mendelian Inheritance in Man (OMIM), and SWISS-PROT to predict the active sites in a protein (Chauhan et al., 2019).

2.9.4 Protein structure modeling

For building the models of the ArsC and ArsH proteins, the sequences obtained from the LC-MS/MS analysis were used. The protein models were built using the four different software including the Modeller (version 9.25) (<https://salilab.org/modeller/>) (Šali & Blundell, 1993), SWISS-MODEL (Waterhouse et al., 2018), I-TASSER (Iterative Threading ASSEmbly Refinement) (Yang et al., 2015), and Phyre2 (Kelley et al., 2015). To identify the template protein, the sequence similarity search of the query sequence was performed against the PDB database using the BLASTP program. The hits showing the higher similarity, maximum query coverage, and lowest e-value score with the query sequence were selected as the templates. The coordinates of the selected template sequences were obtained from the protein data bank (PDB). The energy minimization of the generated models was performed using the Swiss PDB viewer if required. The best protein models obtained from each tool were validated by the PDBsum database ([PDBsum Generate \(ebi.ac.uk\)](http://pdbsum.ebi.ac.uk)) (Laskowski et al., 2018) using the PROCHECK server to analyze the Ramachandran plot. It measures the steric clashes among the side chains and their percentage occurrence in the allowed and disallowed regions of the plot. To further validate the model SAVES (version 6.0)-ERRAT (Colovos & Yeates, 1993) program was used which gives a quality score where a higher value indicates the better structural quality.

2.9.5 Molecular docking of proteins with the arsenate ion and stability/deformability study

Arsenate compounds form oxo-anions in the aqueous solution such as salts of arsenic acid (H_3AsO_4) having a +5-oxidation state. The structure of arsenate ion AsO_4^{3-} was retrieved from the RCSB PDB (Berman et al., 2003). The binding between the proteins and arsenate ligand was studied and analyzed using the molecular docking package AutoDockTools 4.2 (Morris

et al., 2009) for which the MGL Tools 1.5.6 (Holt et al., 2008) was installed and used for preparing parameters for the docking. Parameterization of arsenate ion was carried out as per the standard procedure mentioned on the AutoDock website. The parameters including Rii=4.30 Å (van der Waals radius), epsii=0.200 kcal/mol (van der Waals well depth), vol=41.60787 Å³ (atomic solvation volume), and solpar=-0.00110 (solvation parameter) were manually added to 'AD4_parameters.dat' and 'AD4.1_bound.dat' files which were kept in the directory while running the docking program. The identity of the new parameter file was also manually edited in the grid parameter file (.gpf) while running the program (Sahu et al., 2019). The coordinates of the ligand and protein obtained from the PDB file were loaded into the AutoDockTools 1.5.6 followed by deletion of water molecules, the addition of polar hydrogens, and calculation of partial charges. The modified ligand and protein were saved in the pdbqt format. The size of the grid box was set as it covers the entire proteins and saved as a .gpf file. The final docking was performed using the genetic algorithm approach and all the other parameters were set as default. The obtained docked structures were analyzed by the AutoDockTools using the docking log files and images were generated using the PyMOL 2.3.3 (DeLano, 2002).

The deformability and stability studies of the protein-ligand complex were performed by the normal mode analysis (NMA) using the iMODS server (<http://imods.chaconlab.org/>) (López-Blanco et al., 2014). It analyzes various properties of the protein-ligand complex such as eigenvalues, mobility profiles, and deformability (Banik et al., 2020).

Chapter III

Results and Discussion

3.1 Isolation and characterization of arsenic resistant bacterial strains from khetri copper mines

3.1.1 Bacterial strains with arsenate resistance

The metal-contaminated sites of khetri copper mines were selected for the isolation of arsenic-resistant microorganisms based on our previous study that exhibited the presence of arsenic in the tailing waste of khetri copper mines. Different sites (rhizospheric soil, wastewater, and slag dump) selected for the sample collections have been shown in Fig. 3.1. The pH of the collected samples were found to be 7.86, 8.36, and 6.33 for the rhizospheric soil, wastewater, and slag sample, respectively. The enrichment culture technique used for the isolation of bacteria involves the introduction of specific growth media or nutrient that favors the growth of an organism of interest (Madhuri et al., 2019). The concentration of arsenate was gradually increased from 2 mM to 300 mM in the M9 minimal media containing the collected samples. After the incubation with 300 mM arsenate for 7-8 days at 30 ± 2 °C, four bacterial colonies (named as SMSKVR-1a, SMSKVR-1b, SMSKVR-2 and, SMSKVR-3) from the rhizospheric soil sample, and five colonies (named as SMSKVW-1, SMSKVW-2, SMSKVW-3 and, SMSKVW-4 and SMSKVW-5) from the wastewater sample were isolated. However, from the slag sample, two bacterial colonies were isolated that did not survive during the further subculturing process.

There are several reports on the arsenic-resistant bacteria isolated from arsenic-contaminated water and soil samples. From the soil of the Semaria Ojha Patti village of Bihar, which has groundwater arsenic contamination level up to $1000 \mu\text{g L}^{-1}$, three bacteria *Acinetobacter calcoaceticus* J1, *A. tumefaciens* J2, and *Bacillus cereus* DAS3 were isolated which have exhibited tolerance up to 310 mM of As(V) and 35 mM As(III) (Tripti, 2018). A tolerance of 55 mM for As(III) and 275 mM for As(V) was observed for *Pseudomonas* strain As-11 isolated from the water contaminated with arsenic in Babagorgor Spring, Iran (Jebelli et al., 2017). Recently, a *Micrococcus luteus* strain AS2 has been isolated from the industrial wastewater of Sheikhpura, Pakistan showing tolerance up to 55 mM As(III) and 275 mM As(V) (Sher et al., 2020).

Rhizospheric region



Wastewater region



Slag dumping region



Fig. 3.1 Different sites of sample collection in the khetri copper mines.

There are only a few reports on the isolation of arsenic-resistant bacteria from the mining area which generally belongs to gold and uranium mining sites. Till now, very few reports are available on the isolation and characterization of arsenic-resistant bacteria from the copper mining sites. Domingues et al. (2020) have isolated bacteria from a copper mine in Brazilian Amazonia that represent resistance mechanisms for various metals such as lead, arsenic, cadmium, copper, and zinc. Another study by Chen et al. (2019) has exhibited the highest abundance of the gene coding for arsenic resistance (*arsC*) in the bacterial strains isolated from the heavy metal contaminated area of the Shibahe copper tailings dam area in Mountain Zhongtiaoshan of northern China. All these studies witness the presence of arsenic-resistant bacteria in different mining sites. In the present study, we have reported a bacterial isolate SMSKVR-3 that exhibits tolerance up to 300 mM of As(V) indicating the existence of As(V) resistant microbial flora in the copper mining area as discussed in the earlier section.

3.1.2 Gram staining

All the nine bacterial isolates, isolated from the different sites of khetri copper mines (in the media containing 300 mM arsenate) exhibited gram-negative characteristics. The gram staining characteristic of all the isolates has been shown in Fig. 3.2.

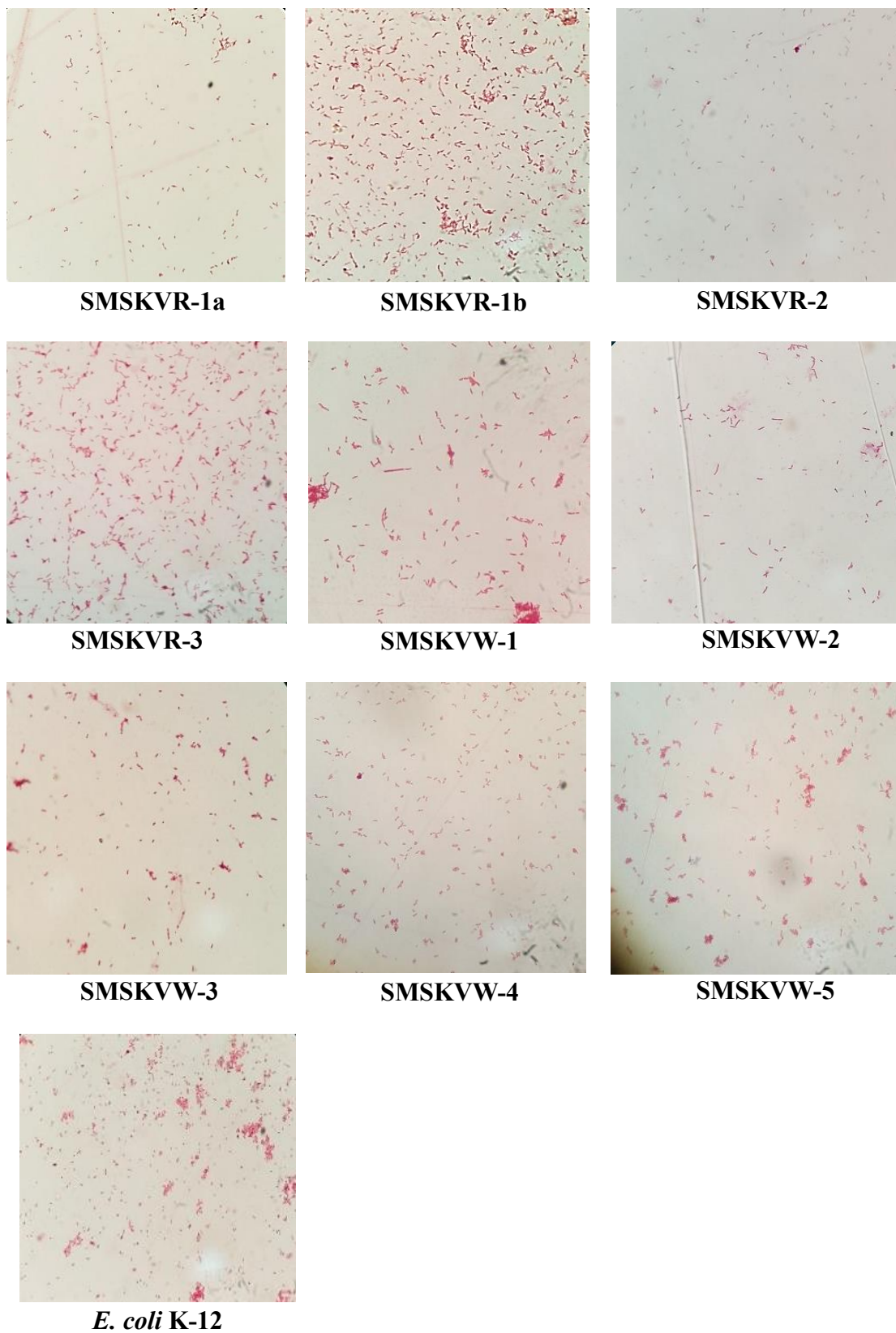


Fig. 3.2 Gram staining of the isolated bacterial strains.

3.1.3 BOX-PCR analysis of the isolated bacterial strains

The BOX-PCR analysis is performed for the typing of bacterial strains to sort out the common strains. To perform the BOX-PCR, the genomic DNA was isolated (Fig. 3.3a) from all the isolates and the BOX elements present in the genome were amplified as described in section 2.2.3.

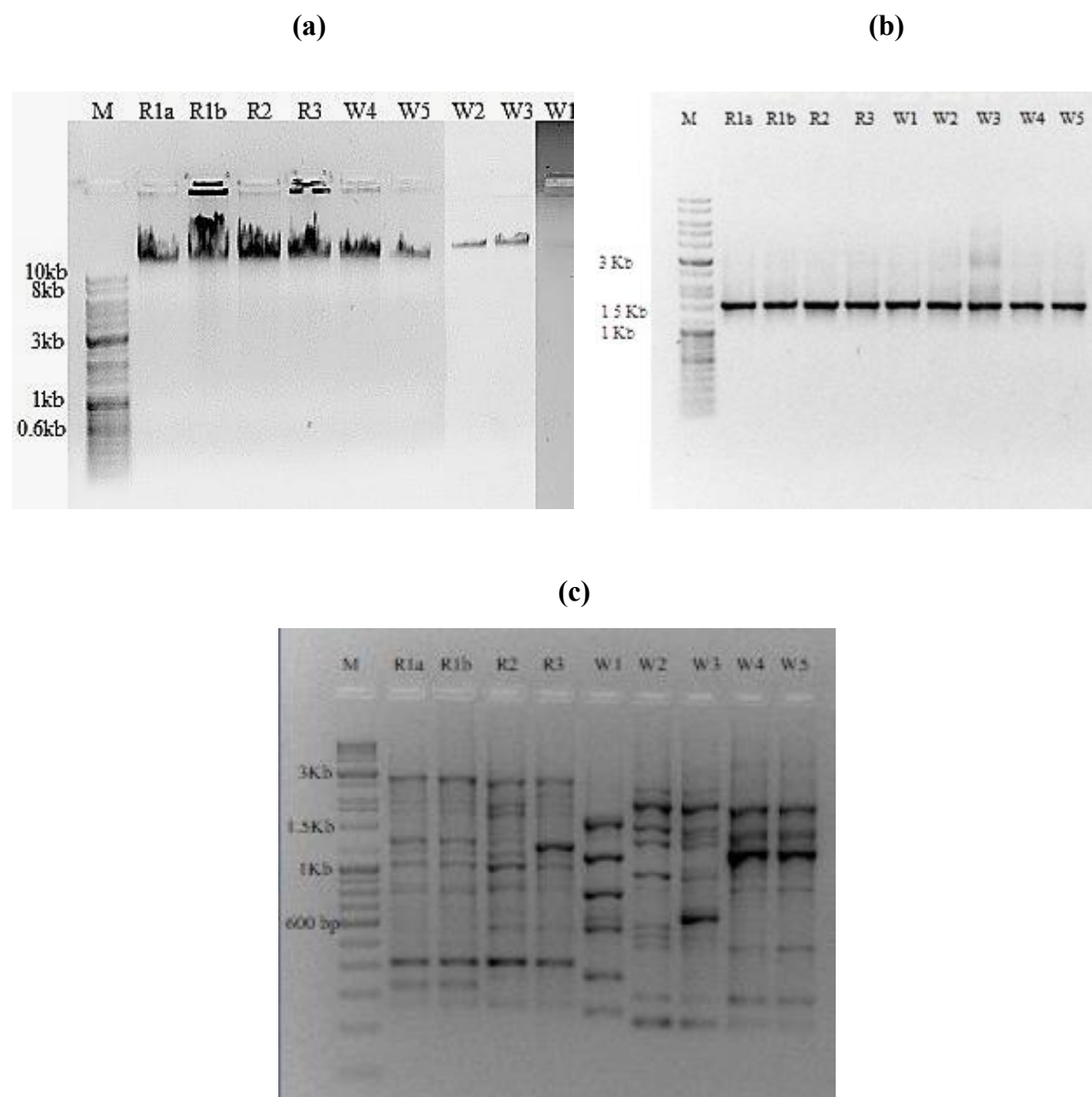


Fig. 3.3 Molecular characterization of the isolates, (a) genomic DNA of the isolates, (b) amplified 16S rRNA genes from the isolates, (c) BOX-PCR profile of all the isolates. (Lane M: SM0311 DNA ladder, Lane 2-9: isolates SMSKVR-1a- SMSKVW-5)

The patterns of amplified BOX elements were compared in all the isolates and the isolates showing similar patterns were considered as the same strains which were not included in the further studies. In the BOX-PCR analysis, SMSKVR-1a and SMSKVR-1b showed the same amplification pattern. Isolate SMSKVW-4 and SMSKVW-5 also showed the same BOX element amplification pattern and were therefore also considered as the same strains. However, all the other isolates represented different BOX element amplification patterns (Fig. 3.3c).

3.1.4 Partial 16S rRNA gene sequencing of the isolates and identification

The 16S rRNA gene was isolated and amplified from all the bacterial isolates which are mentioned in Fig. 3.3b. Based on the result of BOX-PCR analysis, partial 16S rRNA gene sequencing of SMSKVR-1a, SMSKVR-2, SMSKVR-3, SMSKVW-1 SMSKVW-2 SMSKVW-3, and SMSKVW-4 were performed. The results obtained after NCBI-BLAST analysis showed 98% identity of SMSKVR-1a (shown as SMSKVR-1) with *P. stutzeri* ATCC 17588. However, SMSKVR-2, SMSKVR-3, SMSKVW-1, SMSKVW-2, SMSKVW-3, and SMSKVW-4 showed 99.6%, 91%, 97%, 99.4%, 98.9%, and 99% identity with *P. argentinensis* CH01, *P. mendocina* ATCC 25411, *Oceanimonas doudoroffii* NBRC 103032, *Halomonas meridiana* DSM 5425, *H. meridiana* DSM 5425, and *H. stevensii* S18214, respectively. The result of the identification of isolated bacteria has been summarized in Table 3.1. The partial sequences of SMSKVR-1, SMSKVR-3, SMSKVW-1, and SMSKVW-4 were

Table 3.1 Partial characterization of isolated bacteria based on 16S rRNA gene sequencing.

S. No.	Code	Bacterial species	Closest match	Coverage (%)	% Identity
1	SMSKVR-1	<i>Pseudomonas stutzeri</i>	<i>Pseudomonas stutzeri</i> ATCC 17588	99	98
2	SMSKVR-2	<i>Pseudomonas argentinensis</i>	<i>Pseudomonas argentinensis</i> CH01	100	99.6
3	SMSKVR-3	<i>Pseudomonas</i> sp.	<i>Pseudomonas mendocina</i> ATCC 25411	100	91
4	SMSKVW-1	<i>Oceanimonas</i> sp.	<i>Oceanimonas doudoroffii</i> NBRC	99	97
5	SMSKVW-2	<i>Halomonas stevensii</i>	<i>Halomonas meridiana</i> DSM 5425	100	99.4
6	SMSKVW-3	<i>Halomonas meridiana</i>	<i>Halomonas meridiana</i> DSM 5425	99	98.9
7	SMSKVW-4	<i>Halomonas stevensii</i>	<i>Halomonas stevensii</i> S18214	100	99

deposited in the NCBI database under Accession No.- MH493721, MH493722, MH493723, and MH493724 respectively.

Among all the isolates of bacteria, SMSKVR-3 showed rapid growth in the presence of 300 mM arsenate in M9-minimal media (data not shown). Thus, SMSKVR-3 was selected for the full characterization and further studies.

3.1.5 Morphological and biochemical characteristics of SMSKVR-3

The morphological study of the colony of SMSKVR-3 exhibited a small, smooth, and flat colony which was initially off-white and showed a brownish-light yellow color pigmentation after 3-4 days of incubation. The transformation of the off-white colonies into yellow color indicates the presence of carotenoid pigments in the bacterial cell (Palleroni et al., 1970). The light-yellow color colony of SMSKVR-3 matches with *P. mendocina* LYX indicating the possibility of the strain being *P. mendocina* (Li et al., 2020).

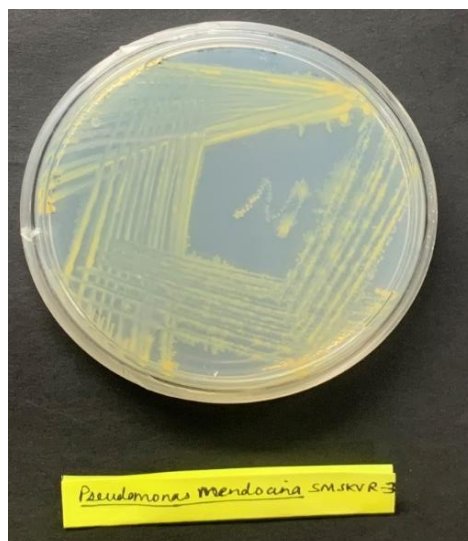


Fig. 3.4 Morphology of SMSKVR-3 in M9-minimal media-agar plate.

The colony morphology of the SMSKVR-3 has been shown in Fig. 3.4. The SMSKVR-3 was also screened for various biochemical characteristics the results of which have been summarized in Table 3.2. The negative results were obtained for the indole, Voges–Proskauer, methyl red, O-nitrophenyl- β -D-galactopyranoside (ONPG), phenylamine deamination, H₂S production, and urease test. However, positive results were obtained for

the citrate utilization, lysine utilization, ornithine utilization, malonate utilization, esculin hydrolysis, oxidase, and nitrate reduction test. The nitrate reduction test determines the ability of bacteria to reduce nitrate (NO_3) to nitrite (NO_2) in the presence of enzyme nitrate reductase. The reduction of nitrate to nitrite by *P. mendocina* LYX has also been reported by Li et al. (2020). The SMSKVR-3 exhibited a positive result towards the oxidase test which is used to differentiate *Pseudomonads* from the other related species of the bacteria. The oxidase test detects the presence of the enzyme cytochrome oxidase that catalyzes the oxidation of cytochrome C. The bacteria showed negative results towards all the tested carbon sources (such as arabinose, xylose, adonitol, rhamnose, cellobiose, melibiose, saccharose, raffinose, trehalose, and lactose) except the glucose.

Table 3.2 Biochemical characterization of selected isolate (SMSKVR-3).

Parameters	SMSKVR-3	Parameters	SMSKVR-3
Gram stain	-ve	Esculin hydrolysis	+ve
ONPG	-ve	Arabinose	-ve
Lysine utilization	+ve	Xylose	-ve
Ornithine utilization	+ve	Adonitol	-ve
Urease	-ve	Rhamnose	-ve
Phenylalanine deamination	-ve	Cellobiose	-ve
Nitrate reduction	+ve	Melibiose	-ve
H ₂ S production	-ve	Saccharose	-ve
Citrate utilization	+ve	Raffinose	-ve
Voges Proskauer's	-ve	Trehalose	-ve
Methyl red	-ve	Glucose	+ve
Indole	-ve	Lactose	-ve
Malonate utilization	+ve	Oxidase	+ve

+ve;positive, -ve;negative

3.1.6 Molecular characterization and phylogenetic analysis of SMSKVR-3

The molecular characterization of SMSKVR-3 was performed by bidirectional sequencing of the 16S rRNA gene using the primer walking technique. The 1.5 kb length of the 16S rRNA gene was amplified and cloned in the Topo-TA cloning vector. The cloned gene was

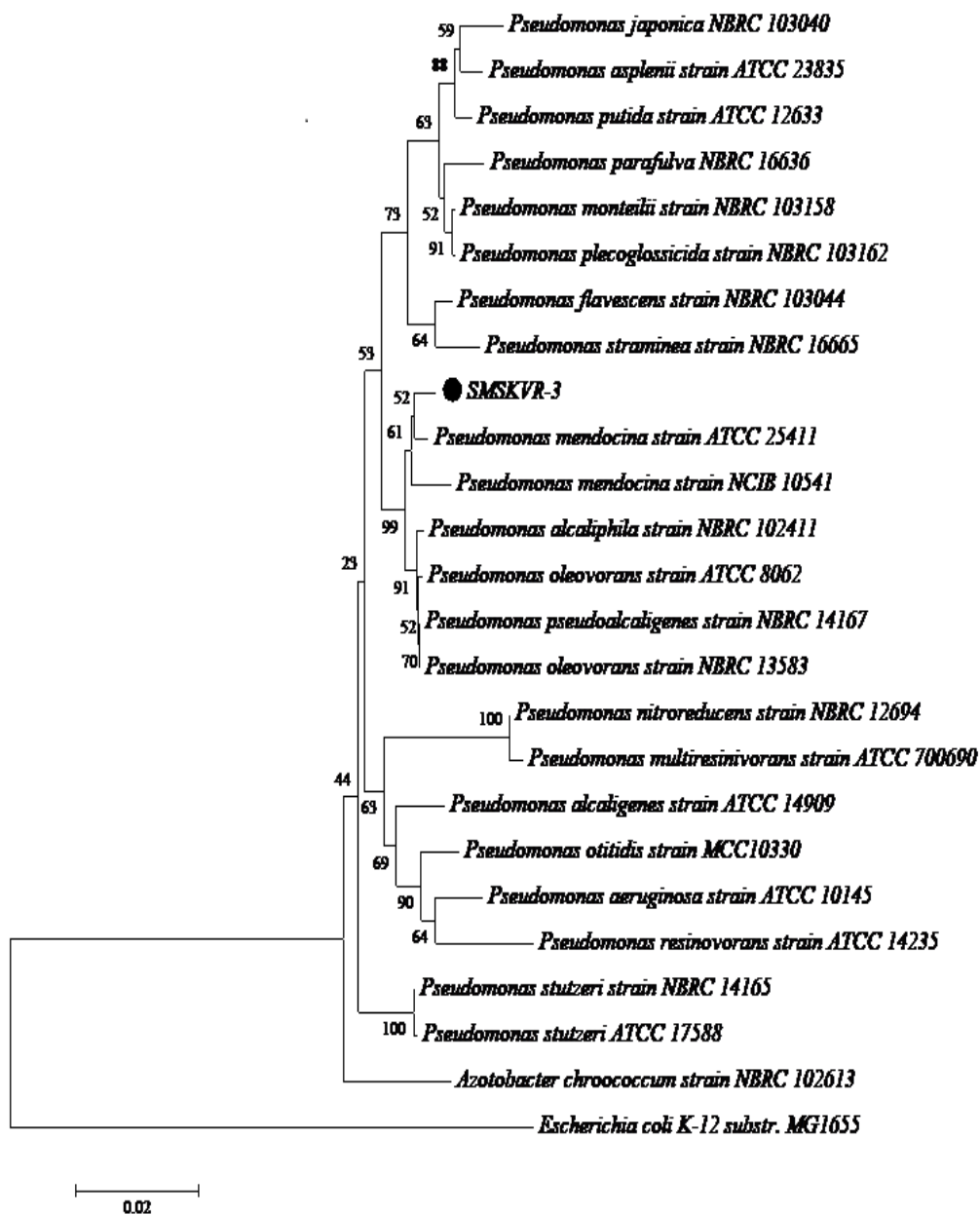


Fig. 3.5 Neighbour-joining phylogenetic tree based on 16S rRNA gene sequences, showing the position of SMSKVR-3 and other related genera. The 16S rRNA gene sequence of the *E. coli* K-12 was used as an outgroup. Bootstrap values (%) are based on 1000 replicates.

sequenced using M13 forward and reverse primers. The obtained 16S rRNA nucleotide sequence was compared with the 16S rRNA gene sequences available in the NCBI-GenBank database using the BLAST algorithm which led to the identification of the closest match for the searched sequence. Some of the closest matches obtained in the BLAST search were further analyzed by the multiple sequence alignment (MSA) followed by phylogenetic tree construction using the neighbor-joining method considering bootstrap values based on 1000 replicates. The SMSKVR-3 represented the closest similarity with *P. mendocina* strain ATCC 25411 belonging to γ -proteobacteria class with 99.04% identity (Fig. 3.5). The 16S rRNA gene sequence was deposited in the GeneBank database under accession no.-MH473722.2. The pure culture of the bacteria was deposited in the Microbial Type Culture Collection (MTCC), Chandigarh, India, under MTCC no.- 12986. The pure culture was also deposited in the National Agriculturally Important Microbial Culture Collection (NAIMCC), Indian Council of Agricultural Research, Mau, Uttar Pradesh, India under NAIMCC no. B-02531.

3.2 Study of physiological parameters required for the bacterial growth

An optimum environmental condition is necessary for the growth of all the bacteria present in nature. The study of the physiological conditions required for the optimal growth of selected bacteria was performed which included the parameters such as temperature, pH, and salt concentration. The growth of bacteria was measured in terms of (a) OD_{600nm}, and (b) intracellular protein concentration. The SMSKVR-3 showed significant growth in the temperature range of 25-40 °C (Fig. 3.6a). The growth of SMSKVR-3 was optimum in M9-media having pH 7 however, it was able to grow in the pH range of 5-9 (Fig 3.6b). The bacteria exhibited almost similar growth in the salt (NaCl) concentration range of 0.25-3.25% (w/v) followed by a sharp decline above 3.25% NaCl concentration. Therefore, 0.25% of NaCl was used in further studies. Very less growth was observed in the 5.25% (w/v) of NaCl concentration (Fig 3.6c). The outcome of this study shows the tolerance of SMSKVR-3 for a diverse range of physiological conditions.

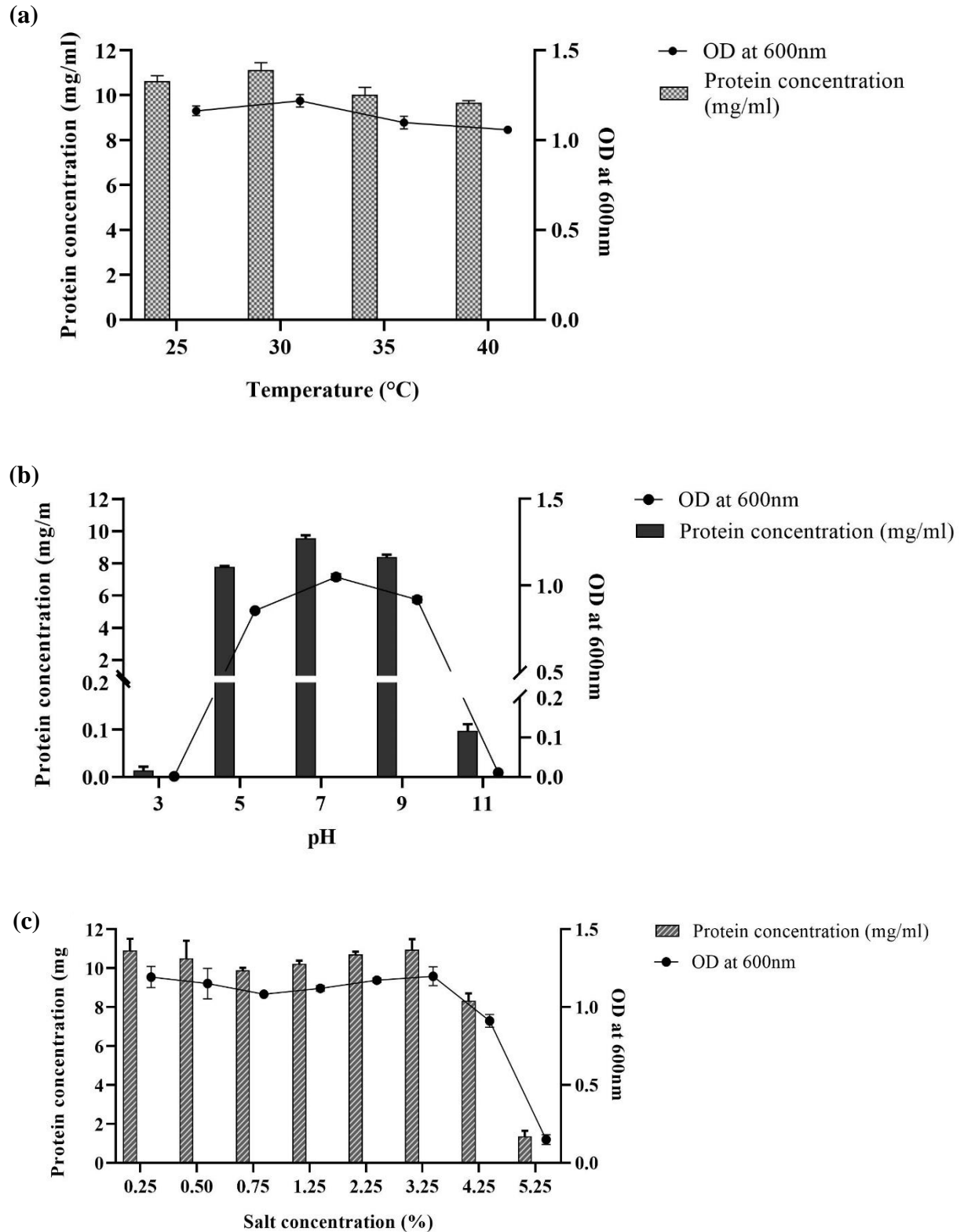


Fig. 3.6 Study of different physiological parameters (a) temperature, (b) pH, and (c) salt (NaCl) concentrations required for the growth of *P. mendocina* SMSKVR-3.

3.3 Analysis of the growth curve

The growth curve of the selected isolate, SMSKVR-3 was plotted between time (in hours) and optical density (600 nm) in three different media conditions- M9 media only, M9 media supplemented with 300 mM As(V), and M9 media supplemented with 1.34 mM As(III) which has been depicted in Fig. 3.7. In all three conditions, the pattern of growth was almost the same where the lag phase showed an extension from 0-6 h. The doubling time of the bacteria in all three conditions showed very little difference and were obtained to be 1.47, 2.66, and 2.62 hours for control (M9 media alone), M9 media supplemented with As(V), and M9 media supplemented with As(III), respectively. This small increase in the doubling time in the media containing As(V) and As(III) might be due to the toxic effect of arsenic on bacteria requiring them some additional time to adapt to this toxic environment. However, the similar growth pattern of bacteria in all these three conditions is an indicator that there is the presence of a strong arsenic resistance mechanism inside the bacterial cell allowing it to grow in the presence of the higher concentration of As(V) and As(III).

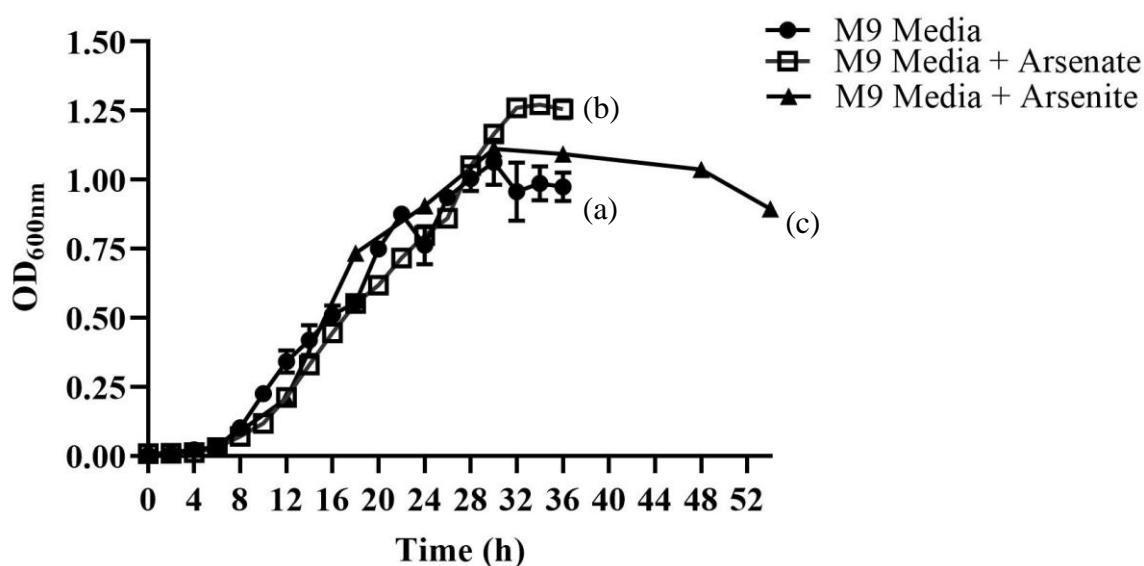


Fig. 3.7 Growth curve of *P. mendocina* SMSKVR-3 in the presence of (a) only M9 minimal media, (b) M9 media having 300 mM arsenate, and (c) M9 media supplemented with 1.34 mM arsenite.

The earlier report by GAD-RAB et al., (2006) on the growth of *Rhodobacter capsulatus* B10 under Cd stress has also shown the inhibition in cell proliferation and extension of lag phase followed by the resumption of growth. The adaptation in the above case involved the distribution of toxic ions inside the cell by adjusting the cellular physiology. Similar results on the extension of the lag phase have been reported for nickel stress in *Rhodospirillum photometricum* (Sarkar & Banerjee, 1987) and antibiotic stress in *P. putida* (Li et al., 2016). All these studies show the importance of lag phase extension in bacterial cells to overcome the toxic effect of metals and other stress-causing agents like antibiotics. However, the SMSKVR-3 showed a very short extension of the lag phase in the presence of As(V) as well as As(III) and thus adapted quickly under the toxic environment which indicates the presence of a strong cellular mechanism to overcome the arsenic toxicity.

3.4 Study of cellular morphology under arsenic stress using SEM analysis

The SEM analysis was performed to investigate the toxic effect of arsenic (arsenate and arsenite) on the cells of SMSKVR-3. The effect of arsenate and arsenite on bacterial cellular morphology has been shown in Fig. 3.8a and b. The bacterial cells exhibited normal cellular morphology as the untreated condition upon treatment with 300 mM arsenate and 1.34 mM arsenite. The enlarged images of bacterial cells (50000 x) in all the conditions (Fig. 3.8 b(i) to (iii)) show the intact cell wall without any damage. The average cell size of bacteria was also found to be the same in all the conditions which were $1.647 \mu\text{m} \times 0.571 \mu\text{m}$, $1.78 \mu\text{m} \times 0.541 \mu\text{m}$, and $1.66 \mu\text{m} \times 0.510 \mu\text{m}$ for control, arsenate treated and arsenite treated cells respectively. However, SMSKVR-3 cells treated with 300 mM As(V) showed aggregation in comparison to control and As(III) treated cells. The results obtained by SEM analysis has confirmed our findings of the growth curve study, where the bacteria showed the same growth pattern in the control, As(V) treated and As(III) treated conditions. This indicates the presence of a strong arsenic resistance mechanism in the SMSKVR-3 allowing it to tolerate the arsenic toxicity. SEM analysis of two bacterial strains As-9 and As-14 isolated by Pandey and Bhatt (2015) from arsenic-rich soil of Rajnandgaon district has shown a fourfold increase in the cell volume of the As(V) treated cell. However, cells were smooth and showed intact cell surfaces in both conditions. Such an increase in the cell volume has been reported as a strategy to acc-

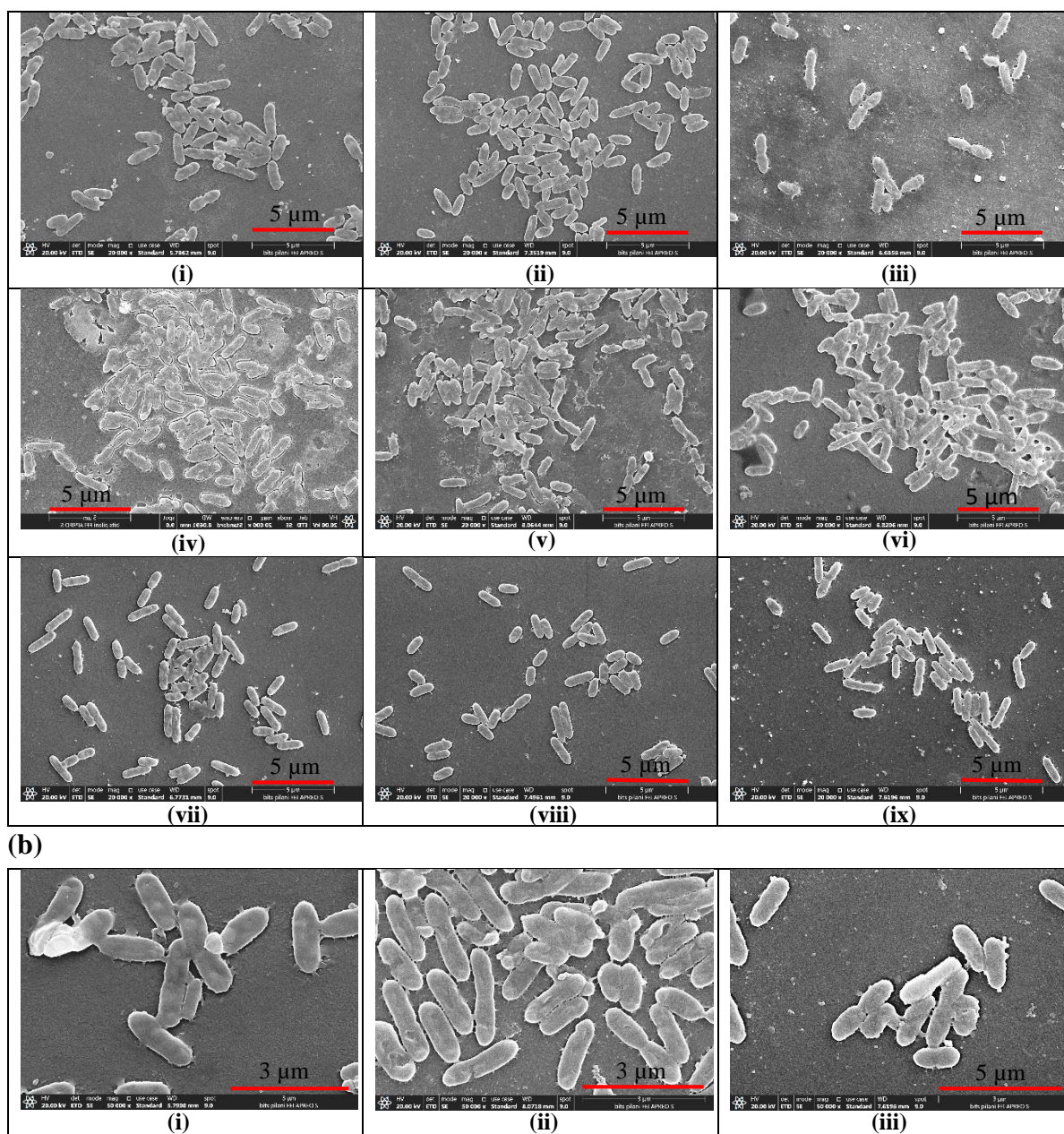


Fig. 3.8 Scanning electron microscopy image of *P. mendocina* SMSKVR-3; a(i), (ii) & (iii) without any treatment (control); a(iv), (v) & (vi) treated with 300 mM arsenate; a(vii), (viii) & (ix) treated with 1.34 mM arsenite at 20000 x magnification; b(i), (ii) & (iii) enlarged image (50000 x) of *P. mendocina* SMSKVR-3 under control, As(V) treated, and As(III) treated conditions.

umulate more arsenic from the surroundings to minimize its toxicity (Pandey & Bhatt, 2015). *R. radiobacter* has a significant change in the cellular morphology exhibiting wrinkled and elongated cells in the presence of 5 mM As(V) (Deepika et al., 2016). In contrast to these

studies, our study has shown the normal cellular morphology, cell size, and volume as the control cells in the As(V) as well as As(III) treated cells. However, the increased colonization of bacterial cells and deposition of the exopolysaccharide layer on the surface of the cells were observed in the cells treated with As(V). Our study was in agreement with the SEM study conducted on *M. luteus* strain AS2 where no significant change in the cellular morphology was observed in the As(III) (15 mM) treated cells in comparison to the untreated ones. This bacteria showed the presence of genetic determinants for arsenic detoxification and resistance. Thus, based on this study, it can be concluded that there is a possibility of a strong arsenic resistance mechanism in the SMSKVR-3 helping it to survive in the stressed condition caused by the exposure of arsenic.

3.5 Investigation of the arsenate resistance mechanisms in *P. mendocina* SMSKVR-3

3.5.1 Siderophores production

The siderophores are non-ribosomal peptides widely known as iron chelators and secreted by microorganisms such as bacteria and fungi. Different types of siderophores include catecholate siderophores containing catechol as the functional group, hydroxamate siderophores having alkylamine or hydroxylated ornithine functional group, citric acid functional group-containing carboxylate siderophores, and mixed type containing a combination of these functional groups (Singh et al., 2021). Besides chelating iron, siderophores are capable of chelating other essential metals such as Fe, Mn, Zn, Cu, and Mg which function as the cofactors of enzymes. The heavy metal resistance in bacteria can be contributed by siderophores production involving sequestration of metals in the extracellular environment and allowing the bacteria to grow in the harsh mine tailing sites (Miranda-Carrasco et al., 2018; Navarro-Noya et al., 2012; Zelaya-Molina et al., 2016). *P. mendocina* SMSKVR-3 exhibited the ability to produce siderophores in the King's B medium for all the tested metals and metalloids. The growth of bacterial culture in King's B-agar plate containing CAS-dye (having bluish-green color) supplemented with desired metal/metalloids led to the formation of orange-yellow halo zone around the bacterial growth that confirmed the production of siderophores by the bacteria. The size of the halo-zone was measured after 48

h of incubation. The production of siderophore by SMSKVR-3 for Fe(III), As(V), and As(III) has been shown in Fig. 3.9.

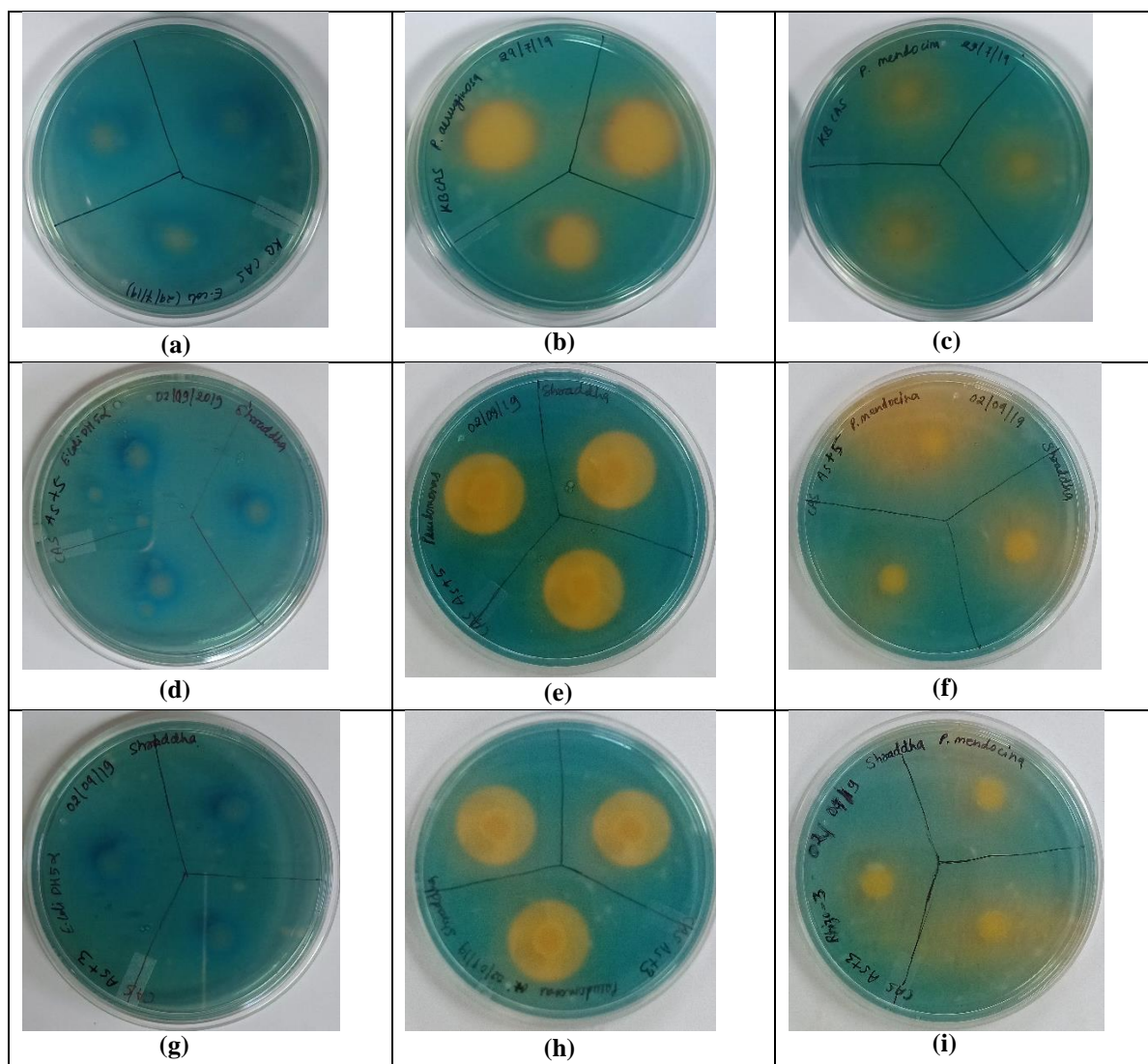


Fig. 3.9 Siderophores production by *P. mendocina* SMSKVR-3 in King's B-agar plate with chrome azurol S dye supplemented with (a) Fe(III), (d) As(V), and (g) As(III) inoculated with negative control (*E. coli* DH5a); King's B media plate with chrome azurol S dye supplemented with (b) Fe(III), (e) As(V), and (h) As(III) inoculated with the positive control (*P. aeruginosa*); King's B-agar plate with chrome azurol S dye supplemented with (c) Fe(III), (f) As(V), and (i) As(III) inoculated with *P. mendocina* SMSKVR-3 and incubated for 48 h.

Siderophores produced by *Pseudomonas* spp. have shown the chelation of biologically non-essential metals, including As, Cd, Cr, Co, Ga, Sn, U, Pb, and Pl. The ability to chelate at least 17 metals has been exhibited by pyoverdine siderophore produced by *P. aeruginosa* (Braud et al., 2009; Nair et al., 2007). The Ni-sequestering hydroxamate siderophores have been reported to be produced by *Streptomyces acidiscabies* (Bazzi et al., 2020). A study conducted on *P. mendocina* P6115 has revealed the production of siderophores to chelate As(V) and As(III) that supports the production of siderophores in the presence of As(V) and As(III) by *P. mendocina* SMSKVR-3 in our study (Miranda-Carrasco et al., 2018). Earlier studies have shown the relation between siderophore production and arsenic detoxification. Many bacteria such as *Pseudomonas* have the ability to oxidize and reduce different arsenic forms such as As(V) and As(III) to minimize their toxic effect which is correlated with the ability of the bacteria to produce siderophores. It has been observed in different strains of *P. fluorescens* that higher production of siderophore is related to the better oxidation of As(III) while bacteria producing low siderophore have efficient As(V) reduction ability. Production of siderophores in higher amounts causes the activation of arsenite oxidase enzyme by the iron which enters the cell through the action of siderophores. However, *Staphylococcus* sp. TA6 containing arsenic operon produced higher siderophore exhibiting strong As(V) reduction ability (Das & Barooah, 2018). The strong arsenate reducers are generally present in the arsenic-rich sites where siderophore produced by bacteria scavenges Fe from the arsenopyrite releasing and As(V) from solid to the liquid phase. This released As(V) enters the cell through phosphate channels and is reduced to As(III) by the arsenate reductase enzyme which is further effluxed via the ArsB transporters. In a similar way, siderophores mobilize arsenic from scorodite containing Fe and As(V) and help in the mitigation of arsenic toxicity (Drewniak et al., 2008; Singh et al., 2021). Based on these studies, we can infer that siderophores produced by *P. mendocina* SMSKVR-3 are helping it to mitigate the arsenic toxicity by possibly reducing As(V) to As(III) and further effluxing it out of the cell which can be confirmed by the arsenate reduction assay.

3.5.2 Study of bacterial resistance to other heavy metal/metalloids

It has been reported in certain cases that bacteria exhibit multiple metal resistance in addition to the metal in which it has been isolated. To check the ability of the selected bacteria to

tolerate other toxic heavy metals/metalloids, the experiment was designed to expose the bacteria to different concentrations of As(III), Mn(II), Mo(VI), Fe(III), Cd(II), Cu(II), Zn(II), Ni(II), Co(II), Cr(VI), and Hg(I) salts incorporated in M9-minimal media. The MIC (lowest concentration of metal or any other antimicrobial compound that prevents the visible growth of bacteria) of each heavy metal/metalloid was determined. The MICs of As(III), Fe(III), Cd(II), Ni(II), Co(II), Cr(VI) and, Hg(I) were obtained to be 18.62, 25.06, 12.53, 0.341, 0.136, 0.115 and 0.01 mM respectively. The MICs of different heavy metals are shown in Table 3.3. The MIC values of Zn(II), Cu(II), Mn(II), and Mo(VI) could not be determined precisely because of the precipitation of metal salts that interrupted the OD measurement. However, plating of bacterial culture on the M9-agar plate supplemented with Zn(II), Cu(II), Mn(II), and Mo(VI) showed the growth of bacteria up to 7.65, 7.85, 25.48, and 14.56 mM concentrations respectively. The results show the presence of a cross-resistance mechanism in the *P. mendocina* SMSKVR-3 for other heavy metals.

Table 3.3 Cross-tolerance of selected isolate for other heavy metals and metalloid(s).

Metals/ Metalloids	MIC	
	(ppm)	(mM)
Arsenite	1400.00	18.62
Manganese	1400.00	25.48
Molybdenum	1400.00	14.56
Iron	1400.00	25.06
Cadmium	1400.00	12.53
Copper	500.00	7.85
Zinc	500.00	7.65
Nickel	2.00	0.341
Cobalt	8.00	0.136
Chromium	6.00	0.115
Mercury	2.00	0.01

3.5.3 Antibiotics sensitivity test

The zone of inhibition test was performed to check the susceptibility of SMSKVR-3 towards some common broad range antibiotics which are reported to have cross-resistance with heavy

metals and other antibiotics. While no ZOI was observed for *P. mendocina* SMSKVR-3 exposed to ampicillin (10 µg) and vancomycin (30 µg), the kanamycin (30 µg) showed a ZOI with a diameter of 11.2 mm. Based on the measured diameter of the zone of inhibition (ZOI) it can be concluded that SMSKVR-3 has resistance (R) towards ampicillin, vancomycin, and kanamycin antibiotics. It also showed intermediate (I) resistance towards chloramphenicol with a ZOI of 13.8 mm but was found to be sensitive (S) for tetracycline and streptomycin with the ZOIs having diameters of 23.8 and 22 mm, respectively (Table 3.4).

Table 3.4 Sensitivity of *P. mendocina* SMSKVR-3 towards different antibiotics.

Antibiotics	Isolate SMSKVR-3	
	Zone of Inhibition (ZOI) (Avg.) (mm)	Sensitivity
Ampicillin	0	R
Chloramphenicol	13.8	I
Kanamycin	11.2	R
Tetracycline	23.8	S
Vancomycin	0	R
Streptomycin	22	S

Resistance to antibiotic - R; Sensitive to antibiotic- S; Intermediate resistance- I

The cross-metal tolerance and antibiotic susceptibility exhibited by SMSKVR-3 can be attributed to multi-drug efflux pumps present in bacteria that have been reported in several studies (Baker-Austin et al., 2006; Bazzi et al., 2020; Pal et al., 2017). Protein TetA(L) is reported to be involved in providing cross-resistance towards tetracycline and cobalt by effluxing them out of the cell (Cheng et al., 1996). The resistance against penicillin/macrolide-type antibiotics as well as As(III) in *A. tumefaciens* 5A and *E. coli* has been attributed to a multi-drug efflux pump MacAB belonging to the ABC transporter family (Shi et al., 2019). Another multi-drug efflux pump, MdrL of *Listeria monocytogenes* confers resistance against erythromycin, josamycin, clindamycin, Zn, Co, and Cr has been reported by Mata et al. (2000). The resistance against Zn, Cd, β-lactams, kanamycin, erythromycin, novobiocin, and ofloxacin is attributed by DsbA-DsbB (Disulfide Bond) efflux pumps in *Burkholderia*

cepacia. The CmeABC efflux pumps provide resistance against some antimicrobials, Co and Cu in *Campylobacter jejuni* (Bazzi et al., 2020). All these studies support our finding that heavy metal/metalloid and antibiotics cross-resistance do exist in SMSKVR-3.

3.5.4 Biotransformation of arsenic

In the arsenic biotransformation studies, either the reduction of arsenate or the oxidation of arsenite is detected using the qualitative silver nitrate microtiter plate assay. This assay employs the reaction of AgNO_3 with Tris-Cl (pH 7.5) buffer containing arsenite or arsenate leading to the production of light yellow to brown colored precipitate. The production of a light-yellow colored precipitate is due to the formation of Ag_3AsO_3 (silverorthoarsenite) and indicates the reduction of arsenate whereas the brown colored precipitate is produced due to the formation of Ag_3AsO_4 (silverorthoarsenate) and indicates the oxidation of arsenite (Simeonova et al., 2004). The formation of the light-yellow color precipitate by *P. mendocina* SMSKVR-3 in As(V) containing Tris-Cl (pH 7.5) buffer after the addition of AgNO_3 at 24 h of incubation shows the reduction of As(V). The intensity of the yellow color increased when it was incubated for a longer time (72 h). However, there was no color change (formation of brown precipitate) in the presence of As(III) in comparison to the control under similar conditions indicating the absence of arsenite oxidation activity in the bacteria. The result of arsenate reduction in SMSKVR-3 is shown in Fig. 3.10. The *P. mendocina* SMSKVR-3 exhi-

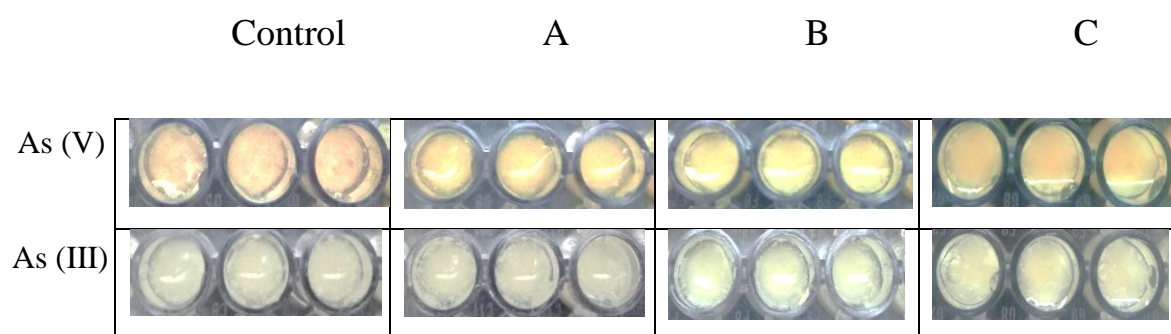


Fig. 3.10 Silver nitrate microtiter plate assay for the analysis of arsenate reduction by *P. mendocina* SMSKVR-3. In each well of microtitre plate 80 μl of 0.2 M Tris-HCl buffer (pH 7.5), 1.33 mM As(V), 20 μl of bacterial cells (OD_{600} range 0.6-0.7) or 20 μl of 0.2 M Tris-HCl buffer (pH 7.5) in control was added. After the incubation for (A) 24 h, (B) 48 h, and (C) 72 h picture was taken after the addition of 100 μl of 0.1 M AgNO_3 .

bited the reduction of As(V) to As(III) after 24 h of incubation under aerobic conditions. While it did not show the ability of oxidizing As(III) due to the lack of arsenite oxidase enzyme.

The mechanism of arsenic reduction and oxidation has been described in many arsenic-resistant bacteria. The reduction of As(V) to As(III) in the bacteria can be mediated by either cytoplasmic arsenate reductase (ArsC) or the respiratory arsenate reductase (Arr) (ArrB). Cytoplasmic ArsC is responsible for the aerobic reduction of As(V) and is encoded by *arsC* gene of the *arsRBC* operon present on the genome of *E. coli*, *S. aureus* plasmid pI258, and *arsRDABC* operon present on the *E. coli* plasmid R773 (Chen et al., 1986; Ji et al., 1994; Sofia et al., 1994). The reduction of As(V) helps the bacteria to mitigate the arsenic toxicity by converting it into the water-soluble form As(III) followed by its efflux through the arsenic-specific transporter ArsB (Biswas et al., 2019; Dey et al., 2016; Ghosh et al., 2015). In contrast to ArsC, the respiratory As(V) reductase enzyme (Arr) performs the reduction of As(V) under anaerobic conditions and are found in the bacteria respiring As(V) such as Strain MIT-13 and *C. arsenatis* (Ahmann et al., 1994; Krafft & Macy, 1998). Mostly, Arr proteins consist of two subunits ArrA which is a larger catalytic subunit, and the smaller unit ArrB. The molecular weight of these subunits differs from organism to organism (Yan et al., 2019). Many arsenic-resistant bacteria have the ability to oxidize As(III) into As(V) which is contributed by either a respiratory arsenite oxidase enzyme encoded by a broadly distributed *aioAB* operon (as identified in *Alcaligenes faecalis*) or a novel arsenite oxidase ArxA encoded by *arxA* gene (identified in a haloalkaliphilic bacteria *A. ehrlichii* strain MLHE-1) (Ellis et al., 2001; Yan et al., 2019; Zargar et al., 2012).

P.mendocina SMSKVR-3 exhibited the reduction of As(V) to As(III) under the aerobic condition that strongly supports the presence of *arsC* gene carrying *ars* operon in this bacteria allowing it to grow under very high concentration of As(V) (300 mM). In addition to this, the previous study has shown the production of siderophore by *P.mendocina* SMSKVR-3 which is also related to the As(V) reduction ability of the bacteria. However, the oxidation of As(III) to As(V) was not observed in this bacteria.

3.5.5 Determination of polyP bodies under arsenic stress

PolyP bodies are the polymer of phosphate that play a potential role in the variety of cellular processes such as survival, phosphate reservoir, tolerance to stress, virulence, antibiotic resistance, energy generation, and metal chelation inside the bacterial cell (Gangaiah et al., 2010; Pokhrel et al., 2019). The concentration of polyP bodies inside the bacterial cells was determined at different time points (from 0 h to 48 h) under the arsenate stress. It was later correlated with the concentration of arsenic inside the cells at the same time point in order to determine the role of polyP bodies in the mitigation of arsenic from the bacterial cell. The concentration of polyPs inside the bacterial cells exhibited a decrease up to 8 h of incubation followed by a slight increase at 24 and 48 h. In the beginning, the concentration of polyPs inside the bacterial cells was $354.8 \mu\text{g}/10^{10} \text{CFU ml}^{-1}$ decreasing to 97, 1.85, and $0.043 \mu\text{g}/10^{10} \text{CFU ml}^{-1}$ at 0.5, 4, and 8 h, respectively. However, after 8 h the polyPs concentration showed a slight increase of $0.8 \mu\text{g}/10^{10} \text{CFU ml}^{-1}$ at 24 h and $0.59 \mu\text{g}/10^{10} \text{CFU ml}^{-1}$ at 48 h (Fig. 3.11a).

The bacterial cells keep polyP bodies as energy and phosphate store which can be seen in the result as the initial highest concentration of polyP bodies. Two enzymes, polyP kinase (PPK) that play role in the synthesis of polyP from ATP reversibly, and exopolyPase (PPX) that catalyzes the degradation of polyP into the inorganic phosphate (P_i) irreversibly, are the crucial enzymes playing crucial roles in the polyP metabolism inside the *E. coli* cells (Akiyama et al., 1993; Keasling & Hupf, 1996; Kulakovskaya, 2018). Another enzyme having a key role in polyP metabolism is polyP-AMP-phosphotransferases (PAP) which phosphorylates AMP to ADP utilizing polyP as a substrate (Kornberg, 1995). The concentration of polyP exhibited a decrease with time which could be resulted due to the PPX-mediated degradation of polyP bodies which later effluxed from the cells in the form of As-phosphate complex through the phosphate transporters. Due to the continuous efflux of the As-phosphate complex, the bacteria exhibited higher arsenic tolerance. This explanation is supported by a similar observation on genetically manipulated *E. coli* cells exhibiting the indirect role of polyP hydrolyzing ability providing tolerance to Cd (Keasling & Hupf, 1996). This study indicated that it is the polyP hydrolyzing ability, not the concentration that play role in metal resistance. Also, the cell having the ability to both synthesize as well as degrade

polyPs showed better Cd resistance. This study also exhibited that the polyP mediated Cd resistance involves intracellular precipitation of Cd by PPX catalyzed polyP degradation or the efflux of Cd-phosphate complex. Apart from Cd, efflux of various other cations has also been reported during the polyP degradation (van Groenestijn et al., 1988).

Based on this study, it can be stated that polyP bodies might be playing a potential role in arsenate resistance in the *P. mendocina* SMSKVR-3 which can be confirmed by studying the change in intracellular arsenic concentration with the time as shown in the following section.

3.5.6 Determination of time-based changes in intracellular and cell surface arsenic concentrations in *P. mendocina* SMSKVR-3

As mentioned above, polyP bodies may contribute to arsenic resistance in bacterial cells. To confirm this hypothesis, a time-based change in the concentration of intracellular arsenic was studied. The result of this study exhibited an initial surge in the concentration of intracellular arsenic at 0.5 h of incubation followed by a linear decrease up to 8 h. The concentration of arsenic was at its minimum at 24 h followed by a slight rise at 48 h. In the beginning, the arsenic concentration was found to be $116.98 \text{ mg L}^{-1} / 10^{10} \text{ CFU ml}^{-1}$ which increased to $346.62 \text{ mg L}^{-1} / 10^{10} \text{ CFU ml}^{-1}$ at 0.5 h. At 4, 8, 24, and 48 h the concentration of arsenic was obtained as 17.43, 2.205, 1.37, and 4.301 $\text{mg L}^{-1} / 10^{10} \text{ cells}$ respectively (Fig. 3.11c). A similar pattern of concentration change was observed for the cell surface-bound arsenic. The initial concentration of $1380.96 \text{ mg L}^{-1} / 10^{10} \text{ CFU ml}^{-1}$ showed a slight increase to $3364.48 \text{ mg L}^{-1} / 10^{10}$ at 0.5 h followed by a gradual decrease of 246.06, 88.65, and 43.36 $\text{mg L}^{-1} / 10^{10} \text{ CFU ml}^{-1}$ at 4, 8, and 24 h, respectively. It was followed by a slight increase of $140.68 \text{ mg L}^{-1} / 10^{10} \text{ CFU ml}^{-1}$ at 48 h of incubation time (Fig. 3.11b).

As discussed earlier, the role of polyPs in heavy metal resistance should be reflected as a positive correlation between time-based change in polyP and intracellular arsenic concentration. This correlation has been witnessed in this study where the same decreasing pattern of the concentrations of polyPs and intracellular arsenic has been obtained. The initial increase in intracellular arsenic concentration may be due to the sudden uptake of arsenic from the outer environment to initiate the detoxification process. However, a slight rise in the

concentrations of intracellular arsenic as well polyPs at 24 h and 48 h could be due to the exhaustion of cellular activity.

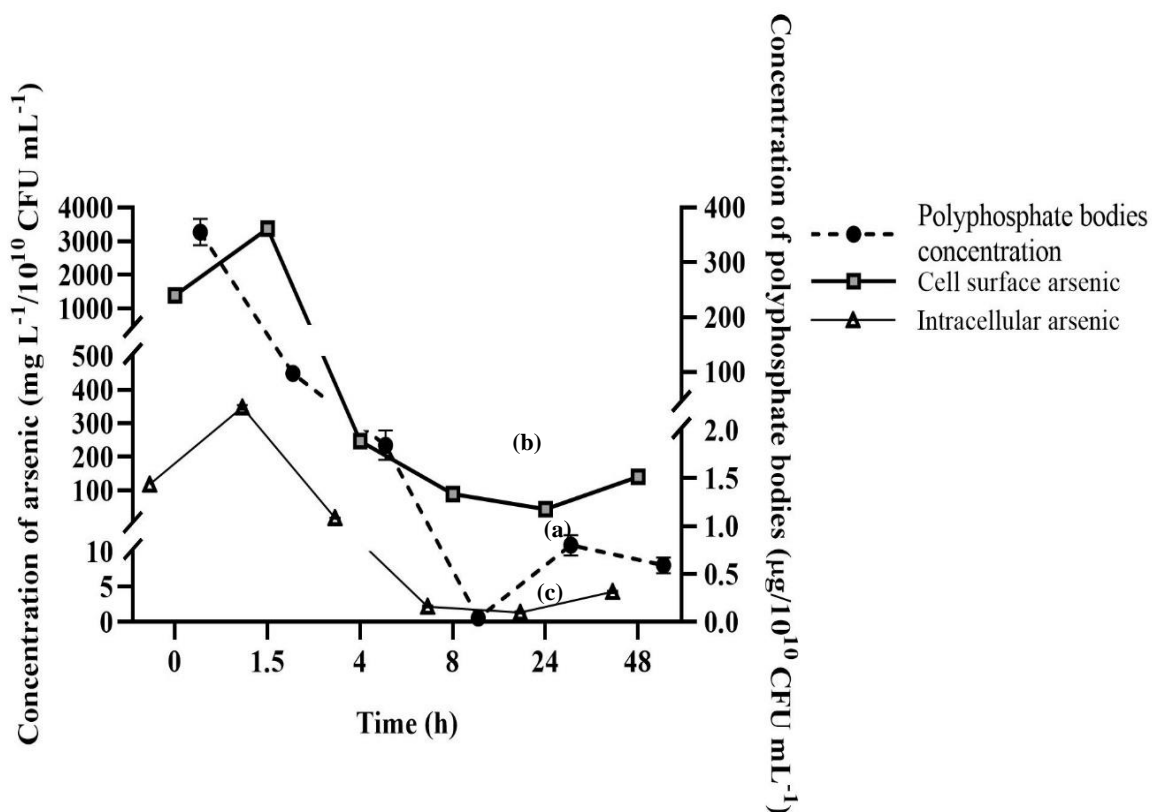


Fig. 3.11 Role of polyphosphate bodies in response to 300 mM As(V) in *P. mendocina* SMSKVR-3; (a) concentration of polyphosphate, (b) concentration of deposited As(V) on the cell surface, (c) concentration of intracellular As(V).

A similar pattern of change in the concentration of surface-bound arsenic was observed indicating polyP-mediated arsenic detoxification. It also exhibited a time-based decrease in concentration because the detoxification process led more amount of arsenic to be effluxed in comparison to its uptake and thus a decrease in the concentration of cell surface-bound arsenic was observed.

Based on the outcomes of all these studies, the involvement of the multiple mechanisms in arsenic detoxification in *P. mendocina* SMSKVR-3 have been hypothesized including multi-drug efflux pump-based resistance, siderophore-based resistance, ArsC-catalyzed transformation of As(V) to As(III), and polyP mediated arsenic resistance. All these mechanisms have been summarized in Fig 3.12.

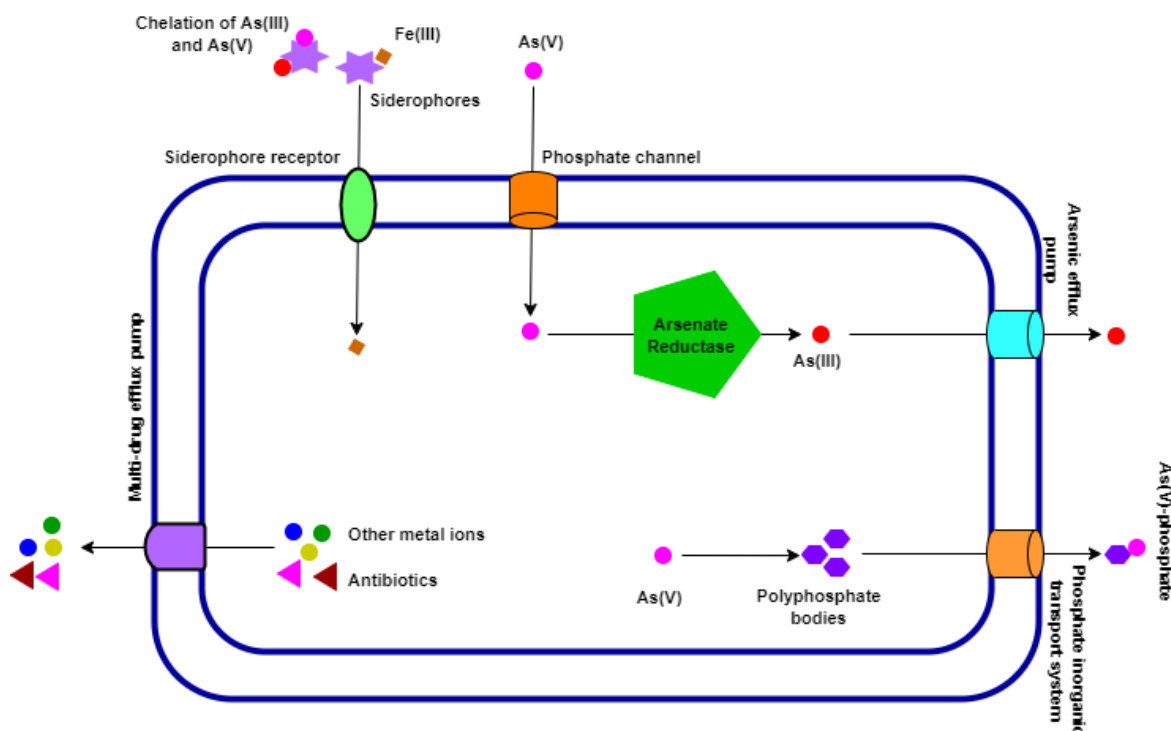


Fig. 3.12 Schematic representation of probable mechanisms of arsenic resistance in *P. mendocina* SMSKVR-3.

3.5.7 PCR amplification of the genes involved in arsenate resistance in *P. mendocina* SMSKVR-3

In order to investigate the As(V) resistance mechanism in *P. mendocina* SMSKVR-3, a further study involving the PCR amplification of genes having a role in As(V) resistance was performed. The genes involved in this study included arsenate reductase (*arsC*),

polyphosphate kinase (*ppk1*), efflux RND transporter component, and arsenic resistance protein (*arsH*). The primers were designed based on the *P. mendocina* gene sequences available in the NCBI database. All the selected As(V) resistance genes were successfully amplified and analyzed on 1.2% agarose gel with the expected amplicon lengths of 354 bp, 2168 bp, 1652 bp, and 607 bp for the *arsC*, *ppk1*, efflux RND transporter component, and *arsH*, respectively (Fig. 3.13). This result confirms the presence of all these genes involved in arsenic resistance in the *P. mendocina* SMSKVR-3 genome.

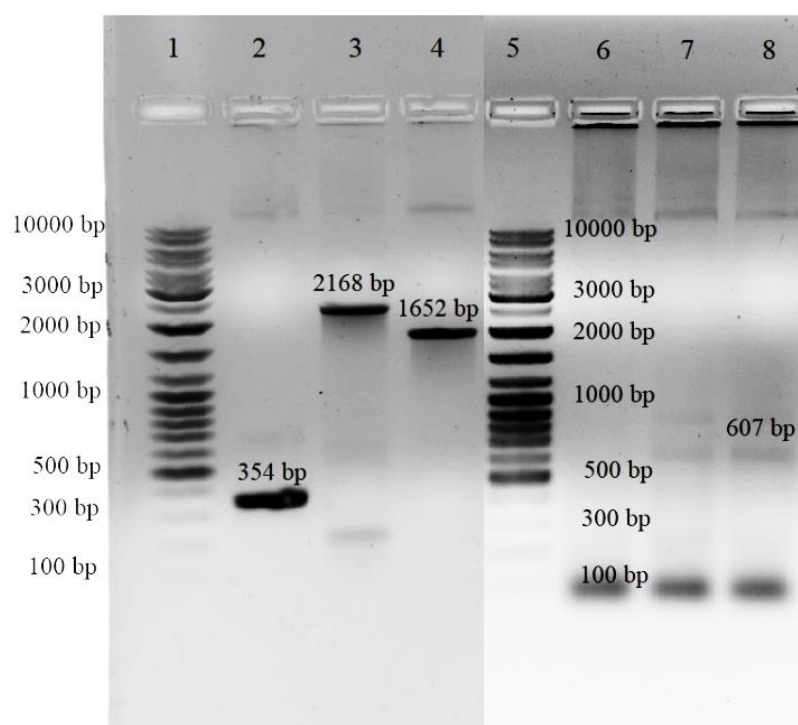


Fig. 3.13 PCR amplification of the genes involved in arsenate resistance in *P. mendocina* SMSKVR-3. Lane 1 & 5: 100-10000 bp ladder (SM0331), Lane 2-4: genes involved in arsenate resistance including arsenate reductase, polyphosphate kinase & efflux RND transporter component, Lane 8: arsenic resistance protein (ArsH).

To further confirm the presence of these As(V) resistance genes in *P. mendocina* SMSKVR-3 along with the other genes involved in As(V) resistance, the analysis of the whole-genome sequence was performed.

3.6 Whole-genome sequencing analysis of *P. mendocina* SMSKVR-3 to explore the presence of arsenate resistance genes

3.6.1 Characteristics of the genome

The genome of *P. mendocina* SMSKVR-3 was sequenced using Illumina HiSeqX10 paired-end sequencing followed by its processing and assembly. The *P. mendocina* SMSKVR-3 showed a circular genome having the length of 5,429,704 bp along with the absence of plasmid. The analysis of 31 contigs using the Prodigal predicted a total of 5155 genes in which 5114 genes represented a significant BLASTX match with the UniProt. The GC content of the genome was found to be 62.52%. The comprehensive genome analysis using PATRIC (version 3.6.9) exhibited the presence of 59 genes coding for tRNA and 3 genes coding for rRNA with no other RNAs and repeating regions (Table 3.5). The annotation of the genome by the PATRIC using the RAST tool kit (RASTtk) represented 1230 hypothetical and 4023 proteins with the functional assignment. Amongst the proteins with the functional assignment,

Table 3.5 Overall properties of the *P. mendocina* SMSKVR-3 genome.

Summary of the genome analysis	<i>P. mendocina</i> SMSKVR-3
Length of the genome	5.4 Mb
Plasmids	0
Number of contigs	31
L50	3
N50	493,613
GC (%)	62.52
Number of predicted genes	5,155
Number of predicted genes with significant BLASTX match (E-value $\leq 1e-3$ and Similarity score $\geq 40\%$) with uniprot	5114
Number of transfer RNA (tRNA)	59
Number of ribosomal RNA (rRNA)	3

1144 proteins contained enzyme commission (EC) numbers, 974 represented gene ontology (GO) annotation and 852 showed mapped KEGG pathways.

3.6.2 The organism annotation

The organism annotation was based on the number of BLASTX hits matched with a particular organism. The name of the organism was extracted by studying the top BLASTX hit of each gene. The top 10 organisms that represented the higher number of BLASTX hits have been shown in Fig. 3.14. The highest number of BLASTX hits (approximately 2000) was shown by *P. mendocina* followed by *Pseudomonas* sp. ALS1131. This also confirms that the analyzed genome sequence belongs to *P. mendocina*.

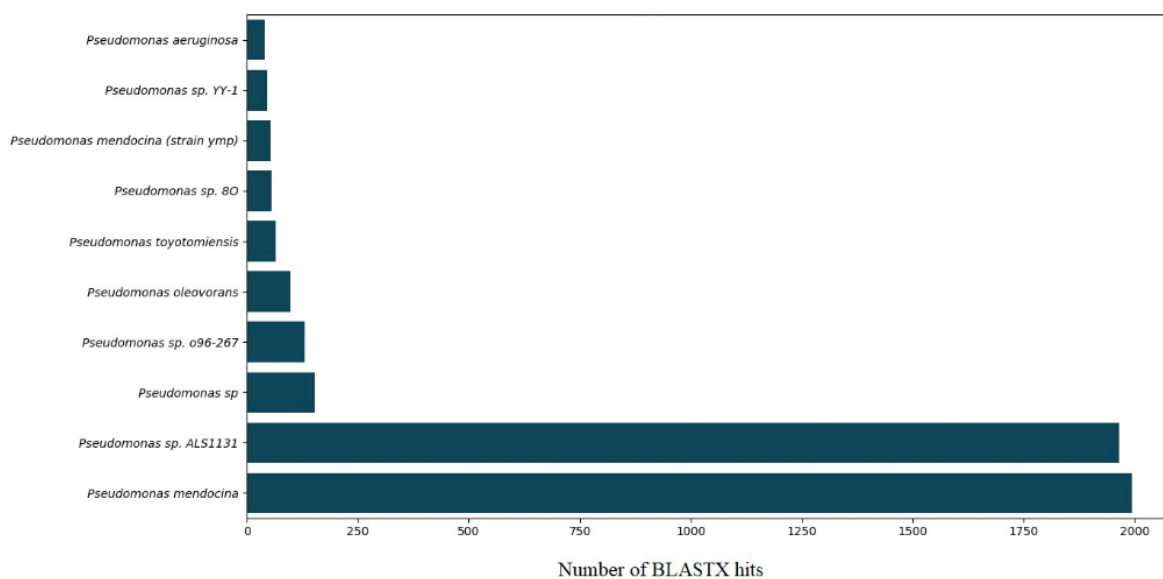


Fig. 3.14 Organism annotation based on the top BLASTX hits.

3.6.3 Phylogenetic analysis

The phylogenetic analysis of the *P. mendocina* SMSKVR-3 genome with the other reference and representative genomes belonging to the same genus and having similarity with it illustrated its close similarity with *P. mendocina* ymp, *P. pseudoalcaligenes* CECT 5344, and

P. alcaliphila 34 (Fig. 3.15). However, the closest similarity was obtained with *P. mendocina* ymp which confirms its accurate molecular characterization or identification mentioned earlier in this study.

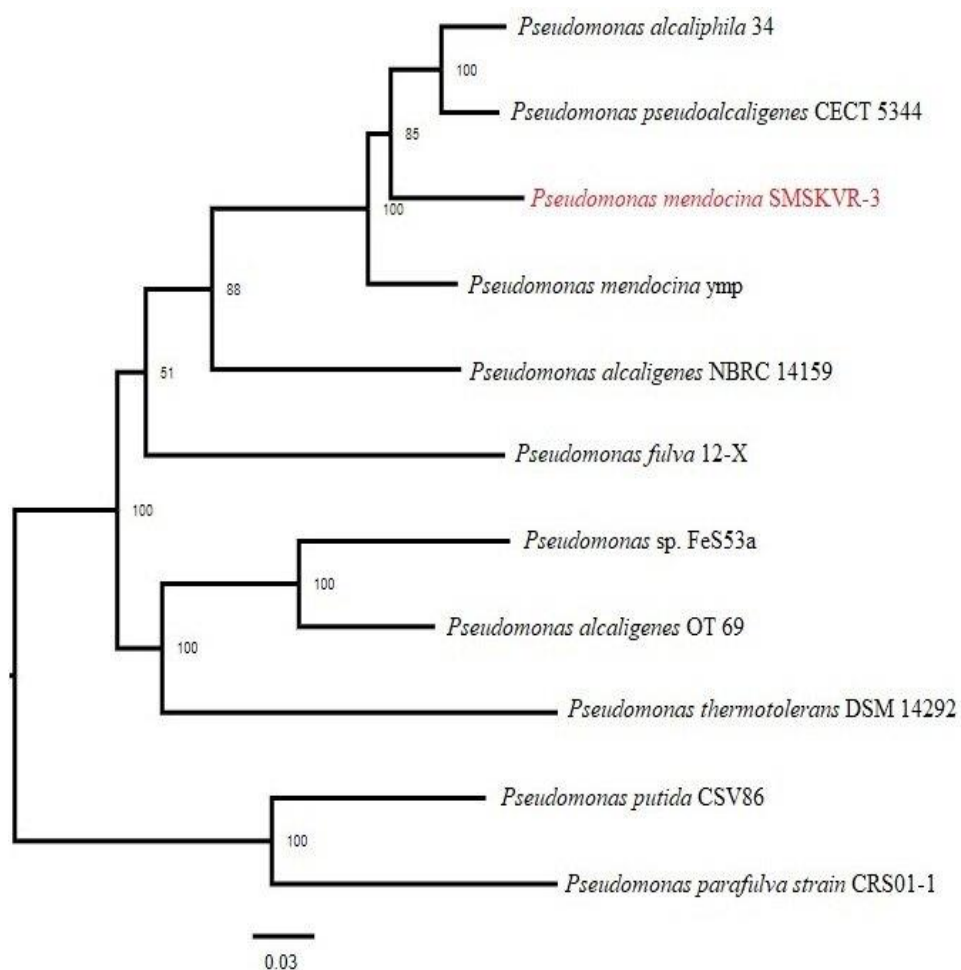


Fig. 3.15 Phylogenetic tree constructed based on the whole-genome sequence of *P. mendocina* SMSKVR-3 and other closest reference and representative genomes belonging to the same genus.

3.6.4 Gene annotation

The annotation of the predicted genes was performed by its comparison with the BLASTX program followed by mapping the GO terms for the genes in three categories of BP, MF, and

CC. The GO annotation based on the BP category revealed that the maximum number (>100) of genes are involved in the regulation of transcription (DNA templated) followed by transmembrane transport (~80), methylation (>60), phosphorelay signal transduction (>60), chemotaxis (>60), signal transduction (60), translation (<60), cell motility (40), DNA recombination (<40) and cell division (<40) (Fig. 3.16). Under the MF category, the highest number of the genes (between 350-400) represented ATP-binding activities followed by DNA binding (>350), metal ion binding (200-250), DNA binding transcription factor (200-250), hydrolase activity (100-150), transmembrane transport (100-150), oxidoreductase activity (100), ATPase activity (around 100), transferase activity (50-100), and electron transfer activity (50-100) (Fig. 3.17). The annotation based on the CC category revealed that the maximum number of the genes are integral component of the membrane (>1000) followed by genes related to the cytoplasmic (around 400), plasma membrane (200-400), outer membrane (<200), and membrane proteins (<200). Proteins belonging to ATP-binding cassette (ABC) transporter complex (<200), ribosomal proteins (<200), integral component of the plasma membrane (<200), proteins localized in periplasmic space (<200), and cellular proteins (<200) were also present in the bacterial genome (Fig. 3.18).

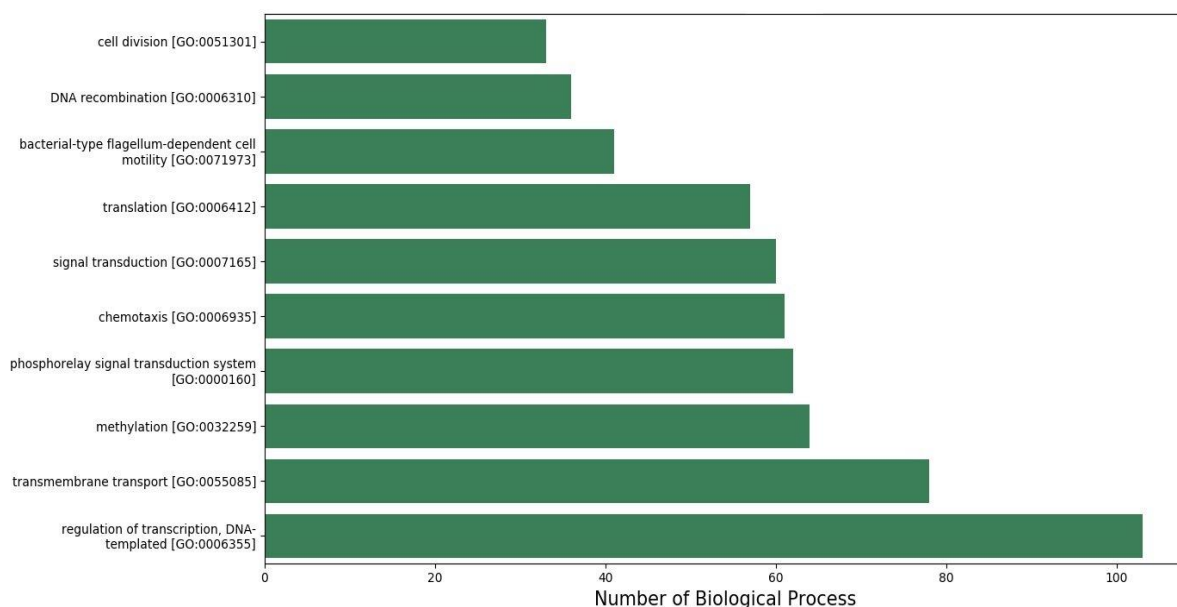


Fig. 3.16 Annotation of the genes based on their biological process.

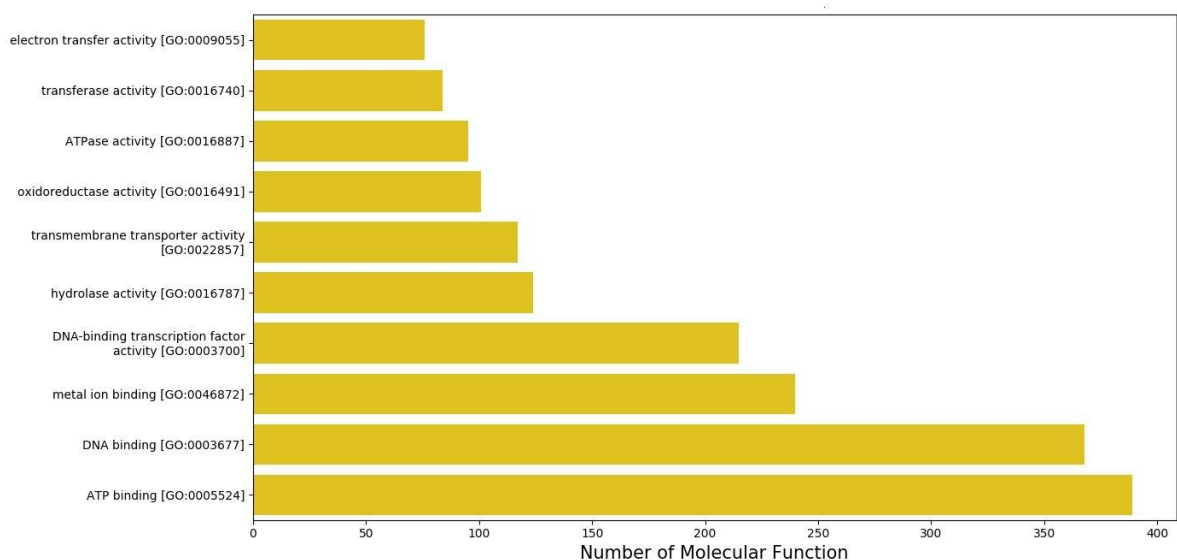


Fig. 3.17 Annotation of the genes based on their molecular function.

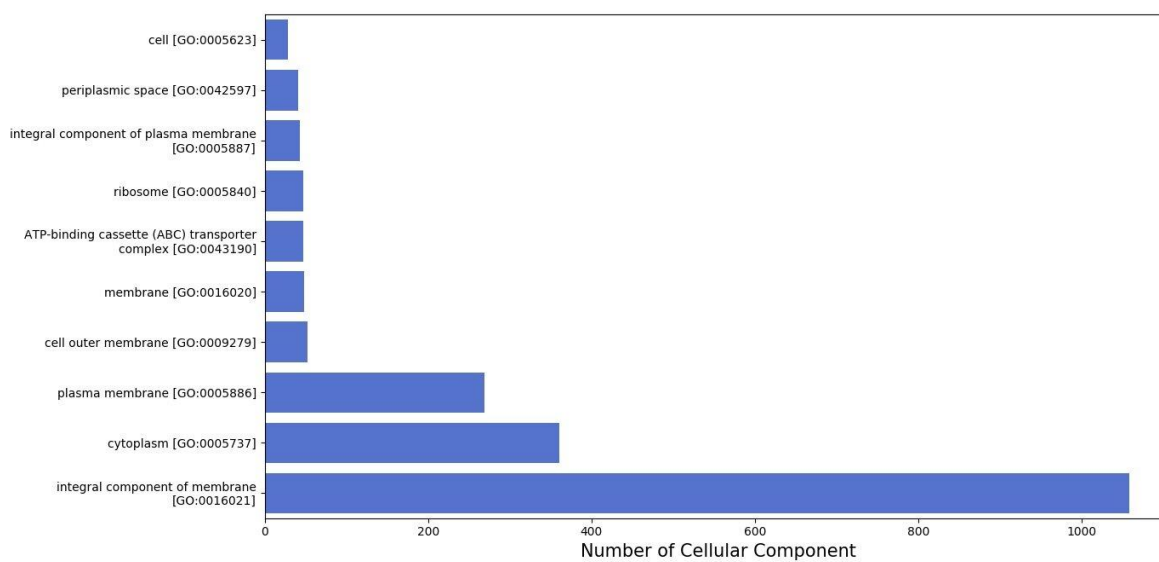


Fig. 3.18 Annotation of the genes based on their cellular component.

The gene annotation performed by RASTtk has generated the complete genome annotation of *P. mendocina* SMSKVR-3 in the form of a circular map represented in Fig. 3.19. The RASTtk annotation of the *P. mendocina* SMSKVR-3 genome has assigned subsystems

to each identified gene product or protein which is a protein group that together execute a specific biological process or form a structural complex. An overview of the subsystem has been depicted in the form of a pie chart in Fig. 3.20. Among different types of subsystems

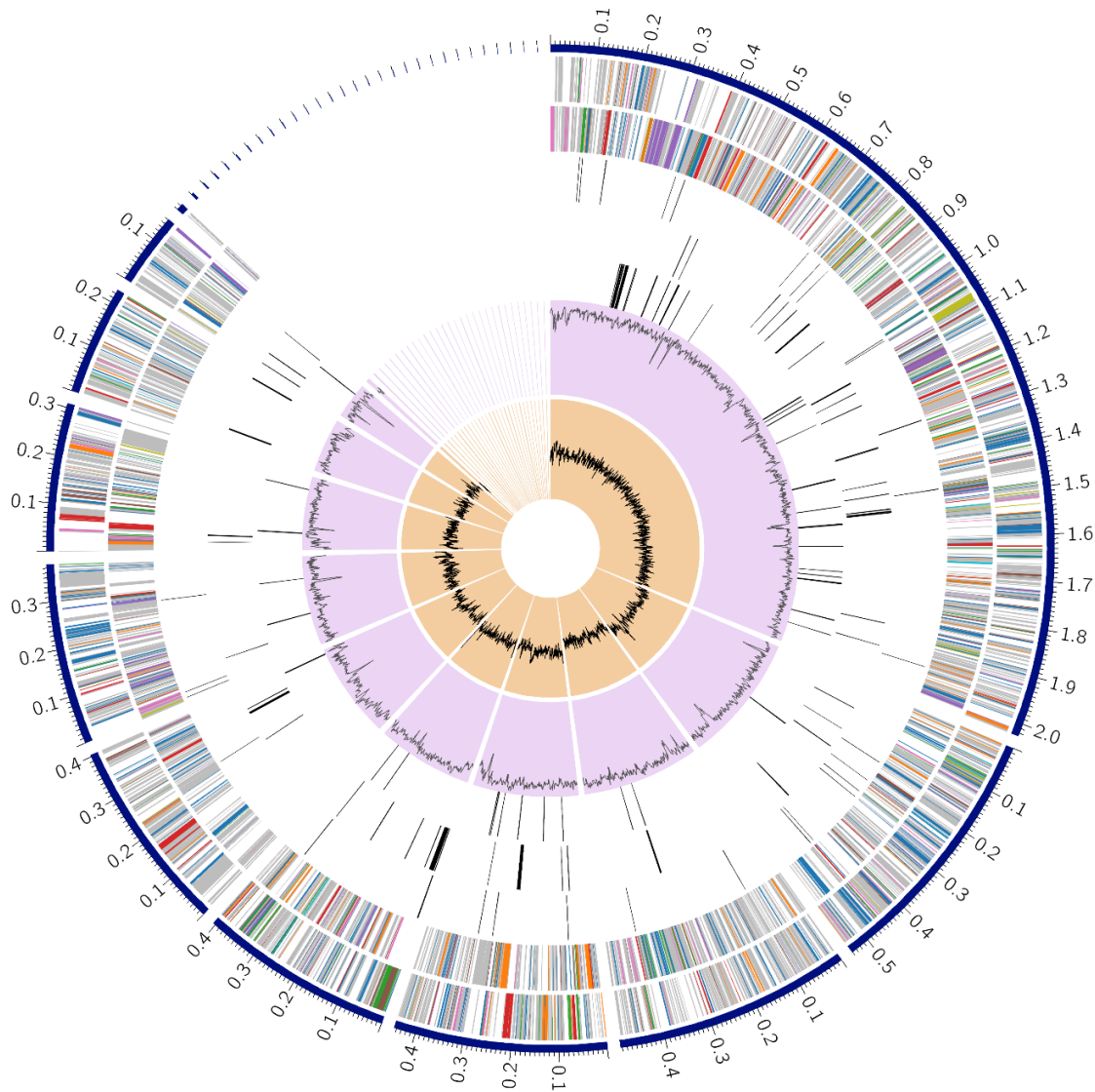


Fig. 3.19 Circular graphical representation of the complete genome annotation of the *P. mendocina* SMSKVR-3. The outer to inner rings include (1) the contigs, (2) forward strand CDS, (3) reverse strand CDS, (4) RNA genes, (5) CDS with homology to known antimicrobial resistance genes, (6) CDS with homology to known virulence factors, (7) GC content, and (8) GC skew. The circular graphical map was constructed using PATRIC (version 3.6.9).

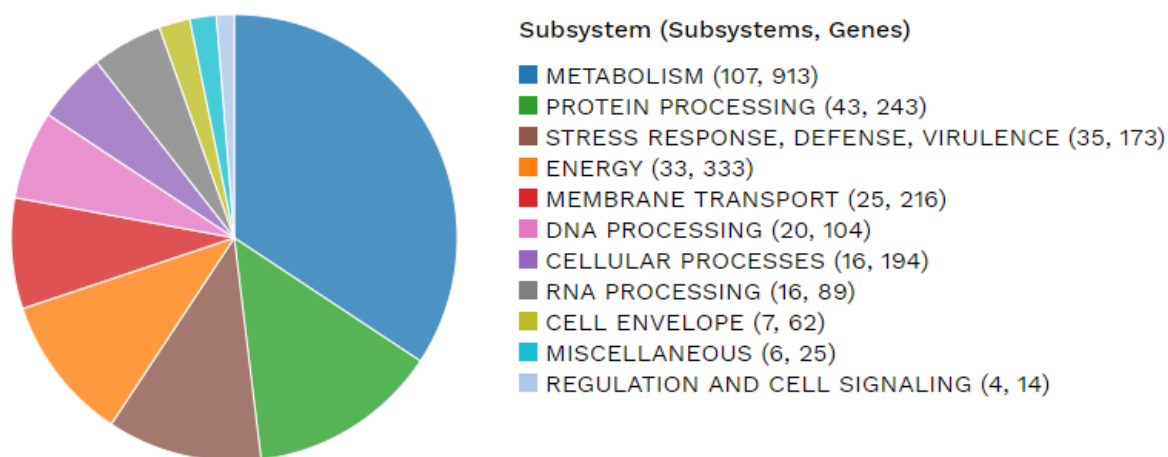


Fig. 3.20 Pie chart representing an overview of the subsystems for the *P. mendocina* SMSKVR-3 genome based on the analysis using PATRIC. The count of the subsystem and genes have been listed right side in parentheses.

found in the bacterial genome, the most abundant subsystem categories were related to (a) metabolic processes with 107 subsystems and 913 protein-coding genes followed by (b) protein processing with 43 subsystems and 243 protein-coding genes and (c) stress response, defense, and virulence having 35 subsystems and 173 protein-coding genes. The other subsystem categories included energy production; with 33 subsystems and 333 protein-coding genes, membrane transport; with 25 subsystems and 216 CDS, DNA processing; with 20 subsystems and 104 CDS, cellular processing; containing 16 subsystems and 194 CDS, RNA processing; with 16 subsystems and 89 CDS, cell envelope; with 7 subsystems and 62 CDS and regulation and cell signaling containing 4 subsystems and 14 CDS. The miscellaneous system category included 6 subsystems and 25 CDS. The larger number of genes related to stress, defense, and membrane transport indicates their possible role in *P. mendocina* SMSKVR-3 As(V) resistance.

3.6.5 Genes related to the transport of different substances across the cell

The analysis of genome sequence revealed the presence of different genes related to the transport of various types of biomolecules across the cell. The products of these genes were

divided into different subclasses and subsystems that have been shown in Table 3.6. The genome analysis exhibited the presence of the genes related to ABC transporter proteins such as MlaA, MlaB, MlaD, MlaC, MlaA, MlaE, and MlaF that are involved in the maintenance of outer membrane lipid asymmetry. Efflux ABC transporters such as YadH and YadG, glycerol ABC transporters including glycerol kinase GlpD, GlpP, GlpQ, GlpR, GlpS, GlpT, GlpU, and GlpV protein-coding genes were also found to be present. Genes coding for proteins related to different multidrug efflux pumps were also present such as LapE, MdtA, MdtB, MdtC, and OmpH belonging to tripartite multidrug efflux systems (of RND type). Other multidrug efflux pumps related genes included the genes coding for RND efflux system, inner membrane transporter, transcriptional regulator (AcrR family), RND efflux system, membrane fusion protein, MexE, MexF, OprN belonging to MexEFOprN subsystem. These multidrug efflux pumps play a very important role in the co-transport of different heavy metals (such as As) and antibiotics. Gene related to cation transporter such as CopZ, copper-translocating P-type/ (lead, cadmium, zinc, and mercury transporting) ATPase, type cbb3 cytochrome oxidase biogenesis protein CcoI, azurin, copper tolerance protein related to copper transport were exhibited in the bacterial genome. Other than these, genes involved in the uptake of potassium (TrkH, TrkA) and transport of Mg (MgtC, MgtE, CorA, CorC) were also found in the bacterial genome. The genes related to uni-, sym-, and antiporters such as Na⁺/H⁺ antiporter NhaD type and Na⁽⁺⁾ H⁽⁺⁾ antiporter subunit A/B, C, D, E, F, G belonging to multi-subunit action antiporter were also present. In addition to the above-mentioned genes, several other genes belonging to bacterial secretion systems II, IV, and VI were also reported which are the virulence factor secreted by pathogenic bacteria to invade the host cell. Type II secretion system included different proteins related to the general secretion pathway such as general secretion pathway protein GspC, GspD, GspE, GspF, GspH, GspI, GspJ, GspK, GspL, and GspM. Type IV secretion system included proteins related to pilus assembly including PilR, PilA, PilQ, PilO, PilN, PilM, PilS, PilB, PilC, PilP, PilT, multimodular transpeptidase-transglycosylase, and 3-dehydroquinate synthase leader peptidase (Prepilin peptidase)/N-methyltransferase (PilD). However, some other genes coding for multimodular transpeptidase-transglycosylase and 3-dehydroquinate synthase were also found under this subsystem. The other subsystem of this, type IV secretion system included proteins related to

conjugative transfer including VirD2, VirD4, CopG domain-containing protein, TraF, TrbB, TrbD, TrbF, TrbK TrbE, TrbC, TrbL, TrbG, TrbI, TrbJ, and TrbK. Type VI secretion system included the genes for PppA, TssA, TssB, TssC, TssE, TagF, TssG, TssM, TssL, TssK, TssF, Hcp, VgrG, PpkA, ImpI and ClpV proteins.

Table 3.6 Annotated subclasses, subsystems, and gene products related to transport.

Subclass	Subsystem	Gene products
ABC transporters	Maintenance of outer membrane lipid asymmetry	MlaA, MlaB, MlaD, MlaC, MlaA, MlaE, MlaF
	Efflux ABC transporter YadGH	YadH, YadG
	Glycerol ABC transporter	Glycerol kinase GlpD, GlpP, GlpQ, GlpR, GlpS, GlpT, GlpU, GlpV
Uni- Sym- and Antiporters	Multi-subunit cation antiporter	Na(+) H(+) antiporter subunit A/B, C, D, E, F, G
Uni- Sym- and Antiporters	Na(+) H(+) antiporter	Na+/H+ antiporter NhaD type
Multidrug efflux systems	Tripartite multidrug efflux systems (of RND type) in <i>Pseudomonas</i>	LapE, MdtA, MdtB, MdtC, OmpH,
	Multidrug resistance RND efflux system MexEFOprN	RND efflux system, inner membrane transporter, transcriptional regulator, AcrR family, RND efflux system, membrane fusion protein, MexE, MexF, OprN
Cation transporters	Magnesium transport	MgtC, MgtE, CorA, CorC
	Copper transport system	CopZ, Copper-translocating P-type/ Lead, cadmium, zinc and mercury transporting ATPase, Type cbb3 cytochrome oxidase biogenesis protein CcoI, Azurin, copper tolerance protein
	Trk and Ktr potassium uptake systems	TrkH, TrkA

Protein secretion system, Type II	General Secretion Pathway	GspC, GspD, GspE, GspF, GspH, GspI, GspJ, GspK, GspL, GspM
Protein and nucleoprotein secretion system, Type IV	Type IV pilus	PilR, PilA, PilQ, PilO, PilN, PilM, PilS, PilB, PilC, PilP, PilT, PilD, multimodular transpeptidase-transglycosylase, 3-dehydroquinase synthase
	Conjugative transfer	VirD2, VirD4, CopG domain-containing protein, TraF, TrbB, TrbD, TrbF, TrbK TrbE, TrbC, TrbJ, TrbL, TrbG, TrbI, TrbK
Protein secretion system, Type VI	Type VI secretion system	PppA, TssA, TssB, TssC, TssE, TagF, TssG, TssM, TssL, TssK, TssF, Hcp, VgrG, PpkA, ImpI, ClpV

3.6.6 Genes related to the arsenic resistance

The analysis of the subsystems of genes present in the bacterial genome revealed the occurrence of genes linked to arsenic resistance such as *gloA1*, *arsC*, *acr3*, *arsJ*, *arsR*, and *arsB*. These genes code for the proteins lactoylglutathione lyase, arsenate reductase (ArsC) (thioredoxin-coupled, LMWP family), arsenical-resistance protein (ACR3), MFS-type efflux pump ArsJ (specific for 1-arseno-3-phosphoglycerate), arsenical resistance operon repressor (ArsR), and arsenite/antimonite:H⁺ antiporter (ArsB) respectively. Gene coding for the NAD-dependent glyceraldehyde-3-phosphate dehydrogenase for arsenate detoxification also existed in the genome. All these gene products are known to provide arsenic resistance in several bacteria (Li et al., 2010; Yan et al., 2019) and are also probably involved in the higher As(V) tolerance of *P. mendocina* SMSKVR-3 which can be further verified by the proteomic studies.

The ArsC is a very important enzyme involved in the arsenic detoxification which catalyzes the reduction of As(V) to As(III) and is encoded by *ars* operon. The thioredoxin coupled ArsC catalyzes this reduction by the formation of a cascade of intramolecular thiol-disulfide (Li et al., 2007). Arsenite/antimonite:H⁺ antiporter (ArsB) is a protein that is the integral component of the membrane and involved in the efflux of the As(III) and antimonite

either based on the protein electrochemical gradient or by hydrolyzing ATP while coupled with ArsA (Achour et al., 2007). The *arsR* gene of *ars* operon encodes a regulatory protein ArsR which is a repressor and controls the expression of *ars* operon (Shi & Rosen, 1996). Various studies have shown that in bacteria the efflux of arsenic is mediated by two types of transporters family. The first one is ArsB which has already been described in the earlier sections and the other one is a less studied ACR3 family transporter that exhibit similarity with the yeast *Saccharomyces cerevisiae* ACR3 transporter and is involved in the efflux of As(III) utilizing proton-motive force (Xia et al., 2008). The NADPH-flavin mononucleotide (FMN)-dependent oxidoreductases (ArsH) catalyzes the oxidation of trivalent organoarsenicals such as methylarsenite [MAs(III)], aromatic arsenicals phenylarsenite [PhAs(III)], and trivalent roxarsone [Rox(III)] (Yang & Rosen, 2016). Various arsenic resistance operon contains two genes having unknown functions which include *gapdh* that encodes NAD-dependent glyceraldehyde-3-phosphate dehydrogenase and *arsJ* encoding major facilitator superfamily (MFS) protein. Both of these genes confer resistance to As(V). One study has proposed a new pathway of As(V) resistance representing ArsJ to be an efflux permease that pumps organoarsenical 1-arseno-3-phosphoglycerate (1As3PGA) out of the cell (Chen et al., 2016). The lactoylglutathione lyase (*gloA1*) is shown to be involved in the detoxification of methylglyoxal (MG). Its role in arsenic resistance is not known but it is categorized under the arsenic resistance system based on the annotation.

Table 3.7 Genes related to arsenic resistance in *P. mendocina* SMSKVR-3 genome.

S. No.	Name of the gene product	Gene
1.	Arsenate reductase thioredoxin-coupled, LMWP family	<i>arsC</i>
2.	Arsenical-resistance protein ACR3	<i>acr3</i>
3.	MFS-type efflux pump ArsJ specific for 1-arseno-3-phosphoglycerate	<i>arsJ</i>
4.	Arsenical resistance operon repressor (ArsR)	<i>arsR</i>
5.	NAD-dependent glyceraldehyde-3-phosphate dehydrogenase for arsenate detoxification	<i>gapdh</i>
6.	Arsenite/antimonite:H ⁺ antiporter (ArsB)	<i>arsB</i>
7.	Lactoylglutathione lyase	<i>gloA1</i>

3.7 Analysis of differential protein expression in *P. mendocina* SMSKVR-3 using 2-DGE

3.7.1 SDS-PAGE analysis of the protein expression under arsenate stress

The protein expression in *P. mendocina* SMSKVR-3 was studied using the SDS-PAGE (12% resolving gel) analysis under arsenate untreated (control) and treated conditions at different time points (at 0, 4, 8, 16, and 24 hours). The protein expression profile of the bacteria under As(V) treated condition at 0 h was same as the control condition where no significant change in the protein expression was observed. However, a significant change in the protein expression was observed from 4 h to 24 h of As(V) treatment. The treatment of bacteria with As(V) for 4 h exhibited the under-expression of 18 and over-expression of 3 protein bands as compared to the control sample which is shown in Fig. 3.21b. At the 8 h of As(V) treatment, 6 protein bands showed under-expression, and 14 protein bands showed over-expression which was the highest number of over-expressed protein bands in this study. The number of under-expressed protein bands was lesser than the over-expressed ones where the molecular weights of the three protein bands ranged between 30-40 kDa, however, the remaining three protein bands had the molecular weight of ~25, ~60, and ~100 kDa. Among the fourteen over-expressed protein bands, the molecular weight of three protein bands ranged from 215-20 kDa, three bands were in the range of 25-30 kDa, four bands had the molecular weight range of 30-50 kDa and four protein bands showed a range from 60-100 kDa (Fig 3.21c). When *P. mendocina* SMSKVR-3 was exposed to As(V) for 16 h, thirteen protein bands showed under-expression and four protein bands exhibited over-expression (Fig 3.21d). The protein expression profile of the 24 h sample showed under- and over-expression of 9 and 3 protein bands, respectively (Fig 3.21d). The result of protein expression analysis using SDS-PAGE showing under- and over-expressed protein bands has been summarized in Fig. 3.22.

The earlier studies on the protein expression profiles of prokaryotes under heavy metal stress have proposed the role of various intracellular proteins in heavy metal resistance which either get upregulated/over-expressed or are specifically expressed under the metal stress. In addition to these, many proteins exhibit downregulation/under-expression. The SDS-PAGE profile of protein expression in As(V) treated *Staphylococcus* sp. strain NBRIEAG-8 exhibit-

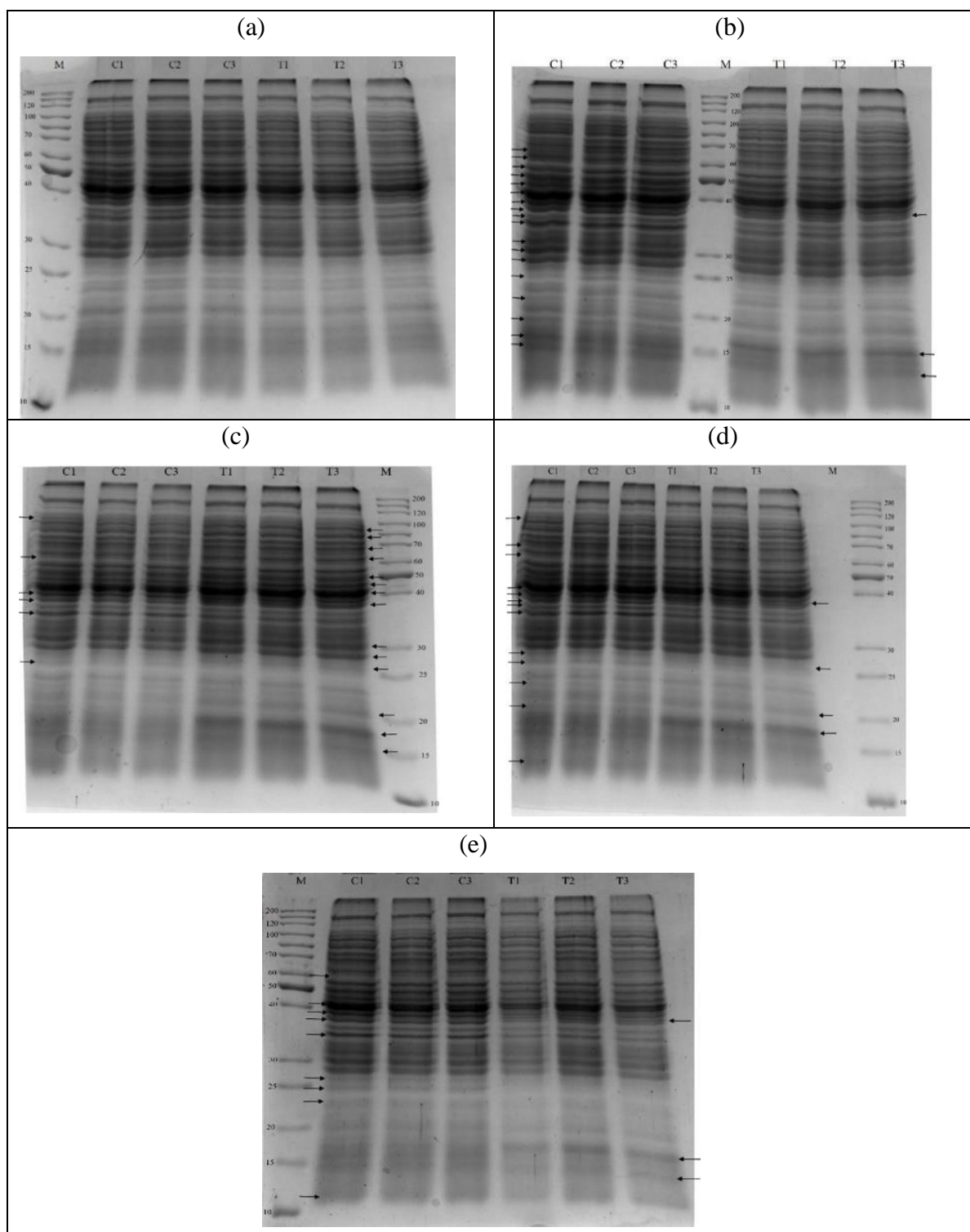


Fig. 3.21 Study of protein expression in *P. mendocina* SMSKVR-3 at (a) 0 h, (b) 4 h, (c) 8 h, (d) 16 h, and (e) 24 h under arsenate untreated (control; C1, C2 and C3) and 300 mM As(V) treated (Treated; T1, T2 and T3) condition.

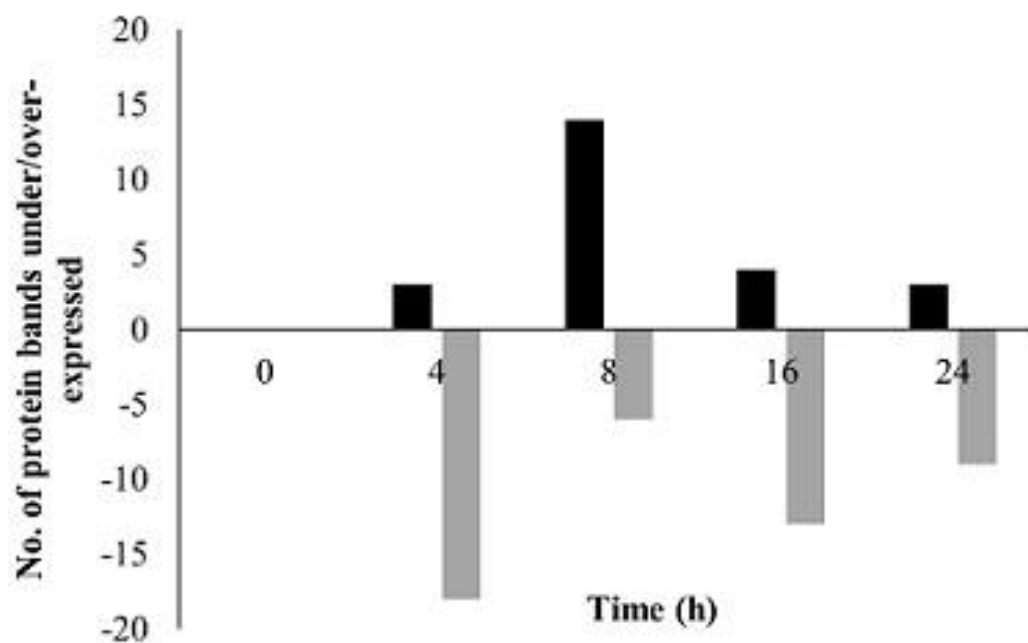


Fig. 3.22 Graphical representation of the SDS-PAGE analysis of the proteins over-expressed and under-expressed at different time intervals under As(V) treated condition in *P. mendocina* SMSKVR-3.

ed a significant change in the protein profile showing over-expression (Srivastava et al., 2012). On the other hand, the wild type and the arsenic-adapted *Aeromonas hydrophila* revealed no significant change in the protein expression profile till the late-log phase. However, the arsenic-adapted bacteria displayed the expression of two unique proteins having an approximate molecular weight of 85 kDa and 79 kDa indicating their role in the arsenic resistance mechanisms of this bacteria (Goswami et al., 2011). Recently, a similar protein expression study conducted on the arsenic resistant *M. luteus* strain AS2 under As(V) stress, has exhibited the upregulation of proteins under the molecular weight range of 34-60 kDa possibly playing a role in As(III) resistance (Sher et al., 2020).

Similarly, in the present study, *P. mendocina* SMSKVR-3 isolated from the khetri copper mines has also revealed the over-expression as well as the exclusive expression of several proteins under As(V) stress at the treatment times of 4 h-24 h. The approximate molecular weight of these proteins was ranged between 15-100 kDa. This indicates the

presence of protein-mediated As(V) resistance mechanisms in this bacteria. Based on the observation of SDS-PAGE-protein expression analysis, 8 hour exposure time for As(V) was selected for the further analysis of protein expression in *P. mendocina* SMSKVR-3.

3.7.2 Analysis of the effect of different arsenate concentrations on the protein expression profile

In order to optimize the concentration of As(V) required to cause a significant change in the proteomic profile of bacteria, the protein expression profile of *P. mendocina* SMSKVR-3 upon 8 h As(V) exposure was studied. The protein expression profile analyzed on 12% SDS-PAGE gel exhibited a significant change in the expression of proteins after treatment with the 200 and 300 mM of As(V) as compared to the untreated control. However, at the As(V) concentrations below 200 mM, the expression pattern was same as the control sample (Fig. 3.23). This result exhibited the requirement of As(V) concentration either 200 mM or greater to obtain the significant changes in the protein expression.

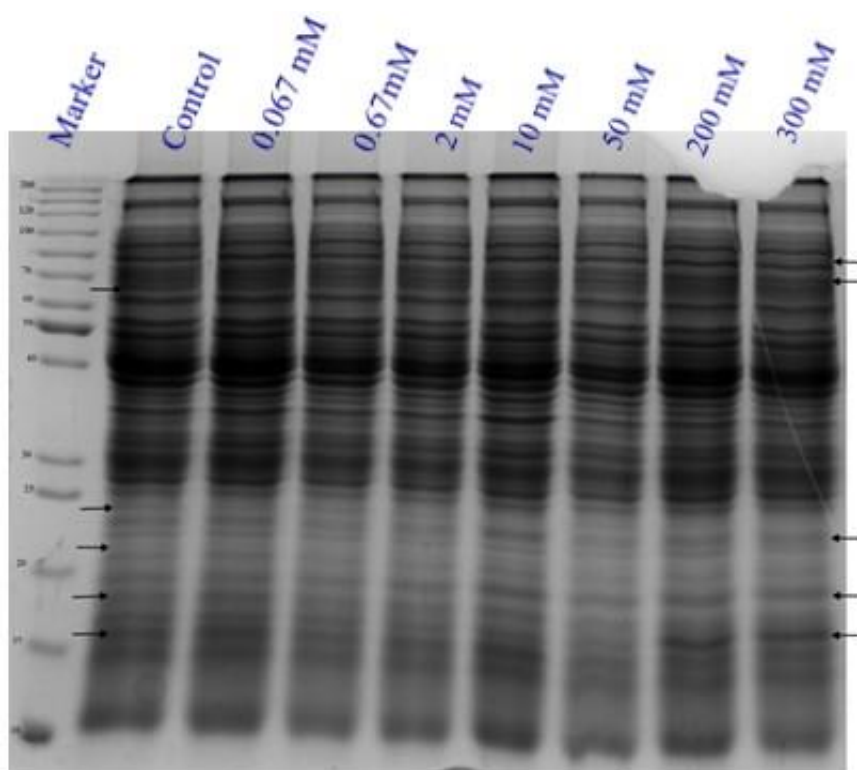


Fig. 3.23 SDS- PAGE analysis of the protein expression in *P. mendocina* SMSKVR-3 under the increasing concentration of As(V).

3.7.3 Analysis of protein expression using two-dimensional gel electrophoresis (2-DGE)

Any kind of alteration in the surrounding environmental conditions may affect the cellular response of bacteria, reflecting changes in the protein expression profile (Daware et al., 2012). The presence of As(V) in the external environment of bacteria may result in a protein profile with altered expressions which can be further explored to get significant information about the proteins responsible for As(V) resistance. The protein expression study of *P. mendocina* SMSKVR-3 by the SDS PAGE analysis has witnessed the change in the expression of proteins under As(V) stress. However, SDS-PAGE analysis does not provide detailed information about the protein expression change as the separation of protein is based on its molecular weight alone. Thus, a 2-DGE analysis was performed to understand the As(V)-induced changes in the protein expression in more detail. For 2-DGE analysis, the protein extracts obtained from the bacteria after the treatment with 300 mM As(V) for the 8 h (treated) and without the As(V) treatment (control) were selected. The result of 2-DGE has been represented in Fig. 3.24a and b. A total of 296 and 320 protein spots were obtained after the

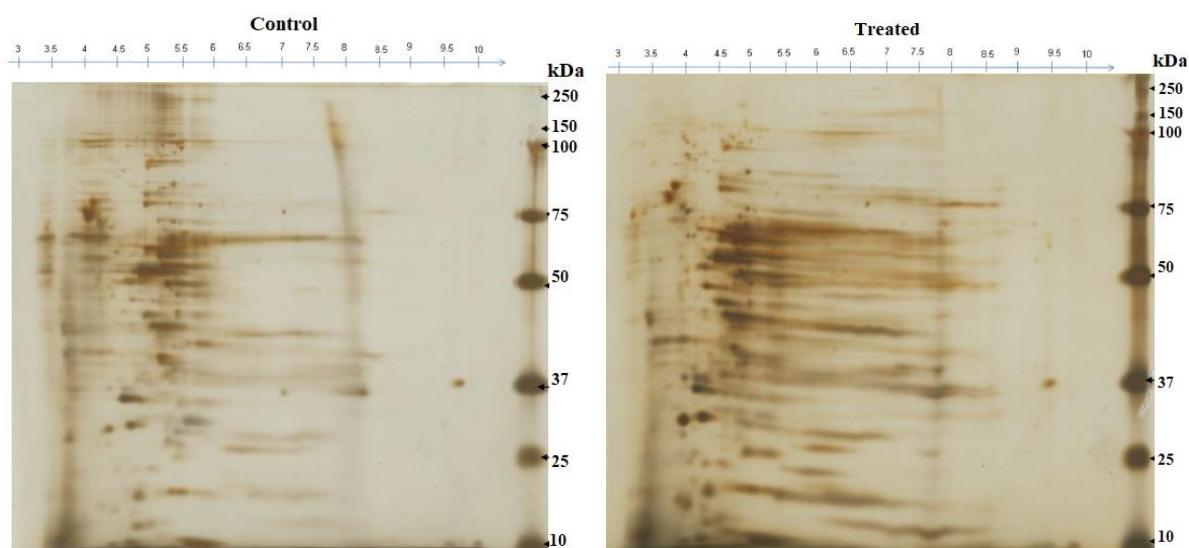


Fig. 3.24 Analysis of protein expression in *P. mendocina* SMSKVR-3 using 2-DGE without As(V) treatment (control) (a), and with 300 mM As(V) treatment (b).

image analysis of the 2-DGE-gels of control and As(V) treated samples having the molecular weight and isoelectric point (pI) ranges of 10-250 kDa and 3-10, respectively. Among all the protein spots observed, the expression of 83 protein bands remained unchanged upon the

treatment with As(V). The 122 (41.22%) and 146 (45.77%) protein spots were unique to control and treated samples, respectively (Fig. 3.25). However, 91 (28.53%) protein spots exhibited differential expression among which 46 showed over-expression while 45 protein spots showed under-expression upon As(V) treatment (Fig. 3.26a and b). Fig. 3.27a, b, and c summarize the overall results of the 2-DGE analysis.

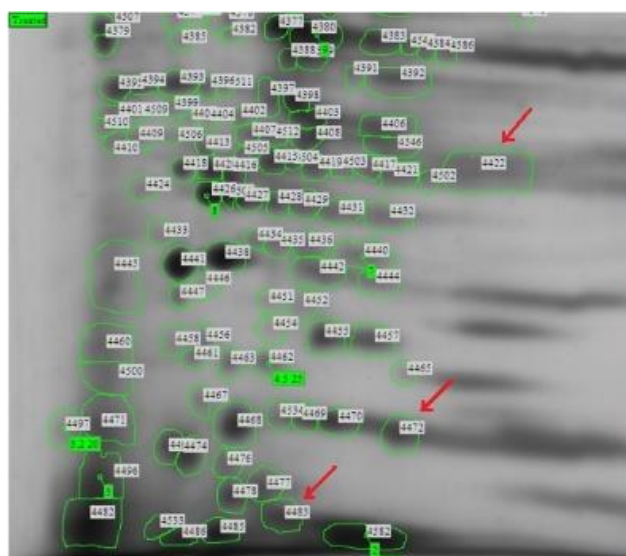
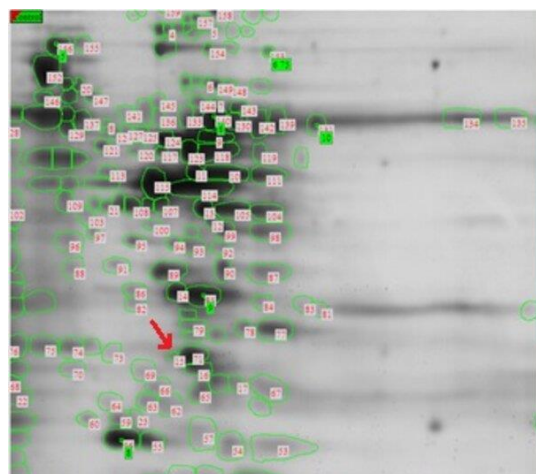


Fig. 3.25 2-DGE gel images showing uniquely expressed proteins in the sample treated with 300 mM arsenate after analysis using Image Master 2D Platinum 7.0 software.

(a)



(b)

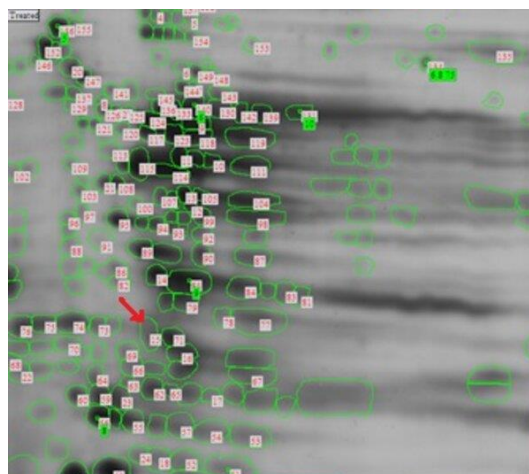
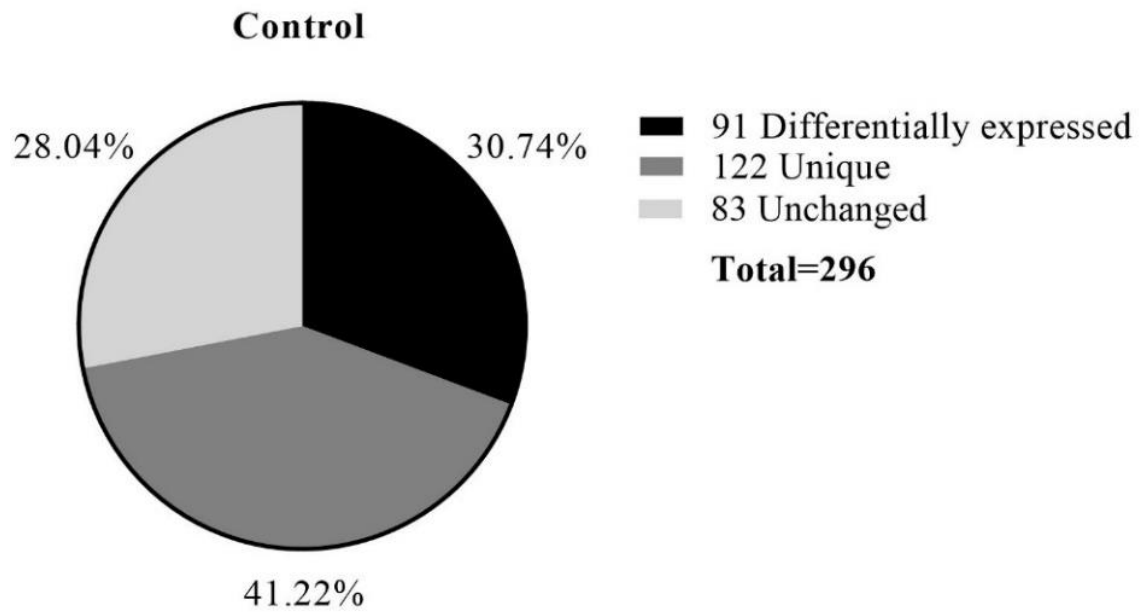
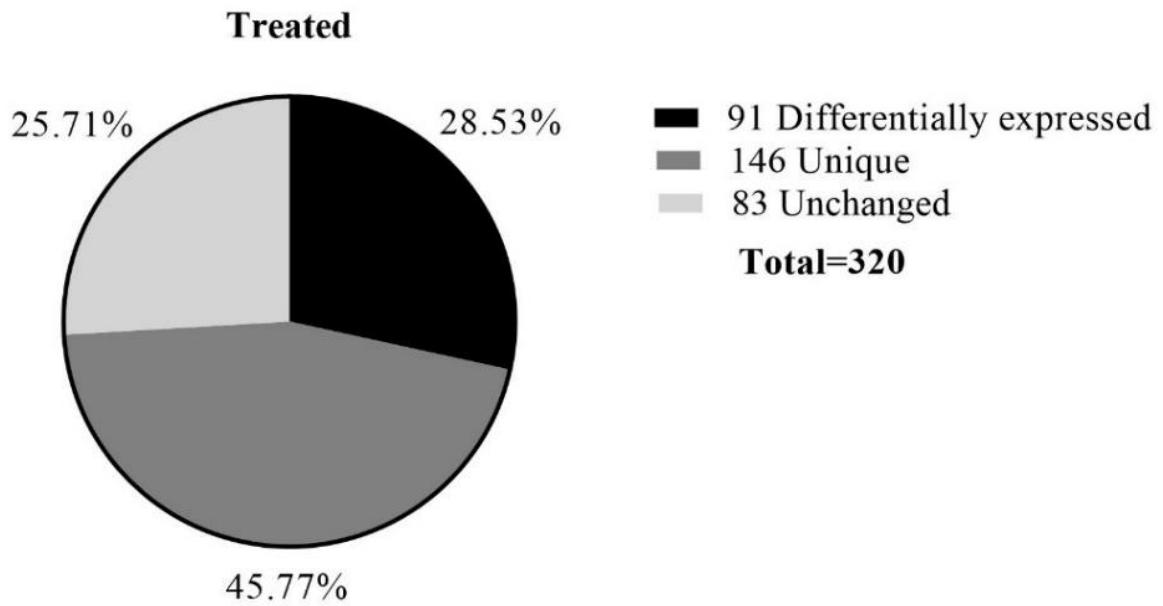


Fig. 3.26 2-DGE gels showing differentially expressed protein in (a) control (without arsenate), and (b) treated (300 mM arsenate) samples after analysis using Image Master 2D Platinum 7.0 software.

(a)



(b)



(c)

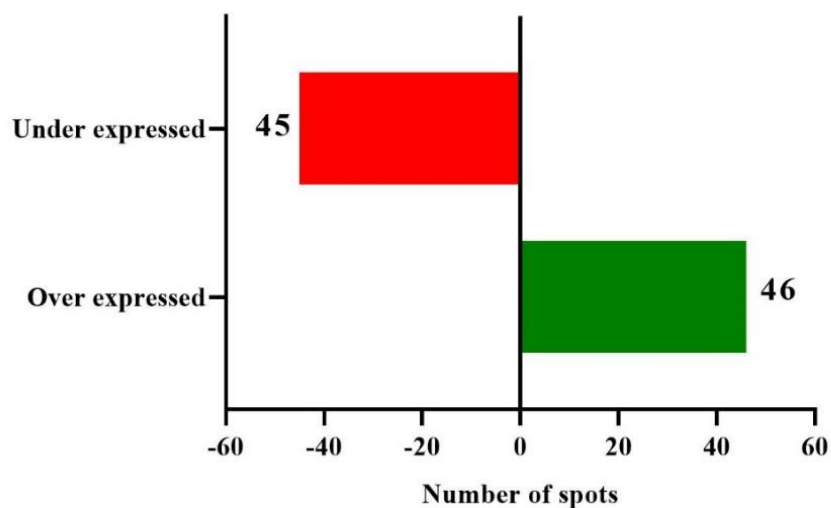


Fig. 3.27 Expression-based categorization of proteins under the (a) control, and (b) treated (300 mM arsenate) conditions in the form of the pie charts; (c) graphical representation of the differentially expressed proteins under 300 mM arsenate treatment.

The levels of expression of proteins expressed exclusively in the control or the As(V) treated sample were represented in the graph as the % volume (Fig. 3.28a and b). Spot 4422 showed the highest % volume (2.539%) among all the unique protein spots obtained in As(V) treated sample. It was successively followed by the % volume of 1.846, 1.204, 1.084, and 1.029% that were exhibited by spots 4445, 4472, 4414, and 4483 respectively. The comparative study of differentially expressed proteins in As(V) treated and control sample revealed highest over-expression of match spot-15 (spot ID-4397) that was represented in terms of fold expression and obtained to be 16.49. It was followed by fold expressions of 6.57, 6.33, 5.30, and 5.05 that were shown by match spot-84, 23, 24, and 19, respectively. The graphical representation of the fold expression change and the heat map comparing the % volume of the differentially expressed proteins has been represented in Fig. 3.29a and b, respectively.

Based on the result of 2-DGE some of the treated-specific protein spots including 4422, 4472, and 4483 (showing higher % volume), and one highly over-expressed spot 4397 (match ID-15) were selected for their characterization using MALDI-TOF/TOF MS analysis.

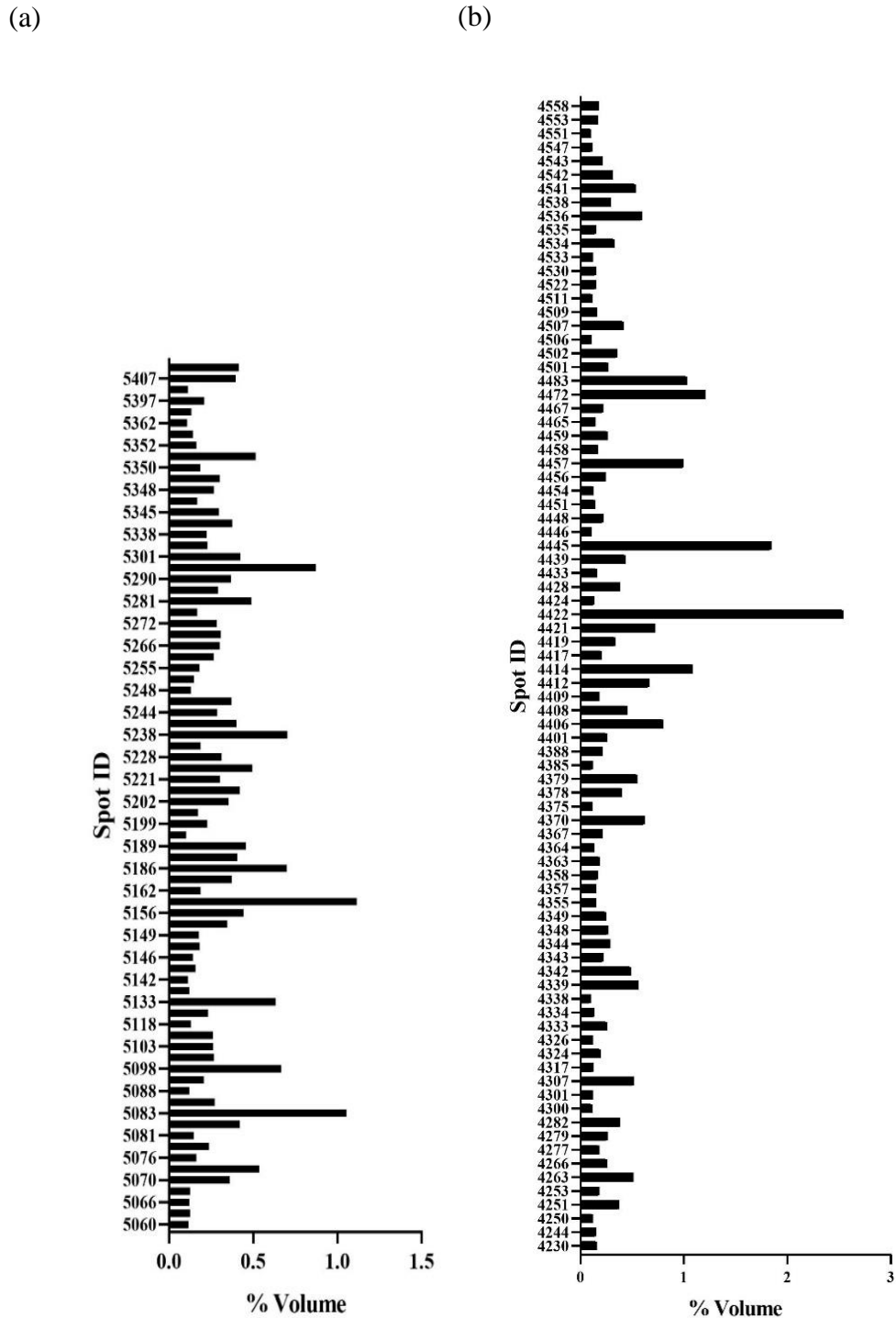
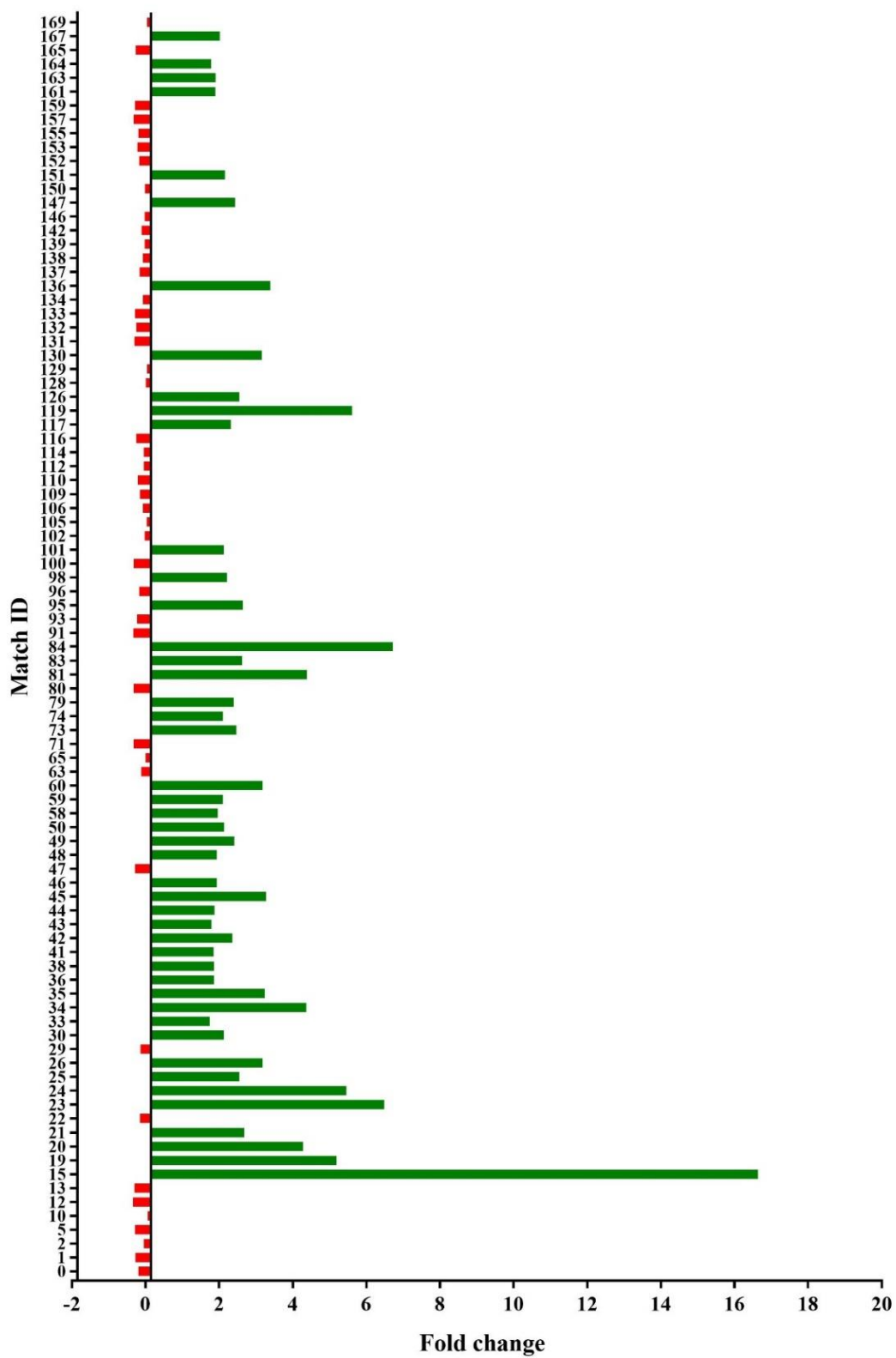


Fig. 3.28 Protein spots expressed exclusively in (a) untreated (control), and (b) 300 mM arsenate treated condition represented in terms of % volume (only % volume ≥ 0.1 has been considered).

(a)



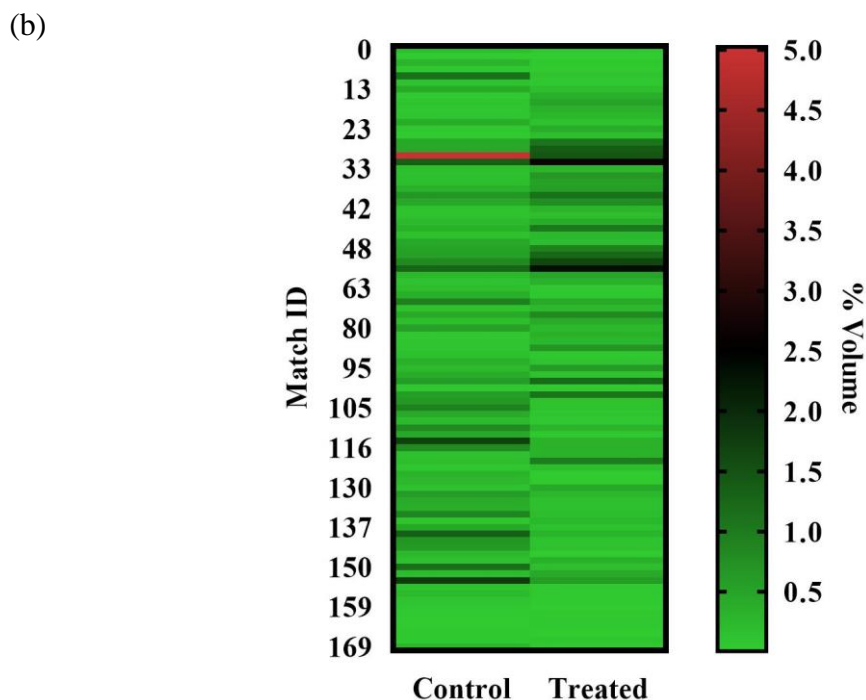


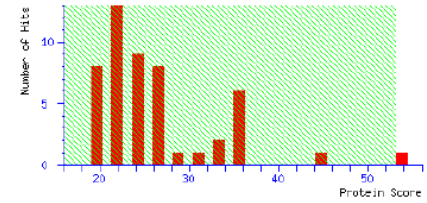
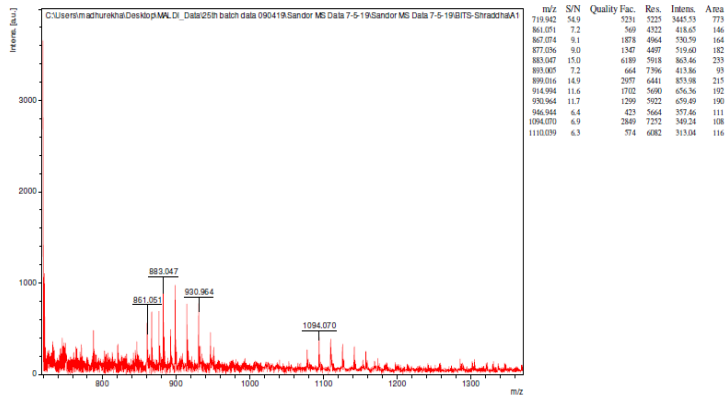
Fig. 3.29 Graphical representation of the under-expressed or over-expressed protein spot in arsenate treated sample in comparison to control sample in terms of fold change (a); over-expression and under-expression of proteins in As(V) treated sample in comparison to control represented as a heat map (b).

It was followed by their identification using MASCOT search to understand their role in arsenate resistance in *P. mendocina* SMSKVR-3.

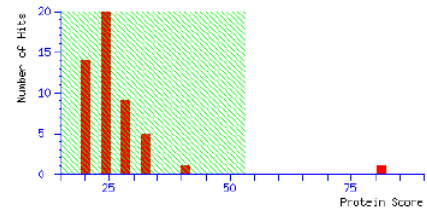
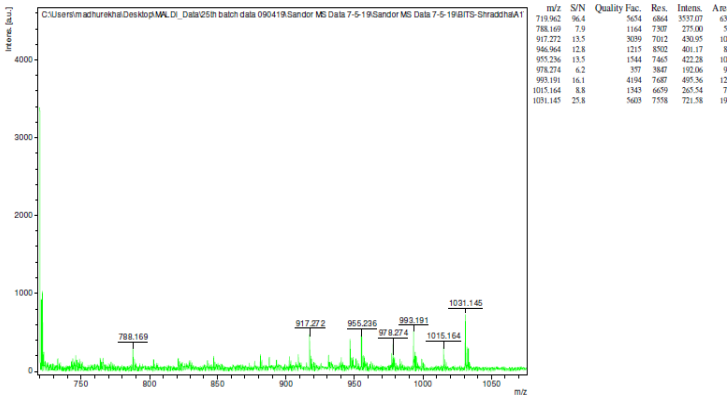
3.7.4 Analysis of the selected protein spots using MALDI-TOF/TOF MS and MASCOT

Based on the higher expression values the characterization of four 2-DGE protein spots 4422, 4472, 4483, and 4397 (match ID-15) was performed using MALDI-TOF/TOF MS analysis. The identification of protein from the MALDI-TOF/TOF MS data was performed using MASCOT search against the primary sequence database of the proteins (Fig. 3.30a to d). The information about the identified proteins has been summarized in Table 3.8. The MASCOT analysis revealed the similarity of protein spot 4472 with the ribosome-recycling factor having the molecular weight and MASCOT scores of 0.134 kDa and 54, respectively (falling under the acceptable limit of MASCOT score). The Match spot-15 showed the highest fold over-expression upon the As(V) treatment, matching with a 40.877 kDa protein polyphosphate:

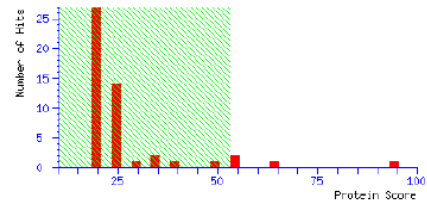
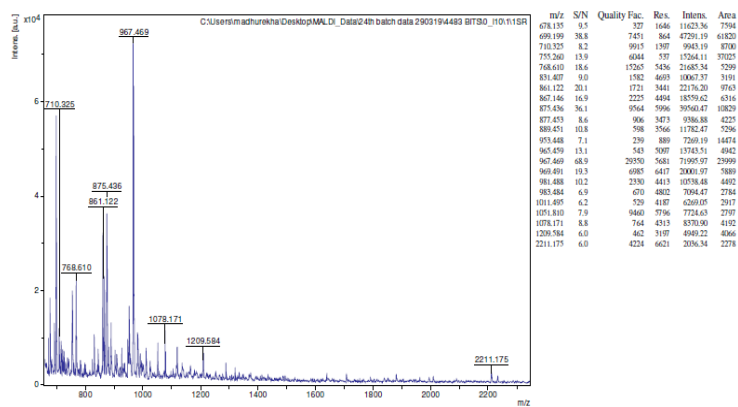
(a)



(b)



(c)



(d)

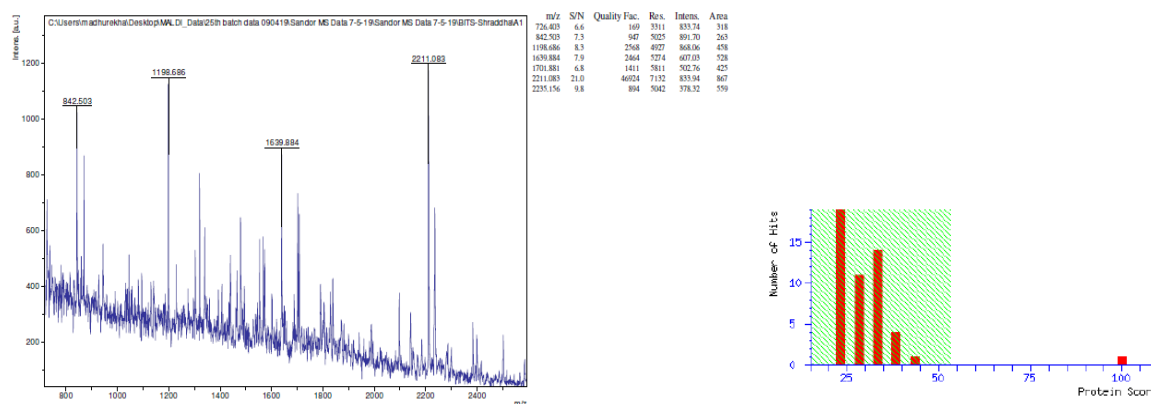


Fig. 3.30 MALDI-TOF/TOF MS spectra and MASCOT histogram plot of the selected spot (a) 4472, (b) match spot 15, (c) 4483, and (d) 4422. In the MASCOT histogram plot, a protein score of >50 is considered as a significant score ($p < 0.05$).

Table 3.8 Identification of selected protein spots using MALDI-TOF/TOF MS analysis followed by MASCOT database search.

Spot/Match ID	Protein Match	Organism Name	Accession	Score	Mass (kDa)
4472	Ribosome-recycling factor	<i>Pseudomonas entomophila</i> (strain L48)	RRF_PSEE4	54	20.134
4397/15	Polyphosphate: ADP/GDP phosphotransferase	<i>Pseudomonas aeruginosa</i> (strain ATCC 15692 / DSM 22644 / CIP 104116 / JCM 14847)	PK21A_PSEAE	81	40.877
4483	Ribonuclease P protein component	<i>Pseudomonas putida</i> (strain GB-1)	RNPA_PSEPG	94	14.958
4422	Cobalt-precorrin-5B C(1)-methyltransferase	<i>Pseudomonas aeruginosa</i> (strain PA7)	CBID_PSEA7	100	38.434

The MASCOT server threshold significance level was set up at $P \leq 0.05$ for a random hit; score ≥ 50 was taken as a significant match/score that indicates extensive homology or identity.

ADP/GDP phosphotransferase with a MASCOT score of 81. The unique protein spot 4483 was identified as the ribonuclease P (RNase P) protein component having the molecular weight and MASCOT score of 14.958 kDa and 94, respectively. The treated-specific protein spot 4422 was identified as cobalt-precorrin-5B C(1)-methyltransferase (38.434 kDa) with the highest MASCOT score of 100. All these proteins, expressed by *P. mendocina* SMSKVR-3, play a potential role in the As(V) resistance which are as follow:

1) Ribosome recycling factor: The spot 4472 that showed the highest similarity to the ribosome recycling factor is involved in the dissociation of post-termination complex that plays an important role in the translation process (Inokuchi et al., 2000). It separates the small 30S and large 50S subunits of the 70S ribosomal complex and influences the release of mRNA and tRNA from the post-translational complex (Chen et al., 2017).

2) Polyphosphate: ADP/GDP phosphotransferase: The highly over-expressed spot (match ID-15) was identified as polyphosphate: ADP/GDP phosphotransferase (PPK2). In *E. coli*, PPK2 is known to play a crucial role in heavy metals tolerance by converting ADP/GDP to ATP/GTP using polyP as the donor of the phosphate group. The degradation of polyPs inside the cell is carried out with the help of polyphosphates enzyme (PPX) which leads to the intracellular metal precipitation or the efflux of the metal-phosphate complex by phosphate specific transporters (Keasling & Hupf, 1996; Nocek et al., 2018). The role of inorganic phosphate transport system which is also involved in the efflux of metal-phosphate complex has been reported in the uptake of divalent metal ions and phosphate in *E. coli* and *A. johnsonii* 210A. This flow of the metals in and outside of the cell creates a proton motive force (PMF) which balances the intracellular metal ion concentration. It also helps the cell to tolerate metal toxicity by throwing it out of the cell (Van Veen et al., 1994). These studies suggest the role of PPK2 in bacterial metal resistance either by generating the energy using polyPs or by producing polyPs which help in the removal of metal. The upregulation of this enzyme in the *P. mendocina* SMSKVR-3 under As(V) stress suggests its role in the As(V) resistance. The polyP mediated removal of As(V) in *P. mendocina* SMSKVR-3 has already been discussed in the previous study mentioned in section 3.5.5. Thus, based on all these findings it can be concluded that polyP bodies are involved in *P. mendocina* SMSKVR-3 As(V) resistance.

3) Ribonuclease P protein (RnaseP): The treated specific spot 4483 has been identified as ribozyme RNase P. It is found in almost all the prokaryotes and eukaryotes and involved in the cleavage of 5'- leader sequences from the precursor tRNA. The RNase P consists of two subunits including one large RNA subunit consisting of 340-420 nt (PvRNA) and a small subunit, containing RnpA protein having a molecular weight of 14 kDa (Jarrous, 2017; Klemm et al., 2016; Marquez et al., 2006). The direct role of RnaseP in bacterial metal tolerance is unknown. However, it might be involved in the stable mature tRNA formation playing an indirect role in the metal resistance.

4) Cobalt-precorrin-5B C(1)-methyltransferase (CbiD)- The unique spot 4422 (having the highest % volume among all the unique spots present in the As(V) treated sample) was identified as CbiD. The CbiD enzyme is known to catalyze the formation of CbiD-6A, an intermediate component of the vitamin B12 synthesis pathway. The mechanism by which CbiD provides metal resistance in the bacteria is still unknown. However, many studies have shown the role of vitamin B12 in metal resistance. It helps the bacteria to grow in the highly acidic and metal-containing environment that otherwise causes oxidative stress inside the cells (Ferrer et al., 2016). Based on the above finding, the indirect role of CbiD in *P. mendocina* SMSKVR-3 As(V) resistance has been suggested involving the increased synthesis of bacterial vitamin B12 under As(V) stress.

Based on the identification and characterization of all the selected protein spots that were either exclusively or over-expressed in the As(V)-treated sample it can be concluded that PPK2, RnaseP, CbiD, and ribosome recycling factor help *P. mendocina* SMSKVR-3 to survive in the presence of 300 mM As(V).

3.8 Analysis of the whole-cell proteins under arsenate stress

The protein expression analysis of *P. mendocina* SMSKVR-3 under As(V) stress using 2-DGE exhibited the expression of some proteins playing an indirect role in As(V) resistance. However, our study focuses on the study of As(V) resistance mechanisms of *P. mendocina* SMSKVR-3 involving arsenic-induced and arsenic binding proteins as well as the identification of candidate proteins for the development of As(V)-specific biosensor and bioremediation strategy. For this purpose, it is required to get an in-depth view of the bacterial

proteome under As(V) stress which cannot be achieved by 2-DGE. Thus, the whole-cell proteomic study of *P. mendocina* SMSKVR-3 under As(V) unstressed and stressed conditions was performed.

3.8.1 Overall result of the proteomic study

The whole-cell proteomic study involved the LC-MS/MS analysis of the total cellular proteins to elucidate the changes in the proteome of *P. mendocina* SMSKVR-3 under As(V) stress and to identify the proteins involved in As(V) resistance. The proteomic analysis of *P. mendocina* SMSKVR-3 under As(V) stressed and unstressed condition (control) resulted in the identification of overall 1557 protein groups, 6882 proteins, and 10109 peptides. Among all these proteins, 281 (4.3%) were specifically expressed in As(V) treated sample, 4957 (75%) were common in the control and As(V) treated sample (differentially expressed), and 1367 (20.7%) proteins were specifically expressed in the control sample (Fig. 3.31).

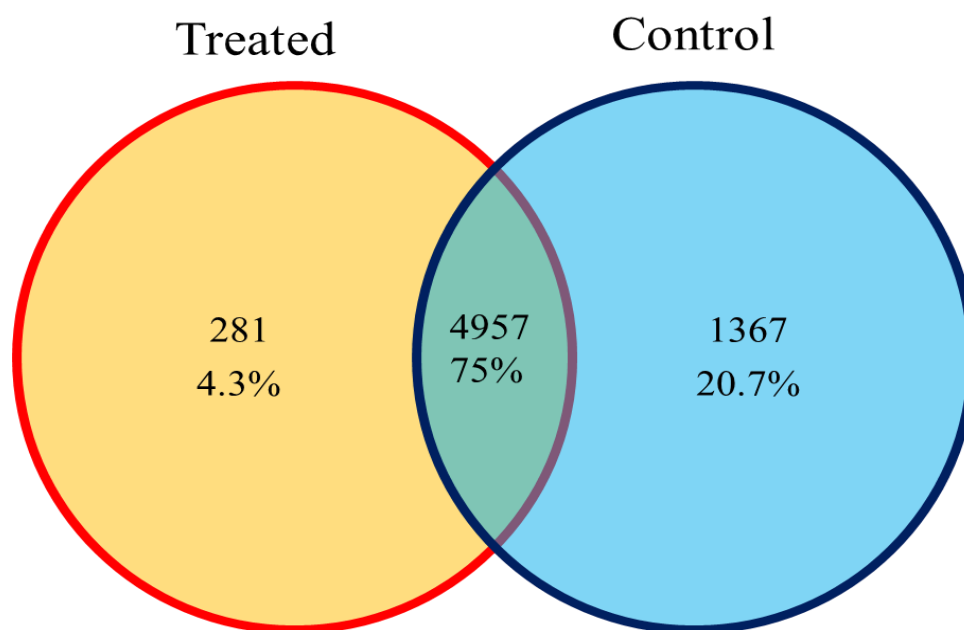


Fig. 3.31 Venn diagram of the total identified proteins in *P. mendocina* SMSKVR-3 under 300 mM As(V) treated and control (untreated) conditions.

The effect of As(V) treatment on the bacterial proteome was analyzed by evaluating the proteins specifically expressed in the control and treated samples along with the proteins showing differential expression. The functional annotation of all the identified proteins was carried out by the PANNZER2 annotation tool based on which the proteins were classified in biological process, molecular function, and cellular component functional groups. Under each functional group, they were further divided into different sub-groups to understand their characteristics more clearly.

3.8.2 Proteins specifically expressed in the control sample

The control sample-specific proteins included the proteins that are expressed in the absence of As(V) and are required for the growth and survival of bacteria under normal conditions. The annotation of all the control-specific proteins based on the biological process functional group has been shown in the form of a pie chart in Fig. 3.32a which represents the majority of the proteins (28.09%) to be unannotated. The major portion of the annotated proteins showed biological function such as metabolic activity (amino acid, nucleotide, vitamin, and other biological compounds), transcription, translation, ion transport, phosphorylation and dephosphorylation, protein targeting, proteolysis, and signaling. Other than these, proteins involved in cell wall synthesis, cell motility, chemotaxis, biofilm formation, pathogenesis, antibiotic biosynthesis, degradation of the aromatic compound, stress response, and defense were also expressed in the control. Among all the control-specific proteins, 5.19% were uncharacterized. The molecular function based annotation revealed that amongst the expressed proteins, a major fraction represents the catalytic function (48.43%) followed by unannotated proteins (19.46%), and proteins having binding properties (such as metal ion, heme, polyamine, transcription factor, Fe-S cluster, nucleotide, DNA, and RNA binding) (14.41%). Other categories included proteins having kinase, ligase, receptor, transducer, and transporter activities. However, 5.19% of proteins were uncharacterized (Fig. 3.32b). In the cellular component functional group, the majority of the proteins were unannotated (50.70%) followed by 21.80% of membrane proteins, 14.41% of cytoplasmic proteins, and 5.19% of uncharacterized proteins. Other proteins belonging to nucleoid, periplasmic space, and organelle were also observed (Fig. 3.32c).

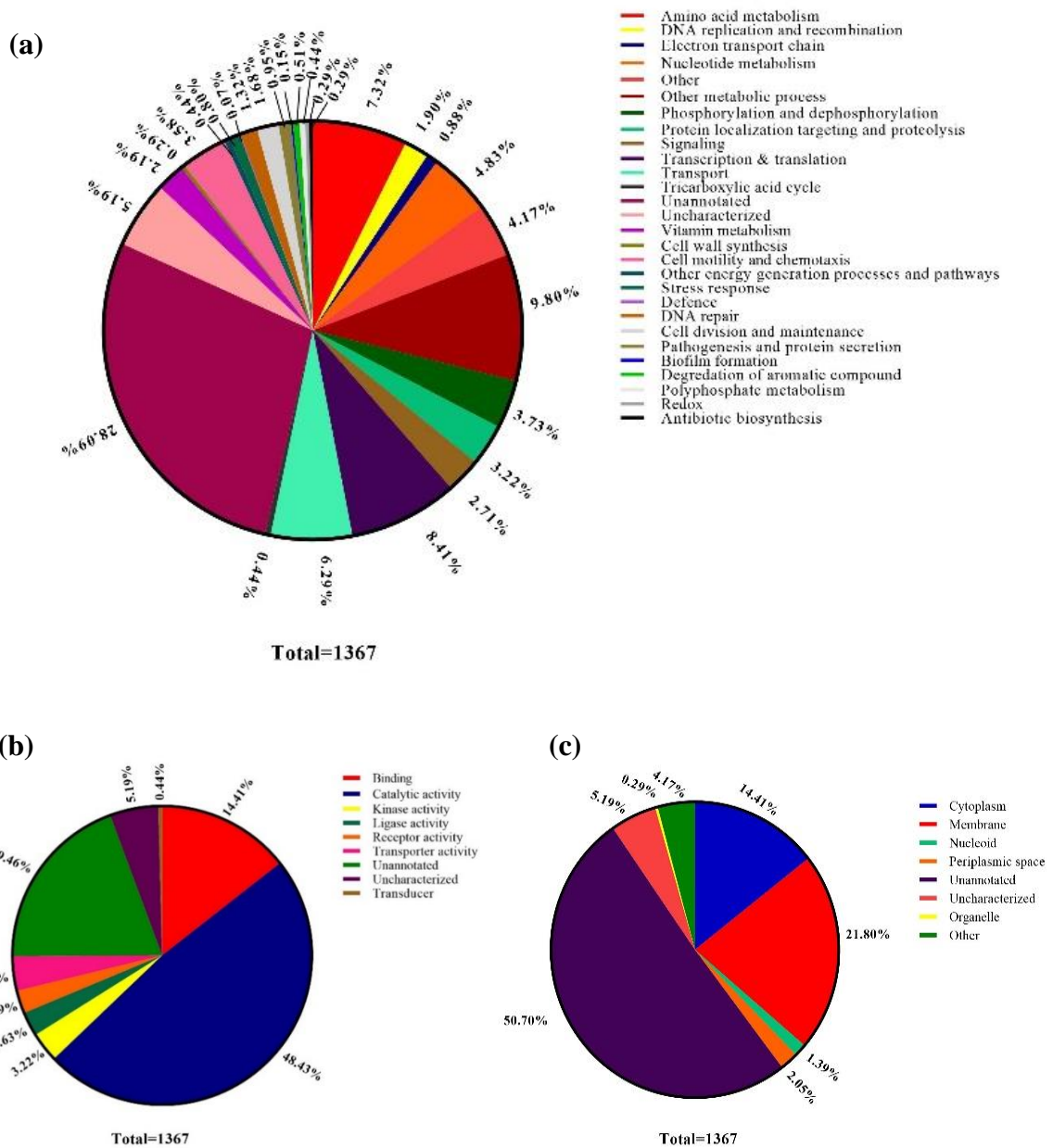


Fig. 3.32 Pie chart representing the distribution of proteins expressed specifically in the control sample based on their (a) biological process, (b) molecular function, and (c) cellular component.

3.8.3 Proteins specifically expressed in the As(V) treated sample

The study of protein specifically expressed in the arsenate-treated samples is crucial as there is a greater likelihood of these proteins being involved in the bacterial As(V) tolerance. The functional annotation of the proteins based on the biological process exhibited 38.79% of the proteins without annotation in the As(V) treated sample exclusively. The majority of the annotated proteins were engaged in the metabolic processes (amino acid, nucleotide, and vitamin) followed by transcription, translation, RNA metabolism, and transport. In addition to these, proteins involved in the electron transport chain (ETC), DNA recombination and integration, tricarboxylic acid cycle (TCA), phosphorylation, dephosphorylation, proteolysis, signaling, degradation of aromatic compound, and nitrogen metabolism were also exclusively expressed in the arsenate treated sample including 5.34% uncharacterized proteins (Fig. 3.33a).

The molecular function-based annotation of the proteins showed 58.36% having catalytic activity followed by 17.44% unannotated, and 11.74% with binding activity. Other proteins having kinase, ligase, receptor, and transporter activities were also expressed including 5.34% of uncharacterized proteins (Fig. 3.33b). Under the cellular component annotation category, the majority of the proteins were cytoplasmic (19.93%) followed by the membrane (13.88%) and periplasmic protein (3.91%). A small fraction of proteins (0.36%) were nucleoid proteins. However, 56.58% of proteins were unannotated and 5.34% were uncharacterized (Fig. 3.33c).

Some of the important proteins that exhibited their expression exclusively in the As(V) treated sample included OsmC family peroxiredoxin, NAD(P)H-quinone oxidoreductase, response regulator receiver protein, BolA family protein, and glutathione synthase protein. These are induced in response to certain environmental stress and protect the bacteria from the oxidative stress generated inside the cell. Proteins related to the transport of different substrates across the cell such as ABC transporter-related protein, lipopolysaccharide export system ATP-binding protein (LptB), phosphate-specific transport accessory protein (PhoU), high-affinity zinc uptake protein ZnuA, and metal ABC transporter substrate-binding protein

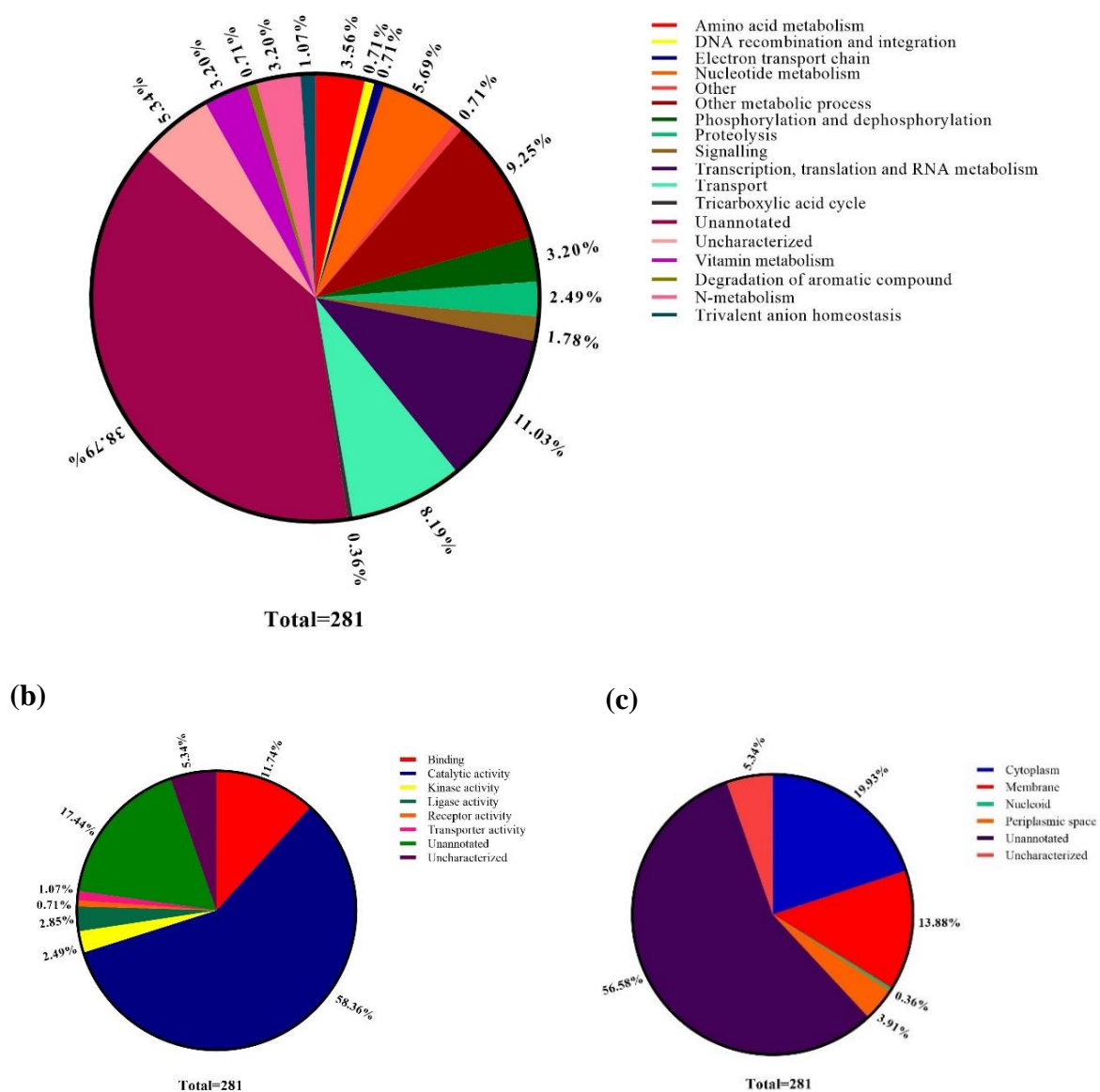


Fig. 3.33 Pie chart representing the distribution of proteins expressed specifically in the 300 mM As(V) treated sample based on their (a) biological process, (b) molecular function, and (c) cellular component.

were induced specifically under As(V) stress. Various transcriptional regulators specifically expressed under As(V) stress include TraR/DksA family transcriptional regulator, AsnC family transcriptional regulator, MarR family transcriptional regulator, and LysR family transcriptional regulator. Other proteins such as copper ion binding azurin, methyl-accepting chemotaxis protein, proteins related to N-metabolism (such as nitrous-oxide reductase and periplasmic nitrate reductase), xanthine dehydrogenase family protein molybdopterin-binding subunit, corrinoid adenosyltransferase, alcohol dehydrogenase (involved in fermentation), sporulation related protein alanine dehydrogenase, copper chaperone, putative antibiotic biosynthesis monooxygenase, and MBL fold metallo-hydrolase were also exclusively expressed under As(V) stress (Table 3.9).

The analysis of proteins specifically expressed under As(V) stress revealed the presence of several proteins such as phosphate-specific transport system accessory protein (PhoU) which helps in the transport of phosphate ions across the cell. In *E. coli* K12, the Pho regulon is reported to encode a phosphate-specific transport (Pst) system in the operon *pstSCAB-phoU* which is also involved in the uptake of As(V) from the outside environment (Mukhopadhyay et al., 2002; Rosen & Liu, 2009). PhoU represses the *pho* regulon under higher phosphate concentrations. PhoU also helps in the survival of the bacterial cells under different stress conditions such as heat, nutrient deficiency, pH, peroxide, presence of energy inhibitors, and antibiotics (such as trimethoprim, gentamicin, ampicillin, tetracycline, and norfloxacin) (Li & Zhang, 2007). The expression of PhoU specifically under As(V) stress shows its involvement in the inhibition of As(V) uptake by repressing the *pho* regulon and thus helping in the mitigation of arsenic toxicity in *P. mendocina* SMSKVR-3 cells. The MBL fold metallo-hydrolase and MarR family transcriptional regulator were found to be over-expressed under As(III) stress in the *Staphylococcus* sp. NIOSBK35. Transcriptional regulator MarR belongs to the family of multiple antibiotic resistance regulators and is involved in the generation of responses related to several environmental stress (such as antibiotics, toxic compounds, oxidative stress), virulence, and catabolism of aromatic compounds. The MarR regulators are transcriptional repressors that bind in the promoter region of the regulon and block the transcription process. However, under stress conditions such as oxidative stress, they form homodimers containing an intermolecular disulfide bond and thus are released from

the promoter (Si et al., 2018). The AsnC family transcriptional regulator is a DNA-binding protein and also called as feast/famine regulatory protein (Romero-Rodríguez et al., 2015). It is involved in the regulation of various metabolic processes such as pili synthesis, amino acid metabolism, DNA repair, recombination, and persistence (Deng et al., 2011). The other transcriptional regulator specifically expressed under the As(V) stress included LysR family transcriptional regulator that has been found to regulate various cellular processes such as motility, stress, metabolism of amino acid, and virulence in *P. aeruginosa* (Modrzejewska et al., 2021). Antibiotic biosynthesis monooxygenase was exclusively expressed under the As(III) stress in *B. casei* #NIOBBA88 (Shah & Damare, 2020). A copper-binding protein azurin was also exclusively expressed under the As(V) stress which is a low molecular weight protein involved in the electron transport chain of several microorganisms. In *P. aeruginosa* it takes part in the protection against oxidative stress.

Table 3.9 Proteins exclusively expressed in *P. mendocina* SMSKVR-3 under As(V) treated condition.

S. No.	Accession No.	Protein Name	Property	Function
1.	A0A5C8YGP4	Azurin	Copper ion binding	Transfers electrons from cytochrome c551 to cytochrome oxidase
2.	A0A550ELL0	OsmC family peroxiredoxin	Peroxiredoxin	Helps in overcoming oxidative stress
3.	A0A550FJJ5	Methyl-accepting protein	chemotaxis Transducer	Chemotaxis signal transduction
4.	A0A550G544	Nitrous-oxide reductase	Copper ion binding	Denitrification pathway
5.	A0A379ITF8	Glutathione synthase	ATP and metal ion binding	Formation of glutathione
6.	A0A5C8YGG6	TraR/DksA family transcriptional regulator	Zn ion binding	Regulation of transcription initiation
7.	A0A550FCW4	Xanthine dehydrogenase family protein molybdopterin-binding subunit	Oxidoreductase activity	Oxidative metabolism of purines
8.	A4XQM8	ABC transporter related protein	ATP-binding	Transport of substrate across the cell

9.	A0A379IXU1	MarR family transcriptional regulator	DNA-binding transcription factor	Degradation of organic compounds and controlling expression of virulence gene
10.	A0A2R3QS71	NAD(P)H-quinone oxidoreductase	Oxidoreductase activity	Reduction of cellular free radicals and detoxification of antibiotics
11.	A0A5C8YEV7	Periplasmic nitrate reductase	Iron and Mo ion binding	Reduction of nitrate to nitrite.
12.	A0A550G436	Metal ABC transporter substrate-binding protein	metal ion binding	Transport of metal ions
13.	A0A379IWK3	Response regulator receiver protein	Phosphorelay signal transduction	Response to environmental changes
14.	A0A379IZ70	BolA family protein	Transcriptional regulator	Stress response
15.	A0A379IZ24	Corrinoid adenosyltransferase	ATP-binding	Biosynthesis of cobalamin
16.	A0A379IMV0	Phosphate-specific transport system accessory protein (PhoU)	Negative regulation of phosphate metabolism	Regulation of phosphate uptake
17.	A0A379IVT2	Alcohol dehydrogenase	oxidoreductase activity	Role in fermentation
18.	A0A2R3QKP7	Lipopolysaccharide export system ATP-binding protein (LptB)	ATP-binding	Transmembrane transport
19.	A0A291KB42	Copper chaperone	Metal-ion binding	Transport of Cu to specific copper proteins
20.	A0A2R3QLQ6	Alanine dehydrogenase	Nucleotide-binding	Role in sporulation
21.	A0A550E3B2	Putative antibiotic biosynthesis monooxygenase	TPR-repeat containing	Virulence associated function
22.	A0A379IPH5	AsnC family transcriptional regulator	DNA-binding	Amino acid metabolism, pili synthesis, DNA transactions during DNA repair and
23.	A0A291K2R3	MBL fold metallo-hydrolase	Hydrolase activity	Hydrolysis of β -lactam antibiotics
24.	A0A379IR28	Putative antibiotic biosynthesis monooxygenase	Monooxygenase activity	Antibiotic synthesis or scavenging reactive oxygen species
25.	A0A2R3QP06	Transporter	Mo binding	Molybdate ion transport
26.	A0A550FCX1	High-affinity zinc uptake system protein ZnuA	Metal ion binding	Transport of zinc ions
27.	A4XXE3	Type IV pilus assembly PilZ	Cyclic-di-GMP binding	Not known
28.	A0A550G5C1	LysR family transcriptional regulator	DNA-binding transcription factor	Regulation of genes involved in virulence, metabolism, quorum sensing, and motility

3.8.4 Proteins differentially expressed (down- or up-regulated) in As(V) treated sample

The differential expression of proteins in the 300 mM As(V) treated sample was studied after 8 h of the As(V) exposure. The analysis of differentially expressed proteins was performed considering the fold change value 2 [\log_2 (abundance ratio) >1.0 was considered as upregulation and <-1.0 was considered as downregulation] as the cut-off. The analysis revealed 1433 proteins to be downregulated (under-expressed) and 383 proteins to be upregulated (over-expressed) in the As (V) treated sample. The functional annotation of all the downregulated proteins in the biological process category showed 34.96% of the proteins to be unannotated, 10.05% proteins related to transport, followed by the proteins involved in metabolism, transcription, translation, and RNA metabolism (7.68%). The proteins engaged in amino acid metabolism, DNA synthesis, replication, ETS, nucleotide metabolism, phosphorylation, dephosphorylation, protein localization, targeting, proteolysis, and signaling were also found to be downregulated. Other downregulated protein groups included proteins involved in TCA, metabolism of vitamins, synthesis and degradation of cell wall and membrane, cell motility, chemotaxis, stress, redox, N-utilization, cell division, glycolysis, pathogenesis, virulence, quorum sensing, and biofilm formation. However, 4.19% of the downregulated proteins were uncharacterized (Fig. 3.34a).

The functional annotation based on the molecular function exhibited a majority of the proteins having catalytic activities (41.24%) followed by the proteins with binding activity (14.38%), receptor function (5.51%), and transporter function (4.33%). Other than these, proteins having kinase, ligase, structural and regulatory activity were also found to be downregulated. However, 24.70% and 4.19% of proteins were found to be unannotated and uncharacterized (Fig. 3.34b). The cellular component-based annotation of downregulated proteins showed 23.73% membrane proteins, 14.93% cytoplasmic proteins, 2.79% periplasmic proteins, 1.95% organelle proteins, 1.05% nucleoid proteins, 46.89% unannotated proteins, and 4.19% uncharacterized proteins (Fig. 3.34c).

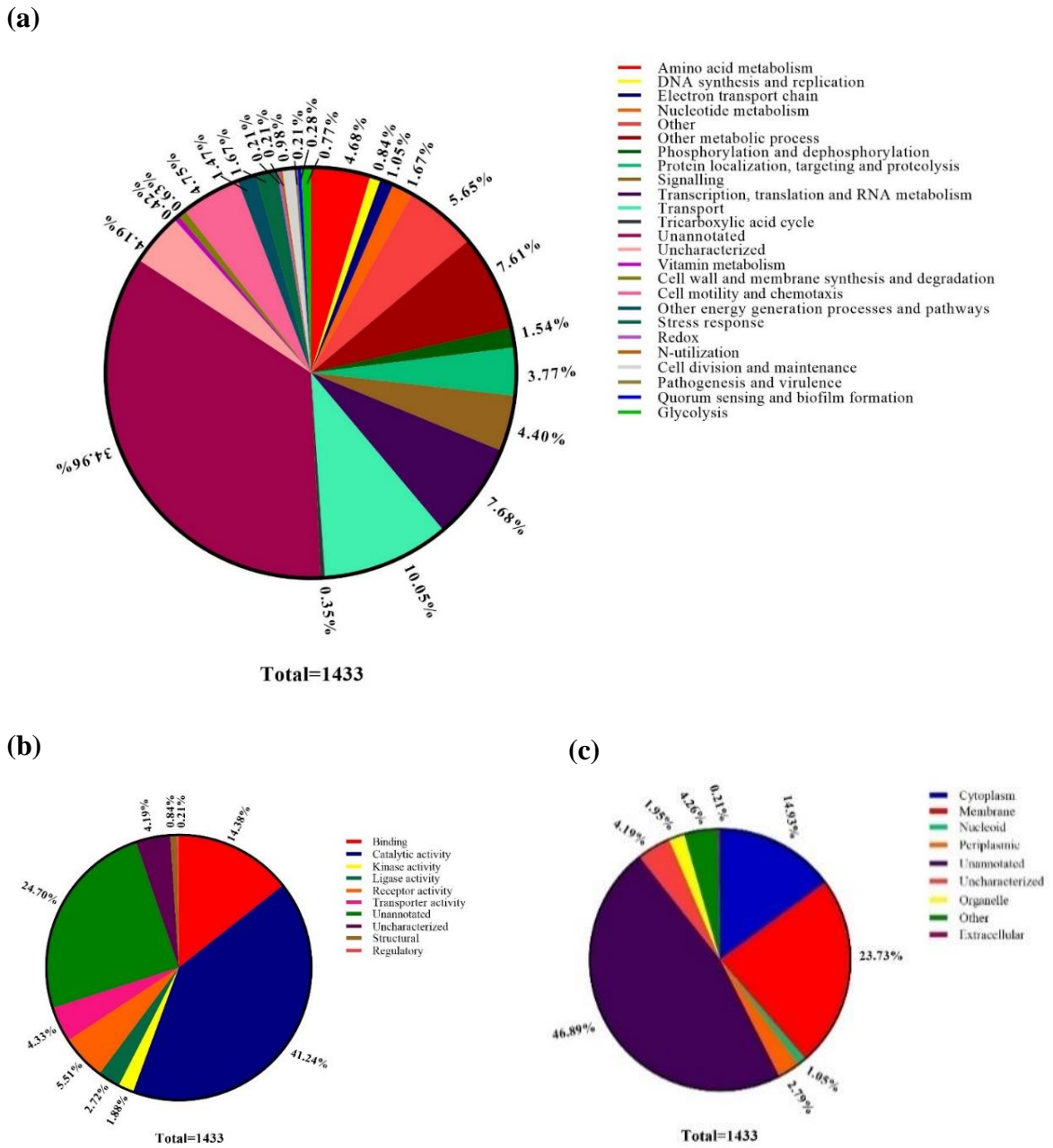


Fig. 3.34 Pie chart representing the distribution of proteins showed downregulation in the 300 mM As(V) treated sample (in comparison to control) based on their (a) biological process, (b) molecular function, and (c) cellular component.

The GO annotation analysis of upregulated proteins in the biological process category displayed 31.07% of them to be unannotated followed by 10.71% proteins related to transcription and translation, 7.31% transport proteins, 6.01% protein involved in amino acid metabolism, and 5.22% protein related to nucleic acid metabolism. Other protein groups included the proteins involved in the other metabolic and biosynthetic processes, DNA synthesis, recombination, ETS, phosphorylation, proteolysis, signaling, TCA, cell wall synthesis, stress, defense, and motility. In addition to these, some specific groups of proteins were also found to be upregulated in As(V) treated samples that included protein involved in DNA repair, fermentation, anaerobic respiration, and carbon utilization. However, 10.97% of the proteins were uncharacterized (Fig. 3.35a). Molecular function-based annotation showed 42.04% of up-regulated proteins having catalytic activity followed by 18.54% with the binding function, 4.18% with transporter activity, and 3.39% with kinase activity. In addition to these, the proteins having ligase and receptor activity were also upregulated along with the 17.23% unannotated and 10.97% uncharacterized proteins (Fig. 3.35b). Based on the cellular component annotation, 15.93% cytoplasmic protein were upregulated followed by 11.49% membrane, 3.39% organelle, 3.13% periplasmic, and 0.26% nucleoid proteins. However, 52.74% of the proteins were unannotated and 10.97% of the proteins were uncharacterized (Fig. 3.35c). All the upregulated and downregulated proteins in the As(V) treated sample are shown in the form of a heat map in Fig. 3.36. The level of the protein expression has been represented in terms of the relative abundance ranging from the value -2 to 2 where the value <0 represents the lower expression or downregulation and value >0 represents the higher level of protein expression or upregulation. However, value 0 represents no change in the protein expression. With the increasing expression level of the protein, the color of the graph is shifting towards red whereas, with the decreasing expression level, it is shifting towards the green color. The heat map representation of differential protein expression clearly indicates that the number of proteins downregulated in As(V) treated sample is relatively higher than the upregulated ones. It has been shown in various studies that the proteins involved in heavy metal (or any other toxic compound) resistance most commonly include, specific transporters,

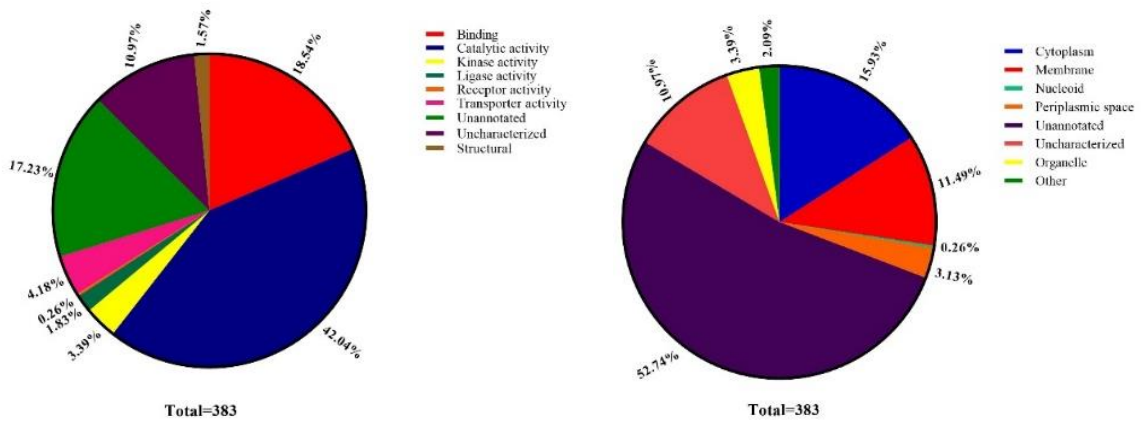
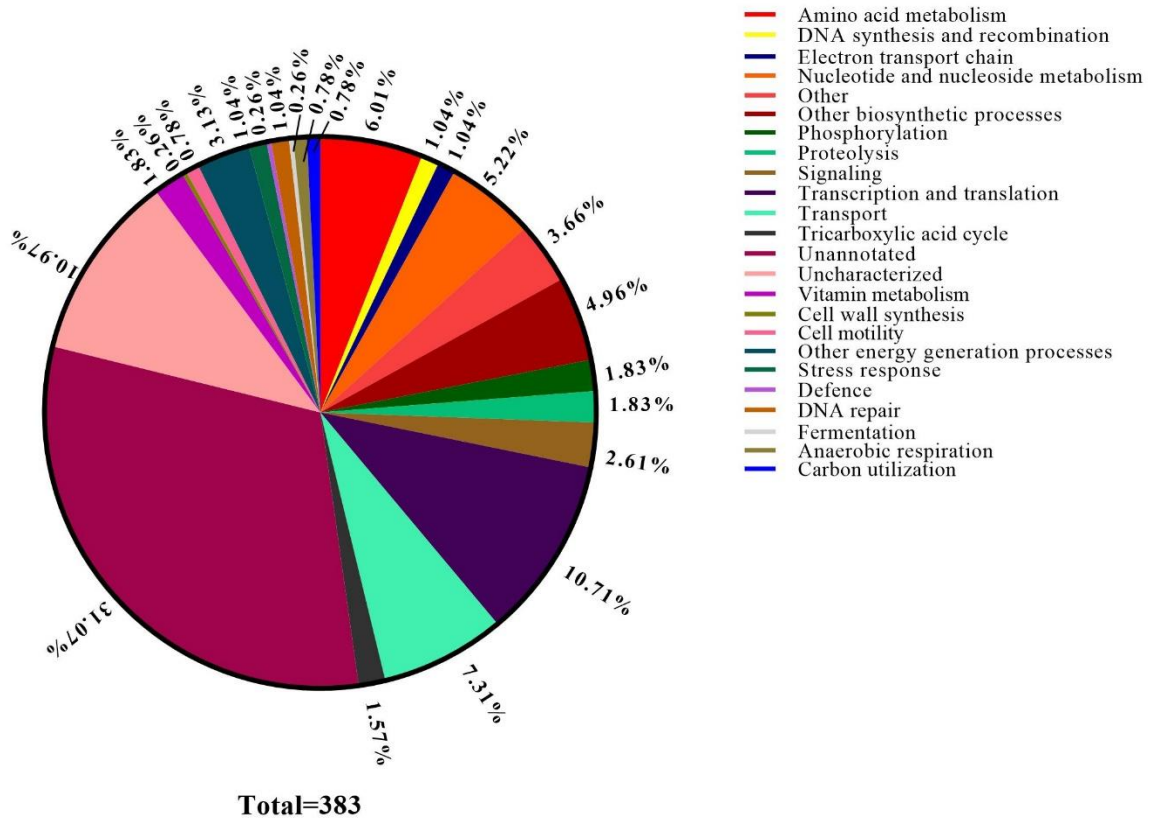


Fig. 3.35 Pie chart representing the distribution of proteins showed upregulation in the 300 mM As(V) treated sample (in comparison to control) based on their (a) biological process, (b) molecular function, and (c) cellular component.

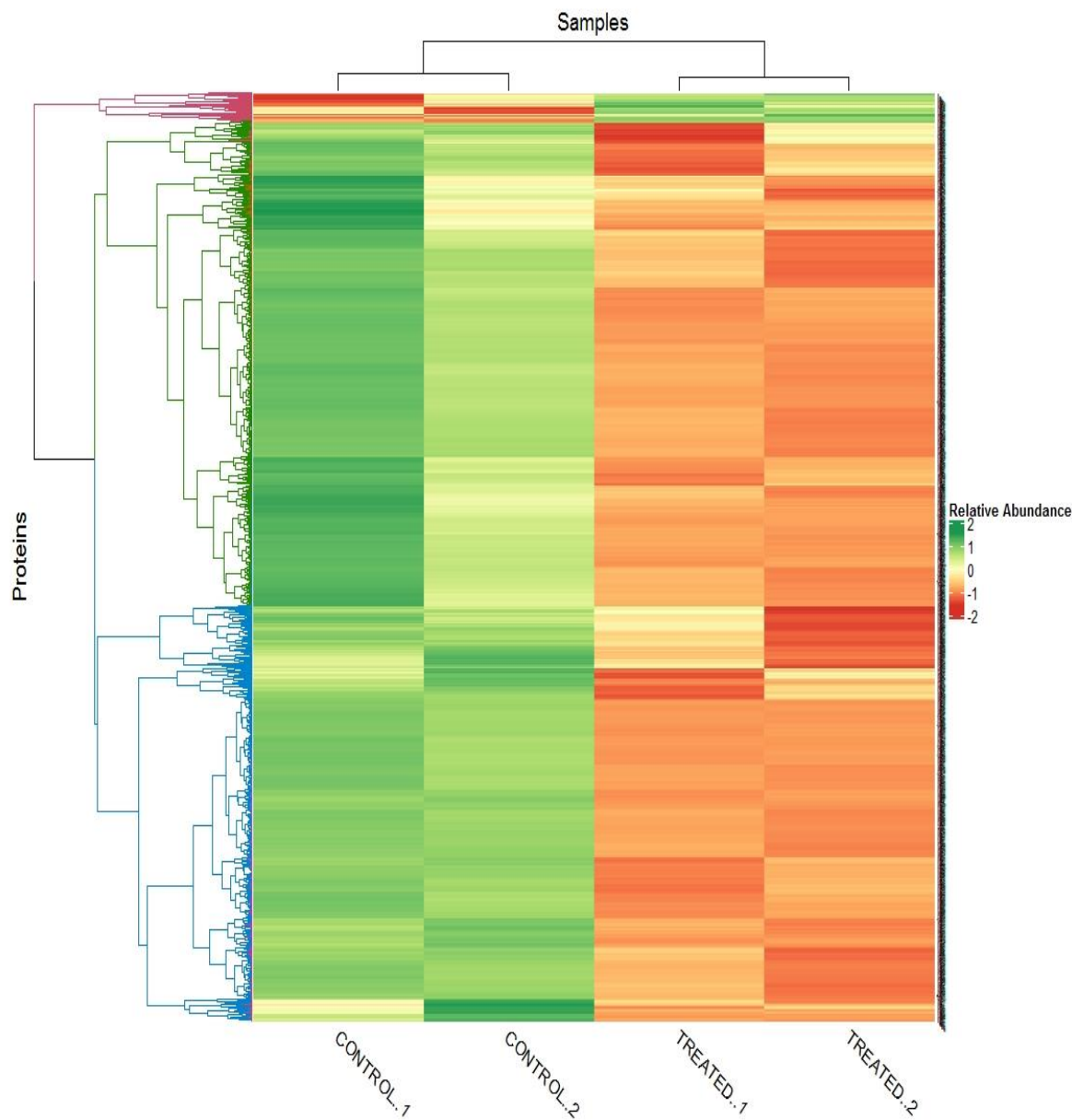


Fig. 3.36 The Heat map of differentially expressed proteins in As(V) treated sample (in comparison to control). The result of samples in duplicates has been represented. Over-expressed and under-expressed proteins have been shown in green and red colors respectively. The level of expression has been represented in the form of relative abundance on the bar shown right side.

proteins related to behavioral changes like moment, stress-induced proteins, and proteins specific to the metal-resistance (Gang et al., 2019) as discussed in the following section.

3.8.4.1 Proteins related to the cell membrane and transport

In the presence of As(V) upregulation and downregulation of several cell membrane and transport associated proteins were observed. The expression level of proteins was calculated in the form of \log_2 abundance ratio indicating the abundance of protein in the treated sample as compared to the control. The number of downregulated proteins was found to be higher as compared to the upregulated protein. The proteins including several outer membrane proteins such as lipoprotein (OprI), lipoprotein-sorting protein, chaperone Skp (OmpH), copper receptor (OprC), assembly factor BamC and BamD, extracellular solute-binding protein, succinate dehydrogenase hydrophobic membrane anchor subunit, putative transmembrane sensor, periplasmic lipoprotein-like protein, inner membrane protein (YqiK), and membrane protein insertase (YidC) showed decreased expression under the treated condition (Table 3.10). A large number of proteins related to transport were downregulated in the As(V) treated sample majority of them belonging to the ABC transporter family involved in the transport of carbohydrates, hemin, leucine, methionine, C4-dicarboxylate, selenate, phosphonate, glycine/betaine, ectoine/hydroxyectoine, spermidine/putrescine, sulfate, choline, and Fe^{3+} . Several other proteins such as porins (OprD, LamB family, carbohydrate, and outer membrane porin), tripartite ATP-independent periplasmic transporter (TRAP) proteins, proteins related to the transport/export of biopolymer (ExbD/TolR), thiosulfate, and lipopolysaccharide (LptA), proton channel protein (MotA/TolQ/ExbB), alanine: cation symporter family protein, Na(+)-translocating NADH-quinone reductase subunit C, and HlyD family efflux transporter periplasmic adaptor subunit proteins were also found to be under-expressed in the As(V) treated sample (Table 3.10).

The number of upregulated proteins was comparatively less which included the proteins involved in the transport of arginine/ornithine (AotP), dicarboxylate, tricarboxylate, glucose or sugar, lipopolysaccharide (LptC), and branched-chain amino acid. The multidrug resistance protein, efflux RND transporter periplasmic adaptor subunit was also found to be upregulated along with some other proteins such as phosphotransferase system phosphocarrier protein (HPr), PhoP/Q and low Mg^{2+} inducible outer membrane protein H1, outer membrane protein assembly factor (BamA), OmpA family protein, OMP_b-brl domain-containing protein, and glycine betaine/L-proline ABC transporter ATP-binding protein (Table 3.11).

There are very few proteomic studies involving the whole cell proteome analysis of bacteria under arsenate stress. However, there are some studies that have shown the downregulation of a larger number of proteins under arsenic stress. However, a lesser number of the proteins exhibited upregulation (Shah & Damare, 2020; Shah & Damare, 2018). A similar trend of protein expression was observed in the present study, where a larger number of proteins were downregulated in the As(V) treated *P. mendocina* SMSKVR-3 cells. The arginine inducible arginine/ornithine transport protein (AotP) is known to be involved in the energy-coupled transport of arginine and ornithine (Johnson et al., 2008). Both of these amino acids are the parts of the urea cycle and are involved in the removal of nitrogenous waste from the cells. Its over-expression under the As(V) stress in the present study suggests its involvement in the removal of nitrogenous waste generated due to the degradation of proteins. Proteins belonging to the ABC transporter category such as ABC transporter substrate-binding protein, glycine betaine/L-proline ABC transporter substrate-binding protein, and multidrug transporter protein (efflux RND transporter periplasmic adaptor subunit) are over-expressed under the As(III) stress in *Staphylococcus* sp. NIOSBK35. Which indicates their direct or indirect role in As(III) detoxification (Shah & Damare, 2018). The role of multidrug efflux systems in heavy metal and antibiotic resistance has already been discussed in section 3.5.3. Phosphocarrier protein (HPr) is a low-mass protein involved in the phosphoenolpyruvate sugar phosphotransferase system playing a role in the sugar transport as well as in the signal transduction regulating the catabolite repression. The Hpr has been expressed in *Streptococcus oralis* under acidic stress (Wilkins et al., 2003). The PhoP/Q and low Mg^{2+} inducible outer membrane protein H1 precursor were found to be overexpressed under the heat stress in *P. putida* (NBAIL-RPF9). It is a two-component regulatory system that allows the pathogenic bacteria to grow under adverse environmental conditions (Rangeshwaran et al., 2013). In *P. aeruginosa* a homolog of PhoP/Q is involved in resistance to polymyxin B under the Mg^{+2} deprived condition (Macfarlane et al., 1999). The outer membrane protein family OmpA is a group of surface-exposed porins present in the outer membrane of gram-negative bacteria in a high copy number. It plays an important role in the adhesion as well as in the evasion of host defense. It allows the survival of bacteria under osmotic stress showing increased expression under the anaerobic growth conditions, nitrogen deprivation, and exposure to polyamine (Confer & Ayalew, 2013). The function of TRAP dicarboxylate transporter, tripartite

tricarboxylate transporter substrate-binding protein, OMP_b-brl domain-containing protein, and binding-protein-dependent transport system in the metal stress is not known. However, these proteins were over-expressed under the As(V) stress. The upregulation of all these membrane and transport-related proteins in As(V) treated *P. mendocina* SMSKVR-3 cells indicates their either direct or indirect role in As(V) resistance.

Table 3.10 The membrane and transport-related proteins downregulated under As(V) treated condition in *P. mendocina* SMSKVR-3.

Protein description	Log₂ (abundance ratio)	Molecular weight (kDa)	pI
Membrane proteins			
Outer membrane lipoprotein (OprI)	-4.10	8.8	8.16
Outer membrane protein assembly factor (BamD)	-4.04	37.4	5.29
Membrane protein-like protein	-3.77	14.5	8.53
Periplasmic binding protein	-3.77	31.4	6.00
Extracellular solute-binding protein	-3.75	64.6	5.21
OmpA-like domain-containing protein	-3.26	29.7	7.44
Succinate dehydrogenase membrane anchor subunit	-2.78	13.7	8.56
OmpA/MotB domain protein	-2.68	22.0	4.73
TolC family protein	-2.50	54.7	5.41
Putative transmembrane sensor	-2.24	35.8	7.33
Periplasmic lipoprotein-like protein	-2.17	38.3	5.44
Outer membrane lipoprotein-sorting protein	-2.16	51	8.43
Outer membrane chaperone Skp (OmpH)	-1.91	19.2	9.35
Outer membrane copper receptor (OprC)	-1.84	75.4	5.53
Membrane protein insertase (YidC)	-1.65	65.9	5.90
OmpH family outer membrane protein	-1.65	19.2	9.20
Efflux outer membrane protein	-1.49	54.5	5.50
Inner membrane protein (YqiK)	-1.43	74.9	5.20
TolC family type I secretion outer membrane protein	-1.35	52.2	5.08
Outer membrane protein assembly factor (BamC)	-1.31	40.5	4.92
Outer membrane beta-barrel protein	-1.23	24.3	4.89
Transporter proteins			
Carbohydrate ABC transporter substrate-binding protein, CUT1 family	-4.23	64.7	5.10
Na(+)-translocating NADH-quinone reductase subunit C	-3.86	27.9	5.49
Transport-associated protein	-3.78	19	9.99
Hemin ABC transporter substrate-binding protein	-3.73	31.2	6.23

MotA/TolQ/ExbB proton channel family protein	-3.60	48.3	5.83
Leucine ABC transporter subunit substrate-binding protein (LivK)	-3.26	39.3	5.38
ABC transporter substrate-binding protein	-3.09	27.4	4.89
Branched-chain amino acid ABC transporter substrate-binding protein	-3.04	39.2	5.21
C4-dicarboxylate ABC transporter	-2.95	36.4	5.19
OprD family porin	-2.83	46.5	4.92
TRAP transporter substrate-binding protein	-2.70	39.7	5.63
Transporter substrate-binding domain-containing protein	-2.41	27.4	4.94
Outer membrane porin	-2.38	47.1	6.20
DctP family TRAP transporter solute-binding subunit	-2.36	37.4	7.42
Putative selenate ABC transporter substrate-binding protein	-2.21	30.5	5.74
Periplasmic phosphonate-binding protein (ABC transporter)	-2.19	30.5	5.74
Amino acid ABC transporter	-2.18	27.4	4.94
Channel protein (TolC)	-2.15	50.8	5.57
Biopolymer transport protein ExbD/TolR	-2.08	15	5.11
ABC transporter ATP-binding protein	-1.97	59.2	8.53
Glycine/betaine ABC transporter substrate-binding protein	-1.95	30.7	6.28
Ectoine/hydroxyectoine ABC transporter substrate-binding protein (EhuB)	-1.93	29.9	5.54
Phosphonate ABC transporter substrate-binding protein	-1.93	30.6	5.59
Spermidine/putrescine ABC transporter substrate-binding protein	-1.81	38.6	4.88
ABC transporter	-1.79	99.2	6.65
Ribosome-associated ATPase/putative transporter (RbbA)	-1.79	99.1	6.52
Carbohydrate porin	-1.71	45.8	5.60
Alanine:cation symporter family protein	-1.70	52.9	7.84
Lipopolysaccharide export system protein (LptA)	-1.69	19.8	5.71
Sulfate ABC transporter substrate-binding protein	-1.63	37.6	6.44
Choline ABC transporter substrate-binding protein	-1.58	33.9	5.30
Thiosulfate transporter subunit	-1.25	37.7	6.57
Methionine ABC transporter substrate-binding protein	-1.23	28.3	6.38
ABC-type Fe ³⁺ transport system periplasmic component-like protein	-1.20	38.1	5.45
HlyD family efflux transporter periplasmic adaptor subunit	-1.17	38.3	8.32
Porin, LamB type	-1.14	45.7	5.58

Table 3.11 The membrane and transport-related proteins upregulated under As(V) treated condition in *P. mendocina* SMSKVR-3.

Protein description	Log₂ (abundance ratio)	Molecular weight (kDa)	pI
PhoP/Q and low Mg ²⁺ inducible outer membrane protein H1	1.35	21.5	7.43
Outer membrane protein assembly factor (BamA)	1.41	87.1	4.94
Membrane protein	1.68	6.6	4.36
OmpA family protein	4.42	28.6	8.56
OMP_b-brl domain-containing protein	4.89	27.6	5.15
Arginine/ornithine transport protein (AotP)	1.12	28.0	8.06
Tripartite tricarboxylate transporter substrate binding protein	1.18	35.5	5.55
Binding-protein-dependent transport system inner membrane protein	1.19	31.8	9.13
Glucose ABC transporter membrane protein	1.19	31.8	9.32
TRAP dicarboxylate transporter, DctP subunit	1.20	37.2	5.39
Glucose ABC transporter ATP-binding protein	1.25	41.4	6.58
Efflux RND transporter periplasmic adaptor subunit	1.29	58.9	6.20
Phosphotransferase system, phosphocarrier protein (HPr)	1.30	9.6	5.08
ABC transporter ATP-binding protein	2.25	41.2	6.79
Lipopolysaccharide export system protein (LptC)	2.27	20.9	8.34
High-affinity branched-chain amino acid transport ATP-binding protein	3.40	25.5	5.99
ABC transporter substrate-binding protein	3.58	27.5	5.92
Glycine betaine/L-proline ABC transporter ATP-binding protein	5.16	44.2	5.38

3.8.4.2 Proteins related to the cell adhesion, signal transduction, chemotaxis, motility, and receptor family

Proteins belonging to cell adhesion, signal transduction, chemotaxis, motility, and receptor family were also found to be downregulated in the As(V) treated sample. This includes the proteins that constitute bacterial type I, IV, V, and VI secretory systems such as type I secretion outer membrane protein (TolC family), Type IV pilus secretin (PilQ), type V secretory pathway adhesin (AidA), type VI secretion system contractile sheath small & large subunit and type VI secretion protein. The proteins constituting flagellar and pilus systems such as flagellin, FlgN family protein, flagellar motor protein (MotA), flagellar protein (FlaG),

flagellar hook protein (FlgE), Tfp pilus assembly protein (FimV-like protein), Type IV pilus biogenesis/stability protein (PilW), and pili assembly chaperone were also downregulated under the As(V) stress. The other downregulated proteins included receptors (such as TonB-dependent hemoglobin/transferrin/lactoferrin family receptor, putative siderophore receptor, outer membrane heme receptor, TonB-dependent siderophore and copper receptor), chemotaxis proteins, adhesin, putative CheA signal transduction histidine kinase, H-NS family protein (MvaT), and signal peptidase I. However, very few proteins under this category were found to be upregulated including secretion protein HlyD family protein, signal transduction protein with CBS domains, flagellar motor switch protein (FliN), putative secreted protein (NlpA lipoprotein), and HopJ type III effector protein (Fig. 3.37).

The number of downregulated proteins was higher than the ones that were upregulated in *P. mendocina* SMSKVR-3 under the As(V) stress. The downregulated proteins included various receptors such as TonB-dependent siderophore receptor which is known to mediate the transport of siderophores into the periplasm of gram-negative bacteria forming the complex with membrane-spanning proteins ExbB and ExbD (Ferguson & Deisenhofer, 2002). The binding of siderophores causes signal transduction resulting in the transport of iron (Ferguson & Deisenhofer, 2002). The expression of TonB-dependent receptor, siderophore receptor, and hemoglobin/transferrin/lactoferrin receptor genes are reported to be downregulated under the heat and cold stress in *Psychrobacter* sp. G. Both of these receptors take part in the iron uptake and transport which is essential for the bacteria to survive under the aerobic conditions. The downregulation of these genes are caused due to the reduction of aerobic respiration under temperature stress (Wang et al., 2017). Based on these findings it can be concluded that downregulation of these receptors might be related to the decreased iron uptake and aerobic respiration in *P. mendocina* SMSKVR-3. However, in the present study, it has been proposed that the siderophores produced by *P. mendocina* SMSKVR-3 in the presence of As(V) and As(III) are involved in the As(V) resistance. The downregulation of AidA, which is an adhesion protein involved in bacterial virulence suggests that the presence of As(V) decreases the adhesion of bacteria with the host cell leading to decreased virulence. Some other virulence proteins such as type I, V, and VI secretory pathway proteins were also found to be downregulated. Studies have shown contrasting results on the virulence of bacteria under different stress conditions. A study has shown the upregulation of virulence genes under

the heat and oxidative stresses, while downregulation of them under the starvation and osmotic stress (Bui et al., 2012). The upregulated secretion protein belonging to HlyD family which is a component of the bacterial type I secretion system is involved in the formation of a three-component ABC transporter complex. However, its contribution to bacterial stress tolerance is not yet studied.

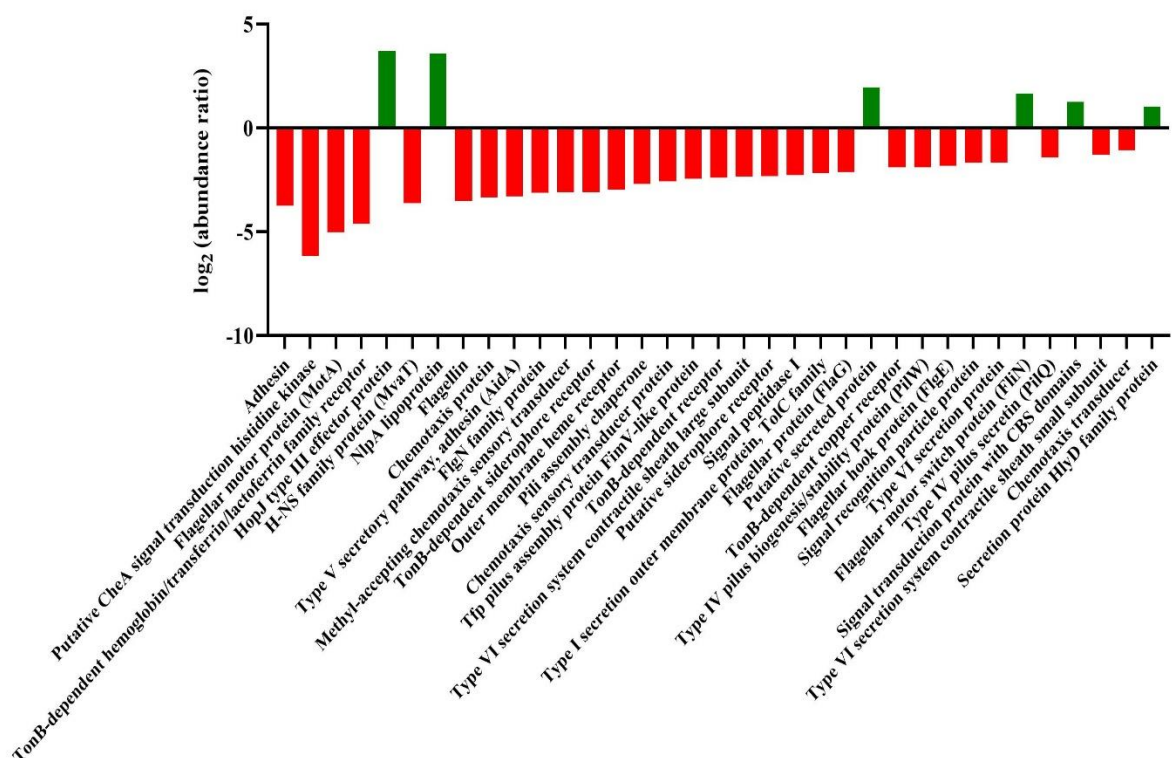


Fig. 3.37 Differential expression of proteins belonging to cell adhesion, signal transduction, chemotaxis, motility, and receptor family represented in terms of log₂ value of the abundance ratio (treated/control).

Some flagellar proteins such as the flagellar hook-associated protein FlgL, the flagellar hook-filament junction protein FlgK, and flagellin FliC were found to be overexpressed under the prolonged Cr(VI) exposure in *Shewanella oneidensis* MR-1 (Gang et al., 2019). However, some studies have shown the stress-sensitive nature of the flagellar assembly pathway. It has also been revealed that bacteria tend to aggregate and acquire abnormal cellular morphology under metal stress (Gang et al., 2019; Qin et al., 2011; Wang et al., 2015). The present study shows the upregulation of FliN (determines the direction of flagellar movement) while the

downregulation of FlgE, MotA, FlgG, FlgN, and the proteins involved in chemotaxis which indicates the inhibition of flagellar movement in *P. mendocina* SMSKVR-3 under the As(V) stress. The SEM study confirms this finding showing the aggregation of bacteria under As(V) stress. However, to get the nutrient from the surrounding environment there is still some movement in the proper direction which has been witnessed by the over-expression of FliN.

3.8.4.3 Proteins related to the stress response

Under As(V) stress condition various stress-related proteins were found to be downregulated and upregulated that have been shown in Fig. 3.38. The downregulated proteins included alkyl hydroperoxide reductase C, cold-shock and heat shock proteins, DJ-1/PfpI family protein, dihydrolipoyllysine-residue succinyltransferase, thioredoxin reductase, stress response translation initiation inhibitor (YciH), proteins components of pyruvate dehydrogenase, thiol peroxidase, peroxiredoxin, glutathione peroxidase, HDOD domain-containing protein, DEAD/DEAH box helicase, glutaredoxin, and two-component response regulator (PilR). In addition to these, peptide methionine sulfoxide reductase, tail-specific protease, 3-isopropylmalate dehydratase, GTPase (Obg), alkyl hydroperoxide reductase, fatty acid oxidation complex subunit alpha, osmolarity response regulator, and glucose/maltose/N-acetylglucosamine-specific phosphotransferase system IIC component were also found to be downregulated. There were also several chaperones such as 10 kDa chaperonin (groS), 60 kDa chaperonin, 33 kDa chaperonin, chaperone protein (HtpG), chaperone protein HscA homolog, chaperone protein (ClpB), co-chaperone protein HscB homolog, chaperone (SurA), MoxR family ATPase, molecular chaperone, and copper chaperone (PCu(A)C) which found to be downregulated under the As(V) stress.

Several stress-related proteins including superoxide dismutase, toluene tolerance protein, nucleotide pyrophosphohydrolase, lon protease, UPF0229 protein NCTC10899_01085, putative serine protein kinase (PrkA), 3-hydroxyisobutyrate dehydrogenase, tetratricopeptide repeat protein, UPF0301 protein NCTC10899_04954, thiazole synthase, UspA domain-containing protein, translational regulator (CsrA), universal stress protein, ATP-dependent RNA helicase DeaD, UPF0229 protein CO724_04580, HPF/RaiA family ribosome-associated protein, osmoprotectant NAGGN system M42 family peptidase, and CsbD family protein were upregulated under the As(V) stress. In addition to

these, several arsenic-resistance specific proteins were also over-expressed including ArsC family reductase, polyphosphate kinase, arsenical resistance protein ArsH, glyceraldehyde-3-phosphate dehydrogenase, and NAD-dependent aldehyde dehydrogenase.

The downregulated protein alkyl hydroperoxide reductase C (AhpC) is a thiol-specific peroxidase that protects the bacterial cell from the oxidative stress caused by peroxides. A study has exhibited that the *C. jejuni* mutant to AhpC exhibited increased biofilm formation indicating its role in the repression of biofilm formation (Oh & Jeon, 2014). This study suggested that the downregulation of AhpC in *P. mendocina* SMSKVR-3 is probably resulting in the stress-induced biofilm formation. In other studies, protein superoxide dismutase and UspA domain-containing proteins have been overexpressed under the arsenic stress. The former acts as an antioxidant and protects the cells from the reactive oxygen species while the other allows the bacteria to grow under different environmental stress conditions. (Belfiore et al., 2013; Shah & Damare, 2020). A study has shown the downregulation of heat shock protein family chaperon under As(III) stress that has been witnessed in the present study as well. However, the heat shock protein, cold shock proteins, and different chaperone proteins have been downregulated under the As(III) stress indicating no significant role of these proteins in the arsenic detoxification process (Shah & Damare, 2018).

The proteins directly involved in the As(V) resistance were also found to be upregulated in the *P. mendocina* SMSKVR-3 including the ArsC family reductase, polyphosphate kinase, arsenical resistance protein ArsH, glyceraldehyde-3-phosphate dehydrogenase, and NAD-dependent aldehyde dehydrogenase. The presence of the genes of these proteins in the studied bacteria has been shown in the whole-genome sequencing analysis described in section 3.6.6. The over-expression of arsenic-resistance proteins such as arsenic resistance operon repressor (ArsR) and arsenical pump-driving ATPase under the As(III) stress is also reported in *Staphylococcus* sp. NIOSBK35 (Shah & Damare, 2018). However, another study has shown the exclusive expression of ArsR protein in *B. casei* #NIOSBA88 under the arsenic exposure (Shah & Damare, 2020). The role of these proteins in the bacterial arsenic resistance has been already described in section 1.4. The summarized result of the whole-cell proteomic study describing the upregulation, downregulation, and

exclusive expression of several proteins under As(V) stress has been shown in Fig. 3.39. All these proteins are playing important role in As(V) resistance in *P. mendocina* SMSKVR-3.

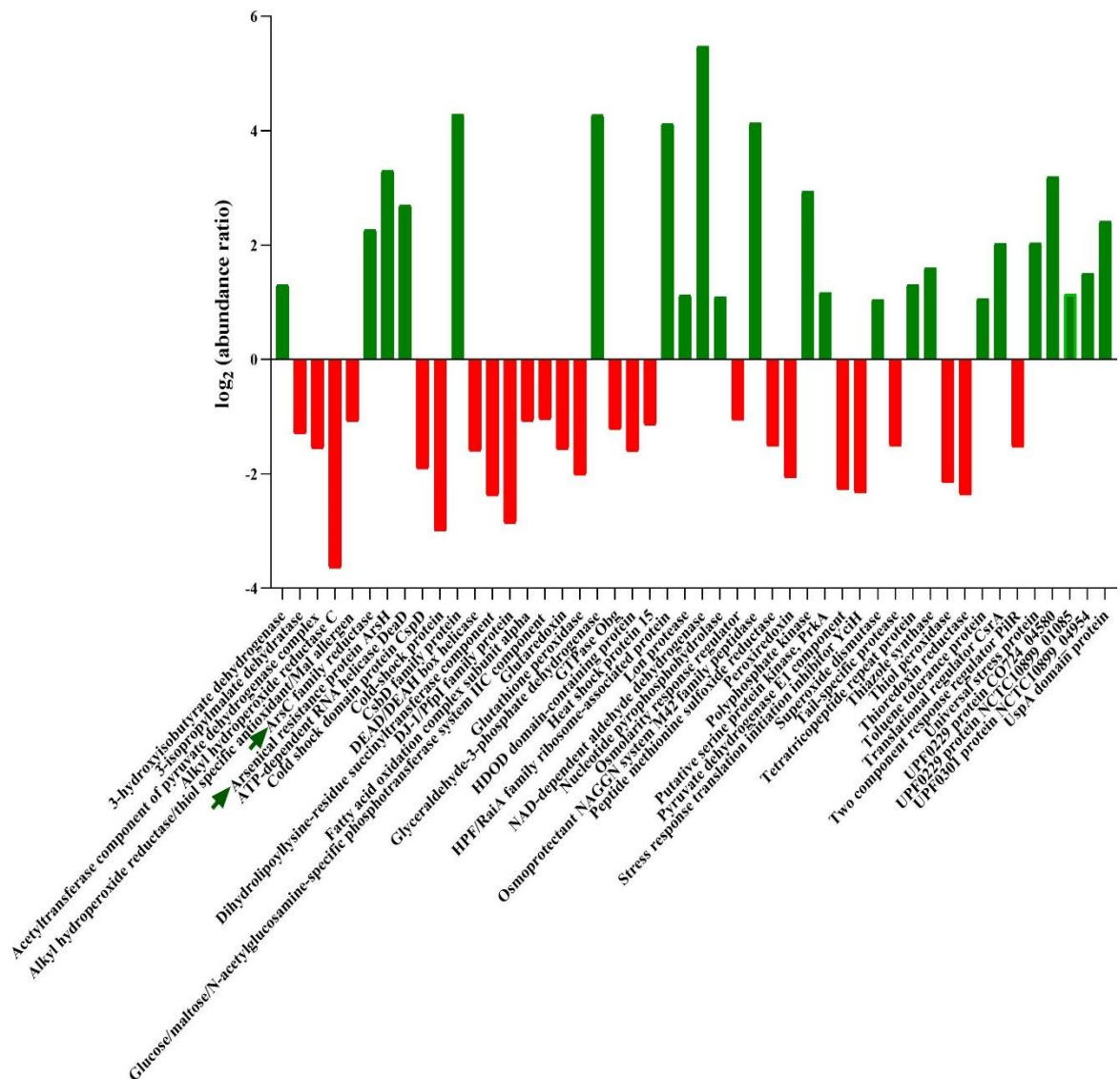


Fig. 3.38 Differential expression of the proteins related to stress response represented in terms of log₂ value of the abundance ratio (treated/control).

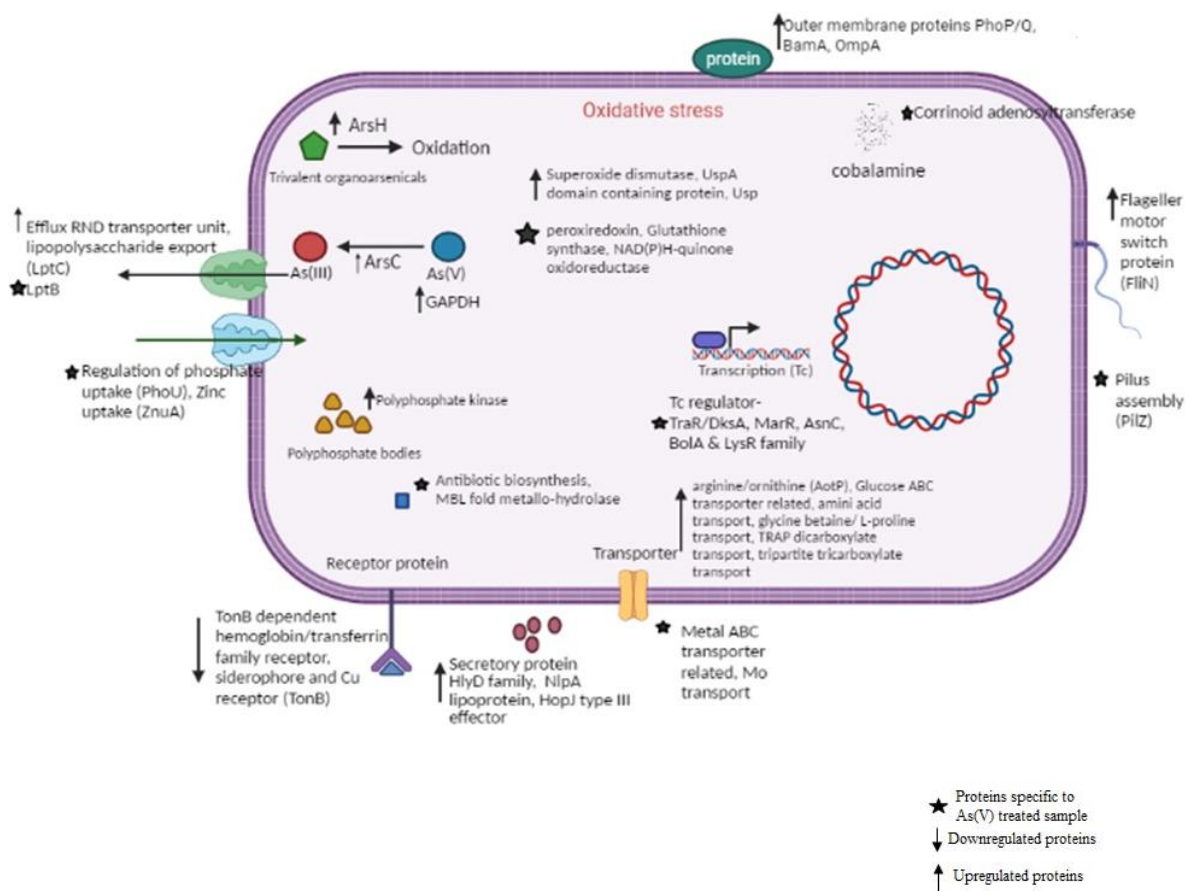


Fig. 3.39 Overview of the whole-cell proteomic analysis of *P. mendocina* SMSKVR-3 under the As(V) stress representing some important proteins upregulated, downregulated, and specifically expressed.

The results of the whole-cell proteomic study were found to be correlated with the outcomes of the experiments conducted to identify the As(V) resistance mechanisms in *P. mendocina* SMSKVR-3, whole-genome analysis, and 2-DGE analysis. Collectively, all of these studies are showing the role of siderophores, polyP bodies, multidrug efflux pumps, vitamin B12 synthesis, and several arsenic resistance proteins such as ArsC and ArsH in *P. mendocina* SMSKVR-3 As(V) resistance.

Among all the over-expressed and exclusively expressed stress-related proteins observed in the whole proteome study, arsenic-specific proteins ArsC, and ArsH were selected for the *in silico* study which was performed to check the interaction of As(V) with these proteins.

3.9 *In silico* study of the binding of arsenate with the selected arsenate binding proteins

The ArsC and ArsH proteins involved in the As(V) resistance in *P. mendocina* SMSKVR-3 were selected for the *in silico* As(V) binding study. These proteins are very well known for their important roles in the As(V) resistance in different bacterial species (Chen et al., 2015; Rosen, 2002) and thus were selected for the *in silico* study. The *in silico* binding study involved the prediction of 3D structures of these proteins using different protein modeling tools using the known PDB structure as the template. After that, the binding of As(V) with these proteins was studied by the docking which was followed by the analysis of deformability and stability of the protein-As(V) complex. The significant binding of As(V) with these proteins be employed for the development of As(V) specific biosensors as well as the bioremediation strategy for its removal.

3.9.1 Analysis of the physicochemical and functional characteristics of ArsC and ArsH

The sequences of ArsC and ArsH proteins obtained from the LC-MS/MS analysis were analyzed for their Physico-chemical characteristics which were determined using ExPASy's ProtParam tool (Table 3.12). The ArsC and ArsH monomer has 135 and 237 amino acid residues and the molecular weight of 15452.52 and 27121.10 g/mol, respectively. The ArsH protein in the solution at room temperature exists predominantly in the tetrameric form. The pI values of the ArsC and ArsH were obtained to be 6.36 and 6.46. The half-life of the ArsC and ArsH inside the *E. coli* system was found to be >10 h. The hydrophilic and hydrophobic nature of the protein was determined using GRAVY where a negative value indicates the hydrophilic and a positive value indicates the hydrophobic nature. It is calculated by dividing the sum of the hydropathy values of the amino acids by the total number of amino acids in a protein sequence. The ArsC and ArsH had a GRAVY value of -0.621 and -0.427, respectively indicating their hydrophilic nature (Yang et al., 2013). The numbers of positively charged residues in ArsC and ArsH were 18 and 32 while the numbers of negatively charged residues were 20 and 33. The thermostability of a protein is determined by calculating the aliphatic index of a protein which is the volume of a protein covered by aliphatic amino acid side chains. The higher aliphatic index indicates the higher thermostability of a protein. The aliphatic index of the ArsC and ArsH were obtained to be 74.59 and 82.70 indicating them to be highly

thermostable. The *in vitro* stability of a protein is determined by calculating the instability index. The instability index <40 indicates a stable protein while >40 indicates the unstable protein. The instability index for the ArsC and ArsH were obtained to be 37.83 and 48.76, respectively showing ArsC to be stable while ArsH to be less stable.

The stability of a protein structure is determined by the formation of disulfide bonds between the cysteine amino acid residues of a protein. The identification of the cysteine amino acid residues of the ArsC and ArsH was done by CYS_RES tool that showed the presence of 2 (at positions 101 and 141) and 3 (position 6, 31, and 67) cysteine residues in these proteins. The protein families were predicted by Pfam showing ArsC belonging to ArsC family and ArsH belonging to the FMN_red family. The CDD and CDART search also confirmed that the ArsC and ArsH belong to the ArsC (thioredoxin_like superfamily) and the FMN_red families, respectively. The motifs, that are the part of protein having a particular biological function were determined using MotifFinder. The obtained motifs are listed in Table 3.13. The ArsC protein showed the presence of three motifs ArsC, Ish1, and glutaredoxin at positions 26-132, 37-47, and 25-74, respectively belonging to ArsC, putative nuclear envelope organization protein, and glutaredoxin family. However, ArsH protein represented two motifs FMN_red, and flavodoxin_2 at positions 31-174 and 32-147, respectively belonging to NADPH-dependent FMN reductase and flavodoxin-like fold family.

Table 3.12 Physiochemical characteristics and numbers of cysteine residues in ArsC and ArsH proteins.

Protein characteristics	ArsC	ArsH
Number of amino acids	135	237
Molecular weight (g/mol)	15452.52	27121.10
Theoretical pI	6.36	6.46
Aliphatic index	74.59	82.70
Positively charged residues	18	32
Negatively charged residues	20	33
Estimated half-life (h) (<i>Escherichia coli</i> , in vivo)	>10	>10
Instability index	37.83 (stable)	48.76 (unstable)
GRAVY	-0.621	-0.427
No. of Cys residues	2 (position 101 and 141)	3 (position 6, 31 and 67)

Table 3.13 Motifs present in proteins determined by the MotifFinder.

Protein	Motif name	Position	Description
ArsC	ArsC	26-132	ArsC family
	Ish1	37-47	Putative nuclear envelope organization protein
	Glutaredoxin	25-74	Glutaredoxin
ArsH	FMN_red	31-174	NADPH-dependent FMN reductase
	Flavodoxin_2	32-147	Flavodoxin-like fold

3.9.2 Protein secondary structure prediction

The protein secondary structures are the local three-dimensional structures in the proteins formed by the hydrogen bonding between the hydrogen atom of the amino group and the oxygen atom of the carboxyl group. In the present study, the protein secondary structures as determined by the SOPMA tool exhibited 42.96 and 49.79% of alpha-helix, 17.78 and 10.55% of the extended strand, 7.41 and 4.64% of beta-turn, and 31.85 and 35.02% of the random coil in the ArsC and ArsH proteins respectively. However, other secondary structures such as 3_{10} helix, Pi helix, beta bridge, bend region, ambiguous states, and other states were absent in both the proteins (Table 3.14). The presence of transmembrane regions in the protein was studied using the PSIPRED 4.0 which showed the absence of any transmembrane region in the proteins indicating that proteins are not associated with the membrane (Fig. 3.39a and b).

Table 3.14 Content of different secondary structures in ArsH and ArsC proteins.

Secondary structure	Percentage (%) (ArsC)	Percentage (%) (ArsH)
Alpha helix	42.96	49.79
3_{10} helix	0.00	0.00
Pi helix	0.00	0.00
Beta bridge	0.00	0.00
Extended strand	17.78	10.55
Beta turn	7.41	4.64
Bend region	0.00	0.00
Random coil	31.85	35.02
Ambiguous states	0.00	0.00
Other states	0.00	0.00

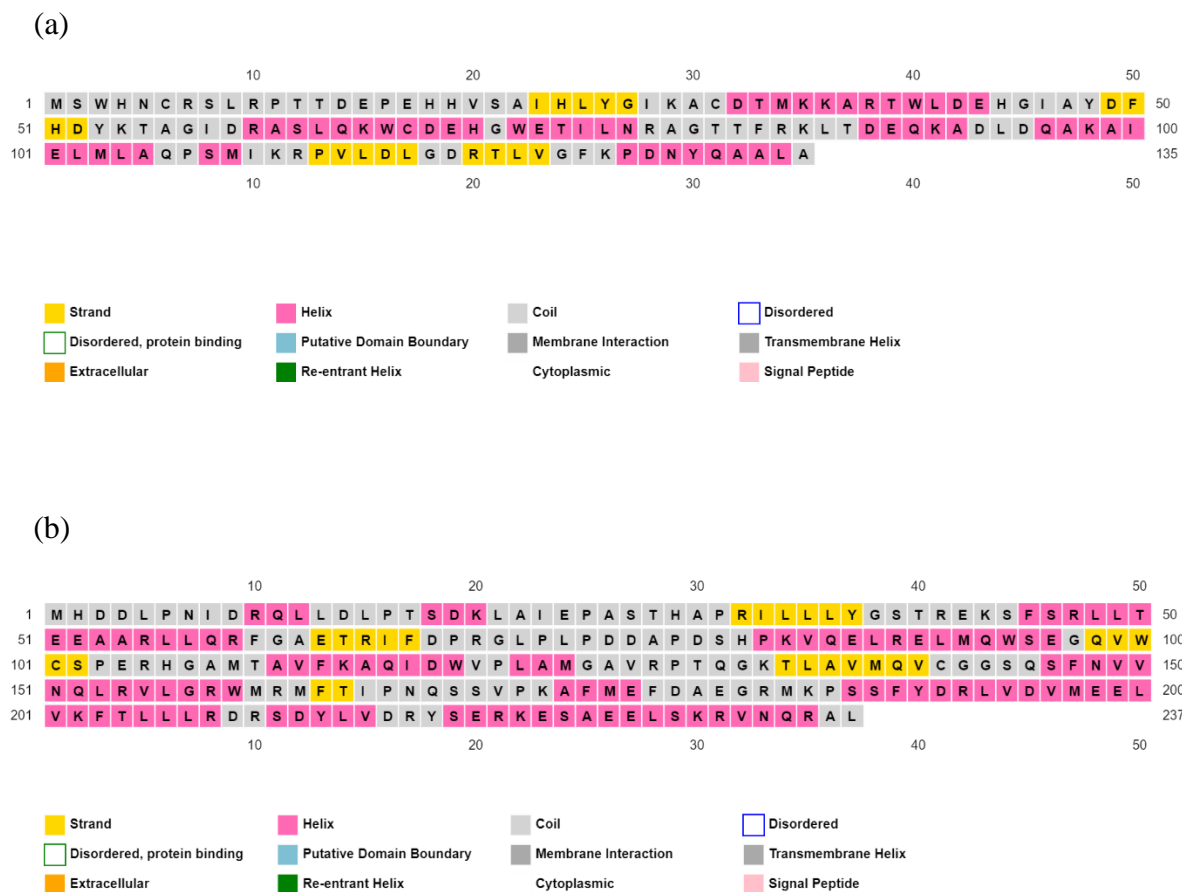


Fig. 3.40 Presence of secondary structures in *P. mendocina* SMSKVR-3 (a) ArsC, and (B) ArsH proteins analyzed by PSIPRED.

3.9.3 Modeling of protein 3D structure

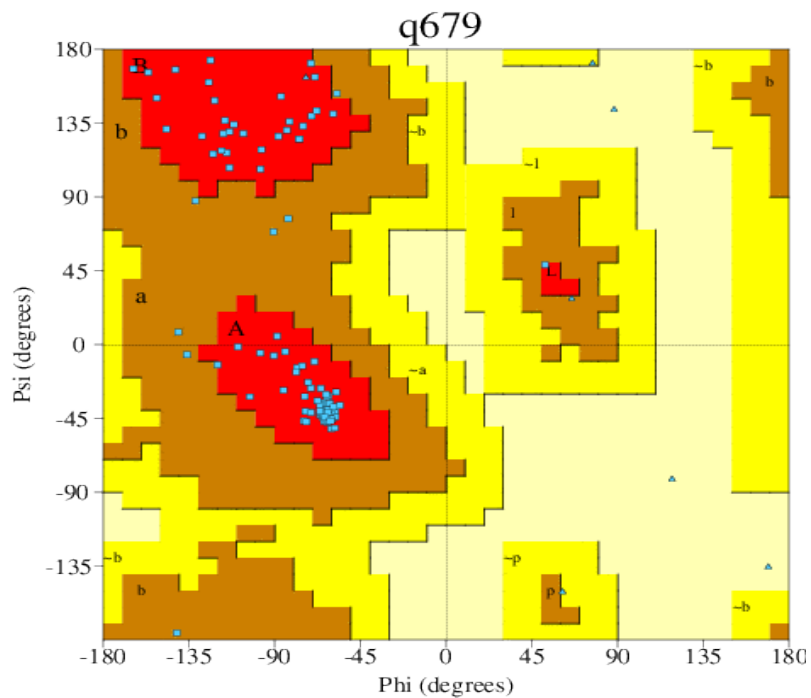
The modeling of protein 3D structure was performed using the four different tools viz. Modeller 9.25, SWISS-MODEL, Phyre2, and I-TASSER. However, the 3D structures of homotetrameric ArsH protein were generated using the Modeller 9.25, and SWISS-MODEL because Phyre2, and I-TASSER do not support the generation of multimeric protein structure. The model validation was performed by comparing the percentage of the amino acid residues in the allowed and disallowed regions of the Ramachandran plot and by the ERRAT scores of the models obtained from different modeling tools. An ERRAT score greater than 90 along with the > 90% fraction of the amino residues in the allowed region of the Ramachandran plot indicated the acceptable protein model. The models of ArsC and ArsH showing the best values

of these parameters were selected for further studies (Table 3.15). The structure of the ArsC protein obtained from the Modeller exhibited 85.1% and 1.7% amino acid residues in the allowed and disallowed region, respectively with an ERRAT score of 57.94. The model generated via SWISS-MODEL exhibited 93.1% amino acid residues in the allowed region with no amino acid residues in the disallowed region (Fig. 3.41a) showing an ERRAT score of 100 (Fig. 3.42a). Thus, this 3D structure was considered the best protein model for the *P. mendocina* SMSKVR-3 ArsC protein. The model constructed using Phyre2 tool showed 89.2% residues in the allowed region with the absence of any amino acid residue in the disallowed region having an ERRAT score of 92.38. However, the I-TASSER model showed 69.4% and 3.3% amino acid residues in the allowed and disallowed regions, respectively with a 90.55 ERRAT value. Hence, based on these results it can be concluded that the best protein 3D structure for ArsC was obtained by the SWISS-MODEL which was selected for further studies. In the case of ArsH, the 3D structure obtained by the Modeller showed 92.0% and 0.4% amino acid residues respectively in the allowed and disallowed regions of the Ramachandran plot with a 64.82 ERRAT value. While the best protein model was obtained by the SWISS-MODEL exhibiting 95.3% amino acid residues in the allowed region and no amino acid residues in the disallowed region (Fig. 3.41b) with an ERRAT score of 91.65 (Fig. 3.42b to e).

Table 3.15 Ramachandran plot analysis and ERRAT scores of the proteins 3D structures obtained by different modeling tools.

Tools used for the modeling	Ramachandran plot				ERRAT score	
	Residues in the most favored region (%)		Residues in the disallowed region (%)		ArsC	ArsH
	ArsC	ArsH	ArsC	ArsH		
Modeller 9.25	85.1	92.0	1.7	0.4	57.94	64.82
SWISS-MODEL	93.1	95.3	0.0	0.0	100	91.65
Phyre2	89.2	-	0.0	-	92.38	-
I-TASSER	69.4	-	3.3	-	90.55	-

(a)



(b)

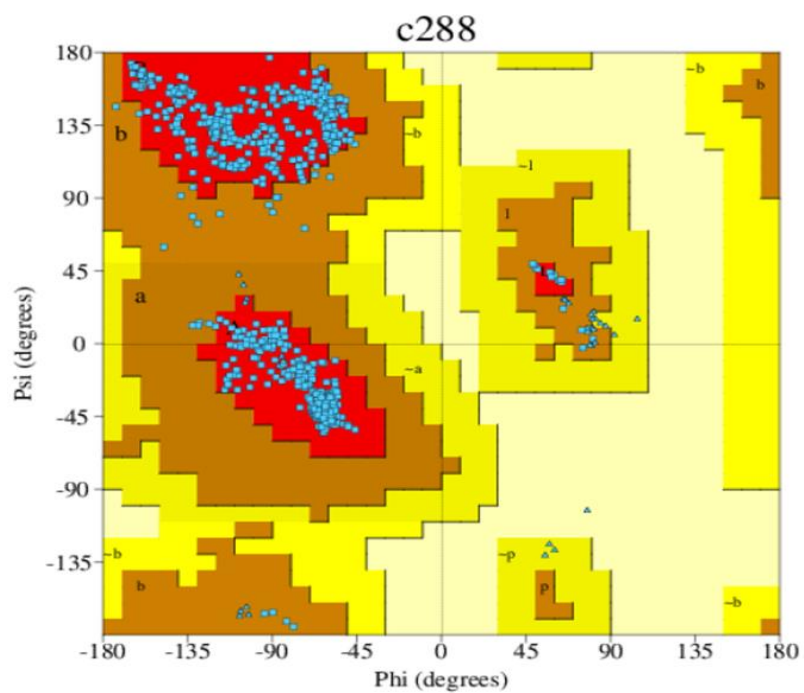
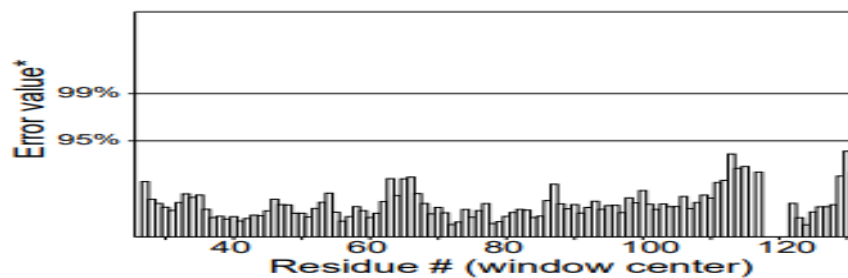


Fig. 3.41 PDBSum-PROCKECK analysis of the protein structures: (a) Ramachandran plot of the SWISS-MODEL structure of the ArsC (b) Ramachandran plot of the SWISS-MODEL structure of the ArsH showing amino acid residues in allowed and disallowed regions.

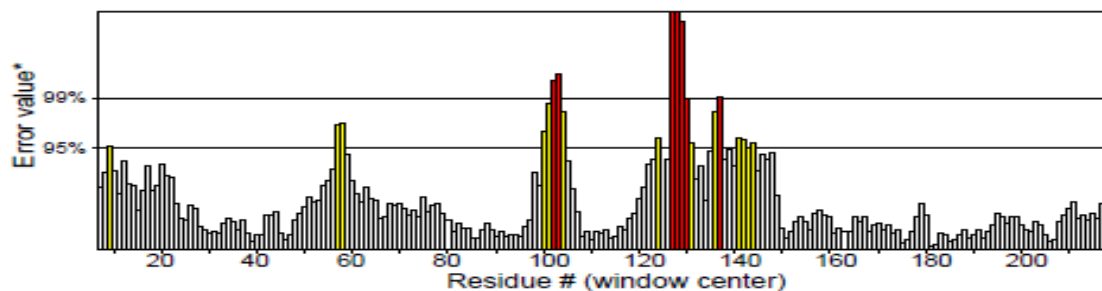
(a)

Program: ERRAT2
File: bestmodel.pdb
Chain#:A
Overall quality factor**: 100.000



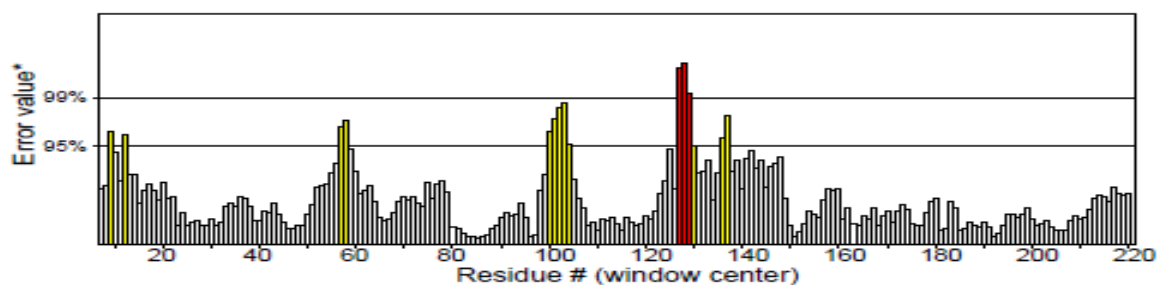
(b)

Program: ERRAT2
File: model 01.pdb
Chain#:A
Overall quality factor**: 91.647

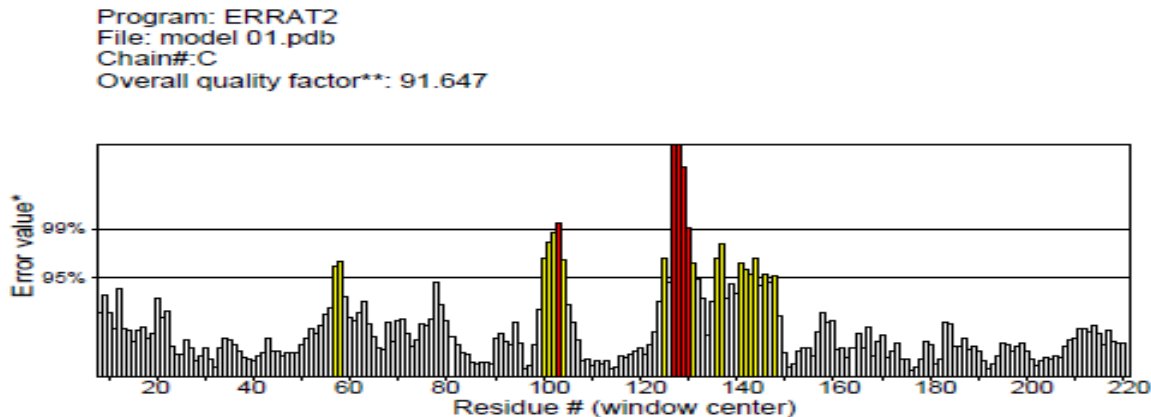


(c)

Program: ERRAT2
File: model 01.pdb
Chain#:B
Overall quality factor**: 91.647



(d)



(e)

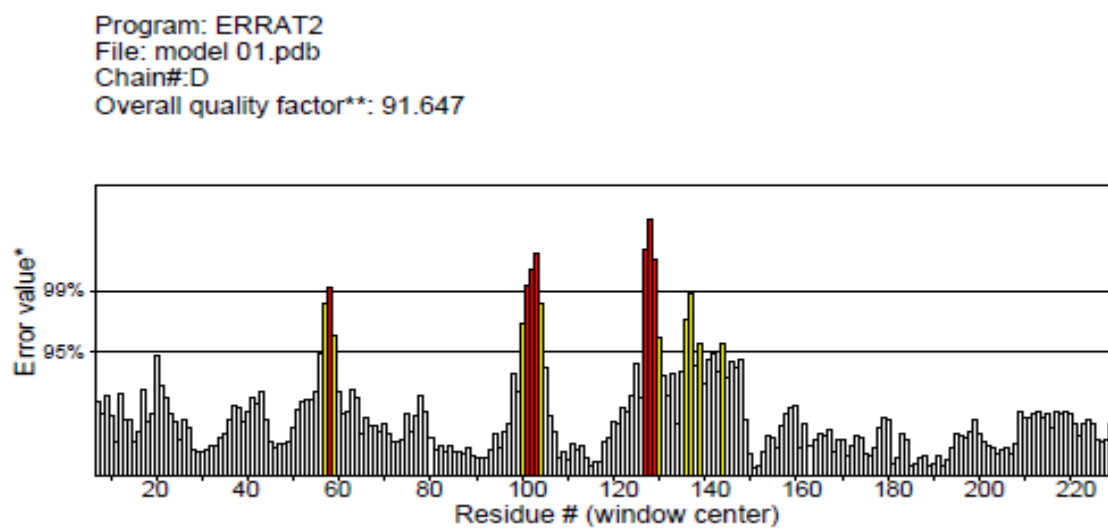
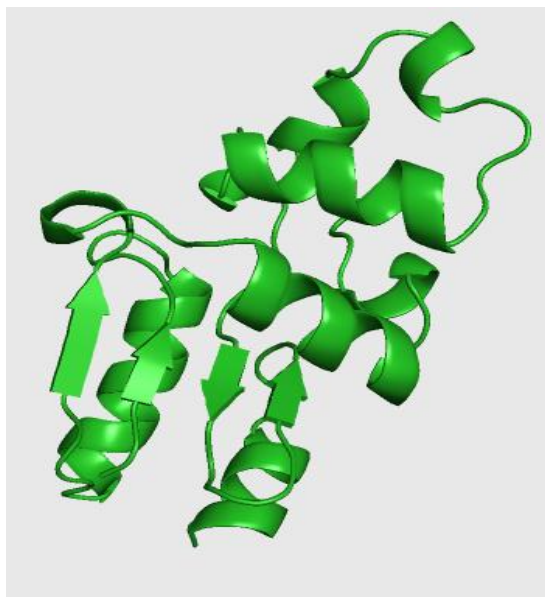


Fig. 3.42 Analysis of the ERRAT score for (a) Structure of ArsC protein obtained from SWISS-MODEL, (b) SWISS-MODEL structure of the homotetrameric structure of ArsH-chain A, (c) ArsH chain B, (d) ArsH chain C, and (e) ArsH chain D.

The ERRAT value is considered as the overall quality factor of a protein structure. It is defined as the percentage of protein for which the calculated error value falls below the rejection limit of 95%. The high-resolution structure generally shows an ERRAT value of 95% or higher. However, lower resolution structures show the ERRAT value of 91%. Based

on the analysis of the Ramachandran plot and ERRAT score it can be concluded that the structure ArsC and ArsH proteins generated through the SWISS-MODEL are of acceptable quality and can be further used for the docking studies (Fig. 3.43a and b).

(a)



(b)

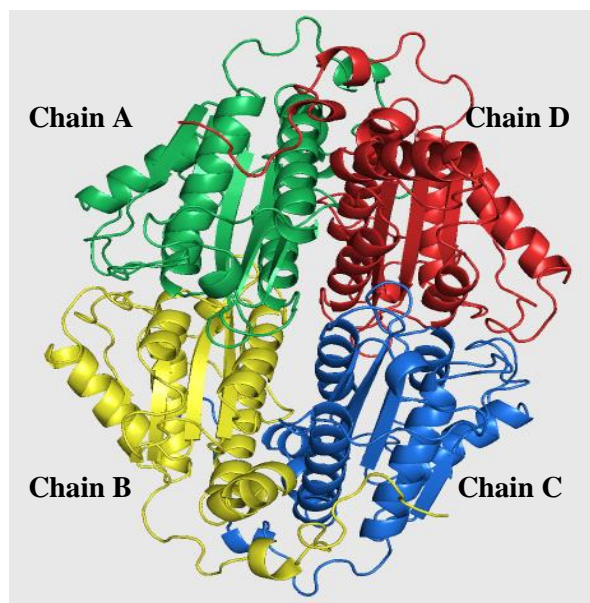


Fig. 3.43 Best protein models obtained by SWISS-MODELER for (a) ArsC protein containing one chain only, and (b) homotetrameric ArsH proteins where green color represents chain A, yellow- chain B, blue- chain C, and red-chain D.

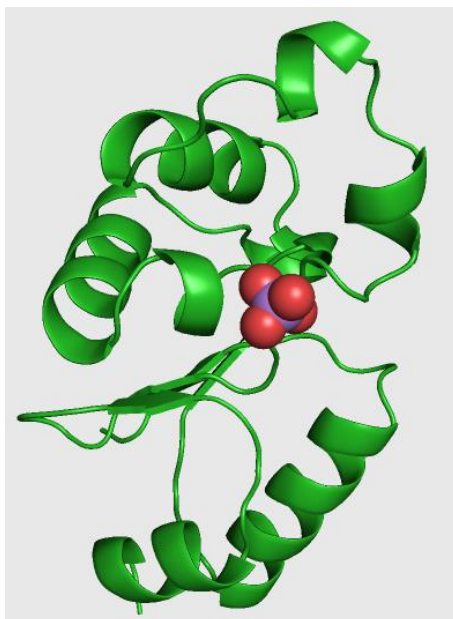
3.9.4 Prediction of active sites in the proteins

The active sites or the binding pockets present in the proteins were predicted by CASTp that finds the residues with As(V) ion binding ability. The analysis of ArsC protein using CASTp showed the presence of a total of three binding pockets with pocket 1 having the largest area and volume of 6064.83 Å² and 3096.21 Å³, respectively. However, the homotetrameric structure of ArsH protein represented 395 pockets with pocket 1 having the largest area and volume of 2015.73 Å² and 1781.52 Å³, respectively. It was followed by pocket 2 having an area and volume of 1191.589 Å² and 1250.541 Å³, respectively. These binding pockets on the proteins can provide space for the As(V) ion binding.

3.9.5 Molecular docking of proteins ArsC and ArsH with the arsenate ion followed by deformability and stability study

The *in silico* docking study involving the binding of ArsC and ArsH with the arsenate ion (AsO₄³⁻) was performed using the AutoDock Tools by manually entering the arsenic parameters in the parameter file (as AutoDock doesn't contain parameters for the arsenic). The docking study revealed the significant binding of arsenate ion with the ArsC (Fig. 3.44a and b) and ArsH (Fig. 3.45a and b) proteins. The binding energy of the ArsC and arsenate ion was calculated as -4.31 kcal/mol with an inhibition constant (K_i) of 697.56 μM. However, the free energy of the binding of ArsH with arsenate ion was calculated as -4.60 kcal/mol with a K_i of 423.62 μM (Table 3.16). The result of the docking confirms the binding of As(V) ions with the Glu 73, Leu 76, Ala 79, Arg 78, and Lys 111 residues of the ArsC protein that were also predicted as the potential binding sites in the 1st binding pocket of ArsC as shown by the CASTp (Fig. 3.44b). The amino acid residues of the ArsH protein involved in the As(V) ion-binding included Ser 39, Lys 43, Ser 44, Phe 45, and Ser 46 residues of the chain B of the protein as it is a homotetrameric protein (Fig. 3.45b). The analysis of the binding pockets using CASTp also showed the presence of these residues in the 2nd binding pocket of the ArsH protein.

(a)



(b)

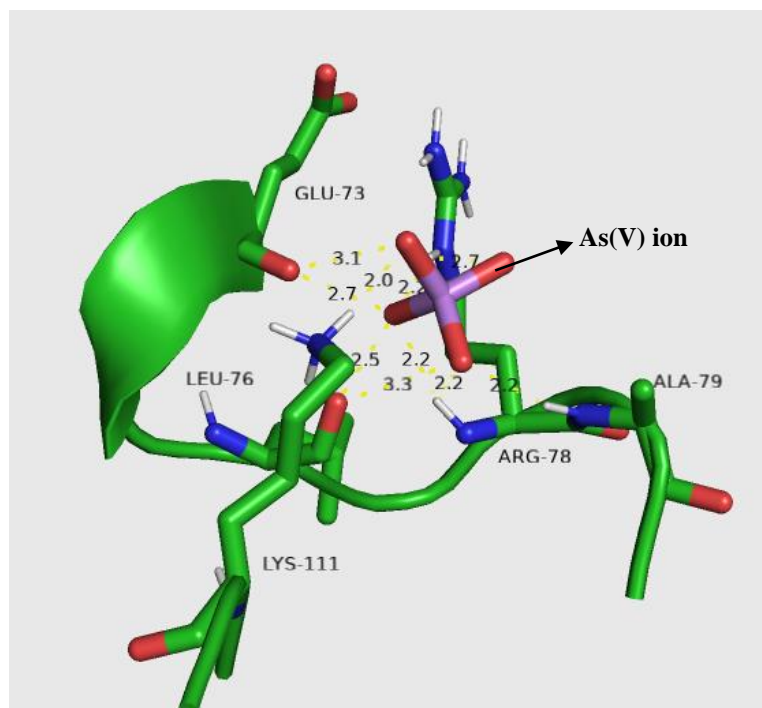
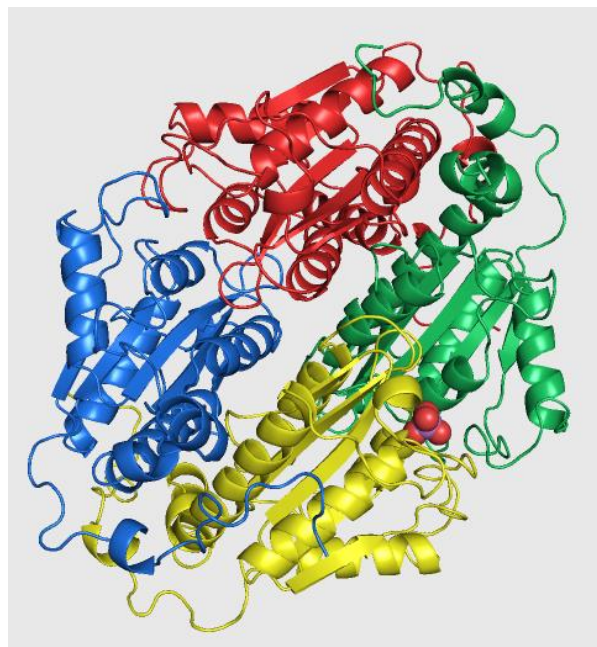


Fig. 3.44 Docking of arsenate ion ligand with the *P. mendocina* SMSKVR-3 ArsC protein (a) complete protein structure, and (b) putative binding site in the protein involving Glu 73, Leu 76, Ala 79, Arg 78, and Lys 111.

(a)



(b)

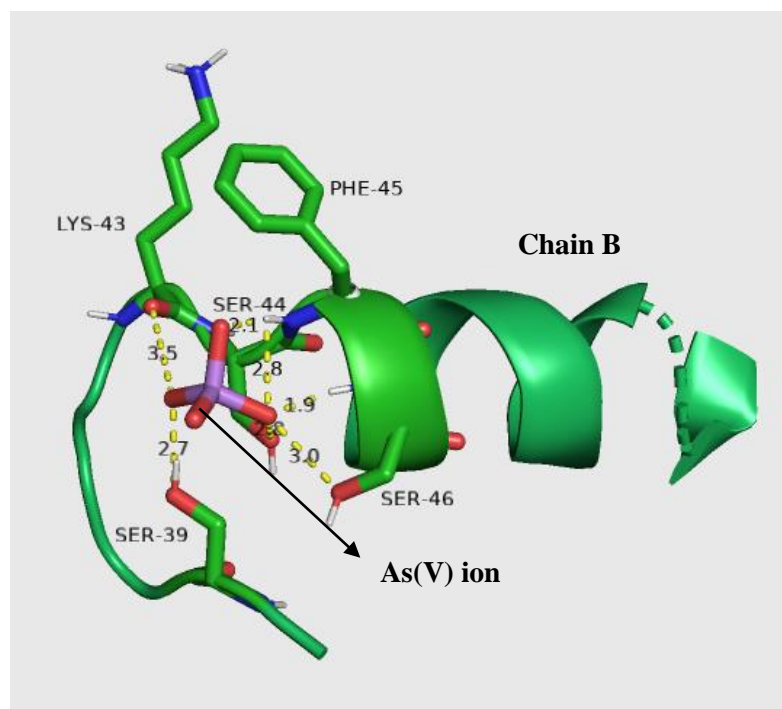


Fig. 3.45 Docking of arsenate ion ligand with the *P. mendocina* SMSKVR-3 ArsH protein (a) complete protein structure, and (b) putative binding site in the protein involving Ser 39, Lys 43, Ser 44, Phe 45, and Ser 46 of the chain B.

Table 3.16 Free energies of the binding and inhibition constants obtained by the docking of *P. mendocina* SMSKVR-3 proteins ArsC and ArsH with the As(V) ion.

Protein	Free energy of the binding (kcal/mol)	Inhibition constant (Ki) (μM)
ArsC	-4.31	697.56
ArsH	-4.60	423.62

The analysis of stability and deformability of the protein-ligand complex was performed using the server-based simulation tool, iMODS applying the NMA. Due to the deformability, the individual residues of the protein represented a distortion that has been shown by the chain hinges for ArsC and ArsH (Fig. 3.46a and b). Deformability is the measure of the ability of each residue of a given molecule to deform independently. The high deformability regions of the protein have been reprinted as the chain hinges. The eigenvalues were obtained to be 3.785×10^{-4} and 8.498×10^{-5} for ArsC and ArsH proteins, respectively (Fig. 3.46c and d). The eigenvalue represents the motion stiffness and is directly proportional to the amount of energy required to deform the protein structure. The lower eigenvalue represents the easier deformation. The variance which is inversely proportional to the eigenvalue was found to be gradually decreased for both ArsC and ArsH proteins (Fig. 3.46e and f). These results indicate the stable binding of the As(V) ion with ArsC and ArsH (Khan et al., 2021; Samad et al., 2020).

The arsenate reductase (ArsC) is a protein that catalyzes the conversion of As(V) to As(III) which is a very well-known mechanism of arsenic detoxification in bacteria. The structure of various bacterial arsenate reductase has been crystallized and available in PDB. However, the structure of *P. mendocina* ArsC is still not available in the PDB. The 3D structure prediction of *P. mendocina* SMSKVR-3 ArsC was performed using *P. aeruginosa* YffB protein (PDB ID- 1RW1) which is a glutathione-dependent thiol reductase, as a template. YffB showed 80.18% identity with the ArsC of *P. mendocina* SMSKVR-3 and thus is a suitable template for it. The 3D structure of ArsC showed the presence of 7 alpha helices and 4 beta-strands sandwiched between the helices similar to the YffB protein having α/β -domain topology (Teplyakov et al., 2004).

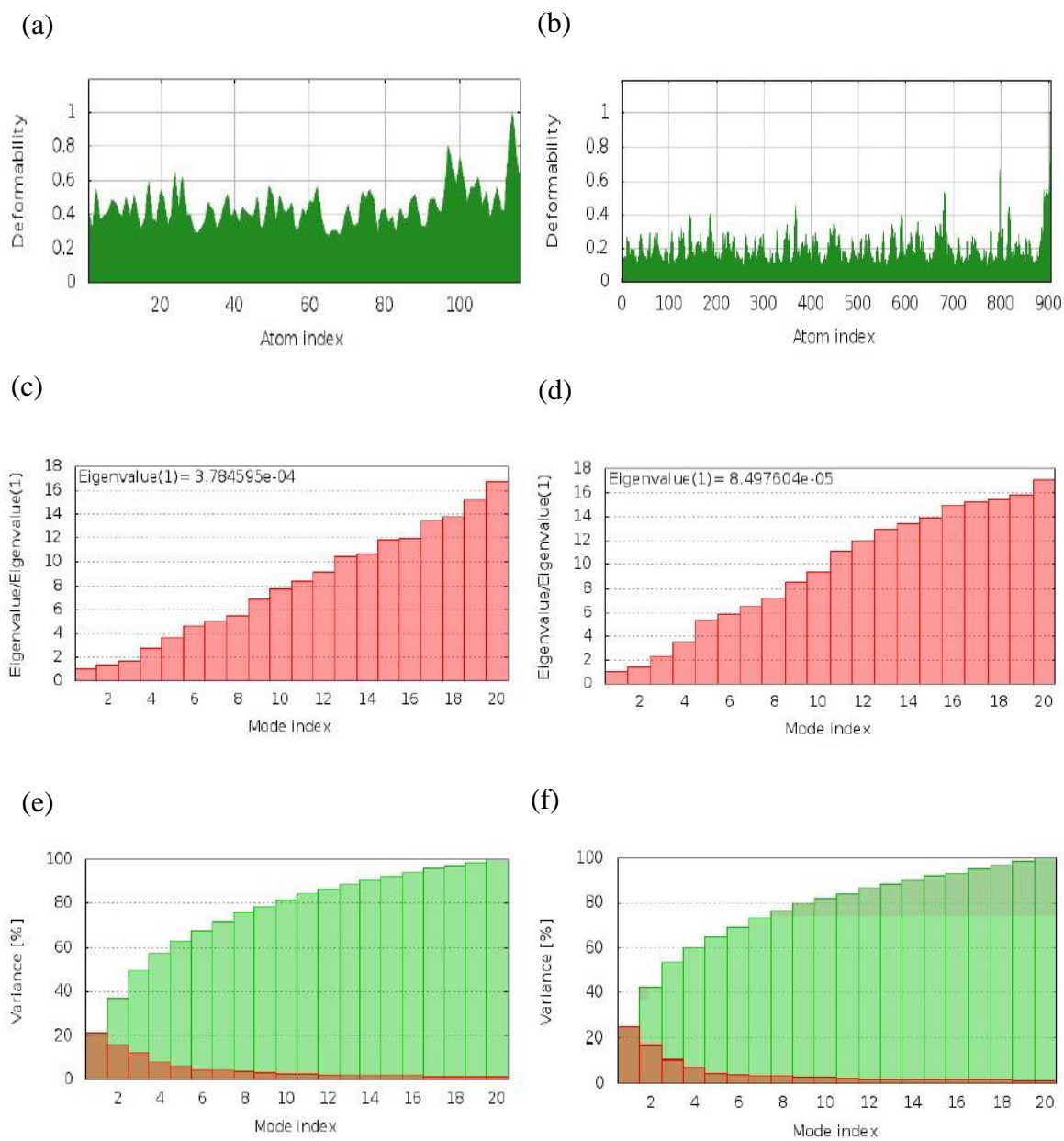


Fig. 3.46 Molecular dynamic simulation studies of ArsC and ArsH proteins using iMODS. Different simulation plots represent (a) and (b) index of deformability, (c) and (d) eigenvalues, and (e) and (f) NMA variance for the *P. mendocina* SMSKVR-3 ArsC and ArsH proteins, respectively.

The sequence comparison of *P. mendocina* SMSKVR-3 and *P. aeruginosa* YffB ArsC showed the variation in the length with the extra sequences in the *P. mendocina* SMSKVR-3 ArsC. The *P. mendocina* SMSKVR-3 ArsC sequence exhibited very little similarity with the *E. coli* ArsC (*P. mendocina* SMSKVR-3 ArsC contains 135 amino acids whereas the *E. coli* ArsC has 141 amino acids) indicating a different mechanism of arsenic binding and detoxification. To understand the binding of *P. mendocina* SMSKVR-3 ArsC with the As(V) ion, a manual docking study was performed that revealed the contribution of Glu 73, Leu 76, Ala 79, Arg 78, and Lys 111 residues of the protein in the As(V) ion binding present at the distance of 4 Å. However, in *E. coli* ArsC, Cys12 is the crucial residue along with the three arginine residues Arg60, Arg94, and Arg107 which binds with the substrate and stabilize the intermediate product formed in the reaction. This indicates a completely different mechanism of arsenic detoxification in *P. mendocina* SMSKVR-3 signifying the role of Arg78 in As(V) ion binding. An earlier study has also shown a very different arsenate reductase mediated arsenic detoxification in *D. indicus* DR1 isolated from the Dadri, Uttar Pradesh, India. This study exhibited the contribution of Glu 9, Asp 53, Arg 86, and Glu 100 residues in the As(V) binding without the involvement of any cysteine residue (Chauhan et al., 2019). This suggests that the presence of cysteine residue in the active site of the arsenate reductase protein is not always required for its catalytic activity and other amino acid residues may also be involved in the As(V) ion-binding.

The protein ArsH is a NADPH-dependent flavin mononucleotide reductase that plays a role in both As(V) and As(III) tolerance. The protein structures of *Shigella flexneri*, *S. meliloti*, and *Synechocystis* sp. (approximate molecular weight of 26 kDa) ArsH are available in the PDB database (Páez-Espino et al., 2020; Vorontsov et al., 2007; Xue et al., 2014; Ye et al., 2007). However, the structure of *P. mendocina* ArsH is not known. The 3D structure of *P. mendocina* SMSKVR-3 was predicted by SWISS-MODEL using the homotetrameric ArsH of *S. meliloti* (PDB ID- 2Q62) as the template showing 74.03% identity with the *P. mendocina* SMSKVR-3 ArsH protein sequence. Each monomer of *P. mendocina* SMSKVR-3 ArsH exhibited a five-stranded beta-sheet parallelly arranged and forming the core domain and 10 alpha-helices similar to *S. meliloti*. The docking study of *P. mendocina* SMSKVR-3 ArsH protein with the As(V) ion was performed to analyze the potential As(V) ion binding sites. The result of the docking study showed the involvement of Ser 39, Lys 43, Ser 44, Phe 45,

and Ser 46 residues of the B monomer of the ArsH in the As(V) ion-binding. The binding pocket study by CASTp also displayed the presence of these amino acid residues in the predicted 2nd binding pocket showing these residues to be crucial for the As(V) ion binding. These results indicate the significant binding of arsenate ion with these proteins. Thus, these proteins can be used as suitable candidates for the development of As(V) bioremediation strategy and biosensor for As(V) detection in the future.

Chapter IV

Summary and Conclusions

Summary and conclusions

The study of arsenic-resistant bacteria is getting a lot of attention because of their arsenic bioremediation potential. Earlier studies on arsenic resistance in the microbes are based on the bacteria isolated from the arsenic-contaminated groundwater and soil but there are very few studies on the arsenic-resistance mechanism present in bacteria that are native to the mining area. Bacterial populations growing in the arsenic-rich environment have shown the presence of arsenic resistance mechanisms involving various proteins and enzymes. In addition to arsenic-specific resistance systems, various other proteins are also induced or overexpressed in presence of arsenic providing resistance to it. The genomics and proteomic approaches provide a great opportunity to understand the expression of proteins in the presence of arsenic. The arsenic resistance machinery consists of several arsenic binding proteins that are specific to the arsenic. The study of the arsenic binding ability of these proteins can be used for the development of an efficient arsenic bioremediation strategy and biosensor for As(V). The summary of the work done is described below-

1) A total of seven (7) arsenic-resistant bacteria designated as SMSKVR-1, SMSKVR-2, SMSKVR-3, SMSKVW-1, SMSKVW-2, SMSKVW-3, and SMSKVW-4 were isolated from the different sites of the khetri copper mines, located in the Jhunjhunu district of Rajasthan. All the strains showed gram-negative characteristics and were able to grow at the 300 mM As(V) containing M9-minimal media. All the strains were analyzed by BOX-PCR and partially characterized by 16S rRNA gene sequencing. These strains exhibited similarity with the genera *Pseudomonas*, *Oceanimonas*, and *Halomonas*. However, among all the isolated strains, SMSKVR-3 belonging to *Pseudomonas* genera was selected for further studies because of its faster growth in the presence of 300 mM As(V).

2) The morphological characterization of SMSKVR-3 showed yellow pigmentation on 3-4 days of growth. The biochemical tests exhibited positive results for citrate, lysine, ornithine, and malonate utilization, esculin hydrolysis, oxidase, and nitrate reduction test. The bacteria showed negative test results for the utilization of all the tested carbon sources, except glucose. The full-length 16S rRNA-based molecular characterization of the bacteria led to the identification of SMSKVR-3 as *Pseudomonas mendocina* strain SMSKVR-3. The study of physiological parameters represented the growth of bacteria in the diverse temperature (25-40

°C), pH (5-9), and salt concentrations (0.25-3.25%) (w/v). However, the optimum growth was observed at the temperature of 30 °C, pH 7, and 0.25% NaCl concentration. The growth study of *P. mendocina* SMSKVR-3 in the absence and presence of 300 mM As(V) and 1.34 mM As(III) exhibited a similar growth pattern in these conditions suggesting the presence of strong arsenic resistance mechanisms in *P. mendocina* SMSKVR-3. The outcome of the growth characteristics study was confirmed by the SEM analysis in the absence (control) and presence of 300 mM As(V) or 1.34 mM As(III) which also exhibited the normal cellular morphology of the *P. mendocina* SMSKVR-3 under all the conditions.

3) The probable As(V) resistance mechanism present in *P. mendocina* SMSKVR-3 was investigated by performing tests including siderophore production, cross heavy metal/metalloid tolerance, antibiotic susceptibility, arsenic biotransformation, and change in polyP bodies and As(V) concentration with the time. *P. mendocina* SMSKVR-3 was found to produce siderophore in the presence of Fe(III), As(V), and As(III) after 48 h of incubation. Tolerance for other heavy metals such as As(III), Mn(II), Mo(VI), Fe(III), Cd(II), Cu(II), and Zn(II) was exhibited by *P. mendocina* SMSKVR-3 along with the tolerance to several broad range antibiotics such as ampicillin (10 µg), vancomycin (30 µg), and kanamycin (30 µg) suggesting the cross-tolerance in *P. mendocina* SMSKVR-3 for heavy metals and antibiotics. The result of the test for the biotransformation of arsenic exhibited the reduction of As(V) to As(III) in *P. mendocina* SMSKVR-3 which is catalyzed by ArsC, a well-known enzyme of the arsenic detoxification pathway. The decrease in the concentration of polyP bodies with the time was also found to be correlated with the decrease in arsenic concentration suggesting the role of polyP bodies in arsenic detoxification in the *P. mendocina* SMSKVR-3. The confirmation of the presence of genes related to these tests such as *arsC*, *ppk1* & efflux RND transporter component gene was done by the PCR amplification of these genes.

4) The whole-genome analysis of *P. mendocina* SMSKVR-3 led to the identification of genes involved in arsenic resistance. The genome of *P. mendocina* SMSKVR-3 has a size of 5.4 Mb. The organism annotation showed a maximum number of BLASTX hits belonging to *P. mendocina*. The phylogenetic analysis also represented its highest similarity with the *P. mendocina* ymp strain. The annotation of the genome showed 4023 proteins with the functional assignment most of which are belonging to the category of metabolic processes

(913 protein-coding genes) followed by protein processing (243 genes), stress response, defense, and virulence (173), energy production (333 genes), membrane transport (216 genes), DNA processing (104 genes), cellular processing (194 genes), RNA processing (89 genes), cell envelop (62 genes), and cell signaling or regulation (14 genes). The analysis of the genome exhibited the presence of genes involved in arsenic resistance such as lactoylglutathione lyase (*gloA1*), arsenate reductase (thioredoxin-coupled, LMWP family) (*arsC*), arsenical-resistance protein (*acr3*), MFS-type efflux pump ArsJ specific for 1-arseno-3-phosphoglycerate, arsenical resistance operon repressor (*arsR*), and arsenite/antimonite:H⁺ antiporter (*arsB*). The other genes involved in arsenic resistance included genes related to multidrug efflux pump such as *lapE*, *mdtA*, *mdtB*, *mdtC*, and *ompH*. Thus, the genome analysis of *P. mendocina* SMSKVR-3 unravels the presence of genes conferring arsenic resistance.

5) The expression of proteins in *P. mendocina* SMSKVR-3 under As(V) stress was standardized. The induction/over-expression of the highest number of protein bands was observed after the 8 h of incubation time with ≥ 200 mM As(V) concentration. Thus, the expression time of 8 h and 300 mM As(V) was used in further studies. The protein expression analysis using 2-DGE exhibited exclusive expression of ribosome-recycling factor, ribonuclease P protein component, and cobalt-precorrin-5B C(1)-methyltransferase with the higher % volume along with the overexpressed polyphosphate: ADP/GDP phosphotransferase (16.49 fold expression). All these proteins play an indirect role in As(V) resistance in *P. mendocina* SMSKVR-3.

6) To get a detailed view of the protein expression profile under As(V) stressed and unstressed conditions, the analysis of the entire proteome of *P. mendocina* SMSKVR-3 was performed using LC-MS//MS analysis. The analysis of proteins exclusively expressed in the presence of 300 mM As(V) showed the presence of phosphate-specific transport system accessory protein (PhoU), stress-induced proteins such as OsmC family peroxiredoxin, NAD(P)H-quinone oxidoreductase, response regulator receiver protein, BofA family protein, and glutathione synthase. Various transcriptional regulators such as TraR/DksA, AsnC, MarR, and LysR were also induced suggesting their direct or indirect involvement in As(V) resistance. The analysis of the upregulated proteins in the As(V) treated sample revealed the highest number of

upregulated proteins involved in the transcription and translation (10.71%) followed by the proteins involved in the transport of various ions (7.31%), amino acid metabolism (6.01%), and nucleic acid metabolism (5.22%). The upregulated proteins involved in As(V) resistance included efflux RND transporter periplasmic adaptor subunit, ArsC family reductase, polyphosphate kinase, arsenical resistance protein ArsH glyceraldehyde-3-phosphate dehydrogenase, and NAD-dependent aldehyde dehydrogenase. Along with these, several stress-related proteins such as superoxide dismutase, universal stress protein, and UspA domain-containing protein were also over-expressed in As(V) treated sample. Thus, the proteomic analysis unravels the role of several arsenic-specific proteins related to the As(V) resistance in *P. mendocina* SMSKVR-3. These arsenic-specific proteins can be employed for arsenic bioremediation and biosensor development to detect arsenic with high selectivity.

7) The arsenic resistance proteins ArsC and ArsH were further studied for their As(V) ion binding capacity using *in silico* approach. It included the modeling of protein 3D structure, docking, and analysis of the deformability and stability. Both the ArsC and ArsH protein exhibited significant binding with As(V) ion showing the binding energies of -4.31 and -4.60 kcal/mol. A comparison of the amino acid residues of ArsC involved in As(V) ion-binding in *P. mendocina* SMSKVR-3 and *E. coli* reveals a different mechanism of ArsC activity in *P. mendocina*. The ArsH showed binding of As(V) ion with the Ser 39, Lys 43, Ser 44, Phe 45, and Ser 46 residues of the B chain of the protein. The interaction of the amino acid residues of ArsC and ArsH proteins with the As(V) ion can be exploited for the development of an efficient bioremediation strategy for As(V) removal and development of the biosensor for As(V).

Future scope of the work

The studies conducted on several arsenic-resistant bacteria have shown their potential application in arsenic bioremediation which could help us to solve the problem of arsenic contamination in the environment. The genomic and proteomic study of *P. mendocina* SMSKVR-3 has confirmed the presence of several arsenic-specific proteins involved in the arsenic resistance which can be exploited for the development of arsenic bioremediation strategies and biosensor specific for arsenic detection. The future works based on the present study may include-

- 1) The study has shown a significant number of proteins to be uncharacterized which are expressed in the presence of As(V). These proteins can be characterized and further studied to explore their role in arsenic resistance as well as their arsenic binding properties.
- 2) Based on the present study, which has shown the significant binding of ArsC and ArsH protein with As(V) ion, strategies can be developed for the construction of biosensor for As(V) detection.
- 3) Affinity of As(V) ion towards the protein ArsC and ArsH can also be exploited to develop the strategies for the bioremediation of As(V).

References

- Abbas, S. Z., Riaz, M., Ramzan, N., Zahid, M. T., Shakoori, F. R., & Rafatullah, M. (2014). Isolation and characterization of arsenic resistant bacteria from wastewater. *Brazilian journal of microbiology*, 45(4), 1309-1315.
- Achour, A. R., Bauda, P., & Billard, P. (2007). Diversity of arsenite transporter genes from arsenic-resistant soil bacteria. *Research in microbiology*, 158(2), 128-137.
- Afkar, E., Lisak, J., Saltikov, C., Basu, P., Oremland, R. S., & Stolz, J. F. (2003). The respiratory arsenate reductase from *Bacillus selenitireducens* strain MLS10. *FEMS microbiology letters*, 226(1), 107-112.
- Aguilar, N. C., Faria, M. C. S., Pedron, T., Batista, B. L., Mesquita, J. P., Bomfeti, C. A., & Rodrigues, J. L. (2020). Isolation and characterization of bacteria from a brazilian gold mining area with a capacity of arsenic bioaccumulation. *Chemosphere*, 240, 124871.
- Ahmann, D., Roberts, A. L., Krumholz, L. R., & Morel, F. M. (1994). Microbe grows by reducing arsenic. *Nature*, 371(6500), 750-750.
- Ajees, A. A., & Rosen, B. P. (2015). As (III) S-adenosylmethionine methyltransferases and other arsenic binding proteins. *Geomicrobiology journal*, 32(7), 570-576.
- Akiyama, M., Crooke, E., & Kornberg, A. (1993). An exopolyphosphatase of *Escherichia coli*. The enzyme and its *ppx* gene in a polyphosphate operon. *Journal of biological chemistry*, 268(1), 633-639.
- Ao, L., Zeng, X.-C., Nie, Y., Mu, Y., Zhou, L., & Luo, X. (2014). *Flavobacterium arsenatis* sp. nov., a novel arsenic-resistant bacterium from high-arsenic sediment. *International journal of systematic and evolutionary microbiology*, 64(10), 3369-3374.
- Arora, K., Prabhakar, N., Chand, S., & Malhotra, B. D. (2007). Immobilization of single stranded DNA probe onto polypyrrole-polyvinyl sulfonate for application to DNA hybridization biosensor. *Sensors and actuators B: chemical*, 126(2), 655-663.
- Arora, N. K., & Verma, M. (2017). Modified microplate method for rapid and efficient estimation of siderophore produced by bacteria. *3 Biotech*, 7(6), 1-9.
- Atlas, R. M. (2010). *Handbook of microbiological media*: CRC press.
- Babkina, S. S., Ulakhovich, N. A., & Zyavkina, Y. I. (2004). Amperometric DNA biosensor for the determination of auto-antibodies using DNA interaction with Pt (II) complex. *Analytica chimica acta*, 502(1), 23-30.

- Badilla, C., Osborne, T. H., Cole, A., Watson, C., Djordjevic, S., & Santini, J. M. (2018). A new family of periplasmic-binding proteins that sense arsenic oxyanions. *Scientific reports*, 8(1), 6282.
- Bafana, A., Khan, F., & Suguna, K. (2017). Structural and functional characterization of mercuric reductase from *Lysinibacillus sphaericus* strain G1. *Biometals*, 30(5), 809-819.
- Bahar, M. M., Megharaj, M., & Naidu, R. (2013). Bioremediation of arsenic-contaminated water: recent advances and future prospects. *Water, air, & soil Pollution*, 224(12), 1722.
- Bai, Y.-N., Lu, Y.-Z., Shen, N., Lau, T.-C., & Zeng, R. J. (2018). Investigation of Cr (VI) reduction potential and mechanism by *Caldicellulosiruptor saccharolyticus* under glucose fermentation condition. *Journal of hazardous materials*, 344, 585-592.
- Baker-Austin, C., Wright, M. S., Stepanauskas, R., & McArthur, J. V. (2006). Co-selection of antibiotic and metal resistance. *Trends in microbiology*, 14(4), 176-182.
- Banik, A., Sajib, E., Deb, A., Ahmed, S. R., Islam, M.-T., Roy, S., Sinha, S., Marma, H., Azim, K. F., & Roy, S. (2020). Identification of potential phytochemical inhibitors as promising therapeutics against SARS-CoV-2 and molecular dynamics simulation.
- Bauer, A. W., Kirby, W. M. M., Sherris, J. C., & Turck, M. (1966). Antibiotic susceptibility testing by a standardized single disk method. *American journal of clinical pathology*, 45(4), 493-496.
- Bazzi, W., Abou Fayad, A. G., Nasser, A., Haraoui, L. P., Dewachi, O., Abou-Sitta, G., Nguyen, V. K., Abara, A., Karah, N., Landecker, H. & Knapp, C. (2020). Heavy metal toxicity in armed conflicts potentiates AMR in *A. baumannii* by selecting for antibiotic and heavy metal co-resistance mechanisms. *Frontiers in microbiology*, 11, 68.
- Belfiore, C., Ordonez, O. F., & Farías, M. E. (2013). Proteomic approach of adaptive response to arsenic stress in *Exiguobacterium* sp. S17, an extremophile strain isolated from a high-altitude Andean Lake stromatolite. *Extremophiles*, 17(3), 421-431.
- Ben Fekih, I., Zhang, C., Li, Y. P., Zhao, Y., Alwathnani, H. A., Saquib, Q., Rensing, C., & Cervantes, C. (2018). Distribution of arsenic resistance genes in prokaryotes. *Frontiers in microbiology*, 9, 2473.
- Berman, H., Henrick, K., & Nakamura, H. (2003). Announcing the worldwide protein data bank. *Nature structural & molecular biology*, 10(12), 980-980.
- Bhattacharjee, H., Li, J., Ksenzenko, M. Y., & Rosen, B. P. (1995). Role of cysteinyl residues in metalloactivation of the oxyanion-translocating ArsA ATPase. *Journal of biological chemistry*, 270(19), 11245-11250.

- Bhattacharya, M., Hota, A., Kar, A., Sankar Chini, D., Chandra Malick, R., Chandra Patra, B., & Kumar Das, B. (2018). *In silico* structural and functional modelling of Antifreeze protein (AFP) sequences of Ocean pout (*Zoarces americanus*, Bloch & Schneider 1801). *Journal of genetic engineering and biotechnology*, *16*(2), 721-730.
- Biswas, R., Majhi, A. K., & Sarkar, A. (2019). The role of arsenate reducing bacteria for their prospective application in arsenic contaminated groundwater aquifer system. *Biocatalysis and agricultural biotechnology*, *20*, 101218.
- Boeck, B., & Schinzel, R. (1996). Purification and Characterisation of an α -Glucan Phosphorylase from the Thermophilic Bacterium *Thermus thermophilus*. *European journal of biochemistry*, *239*(1), 150-155.
- Braud, A., Hoegy, F., Jezequel, K., Lebeau, T., & Schalk, I. J. (2009). New insights into the metal specificity of the *Pseudomonas aeruginosa* pyoverdine–iron uptake pathway. *Environmental microbiology*, *11*(5), 1079-1091.
- Brettin, T., Davis, J. J., Disz, T., Edwards, R. A., Gerdes, S., Olsen, G. J., Olson, R., Overbeek, R., Parrello, B., & Pusch, G. D. (2015). RASTtk: a modular and extensible implementation of the RAST algorithm for building custom annotation pipelines and annotating batches of genomes. *Scientific reports*, *5*(1), 1-6.
- Brusetti, L., Malkhazova, I., Gtari, M., Tamagnini, I., Borin, S., Merabishvili, M., Chanishvili, N., Mora, D., Cappitelli, F., & Daffonchio, D. (2008). Fluorescent-BOX-PCR for resolving bacterial genetic diversity, endemism and biogeography. *BMC microbiology*, *8*(1), 220.
- Bryan, C. G., Marchal, M., Battaglia-Brunet, F., Kugler, V., Lemaitre-Guillier, C., Lièvreumont, D., Bertin, P. N., & Arsène-Ploetze, F. (2009). Carbon and arsenic metabolism in *Thiomonas* strains: differences revealed diverse adaptation processes. *BMC microbiology*, *9*(1), 1-12.
- Buchan, D. W. A., & Jones, D. T. (2019). The PSIPRED protein analysis workbench: 20 years on. *Nucleic acids research*, *47*(W1), W402-W407.
- Bui, X. T., Qvortrup, K., Wolff, A., Bang, D. D., & Creuzenet, C. (2012). Effect of environmental stress factors on the uptake and survival of *Campylobacter jejuni* in *Acanthamoeba castellanii*. *BMC microbiology*, *12*, 232.
- Cervantes, C., Ji, G., Ramírez, J. L., & Silver, S. (1994). Resistance to arsenic compounds in microorganisms. *FEMS microbiology reviews*, *15*(4), 355-367.
- Challenger, F. (1945). Biological methylation. *Chemical reviews*, *36*(3), 315-361.

- Chambers, J. P., Arulanandam, B. P., Matta, L. L., Weis, A., & Valdes, J. J. (2008). Biosensor recognition elements. *Current issues in molecular biology*, 10(1-2), 1-12
- Chang, J.-S., Kim, Y.-H., & Kim, K.-W. (2008). The *ars* genotype characterization of arsenic-resistant bacteria from arsenic-contaminated gold–silver mines in the Republic of Korea. *Applied microbiology and biotechnology*, 80(1), 155-165.
- Chauhan, D., Srivastava, P. A., Agnihotri, V., Yennamalli, R. M., & Priyadarshini, R. (2019). Structure and function prediction of arsenate reductase from *Deinococcus indicus* DR1. *Journal of molecular modeling*, 25(1), 1-9.
- Chen, C.-M., Misra, T. K., Silver, S., & Rosen, B. P. (1986). Nucleotide sequence of the structural genes for an anion pump. The plasmid-encoded arsenical resistance operon. *Journal of biological chemistry*, 261(32), 15030-15038.
- Chen, J., Bhattacharjee, H., & Rosen, B. P. (2015). ArsH is an organoarsenical oxidase that confers resistance to trivalent forms of the herbicide monosodium methylarsenate and the poultry growth promoter roxarsone. *Molecular microbiology*, 96(5), 1042-1052.
- Chen, J., Li, J., Zhang, H., Shi, W., & Liu, Y. (2019). Bacterial heavy-metal and antibiotic resistance genes in a copper tailing dam area in northern China. *Frontiers in microbiology*, 10, 1916.
- Chen, J., & Tian, Y. (2021). Hexavalent chromium reducing bacteria: mechanism of reduction and characteristics. *Environmental science and pollution research*, 28(17), 20981-20997.
- Chen, J., Yoshinaga, M., Garbinski, L. D., & Rosen, B. P. (2016). Synergistic interaction of glyceraldehydes-3-phosphate dehydrogenase and ArsJ, a novel organoarsenical efflux permease, confers arsenate resistance. *Molecular microbiology*, 100(6), 945-953.
- Chen, S.-C., Sun, G.-X., Yan, Y., Konstantinidis, K. T., Zhang, S.-Y., Deng, Y., Li, X.-M., Cui, H.-L., Musat, F., & Popp, D. (2020). The Great Oxidation Event expanded the genetic repertoire of arsenic metabolism and cycling. *Proceedings of the national academy of sciences*, 117(19), 10414-10421.
- Chen, Y., Kaji, A., Kaji, H., & Cooperman, B. S. (2017). The kinetic mechanism of bacterial ribosome recycling. *Nucleic acids research*, 45(17), 10168-10177.
- Cheng, J., Baldwin, K., Guffanti, A. A., & Krulwich, T. A. (1996). Na⁺/H⁺ antiport activity conferred by *Bacillus subtilis* tetA (L), a 5' truncation product of tetA (L), and related plasmid genes upon *Escherichia coli*. *Antimicrobial agents and chemotherapy*, 40(4), 852-857.

- Ciprandi, A., Baraúna, R. A., Santos, A. V., Gonçalves, E. C., Carepo, M. S. P., Schneider, M. P. C., & Silva, A. (2012). Proteomic response to arsenic stress in *Chromobacterium violaceum*. *Journal of integrated OMICS*, 2(1), 69-73.
- Cobbett, C., & Goldsbrough, P. (2002). Phytochelatins and metallothioneins: roles in heavy metal detoxification and homeostasis. *Annual review of plant biology*, 53(1), 159-182.
- Coico, R. (2006). Gram staining. *Current protocols in microbiology*, 00(1), A-3C.
- Colovos, C., & Yeates, T. O. (1993). Verification of protein structures: patterns of nonbonded atomic interactions. *Protein science*, 2(9), 1511-1519.
- Confer, A. W., & Ayalew, S. (2013). The OmpA family of proteins: Roles in bacterial pathogenesis and immunity. *Veterinary microbiology*, 163(3), 207-222.
- Cosnier, S., Mousty, C., Cui, X., Yang, X., & Dong, S. (2006). Specific determination of as (V) by an acid phosphatase-polyphenol oxidase biosensor. *Analytical chemistry*, 78(14), 4985-4989.
- Das, S., & Barooah, M. (2018). Characterization of siderophore producing arsenic-resistant *Staphylococcus* sp. strain TA6 isolated from contaminated groundwater of Jorhat, Assam and its possible role in arsenic geocycle. *BMC microbiology*, 18(1), 104.
- Das, S., Jean, J.-S., Kar, S., Chou, M.-L., & Chen, C.-Y. (2014). Screening of plant growth-promoting traits in arsenic-resistant bacteria isolated from agricultural soil and their potential implication for arsenic bioremediation. *Journal of hazardous materials*, 272, 112-120.
- Davis, J. J., Gerdes, S., Olsen, G. J., Olson, R., Pusch, G. D., Shukla, M., Vonstein, V., Wattam, A. R., & Yoo, H. (2016). PATTyFams: protein families for the microbial genomes in the PATRIC database. *Frontiers in microbiology*, 7, 118.
- Davis, J. J., Wattam, A. R., Aziz, R. K., Brettin, T., Butler, R., Butler, R. M., Chlenski, P., Conrad, N., Dickerman, A., & Dietrich, E. M. (2020). The PATRIC Bioinformatics Resource Center: expanding data and analysis capabilities. *Nucleic acids research*, 48(D1), D606-D612.
- Daware, V., Kesavan, S., Patil, R., Natu, A., Kumar, A., Kulkarni, M., & Gade, W. (2012). Effects of arsenite stress on growth and proteome of *Klebsiella pneumoniae*. *Journal of biotechnology*, 158(1-2), 8-16.
- De Villiers, C. A., Lapsley, M. C., & Hall, E. A. H. (2015). A step towards mobile arsenic measurement for surface waters. *Analyst*, 140(8), 2644-2655.
- Deepika, K. V., Raghuram, M., Kariali, E., & Bramhachari, P. V. (2016). Biological responses of symbiotic *Rhizobium radiobacter* strain VBCK1062 to the arsenic contaminated rhizosphere soils of mung bean. *Ecotoxicology and environmental safety*, 134, 1-10.

- DeLano, W. L. (2002). The PyMOL molecular graphics system. <http://www.pymol.org>.
- DeMel, S., Shi, J., Martin, P., Rosen, B. P., & Edwards, B. F. P. (2004). Arginine 60 in the ArsC arsenate reductase of *E. coli* plasmid R773 determines the chemical nature of the bound As(III) product. *Protein science*, *13*(9), 2330-2340.
- Deng, W., Wang, H., & Xie, J. (2011). Regulatory and pathogenesis roles of *Mycobacterium* Lrp/AsnC family transcriptional factors. *Journal of cellular biochemistry*, *112*(10), 2655-2662.
- Dey, S., Dou, D., & Rosen, B. P. (1994). ATP-dependent arsenite transport in everted membrane vesicles of *Escherichia coli*. *Journal of biological chemistry*, *269*(41), 25442-25446.
- Dey, U., Chatterjee, S., & Mondal, N. K. (2016). Isolation and characterization of arsenic-resistant bacteria and possible application in bioremediation. *Biotechnology reports*, *10*, 1-7.
- Diesel, E., Schreiber, M., & van der Meer, J. R. (2009). Development of bacteria-based bioassays for arsenic detection in natural waters. *Analytical and bioanalytical chemistry*, *394*(3), 687-693.
- Domingues, V. S., de Souza Monteiro, A., Júlio, A. D. L., Queiroz, A. L. L., & dos Santos, V. L. (2020). Diversity of metal-resistant and arsenite-producing culturable heterotrophic bacteria isolated from a copper mine in Brazilian Amazonia. *Scientific reports*, *10*(1), 6171.
- Drewniak, L., Styczek, A., Majder-Lopatka, M., & Sklodowska, A. (2008). Bacteria, hypertolerant to arsenic in the rocks of an ancient gold mine, and their potential role in dissemination of arsenic pollution. *Environmental pollution*, *156*(3), 1069-1074.
- Duval, S., Ducluzeau, A.-L., Nitschke, W., & Schoepp-Cothenet, B. (2008). Enzyme phylogenies as markers for the oxidation state of the environment: the case of respiratory arsenate reductase and related enzymes. *BMC evolutionary biology*, *8*(1), 1-13.
- Edgar, R. C. (2004). MUSCLE: multiple sequence alignment with high accuracy and high throughput. *Nucleic acids research*, *32*(5), 1792-1797.
- Edmundson, M. C., & Horsfall, L. (2015). Construction of a modular arsenic-resistance operon in *E. coli* and the production of arsenic nanoparticles. *Frontiers in bioengineering and biotechnology*, *3*, 160.
- Eis, C., & Nidetzky, B. (2002). Substrate-binding recognition and specificity of trehalose phosphorylase from *Schizophyllum commune* examined in steady-state kinetic studies with deoxy and deoxyfluoro substrate analogues and inhibitors. *Biochemical journal*, *363*(2), 335-340.

- Ellis, P. J., Conrads, T., Hille, R., & Kuhn, P. (2001). Crystal structure of the 100 kDa arsenite oxidase from *Alcaligenes faecalis* in two crystal forms at 1.64 Å and 2.03 Å. *Structure*, 9(2), 125-132.
- Ferguson, A. D., & Deisenhofer, J. (2002). TonB-dependent receptors-structural perspectives. *Biochimica et biophysica acta (BBA) - biomembranes*, 1565(2), 318-332.
- Ferrer, A., Rivera, J., Zapata, C., Norambuena, J., Sandoval, Á., Chávez, R., Orellana, O., & Levicán, G. (2016). Cobalamin protection against oxidative stress in the acidophilic iron-oxidizing bacterium *Leptospirillum* group II CF-1. *Frontiers in microbiology*, 7, 748.
- Finnegan, P. M., & Chen, W. (2012). Arsenic toxicity: the effects on plant metabolism. *Frontiers in physiology*, 3, 182.
- Fru, E. C., Arvestål, E., Callac, N., El Albani, A., Kiliyas, S., Argyraki, A., & Jakobsson, M. (2015). Arsenic stress after the Proterozoic glaciations. *Scientific reports*, 5(1), 1-12.
- Fru, E. C., Somogyi, A., El Albani, A., Medjoubi, K., Aubineau, J., Robbins, L. J., Lalonde, S. V., & Konhauser, K. O. (2019). The rise of oxygen-driven arsenic cycling at ca. 2.48 Ga. *Geology*, 47(3), 243-246.
- Fuku, X., Iftikar, F., Hess, E., Iwuoha, E., & Baker, P. (2012). Cytochrome c biosensor for determination of trace levels of cyanide and arsenic compounds. *Analytica chimica acta*, 730, 49-59.
- Gang, H., Xiao, C., Xiao, Y., Yan, W., Bai, R., Ding, R., Yang, Z., & Zhao, F. (2019). Proteomic analysis of the reduction and resistance mechanisms of *Shewanella oneidensis* MR-1 under long-term hexavalent chromium stress. *Environment international*, 127, 94-102.
- Gangaiah, D., Liu, Z., Arcos, J., Kassem, I. I., Sanad, Y., Torrelles, J. B., & Rajashekara, G. (2010). Polyphosphate kinase 2: a novel determinant of stress responses and pathogenesis in *Campylobacter jejuni*. *PLoS one*, 5(8), e12142.
- Gasteiger, E., Hoogland, C., Gattiker, A., Wilkins, M. R., Appel, R. D., & Bairoch, A. (2005). Protein identification and analysis tools on the ExPASy server. *The proteomics protocols handbook*, 571-607.
- Ge, Y., Ning, Z., Wang, Y., Zheng, Y., Zhang, C., & Figeys, D. (2016). Quantitative proteomic analysis of *Dunaliella salina* upon acute arsenate exposure. *Chemosphere*, 145, 112-118.
- Geer, L. Y., Domrachev, M., Lipman, D. J., & Bryant, S. H. (2002). CDART: protein homology by domain architecture. *Genome research*, 12(10), 1619-1623.

- Geourjon, C., & Deléage, G. (1995). SOPMA: significant improvements in protein secondary structure prediction by consensus prediction from multiple alignments. *Bioinformatics*, *11*(6), 681-684.
- Ghosh, P., Rathinasabapathi, B., Teplitski, M., & Ma, L. Q. (2015). Bacterial ability in AsIII oxidation and AsV reduction: Relation to arsenic tolerance, P uptake, and siderophore production. *Chemosphere*, *138*, 995-1000.
- Ghosh, P. K., Maiti, T. K., Pramanik, K., Ghosh, S. K., Mitra, S., & De, T. K. (2018). The role of arsenic resistant *Bacillus aryabhatai* MCC3374 in promotion of rice seedlings growth and alleviation of arsenic phytotoxicity. *Chemosphere*, *211*, 407-419.
- González-Segura, L., Mújica-Jiménez, C., & Munoz-Clares, R. A. (2009). Reaction of the catalytic cysteine of betaine aldehyde dehydrogenase from *Pseudomonas aeruginosa* with arsenite-BAL and phenylarsine oxide. *Chemico-biological interactions*, *178*(1-3), 64-69.
- Goswami, R., Ghosh, D., Saha, D. R., Padhy, P. K., & Mazumder, S. (2011). Effect of acute and chronic arsenic exposure on growth, structure and virulence of *Aeromonas hydrophila* isolated from fish. *Microbial pathogenesis*, *50*(2), 63-69.
- Gudlavalleti, R. H., Bose, S. C., Verma, S. K., Khatri, P., Scaria, J., Dhewa, S., & Chaubey, V. K. (2017). A novel fluorometric bio-sensing-based arsenic detection system for groundwater. *IEEE sensors journal*, *17*(17), 5391-5398.
- Gurevich, A., Saveliev, V., Vyahhi, N., & Tesler, G. (2013). QAST: quality assessment tool for genome assemblies. *Bioinformatics*, *29*(8), 1072-1075.
- Hassan, K. M., Fukuhara, T., Hai, F. I., Bari, Q. H., & Islam, K. M. S. (2009). Development of a bio-physicochemical technique for arsenic removal from groundwater. *Desalination*, *249*(1), 224-229.
- Holt, P. A., Chaires, J. B., & Trent, J. O. (2008). Molecular docking of intercalators and groove-binders to nucleic acids using Autodock and Surflex. *Journal of chemical information and modeling*, *48*(8), 1602-1615.
- Huang, K., Xu, Y., Packianathan, C., Gao, F., Chen, C., Zhang, J., Shen, Q., Rosen, B. P., & Zhao, F.-J. (2018). Arsenic methylation by a novel ArsM As(III) S-adenosylmethionine methyltransferase that requires only two conserved cysteine residues. *Molecular microbiology*, *107*(2), 265-276.
- Hussein, K. A., & Joo, J. H. (2017). Stimulation, purification, and chemical characterization of siderophores produced by the rhizospheric bacterial strain *Pseudomonas putida*. *Rhizosphere*, *4*, 16-21.

- Hyatt, D., Chen, G.-L., LoCascio, P. F., Land, M. L., Larimer, F. W., & Hauser, L. J. (2010). Prodigal: prokaryotic gene recognition and translation initiation site identification. *BMC bioinformatics*, *11*(1), 119.
- Inokuchi, Y., Hirashima, A., Sekine, Y., Janosi, L., & Kaji, A. (2000). Role of ribosome recycling factor (RRF) in translational coupling. *The EMBO journal*, *19*(14), 3788-3798.
- Irvine, G. W., Tan, S. N., & Stillman, M. J. (2017). A simple metallothionein-based biosensor for enhanced detection of arsenic and mercury. *Biosensors*, *7*(1), 14.
- Jarrous, N. (2017). Roles of RNase P and its subunits. *Trends in genetics*, *33*(9), 594-603.
- Jha, S. K., Mishra, V. K., Damodaran, T., Sharma, D. K., & Kumar, P. (2017). Arsenic in the groundwater: Occurrence, toxicological activities, and remedies. *Journal of environmental science and health, Part C*, *35*(2), 84-103.
- Jebelli, M. A., Maleki, A., Amoozegar, M. A., Kalantar, E., Shahmoradi, B., & Gharibi, F. (2017). Isolation and identification of indigenous prokaryotic bacteria from arsenic-contaminated water resources and their impact on arsenic transformation. *Ecotoxicology and environmental safety*, *140*, 170-176.
- Ji, G., Garber, E. A. E., Armes, L. G., Chen, C.-M., Fuchs, J. A., & Silver, S. (1994). Arsenate reductase of *Staphylococcus aureus* plasmid pI258. *Biochemistry*, *33*(23), 7294-7299.
- Johnson, D. A., Tetu, S. G., Phillippy, K., Chen, J., Ren, Q., & Paulsen, I. T. (2008). High-throughput phenotypic characterization of *Pseudomonas aeruginosa* membrane transport genes. *PLoS genetics*, *4*(10), e1000211.
- Joshi, D. N., Patel, J. S., Flora, S. J. S., & Kalia, K. (2008). Arsenic accumulation by *Pseudomonas stutzeri* and its response to some thiol chelators. *Environmental health and preventive medicine*, *13*(5), 257-263.
- Kale, S. P., Salaskar, D., Ghosh, S., & Sounderajan, S. (2015). Isolation and identification of arsenic resistant *Providencia rettgeri* (KDM3) from industrial effluent contaminated soil and studies on its arsenic resistance mechanism. *Journal of microbial & biochemical technology*, *7*, 1-8.
- Kang, S. H., Singh, S., Kim, J.-Y., Lee, W., Mulchandani, A., & Chen, W. (2007). Bacteria metabolically engineered for enhanced phytochelatin production and cadmium accumulation. *Applied and environmental microbiology*, *73*(19), 6317-6320.
- Kaur, H., Kumar, R., Babu, J. N., & Mittal, S. (2015). Advances in arsenic biosensor development- a comprehensive review. *Biosensors and bioelectronics*, *63*, 533-545.

- Keasling, J. D., & Hupf, G. A. (1996). Genetic manipulation of polyphosphate metabolism affects cadmium tolerance in *Escherichia coli*. *Applied and environmental microbiology*, *62*(2), 743-746.
- Kelley, L. A., Mezulis, S., Yates, C. M., Wass, M. N., & Sternberg, M. J. E. (2015). The Phyre2 web portal for protein modeling, prediction and analysis. *Nature protocols*, *10*(6), 845-858.
- Keng, Y. F., Wu, L., & Zhang, Z. Y. (1999). Probing the function of the conserved tryptophan in the flexible loop of the *Yersinia* protein-tyrosine phosphatase. *European journal of biochemistry*, *259*(3), 809-814.
- Khan, M. S. A., Nain, Z., Syed, S. B., Abdulla, F., Moni, M. A., Sheam, M. M., Karim, M. M., & Adhikari, U. K. (2021). Computational formulation and immune dynamics of a multi-peptide vaccine candidate against Crimean-Congo hemorrhagic fever virus. *Molecular and cellular probes*, *55*, 101693.
- Kim, M., Um, H.-J., Bang, S., Lee, S.-H., Oh, S.-J., Han, J.-H., Kim, K.-W., Min, J., & Kim, Y.-H. (2009). Arsenic removal from vietnamese groundwater using the arsenic-binding DNA aptamer. *Environmental science & technology*, *43*(24), 9335-9340.
- Klemm, B. P., Wu, N., Chen, Y., Liu, X., Kaitany, K. J., Howard, M. J., & Fierke, C. A. (2016). The diversity of ribonuclease P: Protein and RNA catalysts with analogous biological functions. *Biomolecules*, *6*(2), 27.
- Kornberg, A. (1995). Inorganic polyphosphate: toward making a forgotten polymer unforgettable. *Journal of bacteriology*, *177*(3), 491-496.
- Krafft, T., & Macy, J. M. (1998). Purification and characterization of the respiratory arsenate reductase of *Chrysiogenes arsenatis*. *European journal of biochemistry*, *255*(3), 647-653.
- Krizek, B. A., Prost, V., Joshi, R. M., Stoming, T., & Glenn, T. C. (2003). Developing transgenic *Arabidopsis* plants to be metal-specific bioindicators. *Environmental toxicology and chemistry: An international journal*, *22*(1), 175-181.
- Kruger, M. C., Bertin, P. N., Heipieper, H. J., & Arsène-Ploetze, F. (2013). Bacterial metabolism of environmental arsenic-mechanisms and biotechnological applications. *Applied microbiology and biotechnology*, *97*(9), 3827-3841.
- Kulakovskaya, T. (2018). Inorganic polyphosphates and heavy metal resistance in microorganisms. *World journal of microbiology and biotechnology*, *34*(9), 139.
- Kulp, T. R., Hoefft, S. E., Asao, M., Madigan, M. T., Hollibaugh, J. T., Fisher, J. C., Stolz, J. F., Culbertson, C. W., Miller, L. G., & Oremland, R. S. (2008). Arsenic (III) fuels anoxygenic

- photosynthesis in hot spring biofilms from Mono Lake, California. *Science*, 321(5891), 967-970.
- Kumar, S., Verma, S. K., Singhal, A. (2017). Copper bio-leaching technique for tailing waste at Hindustan Copper Limited, Khetri (Rajasthan), advanced technology and innovations in mining industry. Paper presented at the 37th Annual Day National Seminar, Hindustan Copper Limited, Khetri Nagar, Rajasthan, India.
- Laskowski, R. A., Jabłońska, J., Pravda, L., Vařeková, R. S., & Thornton, J. M. (2018). PDBsum: Structural summaries of PDB entries. *Protein science*, 27(1), 129-134.
- Lebrun, E., Brugna, M., Baymann, F., Muller, D., Lièvreumont, D., Lett, M.-C., & Nitschke, W. (2003). Arsenite oxidase, an ancient bioenergetic enzyme. *Molecular biology and evolution*, 20(5), 686-693.
- Legrain, C., & Stalon, V. (1976). Ornithine carbamoyltransferase from *Escherichia coli* W: purification, structure and steady-state kinetic analysis. *European journal of biochemistry*, 63(1), 289-301.
- Li, B., Lin, J., Mi, S., & Lin, J. (2010). Arsenic resistance operon structure in *Leptospirillum ferriphilum* and proteomic response to arsenic stress. *Bioresource technology*, 101(24), 9811-9814.
- Li, B., Qiu, Y., Shi, H., & Yin, H. (2016). The importance of lag time extension in determining bacterial resistance to antibiotics. *Analyst*, 141(10), 3059-3067.
- Li, Y., Hu, Y., Zhang, X., Xu, H., Lescop, E., Xia, B., & Jin, C. (2007). Conformational fluctuations coupled to the thiol-disulfide transfer between thioredoxin and arsenate reductase in *Bacillus subtilis*. *Journal of biological chemistry*, 282(15), 11078-11083.
- Li, Y., Ling, J., Chen, P., Chen, J., Dai, R., Liao, J., Yu, J., & Xu, Y. (2020). *Pseudomonas mendocina* LYX: A novel aerobic bacterium with advantage of removing nitrate high effectively by assimilation and dissimilation simultaneously. *Frontiers of environmental science & engineering*, 15(4), 57.
- Li, Y., & Zhang, Y. (2007). PhoU is a persistence switch involved in persister formation and tolerance to multiple antibiotics and stresses in *Escherichia coli*. *Antimicrobial agents and chemotherapy*, 51(6), 2092-2099.
- López-Blanco, J. R., Aliaga, J. I., Quintana-Ortí, E. S., & Chacón, P. (2014). iMODS: internal coordinates normal mode analysis server. *Nucleic acids research*, 42(W1), W271-W276.

- Lu, S., Wang, J., Chitsaz, F., Derbyshire, M. K., Geer, R. C., Gonzales, N. R., Gwadz, M., Hurwitz, D. I., Marchler, G. H., & Song, J. S. (2020). CDD/SPARCLE: the conserved domain database in 2020. *Nucleic acids research*, 48(D1), D265-D268.
- Macfarlane, E. L. A., Kwasnicka, A., Ochs, M. M., & Hancock, R. E. W. (1999). PhoP–PhoQ homologues in *Pseudomonas aeruginosa* regulate expression of the outer-membrane protein OprH and polymyxin B resistance. *Molecular microbiology*, 34(2), 305-316.
- Madhuri, R. J., Saraswathi, M., Gowthami, K., Bhargavi, M., Divya, Y., & Deepika, V. (2019). Recent approaches in the production of novel enzymes from environmental samples by enrichment culture and metagenomic approach. *Recent developments in applied microbiology and biochemistry*, 251-262.
- Maizel, D., Blum, J. S., Ferrero, M. A., Utturkar, S. M., Brown, S. D., Rosen, B. P., & Oremland, R. S. (2016). Characterization of the extremely arsenic-resistant *Brevibacterium linens* strain AE038-8 isolated from contaminated groundwater in Tucumán, Argentina. *International biodeterioration & biodegradation*, 107, 147-153.
- Malasarn, D., Keeffe, J. R., & Newman, D. K. (2008). Characterization of the arsenate respiratory reductase from *Shewanella* sp. strain ANA-3. *Journal of bacteriology*, 190(1), 135-142.
- Male, K. B., Hrapovic, S., Santini, J. M., & Luong, J. H. T. (2007). Biosensor for arsenite using arsenite oxidase and multiwalled carbon nanotube modified electrodes. *Analytical chemistry*, 79(20), 7831-7837.
- Marquez, S. M., Chen, J. L., Evans, D., & Pace, N. R. (2006). Structure and function of eukaryotic Ribonuclease P RNA. *Molecular cell*, 24(3), 445-456.
- Mata, M. T., Baquero, F., & Perez-Diaz, J. C. (2000). A multidrug efflux transporter in *Listeria monocytogenes*. *FEMS microbiology letters*, 187(2), 185-188.
- Merulla, D., Buffi, N., Beggah, S., Truffer, F., Geiser, M., Renaud, P., & van der Meer, J. R. (2013). Bioreporters and biosensors for arsenic detection. Biotechnological solutions for a world-wide pollution problem. *Current opinion in biotechnology*, 24(3), 534-541.
- Messens, J., Martins, J. C., Brosens, E., Van Belle, K., Jacobs, D. M., Willem, R., & Wyns, L. (2002). Kinetics and active site dynamics of *Staphylococcus aureus* arsenate reductase. *Journal of biological inorganic chemistry*, 7(1), 146-156.
- Miranda-Carrasco, A., Viguera-Cortés, J. M., Villa-Tanaca, L., & Hernández-Rodríguez, C. (2018). Cyanotrophic and arsenic oxidizing activities of *Pseudomonas mendocina* P6115 isolated from mine tailings containing high cyanide concentration. *Archives of microbiology*, 200(7), 1037-1048.

- Mishra, R. K., Pandey, B. K., Pathak, N., & Zeeshan, M. (2015). BOX-PCR-and ERIC-PCR-based genotyping and phylogenetic correlation among *Fusarium oxysporum* isolates associated with wilt disease in *Psidium guajava* L. *Biocatalysis and agricultural biotechnology*, 4(1), 25-32.
- Mistry, J., Chuguransky, S., Williams, L., Qureshi, M., Salazar, G. A., Sonnhammer, E. L. L., Tosatto, S. C. E., Paladin, L., Raj, S., Richardson, L. J., Finn, R. D., & Bateman, A. (2021). Pfam: The protein families database in 2021. *Nucleic acids research*, 49(D1), D412-D419.
- Modrzejewska, M., Kawalek, A., & Bartosik, A. A. (2021). The LysR-type transcriptional regulator BsrA (PA2121) controls vital metabolic pathways in *Pseudomonas aeruginosa*. *bioRxiv*.
- GAD-RAB, S. M. F., Shoreit, A. A. F., & Fukumori, Y. (2006). Effects of cadmium stress on growth, morphology, and protein expression in *Rhodobacter capsulatus* B10. *Bioscience, biotechnology, and biochemistry*, 70(10), 2394-2402.
- Morris, G. M., Huey, R., Lindstrom, W., Sanner, M. F., Belew, R. K., Goodsell, D. S., & Olson, A. J. (2009). AutoDock4 and AutoDockTools4: Automated docking with selective receptor flexibility. *Journal of computational chemistry*, 30(16), 2785-2791.
- Mousavi, S. M., Hashemi, S. A., Iman Moezzi, S. M., Ravan, N., Gholami, A., Lai, C. W., Chiang, W.-H., Omidifar, N., Yousefi, K., & Behbudi, G. (2021). Recent advances in enzymes for the bioremediation of pollutants. *Biochemistry research international*, 2021, 5599204.
- Mu, Y., Zhou, X., Liu, L., Zhou, X.-K., Zeng, X.-C., & Li, W.-J. (2019). *Pseudaminobacter arsenicus* sp. nov., an arsenic-resistant bacterium isolated from arsenic-rich aquifers. *International journal of systematic and evolutionary microbiology*, 69(3), 791-797.
- Mukhopadhyay, R., Rosen, B. P., Phung, L. T., & Silver, S. (2002). Microbial arsenic: from geocycles to genes and enzymes. *FEMS microbiology reviews*, 26(3), 311-325.
- Murphy, J., & Riley, J. P. (1962). A modified single solution method for the determination of phosphate in natural waters. *Analytica chimica acta*, 27, 31-36.
- Navarro-Noya, Y. E., Hernández-Mendoza, E., Morales-Jiménez, J., Jan-Roblero, J., Martínez-Romero, E., & Hernández-Rodríguez, C. (2012). Isolation and characterization of nitrogen fixing heterotrophic bacteria from the rhizosphere of pioneer plants growing on mine tailings. *Applied soil ecology*, 62, 52-60.
- Nair, A., Juwarkar, A. A., & Singh, S. K. (2007). Production and characterization of siderophores and its application in arsenic removal from contaminated soil. *Water, air, and soil pollution*, 180(1), 199-212.

- Ndeddy Aka, R. J., & Babalola, O. O. (2017). Identification and characterization of Cr-, Cd-, and Ni-tolerant bacteria isolated from mine tailings. *Bioremediation journal*, 21(1), 1-19.
- Newman, D. K., Ahmann, D., & Morel, F. M. M. (1998). A brief review of microbial arsenate respiration. *Geomicrobiology journal*, 15(4), 255-268.
- Nickbarg, E. B., & Knowles, J. R. (1988). Triosephosphate isomerase: energetics of the reaction catalyzed by the yeast enzyme expressed in *Escherichia coli*. *Biochemistry*, 27(16), 5939-5947.
- Nocek, B. P., Khusnutdinova, A. N., Ruszkowski, M., Flick, R., Burda, M., Batyrova, K., Brown, G., Mucha, A., Joachimiak, A., & Berlicki, Ł. (2018). Structural insights into substrate selectivity and activity of bacterial polyphosphate kinases. *ACS catalysis*, 8(11), 10746-10760.
- Oh, E., & Jeon, B. (2014). Role of alkyl hydroperoxide reductase (AhpC) in the biofilm formation of *Campylobacter jejuni*. *PLoS one*, 9(1), e87312.
- Oliveira, S. C. B., Corduneanu, O., & Oliveira-Brett, A. M. (2008). In situ evaluation of heavy metal-DNA interactions using an electrochemical DNA biosensor. *Bioelectrochemistry*, 72(1), 53-58.
- Ondov, B. D., Treangen, T. J., Melsted, P., Mallonee, A. B., Bergman, N. H., Koren, S., & Phillippy, A. M. (2016). Mash: fast genome and metagenome distance estimation using MinHash. *Genome biology*, 17(1), 1-14.
- Oremland, R. S., Saltikov, C. W., Wolfe-Simon, F., & Stolz, J. F. (2009). Arsenic in the evolution of earth and extraterrestrial ecosystems. *Geomicrobiology journal*, 26(7), 522-536.
- Oremland, R. S., & Stolz, J. F. (2003). The ecology of arsenic. *Science*, 300(5621), 939-944.
- Páez-Espino, A. D., Nikel, P. I., Chavarría, M., & de Lorenzo, V. (2020). ArsH protects *Pseudomonas putida* from oxidative damage caused by exposure to arsenic. *Environmental microbiology*, 22(6), 2230-2242.
- Pal, C., Asiani, K., Arya, S., Rensing, C., Stekel, D. J., Larsson, D. J., & Hobman, J. L. (2017). Metal resistance and its association with antibiotic resistance. *Advances in microbial physiology*, 70, 261-313.
- Palleroni, N. J., Doudoroff, M., Stanier, R. Y., Solanes, R. E., & Mandel, M. (1970). Taxonomy of the aerobic *Pseudomonads*: the properties of the *Pseudomonas stutzeri* group. *Microbiology*, 60(2), 215-231.
- Pandey, N., & Bhatt, R. (2015). Arsenic resistance and accumulation by two bacteria isolated from a natural arsenic contaminated site. *Journal of basic microbiology*, 55(11), 1275-1286.

- Park, M., Tsai, S. L., & Chen, W. (2013). Microbial biosensors: engineered microorganisms as the sensing machinery. *Sensors*, *13*(5), 5777-5795.
- Parker, K. J., Kumar, S., Pearce, D. A., & Sutherland, A. J. (2005). Design, synthesis and evaluation of a fluorescent peptidyl sensor for the selective recognition of arsenite. *Tetrahedron letters*, *46*(41), 7043-7045.
- Patel, P. C., Goulhen, F., Boothman, C., Gault, A. G., Charnock, J. M., Kalia, K., & Lloyd, J. R. (2007). Arsenate detoxification in a *Pseudomonad* hypertolerant to arsenic. *Archives of microbiology*, *187*(3), 171-183.
- Pokhrel, A., Lingo, J. C., Wolschendorf, F., & Gray, M. J. (2019). Assaying for inorganic polyphosphate in bacteria. *Journal of visualized experiments : JoVE*(143).
- Qamar, N., Rehman, Y., & Hasnain, S. (2017). Arsenic-resistant and plant growth-promoting Firmicutes and γ -Proteobacteria species from industrially polluted irrigation water and corresponding cropland. *Journal of applied microbiology*, *123*(3), 748-758.
- Qin, J., Rosen, B. P., Zhang, Y., Wang, G., Franke, S., & Rensing, C. (2006). Arsenic detoxification and evolution of trimethylarsine gas by a microbial arsenite S-adenosylmethionine methyltransferase. *Proceedings of the national academy of sciences*, *103*(7), 2075-2080.
- Qin, Q.-L., Li, Y., Zhang, Y.-J., Zhou, Z.-M., Zhang, W.-X., Chen, X.-L., Zhang, X.-Y., Zhou, B.-C., Wang, L., & Zhang, Y.-Z. (2011). Comparative genomics reveals a deep-sea sediment-adapted life style of *Pseudoalteromonas* sp. SM9913. *The ISME journal*, *5*(2), 274-284.
- Rahman, A., Nahar, N., Nawani, N. N., Jass, J., Desale, P., Kapadnis, B. P., Hossain, K., Saha, A. K., Ghosh, S., Olsson, B., & Mandal, A. (2014). Isolation and characterization of a *Lysinibacillus* strain B1-CDA showing potential for bioremediation of arsenics from contaminated water. *Journal of environmental science and health, part A*, *49*(12), 1349-1360.
- Rangeshwaran, R., Ashwitha, K., Sivakumar, G., & Jalali, S. K. (2013). Analysis of proteins expressed by an abiotic stress tolerant *Pseudomonas putida* (NBAIL-RPF9) isolate under saline and high temperature conditions. *Current microbiology*, *67*(6), 659-667.
- Rao, N. N., Roberts, M. F., & Torriani, A. (1985). Amount and chain length of polyphosphates in *Escherichia coli* depend on cell growth conditions. *Journal of bacteriology*, *162*(1), 242-247.
- Ravikumar, Y., Nadarajan, S. P., Lee, C. S., & Yun, H. (2017). Engineering an FMN-based iLOV protein for the detection of arsenic ions. *Analytical biochemistry*, *525*, 38-43.

- Richarme, G. (1988). A novel aspect of the inhibition by arsenicals of binding-protein-dependent galactose transport in gram-negative bacteria. *Biochemical journal*, 253(2), 371-376.
- Romero-Rodríguez, A., Robledo-Casados, I., & Sánchez, S. (2015). An overview on transcriptional regulators in *Streptomyces*. *Biochimica et biophysica acta (BBA)-Gene regulatory mechanisms*, 1849(8), 1017-1039.
- Roos, G., Buts, L., Van Belle, K., Brosens, E., Geerlings, P., Loris, R., Wyns, L., & Messens, J. (2006). Interplay between ion binding and catalysis in the thioredoxin-coupled arsenate reductase family. *Journal of molecular biology*, 360(4), 826-838.
- Rosen, B. P. (2002). Biochemistry of arsenic detoxification. *FEBS letters*, 529(1), 86-92.
- Rosen, B. P., & Liu, Z. (2009). Transport pathways for arsenic and selenium: A minireview. *Environment international*, 35(3), 512-515.
- Sahu, S., Sheet, T., & Banerjee, R. (2019). Interaction landscape of a 'C α NN' motif with arsenate and arsenite: a potential peptide-based scavenger of arsenic. *RSC advances*, 9(2), 1062-1074.
- Šali, A., & Blundell, T. L. (1993). Comparative protein modelling by satisfaction of spatial restraints. *Journal of molecular biology*, 234(3), 779-815.
- Samad, A., Ahammad, F., Nain, Z., Alam, R., Imon, R. R., Hasan, M., & Rahman, M. S. (2020). Designing a multi-epitope vaccine against SARS-CoV-2: an immunoinformatics approach. *Journal of biomolecular structure & dynamics*, 1-17.
- Sanllrente-Méndez, S., Domínguez-Renedo, O., & Arcos-Martínez, M. J. (2012). Development of acid phosphatase based amperometric biosensors for the inhibitive determination of As (V). *Talanta*, 93, 301-306.
- Sarkar, A., Kazy, S. K., & Sar, P. (2013). Characterization of arsenic resistant bacteria from arsenic rich groundwater of West Bengal, India. *Ecotoxicology*, 22(2), 363-376.
- Sarkar, P., Banerjee, S., Bhattacharyay, D., & Turner, A. P. F. (2010). Electrochemical sensing systems for arsenate estimation by oxidation of L-cysteine. *Ecotoxicology and environmental safety*, 73(6), 1495-1501.
- Sarkar, P. K., & Banerjee, A. K. (1987). The effect of nickel on growth, morphology and photopigments of *Rhodospirillum photometricum*. *Folia microbiologica*, 32(1), 48-54.
- Satyapal, G. K., Mishra, S. K., Srivastava, A., Ranjan, R. K., Prakash, K., Haque, R., & Kumar, N. (2018). Possible bioremediation of arsenic toxicity by isolating indigenous bacteria from the middle Gangetic plain of Bihar, India. *Biotechnology reports*, 17, 117-125.

- Schubert, M., Lindgreen, S., & Orlando, L. (2016). AdapterRemoval v2: rapid adapter trimming, identification, and read merging. *BMC research notes*, 9(1), 1-7.
- Schwyn, B., & Neilands, J. B. (1987). Universal chemical assay for the detection and determination of siderophores. *Analytical biochemistry*, 160(1), 47-56.
- Shah, S., & Damare, S. (2020). Cellular response of *Brevibacterium casei*# NIOSBA88 to arsenic and chromium-a proteomic approach. *Brazilian journal of microbiology*, 51(4), 1885-1895.
- Shah, S., & Damare, S. R. (2018). Differential protein expression in a marine-derived *Staphylococcus* sp. NIOSBK35 in response to arsenic (III). *3 Biotech*, 8(6), 1-11.
- Shen, S., Li, X.-F., Cullen, W. R., Weinfeld, M., & Le, X. C. (2013). Arsenic binding to proteins. *Chemical reviews*, 113(10), 7769-7792.
- Sher, S., Hussain, S. Z., & Rehman, A. (2020). Phenotypic and genomic analysis of multiple heavy metal-resistant *Micrococcus luteus* strain AS2 isolated from industrial waste water and its potential use in arsenic bioremediation. *Applied microbiology and biotechnology*, 104(5), 2243-2254.
- Shi, K., Cao, M., Li, C., Huang, J., Zheng, S., & Wang, G. (2019). Efflux proteins MacAB confer resistance to arsenite and penicillin/macrolide-type antibiotics in *Agrobacterium tumefaciens* 5A. *World journal of microbiology and biotechnology*, 35(8), 1-10.
- Shi, W., Dong, J., Scott, R. A., Ksenzenko, M. Y., & Rosen, B. P. (1996). The role of arsenic-thiol interactions in metalloregulation of the ars operon. *Journal of biological chemistry*, 271(16), 9291-9297.
- Shi, W., Wu, J., & Rosen, B. P. (1994). Identification of a putative metal binding site in a new family of metalloregulatory proteins. *Journal of biological chemistry*, 269(31), 19826-19829.
- Shrivastava, A., Ghosh, D., Dash, A., & Bose, S. (2015). Arsenic contamination in soil and sediment in India: sources, effects, and remediation. *Current pollution reports*, 1(1), 35-46.
- Shukla, A., & Srivastava, S. (2017). Emerging aspects of bioremediation of arsenic. *Green technologies and environmental sustainability* (pp. 395-407). Springer, Cham.
- Si, M., Chen, C., Su, T., Che, C., Yao, S., Liang, G., Li, G., & Yang, G. (2018). CosR is an oxidative stress sensing a MarR-type transcriptional repressor in *Corynebacterium glutamicum*. *Biochemical journal*, 475(24), 3979-3995.
- Sigrist, C. J. A., Cerutti, L., Hulo, N., Gattiker, A., Falquet, L., Pagni, M., Bairoch, A., & Bucher, P. (2002). PROSITE: a documented database using patterns and profiles as motif descriptors. *Briefings in bioinformatics*, 3(3), 265-274.

- Simão, F. A., Waterhouse, R. M., Ioannidis, P., Kriventseva, E. V., & Zdobnov, E. M. (2015). BUSCO: assessing genome assembly and annotation completeness with single-copy orthologs. *Bioinformatics*, *31*(19), 3210-3212.
- Simeonova, D. D., Lievreumont, D., Lagarde, F., Muller, D. A., Groudeva, V. I., & Lett, M. C. (2004). Microplate screening assay for the detection of arsenite-oxidizing and arsenate-reducing bacteria. *FEMS microbiology letters*, *237*(2), 249-253.
- Singh, A. L., Asthana, R. K., Srivastava, S. C., & Singh, S. P. (1992). Nickel uptake and its localization in a cyanobacterium. *FEMS microbiology letters*, *99*(2-3), 165-168.
- Singh, M., Verma, N., Garg, A. K., & Redhu, N. (2008). Urea biosensors. *Sensors and Actuators, B: Chemical*, *134*(1), 345-351.
- Singh, P., Khan, A., & Srivastava, A. (2021). Biological means of arsenic minimization with special reference to siderophore. *Arsenic toxicity: challenges and solutions*, 253-278.
- Singh, S., Kang, S. H., Mulchandani, A., & Chen, W. (2008). Bioremediation: environmental clean-up through pathway engineering. *Current opinion in biotechnology*, *19*(5), 437-444.
- Smith, D. R., & Nordberg, M. (2015). General chemistry, sampling, analytical methods, and speciation. In *Handbook on the toxicology of metals* (pp. 15-44). Academic Press.
- Sofia, H. J., Burland, V., Daniels, D. L., Plunkett Iii, G., & Blattner, F. R. (1994). Analysis of the *Escherichia coli* genome. V. DNA sequence of the region from 76.0 to 81.5 minutes. *Nucleic acids research*, *22*(13), 2576-2586.
- Song, B., & Leff, L. G. (2005). Identification and characterization of bacterial isolates from the Mir space station. *Microbiological research*, *160*(2), 111-117.
- Sorin, E. J., Alvarado, W., Cao, S., Radcliffe, A., La, P., & An, Y. (2017). Ensemble molecular dynamics of a protein-ligand complex: residual inhibitor entropy enhances drug potency in butyrylcholinesterase. *Bioenergetics: open access*, *6*(1).
- Srivastava, S., & Dwivedi, A. K. (2015). Biological wastes the tool for biosorption of arsenic. *Journal of bioremediation and biodegradation*, *7*(1), 1-3.
- Srivastava, S., Verma, P. C., Singh, A., Mishra, M., Singh, N., Sharma, N., & Singh, N. (2012). Isolation and characterization of *Staphylococcus* sp. strain NBRIEAG-8 from arsenic contaminated site of West Bengal. *Applied microbiology and biotechnology*, *95*(5), 1275-1291.
- Stamatakis, A. (2014). RAxML version 8: a tool for phylogenetic analysis and post-analysis of large phylogenies. *Bioinformatics*, *30*(9), 1312-1313.

- Stamatakis, A., Hoover, P., & Rougemont, J. (2008). A rapid bootstrap algorithm for the RAxML web servers. *Systematic biology*, 57(5), 758-771.
- Stoytcheva, M., Sharkova, V., & Magnin, J. P. (1998). Electrochemical approach in studying the inactivation of immobilized acetylcholinesterase by arsenate (III). *Electroanalysis: an international journal devoted to fundamental and practical aspects of electroanalysis*, 10(14), 994-998.
- Subedi, P., Schneider, M., Philipp, J., Azimzadeh, O., Metzger, F., Moertl, S., Atkinson, M. J., & Tapio, S. (2019). Comparison of methods to isolate proteins from extracellular vesicles for mass spectrometry-based proteomic analyses. *Analytical biochemistry*, 584, 113390.
- Sun, X., Jia, H. L., Xiao, C. L., Yin, X. F., Yang, X. Y., Lu, J., He, X., Li, N., Li, H. & He, Q.Y. (2011). Bacterial proteome of *Streptococcus pneumoniae* through multidimensional separations coupled with LC-MS/MS. *Omics: a journal of integrative biology*, 15(7-8), 477-482.
- Szajn, H., Csopak, H., & Fölsch, G. (1977). Spectral studies of the interaction of *Escherichia coli* alkaline phosphatase with 4-(4-aminophenylazo) phenylarsonic acid. *Biochimica et biophysica acta (BBA)-enzymology*, 480(1), 154-162.
- Tariq, A., Ullah, U., Asif, M., & Sadiq, I. (2019). Biosorption of arsenic through bacteria isolated from Pakistan. *International microbiology*, 22(1), 59-68.
- Tabatabai, L. B., Zehr, E. S., Zimmerli, M. K., & Nagaraja, K. V. (2008). Iron Acquisition by *Ornithobacterium rhinotracheale*. *Avian diseases*, 52(3), 419-425.
- Tencaliec, A. M., Laschi, S., Magearu, V., & Mascini, M. (2006). A comparison study between a disposable electrochemical DNA biosensor and a *Vibrio fischeri*-based luminescent sensor for the detection of toxicants in water samples. *Talanta*, 69(2), 365-369.
- Tepljakov, A., Pullalarevu, S., Obmolova, G., Doseeva, V., Galkin, A., Herzberg, O., Dauter, M., Dauter, Z., & Gilliland, G. L. (2004). Crystal structure of the YffB protein from *Pseudomonas aeruginosa* suggests a glutathione-dependent thiol reductase function. *BMC structural biology*, 4(1), 1-4.
- Tian, W., Chen, C., Lei, X., Zhao, J., & Liang, J. (2018). CASTp 3.0: computed atlas of surface topography of proteins. *Nucleic acids research*, 46(W1), W363-W367.
- Tongamp, W., Takasaki, Y., & Shibayama, A. (2009). Arsenic removal from copper ores and concentrates through alkaline leaching in NaHS media. *Hydrometallurgy*, 98(3-4), 213-218.
- Törönen, P., Medlar, A., & Holm, L. (2018). PANNZER2: a rapid functional annotation web server. *Nucleic acids research*, 46(W1), W84-W88.

- Tripti, K. (2018). Arsenic removing soil indigenous bacteria of hyper arsenic contaminated region in Bihar. *Proceedings of the National Academy of Sciences, India Section B: Biological Sciences*, 88(4), 1605-1613.
- Tsao, D. H. H., & Maki, A. H. (1991). Optically detected magnetic resonance study of the interaction of an arsenic (III) derivative of cacodylic acid with EcoRI methyltransferase. *Biochemistry*, 30(18), 4565-4572.
- Turdean, G. L. (2011). Design and development of biosensors for the detection of heavy metal toxicity. *International journal of electrochemistry*, 2011.
- Tu, Y. G., Zhao, Y., Xu, M. S., Li, X., & Du, H. Y. (2013). Simultaneous determination of 20 inorganic elements in preserved egg prepared with different metal ions by ICP-AES. *Food analytical methods*, 6(2), 667-676.
- Turner, A. P. F. (2000). Biosensors-sense and sensitivity. *Science*, 290(5495), 1315-1317.
- Ungureanu, G., Santos, S., Boaventura, R., & Botelho, C. (2015). Arsenic and antimony in water and wastewater: overview of removal techniques with special reference to latest advances in adsorption. *Journal of environmental management*, 151, 326-342.
- van Groenestijn, J. W., Vlekke, G. J. F. M., Anink, D. M. E., Deinema, M. H., & Zehnder, A. J. B. (1988). Role of cations in accumulation and release of phosphate by *Acinetobacter* strain 210A. *Applied and environmental microbiology*, 54(12), 2894-2901.
- Van Gunsteren, W. F., & Berendsen, H. J. C. (1977). Algorithms for macromolecular dynamics and constraint dynamics. *Molecular physics*, 34(5), 1311-1327.
- Van Veen, H. W., Abee, T., Kortstee, G. J., Pereira, H., Konings, W. N., & Zehnder, A. J. (1994). Generation of a proton motive force by the excretion of metal-phosphate in the polyphosphate-accumulating *Acinetobacter johnsonii* strain 210A. *Journal of biological chemistry*, 269(47), 29509-29514.
- Verma, S. K., & Singh, H. N. (1991). Evidence for energy-dependent copper efflux as a mechanism of Cu²⁺ resistance in the cyanobacterium *Nostoc calcicola*. *FEMS microbiology letters*, 84(3), 291-294.
- Vorontsov, I. I., Minasov, G., Brunzelle, J. S., Shuvalova, L., Kiryukhina, O., Collart, F. R., & Anderson, W. F. (2007). Crystal structure of an apo form of *Shigella flexneri* ArsH protein with an NADPH-dependent FMN reductase activity. *Protein science*, 16(11), 2483-2490.
- Wang, L., Huang, L., Su, Y., Qin, Y., Kong, W., Ma, Y., Xu, X., Lin, M., & Yan, Q. (2015). Involvement of the flagellar assembly pathway in *Vibrio alginolyticus* adhesion under environmental stresses. *Frontiers in cellular and infection microbiology*, 5, 59.

- Wang, Z., Li, Y., & Lin, X. (2017). Transcriptome analysis of the Antarctic psychrotrophic bacterium *Psychrobacter* sp. G in response to temperature stress. *Acta oceanologica sinica*, *36*(2), 78-87.
- Wang, Z., Zhang, H., Li, X.-F., & Le, X. C. (2007). Study of interactions between arsenicals and thioredoxins (human and *E. coli*) using mass spectrometry. *Rapid communications in mass spectrometry*, *21*(22), 3658-3666.
- Wargnies, B., Lauwers, N., & Stalon, V. (1979). Structure and properties of the putrescine carbamoyltransferase of *Streptococcus faecalis*. *European journal of biochemistry*, *101*(1), 143-152.
- Waterhouse, A., Bertoni, M., Bienert, S., Studer, G., Tauriello, G., Gumienny, R., Heer, F. T., de Beer, T. A. P., Rempfer, C., & Bordoli, L. (2018). SWISS-MODEL: homology modelling of protein structures and complexes. *Nucleic acids research*, *46*(W1), W296-W303.
- Wick, R. R., Judd, L. M., Gorrie, C. L., & Holt, K. E. (2017). Unicycler: Resolving bacterial genome assemblies from short and long sequencing reads. *PLOS Computational biology*, *13*(6), e1005595.
- Wilkins, J. C., Beighton, D., & Homer, K. A. (2003). Effect of acidic pH on expression of surface-associated proteins of *Streptococcus oralis*. *Applied and environmental microbiology*, *69*(9), 5290-5296.
- Wong, E. L. S., Chow, E., & Gooding, J. J. (2007). The electrochemical detection of cadmium using surface-immobilized DNA. *Electrochemistry communications*, *9*(4), 845-849.
- Xia, X., Postis, V. L. G., Rahman, M., Wright, G. S. A., Roach, P. C. J., Deacon, S. E., Ingram, J. C., Henderson, P. J. F., Findlay, J. B. C., & Phillips, S. E. V. (2008). Investigation of the structure and function of a *Shewanella oneidensis* arsenical-resistance family transporter. *Molecular membrane biology*, *25*(8), 691-701.
- Xu, C., Shi, W., & Rosen, B. P. (1996). The chromosomal *arsR* Gene of *Escherichia coli* encodes a trans-acting metalloregulatory protein. *Journal of biological chemistry*, *271*(5), 2427-2432.
- Xu, C., Zhou, T., Kuroda, M., & Rosen, B. P. (1998). Metalloid resistance mechanisms in prokaryotes. *The journal of biochemistry*, *123*(1), 16-23.
- Xue, X.-M., Yan, Y., Xu, H.-J., Wang, N., Zhang, X., & Ye, J. (2014). ArsH from *Synechocystis* sp. PCC 6803 reduces chromate and ferric iron. *FEMS microbiology letters*, *356*(1), 105-112.

- Yan, G., Chen, X., Du, S., Deng, Z., Wang, L., & Chen, S. (2019). Genetic mechanisms of arsenic detoxification and metabolism in bacteria. *Current genetics*, 65(2), 329-338.
- Yang, H.-C., Cheng, J., Finan, T. M., Rosen, B. P., & Bhattacharjee, H. (2005). Novel pathway for arsenic detoxification in the legume symbiont *Sinorhizobium meliloti*. *Journal of bacteriology*, 187(20), 6991-6997.
- Yang, H.-C., & Rosen, B. P. (2016). New mechanisms of bacterial arsenic resistance. *Biomedical journal*, 39(1), 5-13.
- Yang, J., Abdul Salam, A. A., & Rosen, B. P. (2011). Genetic mapping of the interface between the ArsD metallochaperone and the ArsA ATPase. *Molecular microbiology*, 79(4), 872-881.
- Yang, J., Rawat, S., Stemmler, T. L., & Rosen, B. P. (2010). Arsenic binding and transfer by the ArsD As (III) metallochaperone. *Biochemistry*, 49(17), 3658-3666.
- Yang, J., Yan, R., Roy, A., Xu, D., Poisson, J., & Zhang, Y. (2015). The I-TASSER Suite: protein structure and function prediction. *Nature methods*, 12(1), 7-8.
- Yang, T., Zhang, X.-X., Yang, J.-Y., Wang, Y.-T., & Chen, M.-L. (2018). Screening arsenic (III)-binding peptide for colorimetric detection of arsenic (III) based on the peptide induced aggregation of gold nanoparticles. *Talanta*, 177, 212-216.
- Yang, Y., Dai, L., Xia, H., Zhu, K., Liu, H., & Chen, K. (2013). Protein profile of rice (*Oryza sativa*) seeds. *Genetics and molecular biology*, 36(1), 087-092.
- Ye, J., Ajees, A. A., Yang, J., & Rosen, B. P. (2010). The 1.4 Å crystal structure of the ArsD arsenic metallochaperone provides insights into its interaction with the ArsA ATPase. *Biochemistry*, 49(25), 5206-5212.
- Ye, J., Yang, H.-C., Rosen, B. P., & Bhattacharjee, H. (2007). Crystal structure of the flavoprotein ArsH from *Sinorhizobium meliloti*. *FEBS letters*, 581(21), 3996-4000.
- Yin, Z., Lu, W., & Xiao, H. (2014). Arsenic removal from copper–silver ore by roasting in vacuum. *Vacuum*, 101, 350-353.
- Yogarajah, N., & Tsai, S. S. H. (2015). Detection of trace arsenic in drinking water: challenges and opportunities for microfluidics. *Environmental science: water research & technology*, 1(4), 426-447.
- Zargar, K., Conrad, A., Bernick, D. L., Lowe, T. M., Stolc, V., Hoefl, S., Oremland, R. S., Stolz, J., & Saltikov, C. W. (2012). ArxA, a new clade of arsenite oxidase within the DMSO reductase family of molybdenum oxidoreductases. *Environmental microbiology*, 14(7), 1635-1645.

-
- Zelaya-Molina, L. X., Hernández-Soto, L. M., Guerra-Camacho, J. E., Monterrubio-López, R., Patiño-Siciliano, A., Villa-Tanaca, L., & Hernández-Rodríguez, C. (2016). Ammonia-oligotrophic and diazotrophic heavy metal-resistant *Serratia liquefaciens* strains from pioneer plants and mine tailings. *Microbial ecology*, 72(2), 324-346.
- Zhang, L., Guo, W., & Lu, Y. (2020). Advances in Cell-Free Biosensors: Principle, Mechanism, and Applications. *Biotechnology journal*, 15(9), 2000187.
- Zhang, W., Liu, Q. X., Guo, Z. H., & Lin, J. S. (2018). Practical application of aptamer-based biosensors in detection of low molecular weight pollutants in water sources. *Molecules*, 23(2), 344.
- Zhang, Z.-Y., Wang, Y., Wu, L., Fauman, E. B., Stuckey, J. A., Schubert, H. L., Saper, M. A., & Dixon, J. E. (1994). The Cys (X) 5Arg catalytic motif in phosphoester hydrolysis. *Biochemistry*, 33(51), 15266-15270.
- Zhu, Y.-G., Yoshinaga, M., Zhao, F.-J., & Rosen, B. P. (2014). Earth abides arsenic biotransformations. *Annual review of earth and planetary sciences*, 42, 443-467.

Appendix I

List of Publications

1. **Mishra S**, Verma SK. Differential expression of proteins in *Pseudomonas mendocina* SMSKVR-3 under arsenate stress. J Basic Microbiol. 2021;1–11.
2. **Mishra S**, Kumar S, Verma SK. Arsenic resistance mechanisms in *Pseudomonas mendocina* SMSKVR-3 strain isolated from Khetri copper mines, Rajasthan, India. Curr Microbiol. 2022. (Under Production; Manuscript No.- CMIC-D-20-01947R3)
3. **Mishra S**, Verma SK. Isolation and characterization of copper-resistant bacteria from khetri copper mines and analysis of the expression of copper-induced proteins. Int J of Biomed Eng Technol. 2021. (Accepted; Manuscript No.- IJBET_293127)

Book Chapter

1. **Mishra S**, Verma SK (2021) Methods of arsenic detection. (Arsenic in Plants: Uptake, Consequences and Remediation Techniques to be published by Wiley & Sons Publisher, U.S.A.) (Accepted)

Details of Conferences/Workshops Attended

Papers & Poster Presentations:

1. **Mishra S**, Verma SK (2020) Isolation and characterization of copper resistant bacteria from khetri copper mines and analysis of the expression of copper-induced proteins. 3rd International Conference on Advanced Scientific Innovation in Science, Engineering, and Technology (ICASISSET-2020) organized by Bharath Institute of Higher Education and Research, Chennai, India. May 15-16. Pg. no. 11, ICASISSET20-318.
2. **Mishra S**, Kumar S, Verma SK (2019) Isolation and characterization of arsenate resistant bacteria from khetri copper mines. 60th Annual Conference of Association of Microbiologists

of India (AMI-2019) held at Central University of Haryana, Mahendergarh. Nov. 15 -18, Pg. no. 176, Abstract no.: EMT-18.

3. **Mishra S**, Poonia S, Singh S, Verma SK (2018) Evaluation of *E. coli* K12 for the presence of metal induced/binding protein(s). 59th Annual Conference of Association of Microbiologists of India (AMI-2018) held at University of Hyderabad. Dec. 9-12, Pg. no. 615 Abstract no.: MM/004 (40214).

Participations:

1. Five Days Online Workshop on Molecular Simulation with GROMACS organized by EdGene BioMed (OPC) Pvt. Ltd. India, June 22 -26, 2020.

2. Webinar on Importance of Biotechnology in Industries organized by Department of Biotechnology, School of Bioengineering & Technology, Noida International University, Gt. Noida, India, June 5, 2020.

3. International Conference on Life Science Research & its Interface with Engineering and Allied Sciences (LSRIEAS-2018) organized by Department of Biological Sciences, BITS Pilani, Pilani Campus, India. Nov. 1-3, 2018.

4. 3rd Workshop on Analytical Instruments for Chemical and Environmental Engineers (WAICEE-2017) organized by Department of Chemical Engineering, BITS Pilani, Pilani Campus, India. Feb. 10-11, 2017.

5. Two days hands-on workshop on Flow Cytometry organized by Department of Biological Sciences, BITS Pilani, Pilani Campus, India. Jan. 18 -19, 2017.

6. Seminar & workshop on Liquid Chromatography Tandem Mass Spectrometry organized by Department of Pharmacy, BITS Pilani, Pilani Campus, India. Aug. 23-24, 2016.

7. BITS Conference on Gene and Genome Regulation (BCGGR 2016) organized by Department of Biological Sciences, BITS Pilani, Pilani Campus, India. Feb. 18 -20, 2016).

Published Article

Received: 10 November 2020 | Revised: 15 December 2020 | Accepted: 2 January 2021

DOI: 10.1002/jbhm.202000671



RESEARCH PAPER

Journal of Basic Microbiology

Differential expression of proteins in *Pseudomonas mendocina* SMSKVR-3 under arsenate stress

Shraddha Mishra | Sanjay K. Verma

Department of Biological Sciences, Birla Institute of Technology and Science, Pilani, India

Correspondence

Sanjay K. Verma, Department of Biological Sciences, Birla Institute of Technology and Science, Pilani Campus, Pilani 333031, India.
Email: skverma@pilani.bits-pilani.ac.in

Funding information

Council of Scientific and Industrial Research, Grant/Award Number: 09/719(0089)/2018-EMR-I

Abstract

This study focuses on analyzing the protein expression pattern of intracellular proteins when *Pseudomonas mendocina* SMSKVR-3 exposed to 300 mM of arsenate to find out the proteins that are overexpressed or exclusively expressed in response to arsenate. The sodium dodecyl sulfate-polyacrylamide gel electrophoresis analysis of protein expression at different time intervals showed the highest number of protein bands (14) that are overexpressed at 8 h of the time interval. It was also observed that treatment with at least 200 mM of As(V) is required to induce a difference in protein expression. Two-dimensional (2D)-PAGE analysis of 8-h sample exhibited 146 unique spots, 45 underexpressed, and 46 overexpressed spots in arsenate-treated sample. Based on the highest percent volume and fold change, three unique spots and one overexpressed spot were selected and analyzed by matrix-assisted laser desorption/ionization-time of flight (MALDI-TOF/TOF) mass spectrometry (MS) analysis followed by the MASCOT search. These proteins were identified as ribosome-recycling factor (20.13 kDa), polyphosphate:ADP/GDP phosphotransferase (40.88 kDa), ribonuclease P protein component (14.96 kDa) and cobalt-precorrin-5B C(1)-methyltransferase (38.43 kDa) with MASCOT score of 54, 81, 94, and 100, respectively. All of these proteins help the bacteria to overcome arsenate stress.

KEYWORDS

Article Accepted for the Publication

Date: 17 Dec 2021
To: "Sanjay Kumar Verma" skverma@pilani.bits-pilani.ac.in
From: "Current Microbiology (CMIC)" aishwarya.kamalakannan@springer.com
Subject: Your Submission CMIC-D-20-01947R3

Dear Dr. Verma,

We are pleased to inform you that your manuscript, "Arsenic resistance mechanisms in *Pseudomonas mendocina* SMSKVR-3 strain isolated from Khetri copper mines, Rajasthan, India", has been accepted for publication in Current Microbiology.

You will receive an e-mail in due course regarding the production process.

Please remember to quote the manuscript number, CMIC-D-20-01947R3, whenever inquiring about your manuscript.

With kind regards,
Erko Stackebrandt, Ph.D,
Editor in Chief
Current Microbiology

Please note that this journal is a Transformative Journal (TJ). Authors may publish their research with us through the traditional subscription access route or make their paper immediately open access through payment of an article-processing charge (APC). Authors will not be required to make a final decision about access to their article until it has been accepted.

Authors may need to take specific actions to achieve compliance with funder and institutional open access mandates. If your research is supported by a funder that requires immediate open access (e.g. according to Plan S principles) then you should select the gold OA route, and we will direct you to the compliant route where possible. For authors selecting the subscription publication route our standard licensing terms will need to be accepted, including our self-archiving policies. Those standard licensing terms will supersede any other terms that the author or any third party may assert apply to any version of the manuscript.

[Find out more about compliance](#)

This letter contains confidential information, is for your own use, and should not be forwarded to third parties.

Recipients of this email are registered users within the Editorial Manager database for this journal. We will keep your information on file to use in the process of submitting, evaluating and publishing a manuscript. For more information on how we use your personal details please see our privacy policy at <https://www.springernature.com/production-privacy-policy>. If you no longer wish to receive messages from this journal or you have questions regarding database management, please contact the Publication Office at the link below.

8/15/2021

BITS Pilani University Mail - Final Refereeing Decision IJBET_293127



SHRADDHA MISHRA <p2014001@pilani.bits-pilani.ac.in>

Final Refereeing Decision IJBET_293127

1 message

Inderscience Publishers <noreply@indersciencemail.com>

Fri, Mar 26, 2021 at 12:38 AM

Reply-To: Inderscience Publishers <noreply@indersciencemail.com>

To: p2014001@pilani.bits-pilani.ac.in, skverma@pilani.bits-pilani.ac.in, Editor <nilmmini.work@gmail.com>

Dear Shraddha Mishra, Sanjay Kumar Verma,

Ref: Submission "Isolation and characterization of copper resistant bacteria from khetri copper mines and analysis of the expression of copper-induced proteins"

Congratulations, your above mentioned submitted article has been refereed and ~~accepted~~ for publication in the International Journal of Biomedical Engineering and Technology. The acceptance of your article for publication in the journal reflects the high status of your work by your fellow professionals in the field.

You need now to login at <http://www.inderscience.com/login.php> and go to <http://www.inderscience.com/ospeers/admin/author/articlelist.php> to find your submission and complete the following tasks:

1. Save the "Editor's post-review version" on your local disk so you can edit it. If the file is in PDF format and you cannot edit it, use instead your last MS Word revised version, making sure to include there all the review recommendations made during the review process. Rename the new file to "authorFinalVersion."
2. Open the "authorFinalVersion" file and remove your reply or any response to reviewers that you might have in the front of your article.
3. Restore the author's identification, such as names, email addresses, mailing addresses and biographical statements in the first page of your local file "authorFinalVersion."
4. IMPORTANT: The paper is accepted providing that you, the author, check, edit and correct the English language in the paper. Please proofread all the text and make sure to correct any grammar and spelling mistakes.

Appendix II

Biography of Prof. Sanjay Kumar Verma

Prof. Sanjay Kumar Verma is working as a Professor in the Department of Biological Sciences and Dean Administration for Birla Institute of Technology and Sciences Pilani, Pilani Campus, Rajasthan. He completed his master's from Banaras Hindu University (BHU) in the area of Botany having specialization in cyanobacteria and applied phycology. He did Ph.D. in the field of Environmental Biotechnology from the same University. Later, he joined the University of Hyderabad and worked as a research associate in the area of microbial and molecular genetics. He started his teaching career in the Department of Biological Sciences, BITS Pilani in the year 1993. He had previously engaged in several administrative responsibilities such as Head of the Department of Biological Science and Chief Warden and University-wide Dean of Academic Research division (Ph.D. program) of the Institute. His major research area includes environmental biotechnology, microbial physiology & genetics. Prof. Verma has successfully finished numerous research projects related to the development of a recombinant bacterial biosensor for environmental application, biodiesel production by microalgae, bioremediation and biodegradation of toxic industrial waste and, bioactive compounds from native microalgae & higher plants from the Shekhawati region which were granted by various National funding agencies such as DAE, CSIR, UGC, DST, MoM ABSTCL and, WIPO. He has also coordinated several national and international level symposiums, conferences and, workshops. He has published more than 40 research articles in the journals of international repute, 7 book chapters, and holds two patents. He has guided 8 Ph.D. students and 70 graduates and Master's projects in the area of Environmental Biotechnology.

Biography of Prof. Suresh Gupta

Prof. Suresh Gupta is working as a Professor in the Department of Chemical Engineering and Associate Dean, Academic - Undergraduate Studies Division (AUGSD) BITS Pilani, Pilani Campus, Rajasthan. He completed his Bachelor's from Ujjain Engineering College, Ujjain in Chemical Engineering in year 2000, and M.Tech. degree in Chemical Engineering from IIT Kanpur in year 2002. He joined the Department of Chemical Engineering, BITS Pilani, Pilani Campus as a Lecturer in year 2002 subsequently completing Ph.D. in the area of Chemical Engineering from BITS Pilani in the year 2008. He served as Head of the Department of Chemical Engineering from September 2012 to August 2016. He has total 20 years of teaching and research experience. Prof Gupta is also a recipient of DST Young Scientist Project awarded to him by the Department of Science and Technology, Govt. of India, New Delhi, India. He has successfully implemented several research projects in the field of Environmental Engineering, funded by DST-SERB, UGC, Birla Cellulosic Kharach, BITS Pilani, and Aditya Birla Science & Technology Company Pvt. Ltd. (ABSTCPL). He has published 41 research papers in peer-reviewed journals, 7 book chapters, and 68 conference proceedings. He has around 60 conference proceedings to his credit. He has guided 4 Ph.D. (as supervisor/co-supervisor) and 19 M.E. dissertation students. Prof Gupta is involved in various academic and administrative committees at BITS-Pilani and other institutes/organizations.

Biography of Shraddha Mishra

Ms. Shraddha Mishra completed M. Tech. in Biotechnology from Birla Institute of Technology, Mesra, Ranchi (Jharkhand). She joined as a full-time research scholar in Birla Institute of Technology & Science, Pilani (Rajasthan) in August 2014 and worked on a project under Prof. S. K. Verma which was funded by WWE (Under Centre of Research Excellence). She has received financial assistance from various funding agencies such as WWE-BITS Pilani, BITS, Pilani, and CSIR during her Ph. D. She qualified GATE exam in 2013. During her research, she was actively involved in teaching several courses in the Department of Biological Sciences, BITS Pilani. She has published research articles in renowned international journals and also presented papers in various National and International conferences.

Appendix III

Submission of 16S rRNA gene sequence of *P. mendocina* SMSKVR-3 in NCBI database

GenBank

Pseudomonas mendocina strain SMSKVR-3 16S ribosomal RNA gene, partial sequence

GenBank: MH493722.2

[FASTA](#) [Graphics](#) [PopSet](#)

[Go to:](#)

LOCUS MH493722 1492 bp DNA linear BCT 09-JUL-2019
 DEFINITION Pseudomonas mendocina strain SMSKVR-3 16S ribosomal RNA gene,
 partial sequence.
 ACCESSION MH493722
 VERSION MH493722.2
 KEYWORDS .
 SOURCE Pseudomonas mendocina
 ORGANISM [Pseudomonas mendocina](#)
 Bacteria; Proteobacteria; Gammaproteobacteria; Pseudomonadales;
 Pseudomonadaceae; Pseudomonas.
 REFERENCE 1 (bases 1 to 1492)
 AUTHORS Verma,S.K. and Mishra,S.
 TITLE Direct Submission
 JOURNAL Submitted (19-JUN-2018) DEPARTMENT OF BIOLOGICAL SCIENCES, BITS
 PILANI, PILANI CAMPUS, Vidya Vihar, PILANI, RAJASTHAN 333031, India
 COMMENT On Jul 9, 2019 this sequence version replaced [MH493722.1](#).

##Assembly-Data-START##
 Sequencing Technology :: Sanger dideoxy sequencing
 ##Assembly-Data-END##

FEATURES
 source Location/Qualifiers
 1..1492
 /organism="Pseudomonas mendocina"
 /mol_type="genomic DNA"
 /strain="SMSKVR-3"
 /isolation_source="rhizospheric soil"
 /db_xref="taxon:300"
 /country="India: Khetri Copper Mines, Jhunjhunu,
 Rajasthan"
 /lat_lon="27.98 N 75.8 E"
 /collection_date="13-Nov-2017"
 /collected_by="S. Mishra"

Appendix IVSubmission of pure culture of *P. mendocina* SMSKVR-3 in MTCC

सूक्ष्मजीव प्ररूप संवर्धन संग्रह एवं जीन बैंक
MICROBIAL TYPE CULTURE COLLECTION & GENE BANK
 ISO 9001:2008 Certified
 सी.एस.आई.आर-सूक्ष्मजीव प्रौद्योगिकी संस्थान
 सेक्टर 39 ए, चंडीगढ़ 160036 भारत
CSIR-INSTITUTE OF MICROBIAL TECHNOLOGY
 (A CONSTITUENT ESTABLISHMENT OF CSIR)
 Sector 39-A, Chandigarh-160036 (INDIA)



सीएसआईआर - इमटेक
 CSIR - IMTECH

Dr. Suresh Korpole
 Senior Scientist
 Date: 20-11-2019

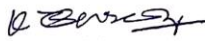
To,
 Dr. SK Verma,
 Department of Biological sciences,
 Faculty division – III, BITS PILANI,
 PILANI Campus-333031
 Rajasthan.

Dear Dr Verma,
 Please find enclosed the MTCC accession number given to your one bacterial strain SMSKVR-3 which was submitted for general deposition.

SI. No.	Strain designation	Identity	MTCC Number
1	SMSKVR-3	<i>Pseudomonas mendocina</i>	12986

Thanking you for your interest in MTCC.

Best regards,
 Yours sincerely,


 (K. Suresh)





FS668168

दूरभाष : +91-172-6665151 (MTCC Office)
 +91-172-6665152 (Information Centre)
 Phone : +91-172-2690562 (Head MTCC)

फैक्स : +91-172-2695215
 Fax : +91-172-2690632

ई-मेल : Information : info.mtcc@imtech.res.in
 E-Mail: Head, MTCC : head.mtcc@imtech.res.in
 Patent Deposits : idamtc@imtech.res.in
 Web : https://www.mtccindia.res.in

Appendix VSubmission of pure culture of *P. mendocina* SMSKVR-3 in NAIMCC


भा.कृ.अनु.प.-राष्ट्रीय कृषि उपयोगी सूक्ष्मजीव ब्यूरो
(भारतीय कृषि अनुसंधान परिषद्)
ICAR-NATIONAL BUREAU OF AGRICULTURALLY IMPORTANT
MICROORGANISMS
(Indian Council of Agricultural Research)
कुशावर, मऊ उत्तर प्रदेश-275103
Kushaaur, Mau Uttar Pradesh- 275103
Tel (फ़ोन): (0547) 2530080, FAX (फैक्स): (0547) 2530381,
E-Mail (ई-मेल): nbaimicar@gmail.com, (Web): www.nbaim.org.in


F.No. NAIMCC/2020-21/1523 Dated: 04.11.2020

National Agriculturally Important Microbial Culture Collection
NAIMCC
Accession Number of Culture(s)

To,
 Depositor/ (s) Name **S.K. Verma***
 Designation Professor
 Address Department of Biological Sciences, Birla Institute of Technology & Science, Pilani-333031, Rajasthan
 Email skverma@pilani.bits-pilani.ac.in
 Phone 7742044100

Thank you for submitting following culture(s) at NAIMCC, ICAR-NBAIM, Mau

	Name of Culture(s)	Accession Number
1.	<i>Pseudomonas mendocina</i> SMSKVR-3	NAIMCC-B-02531

The accession numbers of the submitted culture(s) cited above is/are for your future reference and record.

JPO SS
 In-charge *04/11/2020*
 NAIMCC, ICAR-NBAIM, Mau
 Email: naimcc.nbaim@gmail.com
 Phone: 0547-2530156 Ext. 272/207
 Fax: 0547-2530358

